Investigations of Processes Controlling Trace Element Mobility in Scottish Freshwater Loch Sediments

Ruth Saunders

Ph. D. Thesis
The University of Edinburgh
2003

Declaration

I hereby declare that the work present in this thesis is my own except where appropriate reference has been made in the text. All material included from the work of others has been acknowledged in full and the work has not been presented for and any other degree.

Acknowledgements

The first people I would like to thank are my supervisors Dr Graham and Dr Farmer for their guidance, support and enduring patience without which I would not have had the motivation or confidence to complete this work. I would also like to thank Alex Kirika from the Centre for Ecology and Hydrology for supervising and assisting with the sample trips come rain or, very infrequently, shine. Dr Eades and Dr Thomas gave invaluable advice and training with sample processing and analysis.

My parents have supported me financially and emotionally over the last four years. They have always been there for me especially when I was feeling stressed. I love them very much and hope they are now as relieved as I am. Duncan, my fiancé has also had to cope with ranting, whether excited or nervous, for the last year and has managed wonderfully. My thanks and love go to him for being on hand to fix computers and give hugs day or night.

Finally the research presented in this thesis was funded by the EPSRC and without their financial aid this project would not have been possible.

Abbreviations

AVS	acid volatile sulfates
DOC	dissolved organic carbon
CFF	cross flow filtration
DEAE	cellulose 2-(diethylamino)ethyl cellulose
Amberlite XAD	resin trade name of the Rohm and Haas company
IHSS	International Humic Substance Society
NOM	natural organic matter
IR	infra-red
EDTA	ethylene diamine tetra acetic acid

Abstract

This thesis contains an investigation of the processes controlling trace heavy metal (Pb, Cu and Zn) mobility in three contrasting Scottish freshwater Lochs, Loch Leven, Loch Bradan and Loch Tay. The aim was to determine the relative importance of redox processes (involving Mn and Fe) and of organic matter complexation on the vertical distribution of Pb, Cu and Zn in the sediments and associated porewaters of these lochs. The aim of the project strongly influenced the choice of lochs. Loch Leven was selected because it had well-documented high primary productivity and thus the sediments receive large inputs of authochthonous organic material. Heavy metal contamination was not thought to be extensive. Loch Bradan was included as an example of a water body that received large inputs of catchment derived allochthonous organic material. The Mn-rich nature of the bedrock underlying both the loch and its catchment meant that the sediments also had elevated Mn concentrations. The loch is also shallow and the waters are well-oxygenated throughout the year and so the oxic-anoxic boundary is located within the bottom sediments. Finally, Loch Tay was included because it also had organic-rich sediments with large amounts of the input material being catchment-derived but the past mining activities in the vicinity have lead to documented elevation of the concentrations of heavy metals in the loch sediments.

The sampling strategy started with the collection of multiple cores. Sectioning was always carried out on-site immediately after collection. Samples were then placed in a cold store on return to the laboratory and porewaters extracted from each section within 1-2 days form collection. The porewaters were returned to the cold store and the residual sediments from each section were frozen until required. Characterisation of the porewaters involved UV/vis analysis as a measure of the DOM concentration whilst characterisation of the sediments included determination of moisture content, wet/dry ratio, organic matter content, and ash content. Pseudo-total digestions (hot 8M HNO_3) and readily reducible extractions (0.1 M $NH_2OH.HCl$ (pH 2)) were carried out on dried, ashed sediment samples. The concentrations of Mn, Fe, Pb, Cu and Zn in the digests, extracts and the porewaters were determined initially by AAS but later in the study by ICP-OES. At this stage, additional elements (Al, Ca, Mg, P, S and Si) were also determined by ICP-OES. Centrifugal ultrafiltration was used to separate medium/large colloids (>30 kDa), small colloids (1-30 kDa) and truly dissolved species in the porewaters isolated from one of the Loch Tay cores. Gel electrophoresis was employed to isolate and fractionate humic substances in the porewaters and sediments of a Loch Tay core. ICP-OES analysis of the ultrafilter and gel electrophoretic fractions was used to establish the element-humic associations in the Loch Tay sediment system.

The results comprised vertical pseudo-total, readily reducible and porewater concentration profiles for Mn, Fe, Pb, Cu and Zn (and for certain cores from Loch Bradan and Loch Tay, Al, Ca, Mg, P, S and Si). Solid phase and dissolved organic matter concentration profiles were also obtained. For Loch Tay only, vertical concentration profiles showing the distribution of these elements amongst the medium/large colloidal, small colloidal and truly dissolved fractions were determined.

Element maps showing chnages in elemental concentration across the gel and with vertical depth in the sediment core were produced from the IPC-OES data for the gel electropherograms of humic substances form both the porewaters and the solid phase sediments.

The results showed the redox cycling of Mn and Fe was a process common to the sediments form all three lochs and that this sometimes caused the perturbation of the solid phase profiles of Pb, Cu and Zn. The vertical distributions of Fe, Pb, Cu and Zn in the sediment porewaters were often strongly related to the concentrations of DOM. This was sometimes the case for Mn but centrifugal ultrafilter fractionation of the porewaters showed that, when conditions become sufficiently reducing, it is Mn^{2+} that is released into the porewaters and that association with high molecular weight humic material occurs as Mn diffuses away from the point of release. 'S' and Zn were also present in the truly dissolved fraction at the point of Mn release but further work is required to completely elucidate the process occurring here. Finally, electrophoretic fractionation experiments and ICP-OES determination of associated elemental concentrations (Loch Tay samples only) led to the postulate that there were humic-coated inorganic colloids (containing Fe, Al, Mn and sometime Si) in the porewaters at certain depths an similar entities that could be easily mobilised from the sediment at similar depths. Importantly humic complexation of Fe, Cu and Zn was also established and this was at a maximum in the sediment at the position of the DOC and metal maxima in the porewater. Overall, a much improved understanding of the relative importance of redox processes and of organic matter complexation on the geochemical associations of Pb, Cu and Zn in the sediments and porewaters of freshwater lochs has resulted from this work. This has been due in the main to the approach that has been developed and in particular to the inclusion of ultrafiltration and electrophoresis as tools for the isolation and fractionation of humic materials from both porewaters and sediments.

Chapter 1: Introduction

1.1 The sources and essentiality of metals in the environment

Any element that has been proven to be vital for sustaining the growth of an organism is classed as an essential element. The essential elements play important roles in the metabolic processes of the life form in such a manner that they cannot be fully replaced by any other element (Bowen 1966). The essential elements include the basic biological building blocks C, H and O as well as the other non-metallic elements B, N, P and S. The elements classed as essential include the macronutrients K, Ca and Mg and the micronutrients Mn, Fe, Cu, Zn, Mo, Cl, Ni. Other beneficial elements are Co, Na and Si (Wild 1995).

Detrimental effects develop if the concentration of an essential element falls below a critical level for a given organism. With increasing concentration essential elements cease to be beneficial and become toxic in a similar manner to non-essential elements such as Al, Cd and Pb. The tolerance of an organism for a metal depends on synergistic/antagonistic effects and the bioavailability of the element.

Natural sources of trace metals have to be considered with the earth's crust containing Cu, Pb and Zn at concentrations of 50 μg/g, 14 μg/g and 75 μg/g respectively. Pb occurs naturally as the sulfide, mainly in the form of galena PbS, and Pb and Zn are commonly mined together. Pb has been used for many applications, including plumbing, roofing and paint, since pre-roman times and since 1750 A.D. increases of Pb in the environment have been found (Bunce, 1994). The uses of Zn include pigment in paints, galvanising on iron, and battery components as well as the inclusion of Cu to produce brass. Approximately 65 % of the Pb, Cu and Zn released into the environment in the UK on an annual basis originates in municipal waste disposals (Wild, 1993)

The bioavailability of an element depends strongly not only on the total concentration, but also on the species present (Turner 1995). The concentration of a metal in a lake is governed by the sources of the metal, partitioning and transport processes and the available sinks for the metal. The rates at which these processes occur determine

whether the net result is accumulation or loss of the element from the system. The metal speciation is influenced by environmental variables such as pH, redox conditions and temperature.

1.2 Freshwater environments

The conditions prevalent in a freshwater system will have major influence on the concentrations and fluxes of trace metals between sediments and water. Considerations must include sediment characteristics, water depth and trophic nature of the loch. Shallow lakes tend to remain permanently well mixed due to the surface water movement and thus even at depth the water is oxygenated. Deeper lakes may be subject to thermal stratification as the surface water is heated by solar radiation and the deeper waters where there is little or no light penetration remain cold. In this scenario a thermocline forms separating the warm and oxygenated epilimnion from the cool and anoxic hypolimnion. A temperate winter can break down the stratification and once again produce a well mixed lake that is referred to as holomitic. For very deep lakes the stratification is permanent and although the depth at which the thermocline occurs may vary the lake is never entirely mixed producing a meromitic lake with a mineral enriched stable hypolimnion.

The trophic status of a lake also has a large influence on the biogeochemistry of the waters and sediment. Eutrophic lakes are nutrient rich and productive environments with phytoplankton quotients greater than 2.0. Conversely oligotrophic lakes have low productivity and phytoplankton quotients of less than 0.8 with mesotrophic lakes falling in between these two categories.

1.3 The influence of the colloidal phase

Determination of the speciation and partitioning of a metal is vital for the understanding of the mobility and behaviour of metals in the environment. Modelling of metal behaviour in aquatic environments has focused on partitioning of the metals between the

solid and aqueous phases (Macalady 1998). This is a simplified approach as the colloidal phase plays an important role in metal partitioning and environmental fate.

Colloids are inorganic or organic species that range in size from 1 nm- 1 μm. They are small enough to remain suspended in the water column for extended periods of time under ambient environmental conditions. Due to their small size they exhibit relatively large surface areas (Macalady 1998) and provide reactive sites for adsorption and reaction of other dissolved or suspended species. Colloids can be transported great distances as they are small enough to filter through porous sediments but they can also aggregate to form larger particles that undergo sedimentation and thus be removed from the aqueous phase. The main colloid types are metal (hydr)oxides, clays, silicates, fibrillar extracellular organic substances, biota (cells and viruses), protein-rich cell fragments and humic substances (Leppard 1992).

Organic carbon that remains suspended in the water column has been divided into dissolved and particulate classes according to whether it passes or is retained by a 0.45 μm filter (Butcher 1994). In a study of the particle concentration effect Benoit and Rozan (1999) found that a 3000 Da cut-off was a more suitable lower limit for colloidal material in the water column than the 0.45 μm filter that was previously used to separate colloidal and dissolved species. Thus it was found that >90% of colloidal mass isolated from river water was organic material and the colloidal fraction (0.45 μm-3000 Da) was found to contain 50% of the DOC (defined by the 0.45 μm cut-off) and 32-53% of metals present in the water column. Marley *et al.* (1991) found that ground water colloids occurred primarily in two size bands, 0.45 - 0.1 μm and <3000 Da molecular weight whereas colloids in surface water are more evenly distributed between all the size fractions (0.45-0.1 μm, 0.1 μm-30 kDa, 30-3 kDa and <3 kDa).

Marley *et al.* (1991) found that immediate fractionation of surface water colloids with an auto-sampler in the field produced samples with slightly higher DOC than those produced in the lab after a three week storage period at 3°C. The dissolved organic carbon content of samples, once isolated from the environment, is unstable with respect

to molecular size. Aggregation leads to larger particles that settle out of solution and therefore analysis should be conducted as rapidly as possible.

1.4 Isolation of colloids from natural waters

1.4.1 Isolation of interstitial waters from sediment samples

Interstitial water can be isolated from sediment samples by compression of the sediment during core pressuring or syringe isolation, or by diffusion across a porous filter of a peeper placed within the sediment in situ. Core pressuring, syringe isolation and the peepers isolate colloidal material from interstitial waters by filtration, whereas centrifuging separates colloidal material from sediment samples without applying an arbitrary boundary between colloid and particulate size molecules.

Chin *et al.* (1998) expelled pore water from a sediment core by compressing the core with a piston to force the water through 70 μm filters that had been previously inserted into the centre of the core. Syringe isolation follows a similar method on a smaller scale. Gavin *et al.* (9th IHSS submitted) used a syringe to draw sediment through one of a series of perforations in the apparatus holding the sediment core. The syringe was then fitted with 0.2 μm filter and a second syringe in which the pore water was collected by pushing the liquid released during compression through the filter.

Peepers are porous samplers used to isolate colloidal material in situ. Diffusion processes govern collection of the colloids and therefore long periods of incubation are required. Control experiments, in a study by Chin and Gschwend (1991), showed that Aldrich humic acid required 70 hours for the equilibrium to be reached. Sampling for four weeks produced sufficient material for analysis but allowed possible diagenetic alteration of the organic material. With depth, in the sediment, compaction and the formation of a biofilm on the peeper surface limit diffusion.

Centrifuging of sediment samples results in sedimentation and compaction of solid material and release of interstitial water under increased gravity. The colloidal material is separated from the larger particulate material on the basis that the colloidal material

remains in suspension whereas the particulate material settles out (Thimsen and Keil 1998). The supernatant often displays higher organic carbon and metal concentrations due to rupture of cells and release of intercellular components (Chin and Gschwend 1991)

Centrifuging is free from possible interactions between the membrane and the colloidal material but the concentrations of both organic matter and metals may be altered by cell rupture. Comparison to syringe isolated material may provide insight into the extent of such alterations and produce a more comprehensive study of the nature of the colloidal material.

1.4.2 Concentration of porewater colloids

The colloidal material present in pore water samples can be concentrated into operationally defined fractions according to molecular size by ultrafiltration. Resin adsorption can be used to isolate the colloids by the degree of ionisation or solubility in aqueous solution. Alternatively all of the colloidal material can be concentrated by freeze-drying the entire pore water sample.

Ultrafiltration can be used to concentrate fractions of colloidal material from aqueous solutions by applying large pressures to push the solution through a membrane of selected pore size. Flat membranes have been found to be subject to several operational problems that include non-uniform pore size, adsorption to and electrostatic repulsion from the membrane, macromolecular self-association and concentration polarisation. Hollow-fibre filters have been used to isolate enough colloidal humic material from surface and groundwaters for subsequent spectroscopic characterisation (Marley *et al.* 1992).

Cross-flow ultrafiltration involves the use of hollow fibre filters to produce more accurate molecular size cut-off and allow analysis of larger sample volumes by minimising membrane clogging (Marley *et al.* 1991; Gaffney *et al.* 1996).

Burba *et al.* (1998) reported ultrafiltration to be a suitable technique for distinguishing between the colloidal and solution phase metal ions. Ross and Sherrell (1999)

determined the temporal and spatial patterns of Al, Fe, Mn, Cu, Zn, Cd and Pb after fractionation of stream water colloids by CFF.

Extensive cleaning procedures are required immediately before use of the membranes to minimise the effect of organic and metal contamination of the samples due to leaching from the membrane (Gustafsson *et al.* 1996; Guo and Santchi 1996; Buesseler *et al.* 1996; Dai 1998).

As the membrane cut-offs are operationally defined calibration of the filtration system is required prior to analysis. Marley *et al.* (1991) calibrated a hollow-fibre filter system using natural spherical proteins. However, because they are not discrete and spherical molecules, humic substances do not behave in an ideal manner for comparison to the standard proteins and it was recognised that approximate cut-offs were obtained. As there are no standards suitable for the absolute replication of humic behaviour within the system, a comprehensive range of standard molecules must be applied to the membrane during calibration. Gustafsson *et al.* (1996) applied polystyrene sulfonate, polyethylene glycol, lactalbumin and dextran standards (covering a molecular size range of 1.8 - 40 kDa) to the calibration of a cross-flow filtration system. Large losses of standards to the membrane were observed as well as breakthrough of high molecular weight components.

Resin adsorption isolates fractions of organic matter, with respect to their sorption characteristics, directly from natural water. Ion exchange resins, such as DEAE cellulose, concentrate all organic molecules containing acidic functional groups from water samples by displacement of the mobile ions of the resin during interaction between the organic species with the resin. Humic substances can be isolated from other organic molecules with non-ionic macroporous resins, such as Amberlite XAD resins. The aqueous solubility of the macromolecule and the pH of the solution govern the interaction between the resin and the humic substance. Thus the sorption and elution of humic substances from the column requires the exposure of the macromolecules to strong acidic and alkaline solutions (Gaffney *et al.* 1996; Dunkelog *et al.* 1997; Thurman and Malcolm 1981).

Freeze-drying effectively removes water from the colloidal material under low temperature and pressure conditions, to allowing analysis of the remaining solid material.

All of these techniques are subject to concentration effects, as the volume of solution decreases the interactions between the colloids increase. The organic and metal components of the colloidal material can be isolated from large volumes of water, without exposure to extreme pH conditions, by ultrafiltration. Removing biota and clay colloids during the isolation process (Marley *et al.* 1991 and Buffle *et al.* 1992) can also purify the humic substances.

1.5 Influences on partitioning between particulate/colloidal/dissolved phase

1.5.1 Redox cycling

The two main components in redox cycling are Mn and Fe. The development of anoxic conditions in sediment results in high concentrations of dissolved, reduced Fe and Mn. The standard redox potentials for the half reactions are shown in table 1.1. The reduced Mn and Fe then move away from the point of release vertically in the sediment. When the material migrating up the sediment core reaches the oxic/anoxic boundary oxides form and Fe and Mn are precipitated (Stumm and Morgan, 1996). The movement of Mn and Fe between pore water and solid phases has major implications for trace metal mobility and availability in the sediments and surface waters (Hamilton-Taylor *et al.*, 1996). Trace metals can be adsorbed onto Mn/Fe (oxy)hydroxide surfaces and thus be transported into the sediment on the formation of oxides or be released to the porewater on their dissolution (Canfield et al, 1995,). Balistrieri *et al.* (1995) found that Pb was scavenged by Mn oxides and Fe oxyhydroxides in the oxic portion of the water column and then released as oxides before being reduced in the suboxic-anoxic region. Pb was then incorporated into metal sulfide phases in the anoxic sulphidic zone. The behaviour of Pb was controlled by the redox state and thus controlled by Fe within oxic sediments

Reduction half-reaction	Standard potential at 298K, E^{θ} /V
$MnO_2 + 4H^+ + 2e^- \rightarrow Mn^{2+} + 2H_2O$	+ 1.23
$Fe^{3+} + e^- \rightarrow Fe^{2+}$	+ 0.77

Table 1.1 The half reactions and standard redox potentials for the reduction of the solid phase manganese (IV) and iron (III) to the dissolved phase manganese (II) and iron (II) species

and sulfide where anoxic conditions developed. Taillefert and Gaillard (2002) also found Pb distribution governed by Fe cycling especially redox reactions. The model showed good fit for Pb reaction rates depending stoichiometrically on Fe cycling and suspended material was enriched in Fe and Mn due to oxyhydroxide coatings on the particulates. In a lake polluted by mine and smelter wastes Zn was found to be Mn-oxide bound whereas Cu was associated with Fe components (Jackson and Bistricki, 1995). Murray (1975) found the order of affinity for metals at the Mn dioxide surface to be Mg<Ca<Sr<Ba<Ni<Zn<Mn<Co and the interaction was pH dependent.

Canfield et al (1993) reported standard redox activity of Fe and Mn in Danish coastal sediments with dissolved Mn found at shallower depths than dissolved Fe. On face value the Mn reduction occurs nearer the sediment-water interface than the Fe reduction in accordance with free energy calculations but infact the Fe (II) was oxidised by Mn oxides, resulting in insoluble Fe formation and release of Mn(II). Acid volatile sulfides accumulated below region where Mn oxides concentration decreased and the Mn oxides were implicated in oxidation of AVS to SO_4^{2-}

Laxen *et al.* (1983) investigated the relationship between redox cycling and the size distribution of Fe and Mn in fresh water environments. Samples were taken from Lake Windermere and above the thermocline the Fe was mainly associated with larger, particulate fraction (3μm and >10μm) although some Fe was also found in the truly dissolved phase. Overall Fe was present in the particulate phase whereas Mn was present in the reduced form consistent with redox behaviour and particulate Mn was only found in the epilimnion and thermocline. As Mn is more readily reduced than Fe, Fe is predominant in the particulate phase and the Mn was found in the reduced and soluble form. Aggregation of Fe containing particles was found to be slow, therefore Fe containing particulates remained in suspension for extended periods. Another factor attributing to Fe suspension was the associated of Fe with phytoplankton, which was not found for Mn.

Precipitation of dissolved Fe and Mn occurred in the oxic region of the water column, with sorption to ferric precipitates causing the scavenging of phosphorous (Hongve, 1997).

The redox conditions down through loch sediments are greatly influenced by the content and nature of the organic material in the loch. With burial, increasing depth and the depletion of the oxygen in the sediment the importance of the role of organic matter in redox control increases. The decomposition of the organic material fuels the oxidation-reduction reactions leading to more reducing conditions developing with depth down the sediment column.

1.5.2 Humic substances and metal- organic interactions

Humic substances are refractory macromolecular polymers formed from the breakdown products of proteins, carbohydrates, lipids and lignin. They are ubiquitous in aquatic environments and compose up to 80 % of the DOC in aquatic systems (Aitken *et al.* 1985). They influence the transport and partitioning between the solid and aqueous phases of inorganic (Macalady 1998) and organic pollutants (Hayes *et al.* 1989) as well as micronutrients (Wen *et al.* 1999). They can also influence reactions within the aquatic environment such as the breakdown of non-polar organic molecules by photosensitization and may be involved in redox reactions thus influncing the speciation of metals (Gaffney *et al.* 1996).

Due to their complex nature the structure of these humic molecules has not yet been fully elucidated. Humic substances form polydisperse and highly heterogeneous mixtures and are also susceptible to denaturing and perturbation with changes in pH and temperature (Stevenson 1994). Thus sampling, isolation and characterisation of humic substances can all induce alterations in the molecular shape, size and functional group content of the macromolecules and the results become operationally defined. Under ambient environmental conditions the acidic functional groups of humic substances are significantly ionised and the negative charges are balanced by polyvalent and divalent metals (Schnitzer 1972). Interactions of cations with strands of the humic molecule cause the structure to become more compact and the humic material is thus less soluble in water.

The size of humic molecules and the range of functional groups they contain produce a high affinity for trace metals as well as more abundant ions. The main interaction of metals and humic molecules is via the carboxyl functional groups. Yonebayashi *et al.* (1988) applied several analytical titrations to humic samples and their derivatives to determine the carboxyl, phenolic hydroxyl, carbonyl, total hydroxyl and low pK_a carboxyl contents of humic acids.[13] Sihombing *et al.* (1996) investigated the distributions of functional groups in humic and fulvic acids that were previously fractionated by molecular weight. This study showed that alcoholic carbon (carbohydrates) was more predominant in the highest average molecular weight material, and that carboxylic carbon was more predominant in molecules with molecular weight >2.8-8.2 kDa.

Fe generally is found in association with the larger humic material, classed as the humic fraction by the IHSS fractionation method. The association of Mn with organic material tend tends to be by the formation of weak outer sphere complexes (Gavin, 1999) and in association with the smaller humic molecules i.e. the fulvic fraction. (Cheshire *et al.*, 1977). Riise (1999) also found that anionic and acid sensitive elements, such as Mn, associated with smaller molecular weight fraction (<3kDa) whereas high molecular weight NOM (>10kDa) most important transporting agent for Fe, Al and Pb. It was also proposed that NOM and associated trace elements enter the lake in high molecular weight form then aggregate and settle to become part of the lake sediment

Williams *et al.* (1994) reported that high concentration of organic matter and ion exchange materials affected the ability of sediment to retain metals via adsorption, chelation and ion exchange mechanisms. Thus comparison of the metal concentration and the organic content of interstitial water and sediment samples allowed associations between them to be inferred. Chin *et al.* (1998) found that the increase of DOC with depth in marine sediments was strongly correlated with the Fe (II) concentration, suggesting that they co-accumulate in porewater as iron (II) oxide coated in organic matter.

Gaffney *et al.* (1996) reported that stability constants for metal-DOM interactions suggest the presence of humic substances can dominate the metal speciation in solution.

The binding of metals neutralized repulsive forces and induced the contraction of the polymer and increased hydrophobicity. In the study of the influence of physicochemical factors on Cu-humic acid dissociation kinetics by Rate *et al.* (1993), relatively small changes in pH and ionic strength were found to have noticeable effects on the rate of dissociation.

Tipping and Hurley (1992) studied the binding of ions by humic substances defined by Model V in terms of discrete sites, modified by electrostatic effects and accounting for non-specific binding. The binding strength was reported to be in the order of Mg<Ca<Mn<Co<Zn<Pb<Cu. A different order of sorption was found for metal on humic acid at pH 4.7 by Kerndorff and Shnitzer (1980) Fe, Pb, Cu, Al>Zn>Co>Mn but it was noted that the order found changes with pH. The same process affects the distributions of trace metals in salt water. The colloidal Cu in the Rhone Delta constituted 20-40% total Cu in river water and complexation was dominated by organic matter of 3 kDa (Dai et al 1995).

Vermeer *et al.* (1999) suggested that the adsorption of metal ions on mineral surface increases due to the interaction between negatively charged humic acid and positively charged iron oxide, as compared to isolated oxide.

1.5.3 Additional moieties influencing the mobility of trace metals

Calcite can act as a sink for trace metals through incorporation of the trace metals into the crystal structure, thus effectively removing them from dissolved phase. The more stable solid phases of calcite eg siderite were less effective at removing metals from water but more resistant to subsequent dissolution, inhibiting remobilization of these elements (Rimstidt *et al.*, 1998)

Jackson and Bistricki (1995) investigated the association of trace elements with Fe and Mn in smelter wastes. Adsorbed Cu and Zn was found to be associated with S in the sediments with the lowest sulfide concentration. Dissolved Fe and Mn was released into the water column from anoxic sediments but in the sulfide poor sediments they precipitated as oxyhydroxides on organisms. Under strongly reducing conditions H_2S

production led to FeS precipitation while Mn remained in solution. Therefore sulfides inhibit formation of coatings and suppress release of dissolved Cu and Zn from sediments.

Sulfide dissolution can lead to reducing conditions developing in the water column of a lake and consequent iron oxidation in water, with carbonate and sulfide dissolution leading to increased Ca and Zn concentrations. (Neal C *et al.*, 1986). The concentrations of Fe and Cu in the pore waters of the highly reducing conditions of Delaware marshland were found to be controlled by sulfide formation (Boulegue *et al.*, 1982). Canfield *et al.* (1995) reported the formation of insoluble Pb sulfides at depth in anoxic sediments and sulfide formation was implicated by Carignan and Nriagu (1985) in the decrease in porewater Cu in the zone of suphate reduction.

Williams (1993) found Fe, Mg, Cu, Cd, Co, Pb and Ni in Loch Dee sediments to be in detrital silicates or organic complexes. Adsorbed and reducible oxide phases contained most of the Mn (81%), Ca and Zn. The elevated concentrations of Mn and Co in upper sediments were attributed to secondary oxides and adsorbed species influenced by redox activity. The decline of Pb and Zn below the water sediment interface was attributed to leaching of elements into overlying water. Emerson (1976) found that mobile, reduced iron moved by diffusion to the surface sediments from a large concentration at depth and subsequently precipitatied by combination with phosphorous as vivianite. P dissolution in the reduced zone of the lake sediments and migration to and precipitation in the oxidised zone was also reported by Carignan and Flett (1981).

The interactions of the particulate, colloidal and dissolved phase species inhibiting the mobility of trace metals are highly complex including the adsorption, surface coating, trapping in resistant matrices and co-precipitation. Multi-component interactions complicate the process further with Fe/Mn oxides interacting both with humic substances and with phytoplankton in the water. To elucidate the processes governing the mobility of trace metals a comprehensive sampling, preparation and analysis regime is required.

1.6 Solvents for the extraction of humic substances

Due to the inter and intra-strand associations caused by the electrostatic interactions with polyvalent cations or hydrogen bonding between functional groups the extraction of humic substances from environmental samples requires some perturbation of the macromolecular structure. The ionisation of the functional groups or the replacement of the polyvalent cations with monovalent species produces an expanded and more hydrophilic macromolecule. This perturbation should be minimised, however, if an environmentally relevant material is to be obtained.

The traditional extraction uses sodium hydroxide to isolate the sodium salts of humic molecules from soil or sediment samples (Gaffney *et al.* 1996). The humic material that remains insoluble is classed as humin. The suspension is then acidified to pH 2 with hydrochloric acid. The fraction that precipitates is humic acid and the fraction remaining in solution is fulvic acid. Treatment of humic substances with acid results in the polymerisation and partial decarboxylation of the macromolecules as evidenced by changes in their IR spectra (Stevenson and Goh 1971). Exposure to a strong base in an aerobic atmosphere results in autoxidation of the humic molecules and artefact formation. Extraction with strong base under nitrogen limits the oxidation of the macromolecules but base-catalyzed hydrolysis is not eliminated (Wilson 1991).

Neutral salts of mineral or organic acids can be used to extract humic substances. Sodium pyrophosphate is the most effective (Schnitzer 1972; Stepanov *et al.* 1997; Trubetskoj *et al.* 1995). The pyrophosphate complexes the metals, allowing sodium to neutralise the negative charges. This prevents the reformation of inter-strand interactions and thus the expanded molecules are more readily soluble in aqueous solution. This process can be achieved at near neutral conditions by adjusting the pH of the solution with phosphoric acid (Wilson 1991). The extraction is therefore free from alkaline oxidation effects but may produce a solution that contains organomineral complexes and high molecular weight polysaccharides (Stevenson and Goh 1971). Only the more

oxidised, therefore more acidic, and lower molecular weight materials are isolated by this method (Wilson 1991).

Pyrophosphate extraction has also been carried out under alkaline conditions. A study by Fujitake *et al.* (1998) showed that as the pH of the pyrophosphate solvent increased the concentration of the extracted humic acids increased and in particular the proportion of larger molecules. However, there was also an increase in degradation products formed by the alkali conditions. Belzile *et al.* (1997) found that sodium pyrophosphate-extracted material had lower H/C ratio and higher aromatic carbon content than that extracted by sodium hydroxide. The humic molecules were also found to be of lower molecular weight.

Tris buffers are commonly used in the fractionation of humic substances by gel filtration (Trubetskoi *et al.* 1995) and electrophoresis (Dunkelog *et al.* 1997; Trubetskoj *et al.* 1997). As Tris-borate buffer contains a monovalent base, reactions between the buffer and macromolecule are minimised (Sun 1991). Humic substances can be extracted at near neutral pH with minimum perturbation to the structure. At elevated pH (>9.2) there may be inclusion of borate into the humic molecule (Schmitt-Kopplin *et al.* 1998).

Organic solvents with a high dielectric constant and a high base parameter e.g. dimethylsulphoxide (DMSO) can be used for humic extraction. DMSO can associate with the acidic functional groups in humic molecules and break the hydrogen bonds. The non-polar methyl groups of DMSO can also associate with the non-polar groups of the molecules to enhance the dissolution (Wilson 1991). Belzile *et al.* (1997) found that the organic solvents extracted only a small portion of the organic matter. FT-IR spectra indicated that the extracted material was composed of alkane, fatty acids, long chain alcohols and wax esters.

Solvents from each of the categories have been combined in sequence to produce humic fractions that were more homogeneous than a single alkaline extraction (Belzile *et al.*

1997). Thus a more comprehensive extraction of the organic material can be achieved in combination with a partial fractionation on the basis of functional groups content and molecular size. Schnitzer (1991) extracted soil samples with organic solvent prior to extraction with $Na_4P_2O_7$ and NaOH to isolate the more discrete organic components.

The extraction of humic substances with strong acid or base is not suitable for the isolation of material that is representative of that found in the environment. The sodium hydroxide extraction can be used for the determination of maximum concentration of extractable humic material and for comparisons with other studies. Although the sodium pyrophosphate and Tris-borate solvents can be used to extract humic substances from samples under near neutral pH conditions a comparison of the material extracted by each solvent is required.

1.7 The molecular size determination and fractionation of humic substances and colloidal material

As discussed in section 1.4.2 centrifugal ultrafiltration can be used for the concentration of colloidal material from small water volumes. Ultracentrifugation and determination of molecular weights from the colligative properties of a humic substance yields results that are averaged for the sample under investigation. As the extracted humic material is highly heterogeneous the averaged compositional data are not sufficient to describe the polydisperse and multifunctional humic mixture. Therefore fractionation is required to produce more homogeneous samples for analysis and the two main techniques used (ultrafiltration and gel chromatography) can also produce molecular size distribution data once calibrated with appropriate standards. Electrophoresis fractionates humic substances according to their molecular size and charge and scattering techniques can be used to determine the apparent molecular sizes present within a humic sample.

1.7.1 Ultrafiltration techniques

Ultrafiltration is commonly used to fractionate humic substances and colloidal material in a similar manner to the concentration of pore water colloids discussed in Section 1.5.2. A series of membranes provide sequential size fractionation of the colloids and concentration of the defined fractions. The operational problems encountered for the single membrane procedure are enhanced by the application of a multi-membrane system. Mass balance conducted by Summers *et al.* (1987) revealed an average loss of 5.1% sample weight during the filtration process. High colloidal concentrations and high volumes of sample exacerbate these problems but they can be minimised by use of a stirred cell apparatus to reduce the effects of concentration gradients of molecules at the membrane by agitation of the retentate (Burba *et al.* 1998). Filtrate concentrations were not found to be equivalent when obtained by using different filters reported to be 0.45/0.40μm. Artefacts affected Al, Fe, Mn, Co, Ni, Cu and Zn concentrations while dilution effects were noted for Ca, Mg, Na and SiO_2 (Horowitz *et al*, 1996).
Hollow-fibre membranes are still subject to colloid interactions. The sample volume can be maintained by recirculation of permeate or addition of sample material from external source, thus minimising colloid concentration effects (Dai *et al.* 1998).
Marley *et al.* (1991) added radioactive tracers to surface and sub-surface water samples to assess the binding properties of each colloid size band. The most active sites for binding were for the 100 –30 kDa and greater than 100 kDa particle sizes. Of the trace metals analyzed 10-20% were found to be associated with colloids greater than 30 kDa in size. Iron and zinc were mostly found to be associated with small colloids. Pham and Garnier (1998) tagged colloids with the metal of interest and used coupled frontal cascade ultrafiltration and chromatography to obtain more homogeneous colloidal fractions. Iron was found mainly in the largest size fraction while Mn and Zn were distributed across the entire size range.
Ultrafiltration can provide the simultaneous isolation and fractionation of colloidal material from aqueous samples. The technique is suitable for both organic and metallic colloids but only after extensive washing and calibration procedures. Other analytical

techniques, such as size exclusion chromatography, can be used to confirm the molecular weight distributions obtained from ultrafiltration studies (Chin and Gschwend 1991).

1.7.2 Electrophoresis

A slurry containing sediment and loading buffer can be applied to a flat bed electrophoresis apparatus and the organic matter isolated according to its electrophoretic mobility. The near neutral buffer ionises the acidic groups of the macromolecule and induces a net negative charge. Under an applied electric field the molecules migrate through a stationary, porous medium towards the electrode of opposite charge. Vinogradoff *et al.* (1997) reported that the electrophoretic extraction of humic substances produced a partial fractionation of the complex mixture displayed as a series of bands.

The rate of migration is influenced by the properties of the molecule such as charge, size and shape and can be controlled by the experimental parameters such as voltage, current, buffer pH and ionic strength, temperature and endosmosis. The migration of the solute molecules is also influenced by the porosity of the stationary media. Agarose gel has a relatively large pore size, resulting in sharper bands as the paths of migration through the gel are more direct and zone broadening due to diffusion is minimised (Sun 1991). Thus agarose is suitable for preparative electrophoresis. Other media such as polyacrylamide gels produce a molecular sieving effect more suited to analytical electrophoresis (Hayes *et al.* 1989).

The electrophoretic extraction of humic substances can enhance the efficiency of the buffer for the isolation of the humic material and produce a simultaneous fractionation of the macromolecules. Minimising the steps in the extraction and fractionation procedures will minimise alteration of the natural polymers and produce more environmentally comparable material.

Organic colloids can be dispersed in organic solvents, sodium pyrophosphate or NaOH by ultrasonic vibration. The amount extracted over 3hr can be increased by 20% (Schnitzer 1972). Zone electrophoresis involves a single electrolyte which maintains the pH of the solution and provides the voltage gradient for the migration of the humic molecules. The molecules charge is the basis for the migration and the sample produces discrete zones if the magnitudes of the charges are sufficiently different. In this report the maximum separation of the humic mixture was required but the experimental technique had to conform to the constraint imposed by "natural" pH conditions therefore zone electrophoresis was the chosen method.

Although capillary electrophoresis is reported to be effective, slab electrophoresis was more suitable for the purposes of this project as larger gels could be used to produce larger humic samples. Denaturing agents were not added to the buffer solution, as the most natural electrophoretic system was required. In the absence of denaturing agents the most effective system for the production of discrete bands was sought. Agarose gel was chosen for its high, uniform porosity and Tris-borate buffer was used due to its effectiveness in molecular weight fractionations. As discussed previously (Section 1.5.2) electrophoretic mobility is a function of molecular size, shape and charge as well as experimental parameters. Thus more highly charged molecules migrate more rapidly in the electric field as do smaller molecules.

Capillary electrophoresis has commonly been used for the fractionation of humic substances. The technique is an analytical one and not suitable for the preparative fractionation of samples large enough for extensive characterisation studies. Pompe *et al.* (1996) used capillary electrophoresis to characterise fulvic acids and humic acids of different origins by the development of a catalogue based on functionality. Each sample produced an individual electropherogram but similarities, such as the migration time at which the peaks occurred, were observed within the fulvic and humic acid groups.

De Nobili *et al.* (1990) applied electrofocusing for the fractionation of pyrophosphate extracts. Electrofocusing relies on the isolation of humic molecules across a pH gradient in a similar manner to acid precipitation. It should be noted that perturbation of the humic macromolecules as a result of exposure to acidic pH conditions may be a problem. Pyrolysis, UV spectroscopy and IR spectroscopy confirmed that the fractions showed distinct compositional differences. The increase of electrophoretic mobility was found to accompany an increase of carboxyl content (from IR spectra).

Dunkelog *et al.* (1997) found that borate buffer produced an electropherogram consisting only of one broad band. The highly polydisperse nature of the humic acid resulted in the failure of electrophoretic mobility to produce complete fractionation of the sample. For previously fractionated material Ciavatta *et al.* (1995) found borate buffer to be more useful than the phosphate buffer as it produced better peak resolution, especially for smaller size fractions.

Denaturing agents, such as urea, can be used to disrupt aggregate formation and produce more discrete fractions but artefacts may also be produced. Denaturing agents such as EDTA (Trubetskoj *et al.* 1997), and urea (Trubetskaya *et al.* 1994) have been utilised to disrupt aggregate formation and to obtain more discrete fractions from electrophoretic experiments. Disrupting the non-covalent bonds and neutralising the effect of the divalent cations associated with humic substances will alter the shape of the molecule and produce misleading information regarding effective molecular size.

Electrophoretic fractionation can be used to reduce the heterogeneity of a humic extract but as the separation is charge and size dependent molecules of equal size but with different functionality will migrate at different rates. Thus confirmation of molecular size with a technique based purely on size fractionation or the parallel run of a size standard is required.
The extraction and electrophoretic fractionation of humic substances with Tris-borate would allow further elucidation of the metal-humic interactions.

1.8 Analysis of total and fractionated samples for organic and elemental concentrations

1.8.1 UV-Vis spectroscopy

Molecules that contain chromophores absorb electromagnetic radiation in the UV-visible region due to electronic transitions within and between the chromophores. The absorptivity of the chromophores can be increased by the presence of auxochromes such as hydroxyl and amine groups (Hayes *et al.* 1989). The UV-Vis spectra of humic substances are generally broad due to the high heterogeneity and multifunctionality of the macromolecules. The interpretation of the spectra has therefore produced a range of coefficients and variables for the characterisation of the humic material.

The E4/E6 ratio is among the most frequently quoted variables. This is the ratio of the absorbance at 465 nm to that at 665 nm. Summers *et al.* (1987) found a good log-log correlation of molecular weight and E4/E6 as demonstrated for HA. To overcome the concentration dependence of the absorbance values Yonebayashi and Hattori (1988) measured the absorbance co-efficients for 1% w/v humic acid solutions at wavelengths of 400 nm and 600 nm. The absorbance at 600 nm and the ΔlogK value (difference between absorbance of the 1% solution at 400 nm and 600 nm) were used to estimate the degree of humification. Significant linear correlation was found between between these two factors. Kawahigashi *et al.* (1996) found that the ΔlogK value decreased with increasing particle size. Tomikawa and Oba (1991) concluded that large molecular weight fractions contain a higher proportion of colourless components that exhibit low ΔlogK values.

Summers *et al.* (1987) reported a strong relationship between the absorbance at 254 nm and the DOC content of humic fractions. More recently Garrison *et al.* (1995) used the

absorbance at 254 nm as an indicator of aromatic character. The UV absorbances of interstitial waters at 280 nm analyzed by Krom and Sholkovitz showed close correlation to DOC values (Krom and Sholkovitz, 1977)

The E2/E3 value (the ratio of absorbance coefficients at 250 nm and 365 nm) and the molar absorptivity at 280 nm have been found to correlate to total aromaticity and average molecular weight (Peuravuori and Pihlaja 1997). As the E2/E3 ratio increased the aromaticity and molecular size decreased.

Korshin *et al.* (1997) has interpreted the UV-Vis spectra of humic substances as three overlapped Gaussian functions of energy. For benzene these are the local excitation band at 180 nm, benzenoid band centred at 203 nm and electron transfer band at 253 nm. Trubetskoj *et al.* (1997) used UV-Vis spectroscopy in conjunction with fractionation procedures to determine molecular size distrubutions.

Although the information obtainable from UV-Vis spectra of humic substances is still under debate the rapid analysis of liquid phase samples allows preliminary comparisons between humic samples and preparative techniques to be made. The preparation and analysis of humic solutions containing known weights of humic materials would allow more quantitative data to be obtained from the humic spectra but this would be required for each humic fraction of the study.

1.8.2 Digestion of sediment for metal concentration determination

The metal concentrations of sediments can be determined as pseudo-total concentrations by digestion of all but the most resistant minerals with aqua regia and subsequent analysis by atomic spectroscopy as discussed in Section 1.9.3. The information obtained can be enhanced by sequential extraction of the metals from the sediment, enabling associations between different moieties to be confirmed. A common extraction scheme divides metals into exchangable, carbonate bound, easily reducible, moderately

reducible and organic/sulfide associated fractions (Bryant *et al.* 1997, Mester *et al.*, 1998, Sahuquillo *et al.*, 1999). Generally these involve processing an individual sample through several extraction phases increasing the strength of reagents. This sequential method can lead to alteration of partitioning of the elements as the extractions proceed and thus the production of artefacts. An alternative extraction scheme was used by Gavin *et al.* (9^{th} IHSS submitted publication) for the study of the manganese-humic interaction in loch sediments and water. "Pseudo-total", easily reducible and humic-associated concentrations were determined but the digestions were conducted in parallel with separate sub-samples used for each stage.

1.8.3 Metal analysis

Atomic absorption spectroscopy (AAS) allows the determination of metal concentration by atomisation and absorption of the species present in a 2100 to 3200 K flame. Electromagnetic radiation at the wavelength specific for the element of interest is beamed through the flame and the intensity of radiation is detected at the other side. The concentration of the element present in the sample can be determined from a calibration curve constructed from known standard solutions. AAS is limited to single element analysis and matrix effects can be problematic for highly complex environmental samples. The application of a graphite furnace and a L'vov platform enhances the sensitivity of the technique thus the detection limit is reduced to 1 μgl^{-1} (Schlemmer 1996)

Analysis of the metal inventories of marine sediment pore water and overlying water samples by AAS has allowed assessment of the sediment as a source of trace metals at the sampling site. Williams *et al.* (1998) estimated overall marine sediment fluxes of Cu, Pb, and Mn to the Irish Sea as 160 t yr^{-1}, 180 t yr^{-1} and 38000 t yr^{-1}, respectively.

Inductively coupled plasma (ICP) is an alternative technique for sample introduction to the spectrometer. The plasma can be used to generate light emission from the sample as

in optical emission spectrometry (ICP-OES) or to generate ions prior to analysis by mass spectrometry (ICP-MS). Analysis by ICP allows rapid multi-element determination but the limits of detection are equal to or higher than with AAS (Wolf and Grosser 1997). ICP-OES is applicable to metals and non-metals in solution but does not provide the isotopic information available from ICP-MS. The matrix effects that cannot be overcome in ICP-MS can be overcome with ICP-OES by analysis at interference free wavelengths (Cidu 1996).

1.9 Rationale for the following investigation

Many studies have been conducted on the partitioning, cycling and availability of trace metals in fresh water systems but the focus tends to be narrow, concentrating only on Mn/Fe oxide surfaces or on organic matter. Those that compare more than one major influence in the sediment tend to omit consideration of the porewater. Therefore the aim of this research is to study the speciation and thus the mobility of essential (Fe, Mn, Cu and Zn) and non-essential (Al and Pb) elements within diverse freshwater environments, including consideration of Mn/Fe redox cycling and metal-humic interactions. The research will also investigate the sources, interactions and colloidal nature of metals and humic molecules from sediments, interstitial water and surface water. The influence of the major elements (Ca, Mg, Na, K, S, Si and P) on the distribution of metal concentrations in the sediment matrix will also be investigated.
The areas chosen for the study were very different Scottish loch systems. Loch Leven is a shallow, eutrophic loch with an agricultural catchment and high primary productivity. Loch Bradan has elevated Mn concentrations and has a organic peaty catchment and Loch Tay is a deep, oligotrophic loch and has elevated inventories of Pb, Cu and Zn. The ultimate goal is to evaluate the role of all Mn/Fe redox cycling and metal-humic interactions on the partitioning of the trace metals in the freshwater systems and to compare these roles for the three contrasting freshwater systems.

This aim of this work was to investigate of the processes controlling trace heavy metal (Pb,Cu and Zn) mobility in three contrasting Scottish freshwater lochs, Loch Leven, Loch Bradan and Loch Tay. A particular goal was to determine the relative importance of redox processes (involving Mn and Fe) and of organic matter complexation on the vertical distribution of Pb, Cu and Zn in the sediments and associated porewaters of these lochs.

Chapter 2. Field work and experimental methods

Chapter 2 contains a description of the sampling locations, details of the sampling trips undertaken and the methodology developed for sample processing and analysis.

2.1 Sampling locations

Three Scottish fresh water lochs, Loch Leven, Loch Bradan and Loch Tay, were chosen for their contrasting trophic nature, surrounding geology and usage. Table 2.1 displays the locations and the dates of the sampling trips.

2.1.1 Loch Leven, NE Scotland

Loch Leven (36° 11.5' N, 03° 22.2' W) is the largest sheet of freshwater in the midland valley of Scotland covering an area of 13.3 km^2. It lies at an altitude of 106 m and is located near Kinross in East Scotland, shown in figure 2.2, and is an example of a eutrophic loch. The surrounding catchment is mainly used for agricultural purposes with 70 % of the total land use accounted for by arable crops and improved pastures. The loch is a shallow drift basin with a mean depth of 3.9 m (May, 2002).

The application of fertilisers to the catchment has resulted in the loch being inundated with phosphate rich run-off. Until recently the local woollen mill discharged wastewater into the loch and the release of treated sewage to the loch still continues. All of these inputs to the loch have elevated the nutrient concentration in the water and thus contributed to the eutrophication of the loch (Bailey-Watts and Kirika 1987). The elevated nutrient content of the loch water combined with its clarity and shallow water depth results in high photosynthesis and primary production. Consequently Loch Leven is prone to dense algal blooms throughout the summer months with the density of the blooms controlled by the Daphnia population. When the population of these grazing zooplankton is low an enormous bloom of nano and pico-plankton develops. Frequent blooms subsequently produce declining water clarity, a reduction in the penetration of

LOCATION	DATE
LOCH LEVEN	16/03/00
LOCH BRADAN	10/06/00 – 11/06/00
LOCH TAY	22/06/01 – 24/06/01

Table 2.1 Field work dates and location

Figure 2.2 Map showing the location of Loch Leven, NE Scotland

sunlight and limits the growth of the aquatic plants (SEPA, 2002). Problems also occur when the population of Daphnia is high as although the overall density of the bloom is significantly lower it is dominated by the blue-green algae. The potential toxicity problems generated by these algae blooms threatens the future of the trout fishery and the nature reserve as well as affecting the tourist trade and the paper mill production (May, 2002).

Loch Leven overlies upper devonian strata of Upper Old Red Sandstone comprising of fine grained red/buff sandstones, dark red siltstones and mudstones. (BGS, 1985). The loch is formed in sand and gravel deposits overlying boulder clay and the sediments range from medium and fine sands to silty clays (Bryant *et al.*, 1997). Samples were collected from the shallow Reed Bower site shown in Figure 2.3 and were collected following the regime show in Table 2.4. The cores were predominantly of silty clay and mud. The water column rarely becomes stratified and therefore the oxygen content of the loch is approaching saturation (Bryant *et al.*, 1997) and conditions remain aerobic down to 15 cm into the sediment at the shallow part of the loch (Kirika, 2002).

Figure 2.5 contains a flow chart summarising the processing of the sediment samples and the analysis performed.

2.1.2 Loch Bradan, SW Scotland

Loch Bradan is a drinking water reservoir situated in the Galloway Hills, near Straiton, in SouthWest Scotland (55° 14.8' N, 04° 28.7' W), shown in figure 2.6. The body of water known as Loch Bradan is the product of three projects, in 1913 and 1972, to dam and flood Loch Lure and the original Loch Bradan to produce one larger source of drinking water. In 1913 a dam was constructed on the north-eastern shore and was subsequently breached in 1972 with the construction of two further dams, one at the eastern end of Loch Bradan and the other at the western end of Loch Lure. The map in figure 2.7 shows the original loch basins and the area flooded to raise the water level to that of the present day.

Figure 2.3 Map showing the location of the Loch Leven sampling site marked by •

Core Label	Length /cm	Sectioning regime	Site of collection
LL1	21	0.2 cm top 3 cm then 1cm	Reed Bower
LL2	23	0.2 cm top 3 cm then 1cm	Reed Bower
LL3	12	1cm	Reed Bower

Table 2.4 Sampling and initial processing of Loch Leven sediment cores

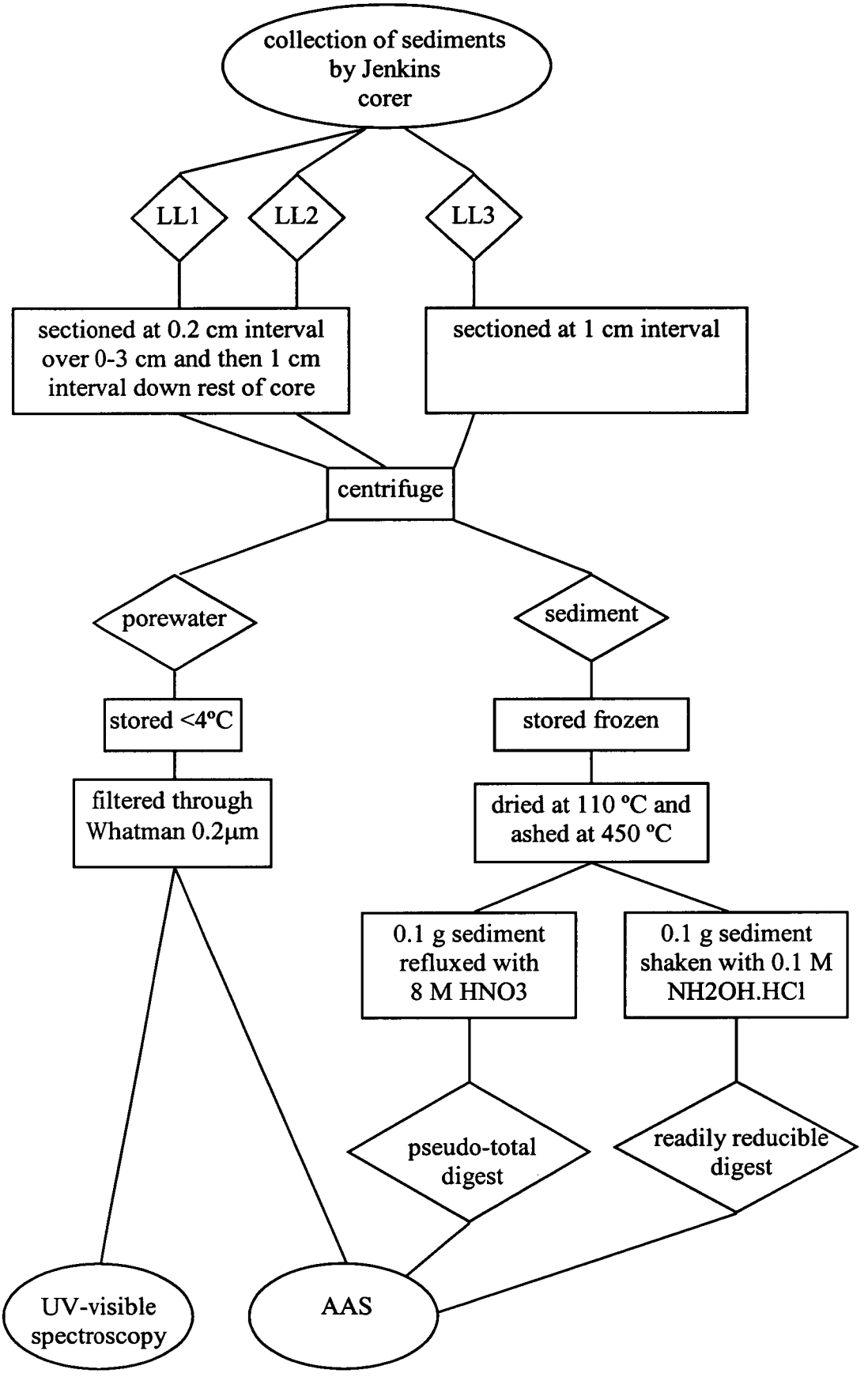

Figure 2.5 Flow chart of sample processing for Loch Leven

Figure 2.6 Sampling locations A and B at Loch Bradan, SW Scotland

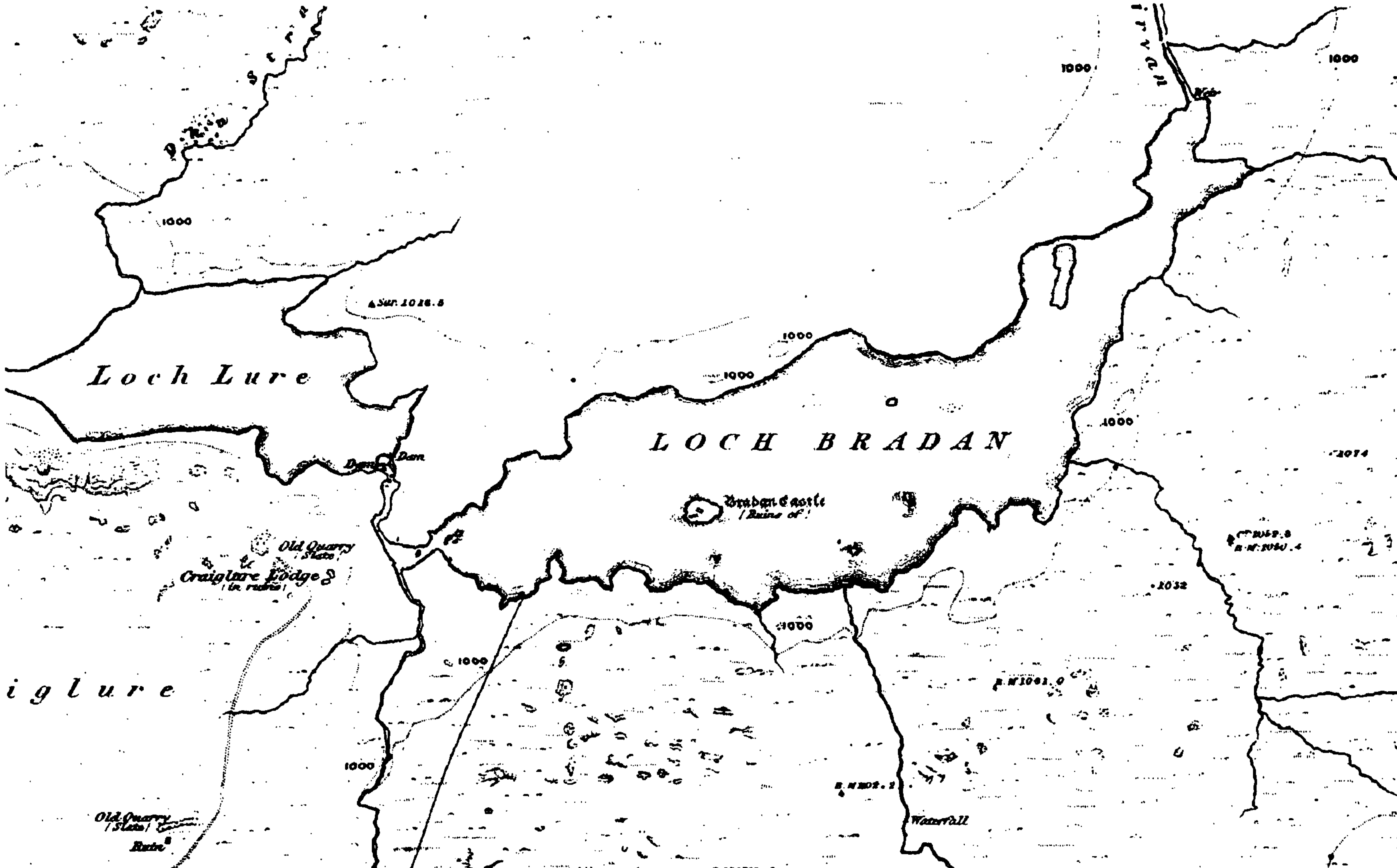

Figure 2.7 Historical map of Loch Bradan showing the original loch basins

Located ~320 m above sea level the loch has a maximum depth of 16 m and an average depth of 10 m. The bottom water and surface sediments are well oxygenated. The major inflow and outflow of Loch Bradan is the Water of Girvan. Entering Bradan from the south-west and leaving the loch to the east, the main flow of water across the loch is therefore west to east. The water of Girvan originates within a region dominated by granite intrusions of Tertiary age, underlying Loch Reicawr. Loch Bradan itself lies on a band of thin to medium bedded greywacke, mainly on the Kirkclom formation of greywacke and thick siltstone. Medium to thick greywacke lies to the north in the Blackcraig formation. Greywacke is a grey or black, fine matrix, sandstone containing quartz, feldspar and rock fragments (Hamilton *et al.*, 1998). They tend to be Mn rich minerals with concentrations of 700 mg/kg reported by Gilkes and McKenzie, 1988. The loch water has elevated levels of Mn often in excess of EC maximum admissible concentration (EC MAC) of 50 $\mu g\ l^{-1}$ and extensive ozonation processes are employed to precipitate MnO_2 from the water during water treatment. Weathering of the Mn rich greywacke has been highlighted as the main source of Mn to the loch sediments (BGS, 1993) but the circum-neutral, well oxygenated nature of the loch water should lead to oxidation of dissolved Mn followed by precipitation and settling to the sediments.

Loch Bradan has a peat rich and thus highly organic catchment. The soils are primarily podzols and peaty podzols (MLURI, 2002) with some peaty rankers and peaty gleys. The southern catchment is dominated by brown forest soils (Soil survey of Scotland, 1982).

The north and west of the catchment is covered by Sitka Spruce which is part of the forestry commission tree plantation while the south and east of the catchment is used for sheep grazing. The role of organic material in the cycling of Mn in Loch Bradan has been the source of investigation, with the suspected inhibition of Mn release from the sediment to the overlying water by interaction with humic material (Gavin *et al.*, 2000).

All sediment cores were collected from within the original Loch Bradan boundaries. Two sites were chosen (shown in figure 2.6) one near the middle of the original basin (Site A, west) and the other near the main inflow to the loch (Site B, east). Table 2.8 shows the details of the cores collected and tables 2.9 and 2.10 detail the observations

Core Label	Length /cm	Site of collection
LBA1	15	Site A, western site
LBA2	14	Site A, western site
LBB1	27	Site B, eastern site
LBB2	25	Site B, eastern site

Table 2.8 Sampling and initial processing of Loch Bradan sediment cores

Depth / cm	Properties of sediment core
0-1	Loose vegetation, dark brown, peaty
1-2.5	Lighter brown
2.5-12.5	Dark brown
12.5-13.5	Grey/silver streaked deposit

Table 2.9 Observed changes in sediment core LBA1 with depth

Depth / cm	Properties of sediment core
0-1	Loose vegetation , dark brown, peaty
1-2.5	Lighter brown with black flecks
2.5-18	Uniform slightly darker brown than above
18-23	Yellow-green streaks in dark brown
23-25	Dark brown with orange nodules, pebble appearance, malleable clay texture

Table 2.10 Observed changes in sediment core LBB1 with depth

made on examination of the sediment cores during sectioning. The flow chart in figure 2.11 shows the processes followed in the preparation and analysis of each sediment core.

2.1.3 Loch Tay, Central Scotland

Loch Tay is an oligotrophic, deep-water loch located in central Scotland near Killin (56° 30' N, 04° 10' W), shown in figure 2.12, and is the forth-largest Scottish freshwater loch by volume. The loch is long and sinuous, extending over 23.4 km, with a mean depth of 61 m and maximum depth of 155 m. The catchment covers an area of 576 km^2 and the inflow is from the Rivers Dochart and Lochay to the west with the outflow to the east via the River Tay.

Surrounding geology consists of slates, phyllites, mica-schist, biotite-gneiss with some quartz and limestone (Farmer *et al.*, 1997). The loch sediment is composed of fine grained silts and the waters are circum-neutral waters. The catchment has been extensively mined for Pb, Cu and Zn, with Pb mining at Tyndrum intermittently from 1739 until 1925. There have been Zn and Cu mines on a smaller scale with associated smelting activity. The loch itself is now used for recreational purposes with two outdoor activity centres located on its southern shore

Five sediment cores were collected at Loch Tay, 3 cores were sectioned at 1cm intervals the other two were sectioned at 0.2 cm intervals down to 3 cm as displayed in table 2.13. Thereafter the processes followed for the sample preparation and analysis are summarised in figure 2.14.

2.2 Sample collection, preliminary preparation and storage

Cores of bottom sediments were collected using a Jenkin sub-surface mud sampler with diving weights added, shown in figure 2.15 (Mortimer, 1971). The water from the top of each core was siphoned off and collected in a 200 ml acid washed, screw-top, polyethylene bottle. At Loch Tay approximately 50 ml of water directly above the

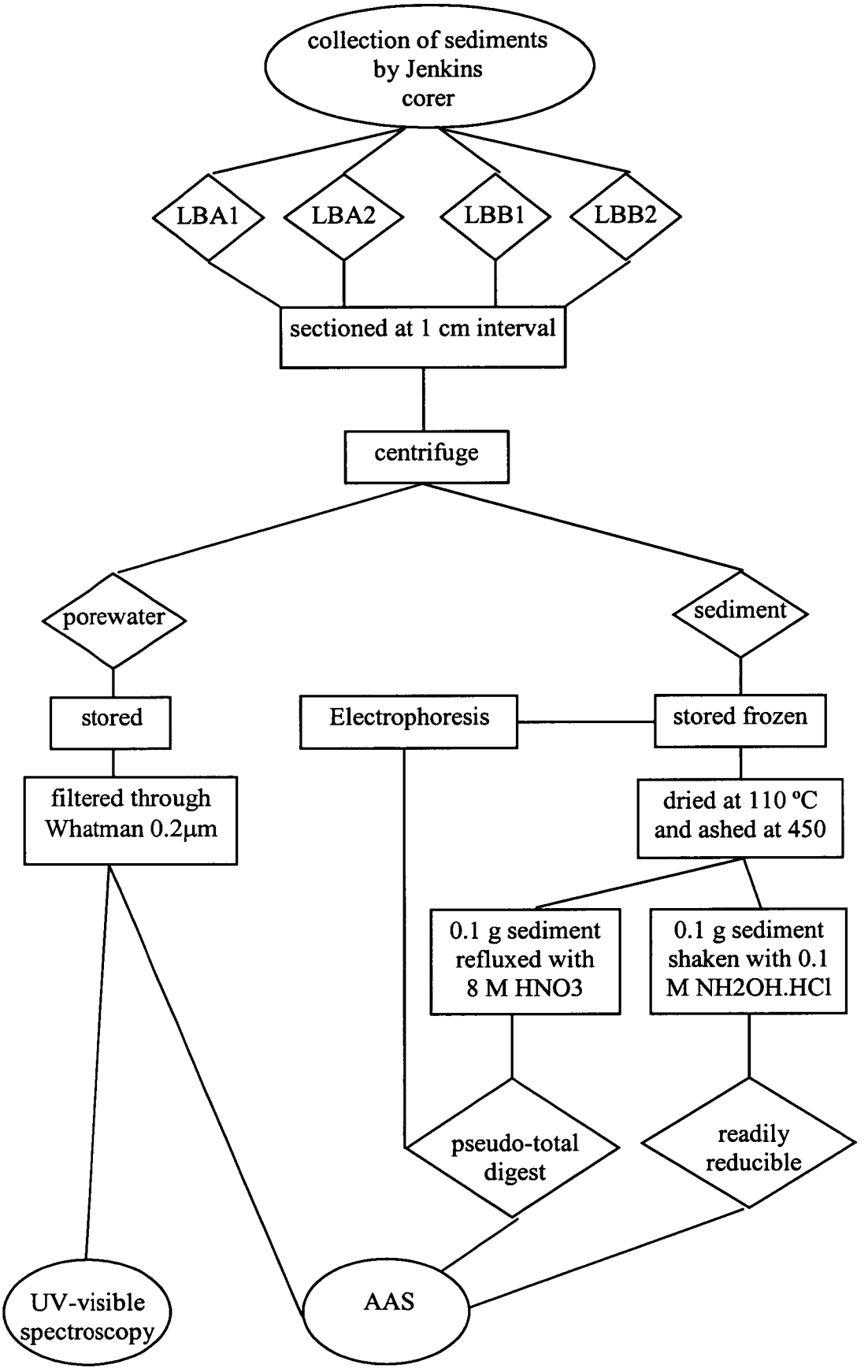

Figure 2.11 Flow chart of sample processing for Loch Bradan

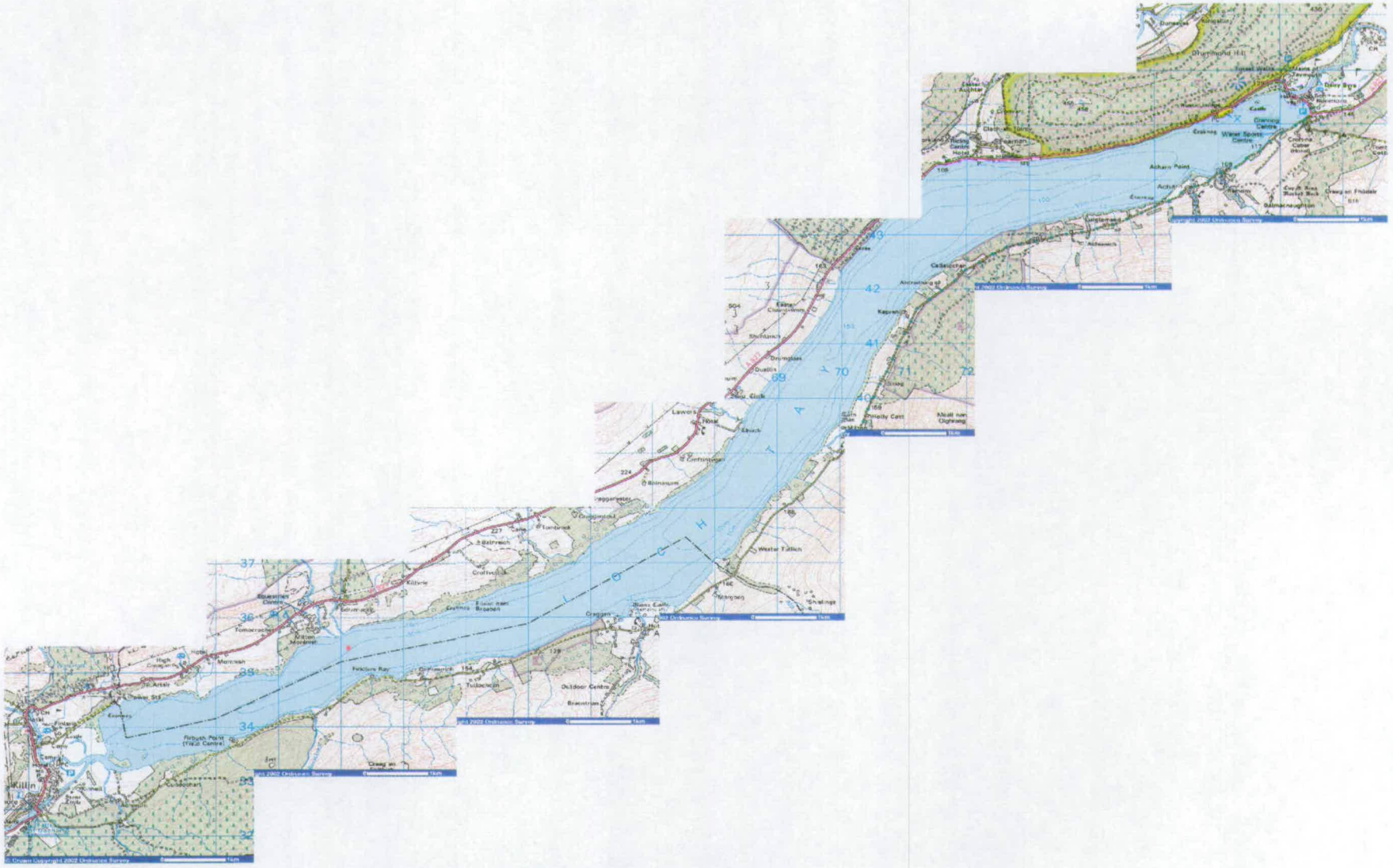

Figure 2.12 Map of Loch Tay, Central Scotland showing the sampling site marked as

Core label	Length of core analysed /cm	Sectioning regime
LT1	22	Sectioned at 1 cm intervals
LT2	23	Sectioned at 1 cm intervals
LT3	25	Sectioned at 1 cm intervals
LT4	3	Sectioned at 0.2 cm over top 3 cm

Table 2.13 Details of sediment samples collected at Loch Tay

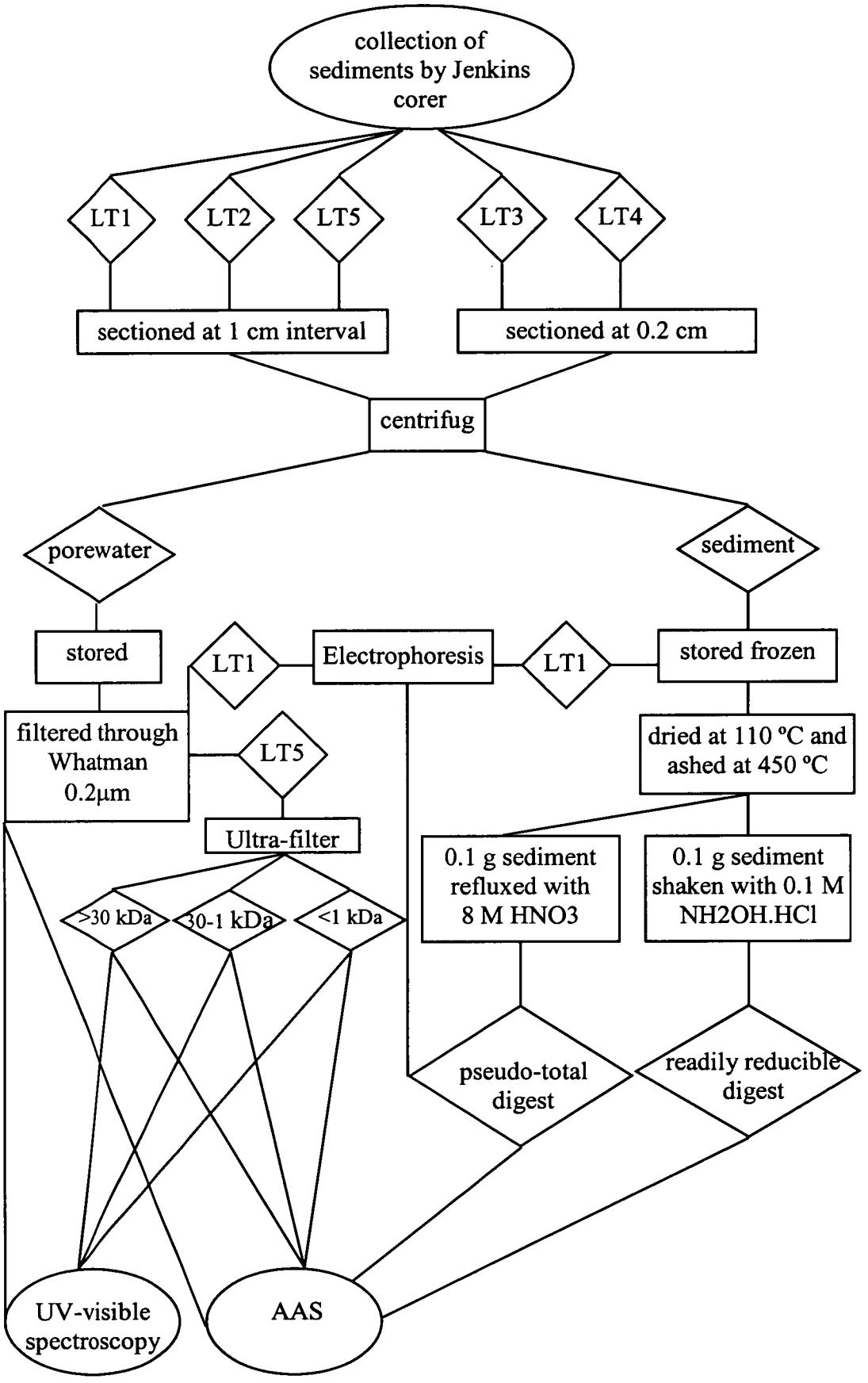

Figure 2.14 Flow chart of sample processing for Loch Tay

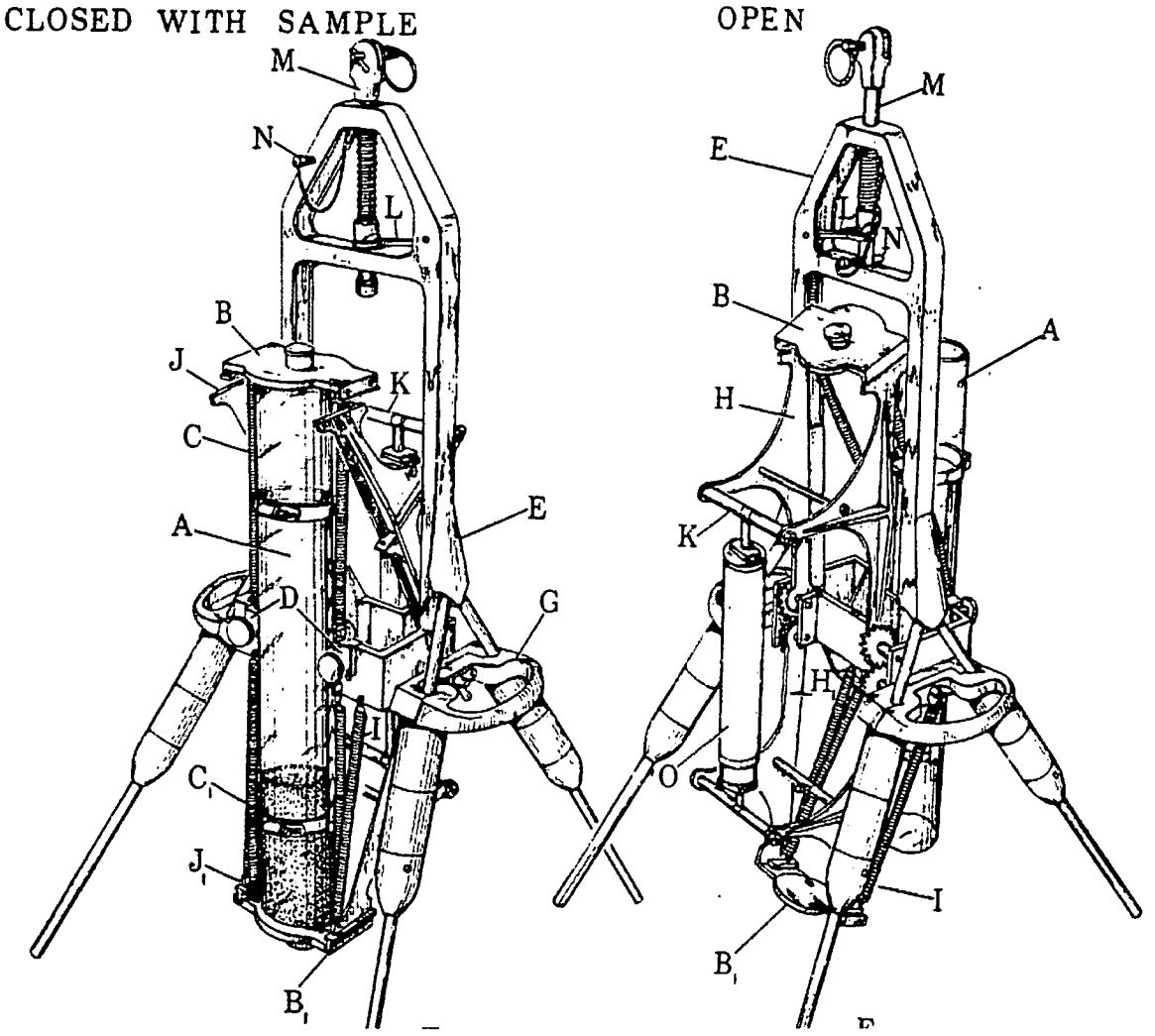

A sampling tube
B and B1 top and bottom lids
C and C1 springs
D harness assembly
E main frame
F legs
G handles
H and H1 arms
I additional springs
J and J1 arms engaging with lids B and B1
K arm assembly pull back from here
L spring loaded release lever
M rod for attachment of cable
N safety pin
O dashpot

Figure 2.15 Diagram of the Jenkin's sub-surface mud sampler (Mortimer, 1971)

sediment–water interface was collected separately. The sediment core was then extruded and sliced into 0.2 cm or 1 cm sections. The sections were placed in tapered polythene bags, which were then sealed.

Surface loch water was collected over the side of the boat in 1 l acid washed polyethylene screw-top bottles. Where possible mid depth loch water was collected using a mini-Friedinger water sampler and was then stored in a 1 l polyethylene bottle as before.

River water samples for Loch Tay were also collected by grab sampling and stored in 1 l acid washed polythene bottles.

All samples were stored in the dark in a cool room, maintained at 3°C, until they were prepared for analysis.

2.3 Apparatus cleaning

All the apparatus was acid-washed prior to use. Borosilicate glassware was washed in 6 M HNO_3 heated to 80°C for 3 hours. It was then rinsed thoroughly with double-deionised water (Millipore Milli-Q SP reagent water system) and reheated to 80°C in double-deionised water for a further 3 hours before being thoroughly rinsed and dried. Plastic apparatus was treated in a similar manner but the solutions were not heated and the apparatus was left to soak overnight.

2.4 Pore water processing

Each sediment sample was emptied into a 50 ml polethylene centrifuge tube and the total sample weight recorded. They were spun in a MSE Mistral 1000 centrifuge at 4500 rpm for three 10 minute intervals and the supernatant was pipetted into sterilin tubes after each run. The water and sediment weights were then recorded and the sediment was then frozen and stored. The pore water was syringe filtered through Whatman 542 filters and, where possible, through 0.45 μm cellulose nitrate filters (Loch Leven samples only). The pore water samples were then stored at 4° C until analysis.

2.5 Centrifugal ultrafiltration of Loch Bradan and Loch Tay porewater

2.5.1 Centrifugal ultrafilter prewash

The centrifugal ultrafilters were subjected to a wash procedure as follows in order to determine any possible contamination of water samples during processing and to eliminate artefact formation in pore water fraction profiles.
A 15 ml aliquot of double deionised water was placed in a centrifugal ultrafilter and was then spun for 1 hour at 4500 rpm. The filtrate was collected and the process was repeated with two further aliquots. This was carried out for two further centrifugal ultrafilters and the fractions were then analysed by UV-visible spectroscopy and AAS to determine the organic content and trace metal concentrations respectively.

2.5.2 Loch Bradan porewater size fractionation

Up to 15 ml of pore water was accurately weighed into a centrifugal ultra-concentrator, of cut-off of 1 kDa, and centrifuged for 3 hours at 4500 rpm (MSE Mistral 1000). The filtrate was weighed and stored in a sterilin tube. The retentate was weighed and made up to 10 ml for AAS analysis (section 2.15) or 5 ml for ICP-OES analysis (section 2.16), with deionised water and stored in a sterilin tube.

2.5.3 Loch Tay porewater size fractionation

The Loch Tay porewater samples from core LT5 was processed in the same manner as the Loch Bradan porewaters, section 2.5.2, but the cut-off of the centrifugal ultra-concentrators used was 30 kDa. The filtrate from the 30 kDa filter was then pipetted into

the reservoir of the 1kDa filter and the process repeated thus producing two size fractions containing colloidal material (>30 kDa and 30-1 kDa) and a fraction of truly dissolved (<1 kDa) material.

2.6 Porewater electrophoresis

2.6.1 Preparation of 0.045 M tris-borate running buffer (pH 8.5)

Approximately 5 g of Tris(hydroxymethyl)methylamine (Acros reagent) and 2.8 g of orthoboric acid (high purity reagent, Fisher) were accurately weighed, dissolved and made up to 1 litre with double-deionised water.

2.6.2 Preparation of the 0.045 M tris-HCl loading buffer (pH 8.5)

0.1 M Tris solution (25 ml, Acros) and 0.1 M HCl (8.6 ml, Analar, BDH) were mixed together and made up to 50 ml with double-deionised water.

2.6.3 Agarose gel preparation

Approximately 3g agarose gel (ultrapure electrophoresis grade, Life Technologies) was accurately weighed and made up to a 300 ml slurry with tris-borate buffer. The mixture was then heated in a microwave at 350 W for several periods of 1 minute until the gel became clear. The gel was then poured into the electrophoresis apparatus and allowed to set (for ~20 minutes).

The sample in loading buffer was then pipetted into the gel well and the reservoirs filled with running buffer. 3 samples of Blue Ranger protein marker mixture was made up in 30 μl deionised water and run alongside the environmental samples to give an indication of molecular size. IHSS Suwannee River natural organic matter was made into a solution of 23 mg in 60 μl tris-HCl and run alongside the environmental samples as a standardised and well characterised humic material , allowing comparison to other

electrophoretic studies. The current was then applied at 150 V for 60 minutes to encourage migration of charged material from the well and fractionation based on particle size and/or charge.

2.6.4 Loch Tay porewater electrophoretic extraction

Selected depths of pore water from Loch Tay core LT1 were allowed to settle out and the overlying colourless water was pipetted off and stored in a sterilin tube. 0.2 ml of the remaining humic rich water mixed with 0.1 ml tris HCl and was pipetted into the well in the agarose gel along side 3 samples of Blue Ranger protein marker mixture made up in 30 µl deionised water. The maximum permitted settings were 150 V, 20 mA, 5 W and the run was voltage controlled for a period of 60 minutes. After the gel was removed from the apparatus it was sliced at 0.5 cm intervals, the position and depth of colour of the bands were noted and the gel was photographed while exposed to UV light using a gel camera (UVP transilluminator, Biodoc-It system).

This procedure was then repeated with a 0.5 % agarose gel. The more diluted gel mixture results in a more open gel with larger pores but the well walls were not strong enough to contain the sample and therefore the gel was discarded.

The 1 % gel method was re-run but no tris HCl was added to the porewater. This allowed comparison of the migration and separation of the natural material and the pore water/ near neutral buffer mix.

The effect of NaOH on the mobility and fractionation of the natural material was then investigated. 0.15 ml of pore water was then mixed with 0.05 ml 0.1M NaOH prior to application to a 1 % gel as before.

The gel strips were weighed into 100 ml beakers and approximately 6 ml of 2 % nitric acid was accurately measured and added. The beakers were then heated gently on a hot plate to dissolve the gel strips. Hydrogen peroxide was added until the solutions were colourless. The solutions were then analysed by ICP-OES (see section 2.16).

2.7 Sediment drying and ashing

Approximately 3 g of wet sediment was accurately weighed into a 100 ml pyrex beaker and then dried in a muffle furnace for 3 hours at 110°C. This was followed by ashing at 450°C for 4 hours and the weight was recorded after each step.

For the fine section cores of the Loch Tay samples only 1 g of the sediment was processed by this method.

2.8 "Pseudo-total" sediment digestion

A 0.1 g sample of dried and ashed sediment was weighed into a 100 ml beaker and 30 ml of 8 M HNO_3 (Aristar) was then added. The beaker was covered with a watch glass and refluxed at 80°C for 2 hours. The suspension was then filtered through Whatman 540 paper to remove residual solid material and the filtrate boiled down to 1 ml. The solution was then made up to 25 ml with 2% HNO_3 (Aristar). This digestion releases all labile material from the sediment including Fe/Mn oxyhydroxides, organics and sulphides.

2.9 Readily reducible sediment digestion

The following procedure was applied to isolate the readily reducible Mn oxyhydroxide phases and to liberate associated trace elements.

A 0.1 g sample of dried and ashed sediment was weighed into a 250 ml conical flask and 25 ml 0.1 M $NH_2OH.HCl$ in 0.01 M HNO_3 was added and the mixture shaken for 30 minutes. The solution was then filtered through Whatman 40 paper and stored at 4 °C in sterilin tubes prior to analysis.

2.10 Electrophoretic extraction of the sediments from Loch Tay core LT1

Approximately 1 g of wet sediment, from selected depths of Loch Tay core LT1, was accurately weighed into a sterilin tube and 2 ml Tris-HCl was added. The mixture was agitated for 24 hours and the resultant slurry was pipetted into a 1 % agarose gel and run as for Loch Bradan sediments for 100 minutes.
This method was then repeated using the surface sediments from Loch Tay core LT1.

2.11 Total digestion of surface waters from Loch Tay

150 ml of overlying water from the sediment core was syringe filtered through a 0.45μm cellulose nitrate filter. 150 μl of concentrated nitric acid (Aristar) was then added and the solution was boiled down to 15 ml prior to being made up to 25 ml with double deionised water.

2.12 Surface water ultrafiltration

2.12.1 Centrifugal ultrafiltration

Approximately 15 ml of Loch Tay 2001 bottom water was syringe filtered through 0.45 μm cellulose nitrate filter. The sample was then placed in 1 kDa centrifugal ultrafilter and centrifuged at 4500 rpm for three 1 hour intervals. The filtrate was pipetted into a sterilin tube and stored for analysis. The retentate was made up to 5 ml with deionised water and stored in a sterilin tube.

2.12.2 Cross flow filtration

About 500 ml double deionised water was circulated through the cross-flow filtration apparatus for 5 minutes and then the retentate was flushed. This was repeated with a further 200 ml. After circulating for a third time with 500 ml of double deionised water

the filtrate was flushed by applying a backpressure until 100 ml was collected. The pH was recorded and the rinsing process continued until the pH was near neutral.
The surface water was syringe filtered through 0.45 μm cellulose nitrate filters. Then 50 ml of the sample was circulated for 5 minutes and then the retentate was flushed. The reservoir was then filled with 400 ml of the sample and the back pressure was applied. The filtrate was collected after discarding the first 20 ml, and the retentate was collected once the reservoir volume was down to 60 ml.
Approximately 200 ml 0.1M NaOH was then circulated for 30 minutes and then the retentate was flushed. A further 100 ml was circulated for 5 minutes and the filtrate was flushed by applying a back pressure. Then filter was then water washed as above before the next sample was filtered

2.13 Digestion of cellulose nitrate filters

Each filter paper was placed in a beaker with 5 ml concentrated nitric acid (Aristar) and approximately 1 ml hydrogen peroxide. This mixture was refluxed for 2 hours in order to completely dissolve the filter paper before being boiled down to 1 ml and then made up to 5 ml with 2 % nitric acid and stored at 4 °C in a sterilin tube prior to analysis by ICP-OES.

2.14 UV-Visible spectroscopy

The UV-Visible absorption of the prepared sample was then measured at wavelengths of 254, 465 and 665 nm using a Unicam UV2-100 UV-visible spectrometer and using deionised water in the reference cell. Dilutions of pore water were made with deionised water where required and the dilution factors are listed in tables 2.16-2.18.

2.15 Flame atomic absorption spectrometry

Single element metal concentrations were determined by flame atomic absorption spectrometry (Solaar Unicam 929). Three measurements were taken each over 1 second

Depth /cm	LBA1 Dilution factors	LBA2 Dilution factors	LBA3 Dilution factors
0.5	4	4	4
1.5	4	8	5
2.5	1	1	1
3.5	4	1	1
4.5	1	1	1
6.5	1	1	1
7.5	1	1	1
8.5	1	1	1
9.5	1	1	1
10.5	1	1	1
11.5	1	1	1
12.5	1	1	1
13.5	1	1	1
14.5	1	N/A	1
15.5	N/A	N/A	4

Table 2.16 The dilution factors for porewater samples from each depth in the sediment cores from Loch Bradan site A (LBA1-3) for UV spectroscopy.

Depth /cm	LBB1 Dilution factors	LBB2 Dilution factors
0.5	3	5
1.5	12	4
2.5	3	1
3.5	3	1
4.5	3	1
5.5	3	1
6.5	3	1
7.5	3	1
8.5	3	1
9.5	3	1
10.5	3	1
11.5	3	4
12.5	3	4
13.5	7	1
14.5	3	3
15.5	3	2
16.5	3	2
17.5	3	2
18.5	3	4
19.5	9	17
20.5	11	4
21.5	10	4
22.5	14	1
23.5	9	3
24.5	10	N/A
25.5	3	N/A
26.5	3	N/A

Table 2.17 The dilution factors for porewater samples from each depth in the sediment cores from Loch Bradan site B (LBB1-2) for UV spectroscopy.

Depth /cm	LT3 Dilution factors
0.5	6
1.5	7
2.5	6
3.5	12
4.5	6
5.5	6
6.5	8
7.5	6
8.5	12
9.5	12
10.5	11
11.5	10
12.5	9
13.5	9
14.5	11
15.5	9
16.5	9
17.5	10
18.5	12
19.5	9
20.5	10
21.5	8
22.5	8
23.5	6
24.5	1

Table 2.18 The dilution factors for porewater samples from each depth in the sediment core from Loch Tay core 3 (LT3) for UV spectroscopy.

intervals in an air-acetylene flame. Details for each element are shown in table 2.19 and the sensitivity of the instrument for each element is shown in table 2.20. Calibration curves were constructed after analysis of standards prepared from 1000 ppm metal solutions (spectroscopic standards in 2% HNO_3 Aristar).

2.16 Inductively coupled plasma optical emissions spectrometry

Multi-element concentrations were determined by inductively coupled plasma optical emission spectrometry (ICPOES). Three measurements were obtained after a 40 second flushing period. Exposure for low wavelengths was 20 second and for high wavelengths 5 seconds. Multi element standards were made from 1000 μgml^{-1} metal solutions (spectroscopic standards in 2% HNO_3 Aristar grade). High concentration elements were added as 2.5 ml aliquots of 1000 ppm solutions and low concentration elements were added as 2.5 ml aliquots of 100 ppm solutions. The mixture was then made up to 50 ml with 2% HNO_3 (Aristar) and was labelled as the top standard. This was diluted 1:10 with 2% HNO_3 (Aristar) to make the middle standard and this process was repeated again for the lowest standard. The operating conditions and instrument specifications are displayed in tables 2.21-22 and the wavelengths used for each element are detailed in table 2.23.

2.17 Analysis of reference materials: quality control

The digestion and analysis methods detailed in sections 2.8, 2.15 and 2.16 were applied to the certified reference material CR7004. The results of the analysis are shown in table 2.24, as the average concentration ± the standard deviation, alongside the reported concentrations for four methods of digestion of the reference material: total digestion by HF, Aqua regia digestion, hot 2 M HNO_3 digestion and cold 2 M HNO_3 digestion.
The reference material was not certified for Fe but the values obtained for each digestion were close at 3.4 %(w/w) ± 0.3. The Mn concentration determined in the pseudo-total digestion was comparable with the reported values for the hot 2 M HNO_3 digestion and

Samples	Element	Wavelength /nm	Flame Angle /°	STAT tube	D_2 Arc background	Bandpass /cm	Burner /cm
LLpw	Fe	248.3	0	N	Y	0.5	5
	Mn	279.5	0	Y	Y	0.5	5
	Pb	217.0	0	Y	Y	0.5	5
	Cu	324.8	0	Y	Y	0.5	5
	Zn	213.9	0	N	Y	0.5	5
LLtsd	Fe	248.3	60	N	Y	0.5	10
	Mn	279.5	25	N	Y	0.5	10
	Pb	217.0	0	Y	Y	0.5	5
	Cu	324.8	0	Y	Y	0.5	5
	Zn	213.9	25	N	Y	0.5	10
LLrrd	Fe	248.3	30	N	Y	0.5	10
	Mn	279.5	25	N	Y	0.5	10
	Pb	217.0	0	Y	Y	0.5	5
	Cu	324.8	0	Y	Y	0.5	5
	Zn	213.9	10	N	Y	0.5	10
LBpw	Fe	248.3	0	N	Y	0.5	5
	Mn	279.5	20	N	Y	0.5	5
	Pb	217.0	0	Y	Y	0.5	5
	Cu	324.8	0	Y	Y	0.5	5
	Zn	213.9	0	N	Y	0.5	5
LBtsd	Fe	248.3	20	N	Y	0.2	10
	Mn	279.5	30	N	Y	0.2	10
	Pb	217.0	0	Y	Y	0.5	5
	Cu	324.8	0	Y	Y	0.5	5
	Zn	213.9	10	N	Y	0.5	5
LBrrd	Fe	248.3	0	N	Y	0.5	10
	Mn	279.5	30	N	Y	0.2	10
	Pb	217.0	0	Y	Y	0.5	5
	Cu	324.8	0	Y	Y	0.5	5
	Zn	213.9	10	N	Y	0.5	5
LTpw	Fe	252.3	25	N	Y	0.5	10
	Mn	279.5	15	N	Y	0.5	10
	Pb	217.0	0	Y	Y	0.5	5
	Cu	324.8	0	Y	Y	0.5	5
	Zn	213.9	0	N	Y	0.5	5
LTtsd	Fe	248.3	0	N	Y	0.5	5
	Mn	279.5	0	Y	Y	0.5	5
	Pb	217.0	0	Y	Y	0.5	5
	Cu	324.8	0	Y	Y	0.5	5
	Zn	213.9	0	N	Y	0.5	5
LTsw	Fe	248.3	0	N	Y	0.5	5
	Mn	279.5	0	Y	Y	0.5	5
	Pb	217.0	0	Y	Y	0.5	5
	Cu	324.8	0	Y	Y	0.5	5
	Zn	213.9	0	N	Y	0.5	5

Table 2.19 Running conditions of AAS

Element	Limiting sensitivity mg/l	Use of slotted atom trap
Mn	0.027	N
Fe	0.06	N
Pb	0.033	Y
Cu	0.013	Y
Zn	0.003	Y

Table 2.20 Limiting sensitivity for each element when analysed by AAS

Pump rate	100rpm
Nebuliser type	Cross flow
Nebuliser pressure	32 PSI
RF power	1150 W
Argon flow	0.5 l/min
Uptake	1.85 ml/min

Table 2.21 Details of ICP-OES instrumental parameters

Autosampler	On
Number of repeats	3
Delay time	5 s
Uptake time at low WL	5 s
Uptake time at high WL	30 s
Acquisition time	30 s
Wash out	15 s

Table 2.22 Details of ICP-OES methodology parameters

Element	Al	Ca	Co	Cu	Fe	K	Mg	Mn	Na	P	Pb
Wave length /angstrom	3961	3179	2286	2247	2599	7698	2795	2576	5889	2136	2169

Element	S	Si	Zn
Wave length /angstrom	1820	2516	2138

Table 2.23 Wavelengths for the determination of elemental concentration by ICP-OES

Digestion method	Fe%(w/w) ± std dev.	Mn %(w/w) ± std dev.	Pb mg/kg ± std dev.	Cu mg/kg ± std dev.	Zn mg/kg ± std dev.
Pseudo-total	3.4 ± 0.3	0.066 ± 0.005	72.1 ± 4.9	163.6 ± 12.7	203 ± 41
Total HF	N/A	0.087 ± 0.00036	93.4 ± 3.4	183 ± 5	227 ± 7
Aqua regia	N/A	0.074 ± 0.00036	83.1 ± 2.3	167 ± 1	198 ± 6
Hot 2 M HNO_3	N/A	0.057 ± 0.00035	82.6 ± 1.9	159 ± 5	169 ± 8
Cold 2 M HNO_3	N/A	0.053 ± 0.00024	71.7 ± 2.5	137 ± 4	119 ± 5

Table 2.24 Comparison of pseudo-total concentrations, determined experimentally during this study, for five replicate samples of certified reference material CR7004 with the reported concentrations from four digestion methods listed on the certificate (Total HF, aqua regia, hot 2 M HNO_3 and cold 2 M HNO_3)

the aqua regia digestion. The concentration for Pb was comparable to that of the cold 2 M HNO_3 digestion. The concentrations obtained for Cu were more variable but still equal or greater than the quoted value for the hot 2 M HNO_3 digestion. The Zn concentration was more variable again but still in the range between the hot 2 M HNO_3 digestion and the aqua regia digestion.

Chapter 3: Results – Loch Leven

3.1 Introduction

The following chapter contains the results of analyses of 3 cores collected at the Reed Bower site on 16/03/00. Section 3.2 describes the characterisation of the sediment sections obtained in each of these cores. Sections 3.3-4 continue the sediment analysis with pseudo-total and readily reducible elemental concentrations, respectively. Section 3.5 consists of the analysis of the pore water elemental concentrations.

3.2 Characterisation of sediment from Loch Leven, Central Scotland

Figure 3.1 displays the depth profiles of percentage moisture, organic matter, ash and wet/dry ratio for all three sediment cores taken from Loch Leven.

3.2.1 Percentage water

The profile for LL1 shows that the sediments have a moisture content of ~ 80 % with a slight decrease with depth notable after 2.9 cm depth.
The LL2 core shows a similar picture with values in the region of 80 % and a slight decrease with depth after 2.9 cm.
The 1 cm sectioned core, LL3, displays lower values of moisture content at ~75 % with a slight maxima at 6.5 cm and then a gradual slight decrease with depth.

3.2.2 Wet/dry ratio

The wet:dry ratio profiles display more clearly the decrease in moisture with depth in the sediment as well as the sharp change between the upper 3 cm of sediment and the remaining core. The cores LL1 and LL2, found in figure 3.1, also display another sharp decreases at the base of the core at 16-17 cm depth. LL3, also found in figure 3.1, shows

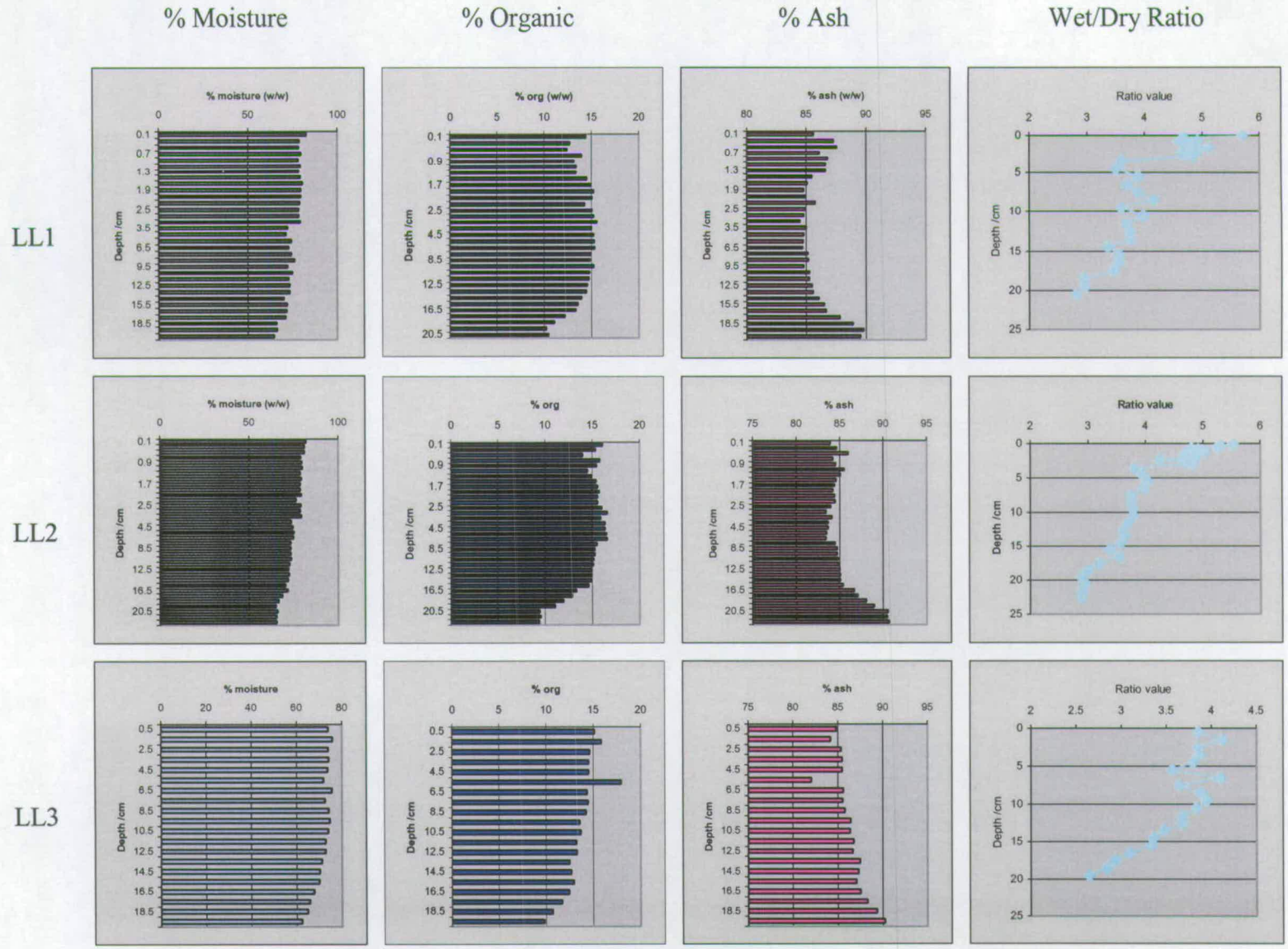

Figure 3.1 Profiles of variation with depth of moisture as % total sample, organic and ash content as % total sediment and wet/dry ratio for Loch Leven sediment cores LL1-3

a slightly different picture as the upper sediment was not fine sectioned. The decrease with depth appears to begin higher in the sediment than previously found, starting at 10 cm depth, and therefore appears to be more gradual.

3.2.3 Organic matter – loss on ignition

The profile of percentage organic matter (% org) for LL1, displayed in figure 3.1, shows a near surface peak of 15 % followed by a decrease to 12 %. The concentration then increases gradually with depth back to maximum of ~16 % at 2.9 cm. From this point the organic concentration then decreases steadily with depth to a minimum of 10 % at 19.5 cm depth.

A near surface maximum of ~ 15 % can also be observed in the LL2 organic matter profile, shown in figure 3.1. Again this is followed by a slight dip at 0.5 cm depth and a maxima of 15 % at 0.7 cm depth. Once again the organic concentration increases steadily with depth but then drop sharply back to 15 % at 6.5 cm depth. The concentration then remains constant until 14.5 cm depth where it decreases rapidly to a minimum value of 9 % 20.5 cm depth.

The 1 cm sectioned core, LL3 also displayed in figure 3.1, does not display the subsurface peak found in the fine sectioned cores. Rather the maxima occur at 1.5 cm as the organic concentration peaks at 16 %. This is followed by a general decrease with depth apart from the peak to ~ 18 % at 5.5 cm depth.

3.2.4 Ash content – mass remaining on ignition

All of the profiles, displayed in figure 3.1, show the inverse of the organic content profiles. The increase in percentage ash content with depth can be clearly observed in all three cores though it more distinct in the longer cores, LL1 and LL2.

3.3 Pseudo-total concentrations of elements in sediment from Loch Leven, Central Scotland

The variations in concentration of trace metals (Fe, Mn, Pb, Cu and Zn) with depth in each of the sediment cores are show in figures 3.2 and 3.3

3.3.1 Redox-active elements, Mn and Fe

Figure 3.2 shows the depth profiles of Fe and Mn for the pseudo-total sediment digestion of LL3. The concentration of Fe remains fairly constant with depth at ~4 % with small maxima at 2.5 cm and 13.5-14.5 cm depth and a slight minima at 9.5 cm depth.
The Mn concentration drops with depth in the sediment from a surface maximum of 0.22 % to 0.09 % at depth. A second subsurface maximum can be observed at 2.5 cm depth as can two small minima at 7.5 cm and 11.5 cm.
Similar profiles with more detail are observed for LL2 as the top 3 cm was sectioned at finer intervals of 0.2 cm. The profile of pseudo-total Fe concentration within the LL2 sediment core has no distinct trends with a concentration ~ 4.5 %.
The pseudo-total Mn concentration profile shows a steady decrease in concentration with depth from a surface peak of 0.27 % to 0.06% at 22.5 cm. Two small minima can be noted of ~0.12 % at 2.1 cm and 6.5 cm with accompanying maxima at 2.5 cm and 7.5 cm depth respectively.
LL1 was also fine sectioned at 0.2 cm intervals over the first 3 cm from the water interface. The Fe concentration generally remains at 4 % with no distinct trends with depth. The pseudo-total Mn profile generally decreases with depth from the maximum concentration of 0.28 % at 0.1 cm depth to a minimum of 0.06 % at 21.5 cm depth. A small maximum can be noted at 3.5 cm depth and a minimum at 15.5 cm depth.
The profiles of Mn/Fe ratio for the pseudo-total concentrations of sediment from Loch Leven cores LL1-3 are shown in figure 3.2. It can be observed that overall the ratio value reflects the variation in Mn concentration as the Fe concentration profiles were fairly uniform. All three profiles had sharp elevations in the ratio value over the upper

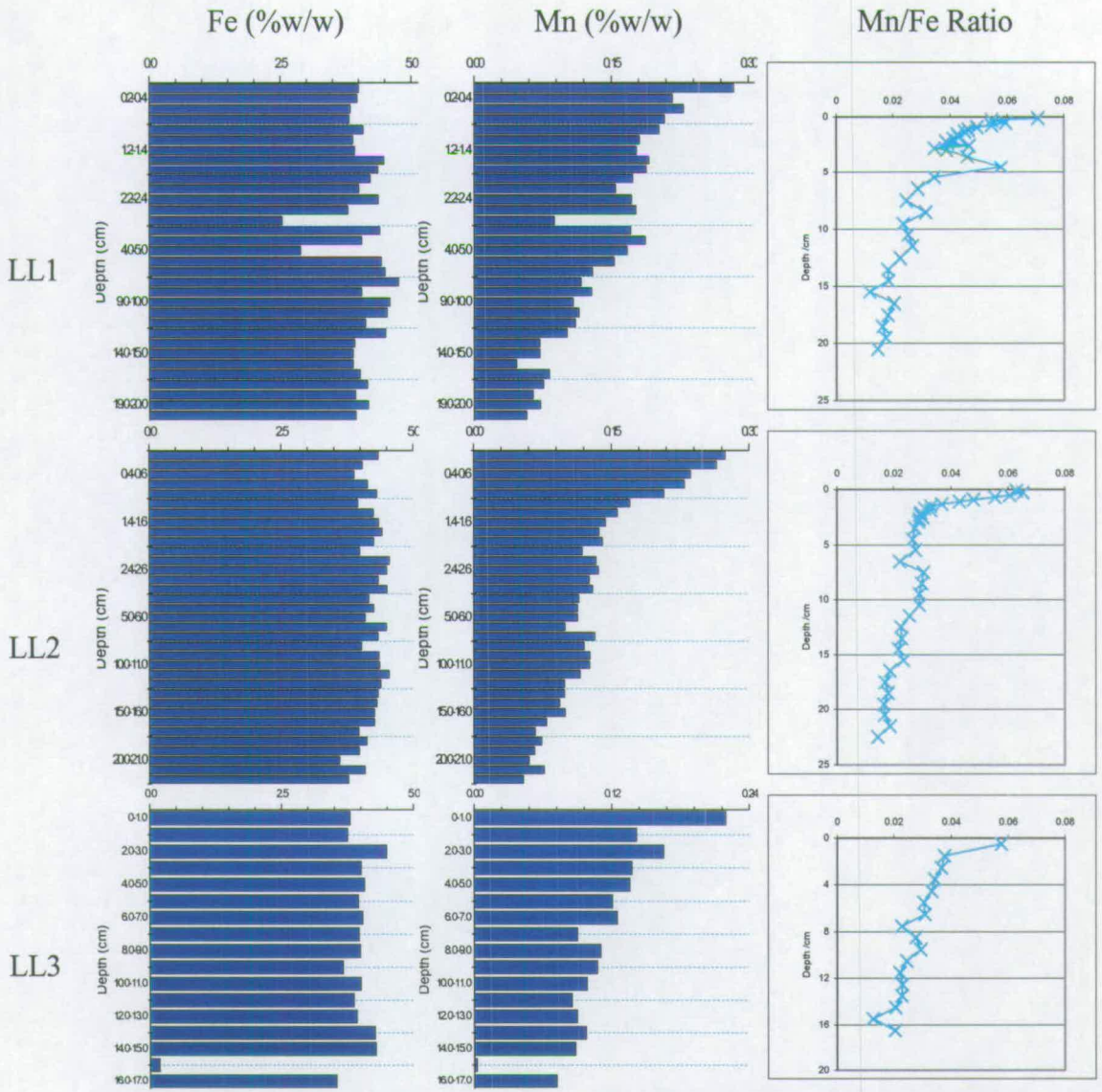

Figure 3.2 Profiles of variation with depth of Fe and Mn sediment conentrations in Loch Leven cores, LL1-3, expressed as % total sediment for Fe and Mn and variation with depth of the Mn/Fe ratio in sediments from Loch Leven cores LL1-3

sediment with maximum values approaching 0.06 at the surface. The fine-sectioned material of cores LL1 and LL2 show that this elevation in Mn/Fe value was indeed confined to the very surface sediments, increasing steadily from 0.8 cm to the surface. All three Mn/Fe profiles also display elevated values over 8-11 cm depth, again corresponding to elevated concentrations of pseudo-total Mn in the sediment.

3.3.2 Trace heavy elements, Cu and Zn

Figure 3.3 shows the trends in the pseudo total concentration of the trace elements for Loch Leven sediment cores 1-3.

The Cu concentration profile for LL3 is fairly constant with depth, ranging from 35 mg/kg to 50 mg/kg, but a single peak in concentration can be seen at 16-17 cm depth. Zinc, like Cu, is spread consistently throughout the sediment core. The maximum concentration found was 225 mg kg at 2-3 cm depth and the minimum value was again at 15-16 cm (175 mg kg).

The Cu concentration of sediment core LL2 ranged from 40 mg/kg to 56 mg/kg and remained fairly constant with depth.

The depth profile of Zn remains constant with depth peaking slightly to 225 mg/kg at 16-17 cm then decreasing to 150 mg/kg over the bottom 3 cm.

Sediment core LL1 has a fairly constant Cu profile. The maximum concentration of 53 mg/kg is found at 15-16 cm. The Zn profile generally increases with depth down to 14-15 cm where it peaks to 225 mg/kg and then decreases over the final 6 cm.

3.4 The concentration of elements in the readily reducible fraction of sediments from Loch Leven, Central Scotland

The following section contains the results of the readily reducible digestions of sediments from cores LL1-LL3 and the subsequent analysis to determine trace element concentrations.

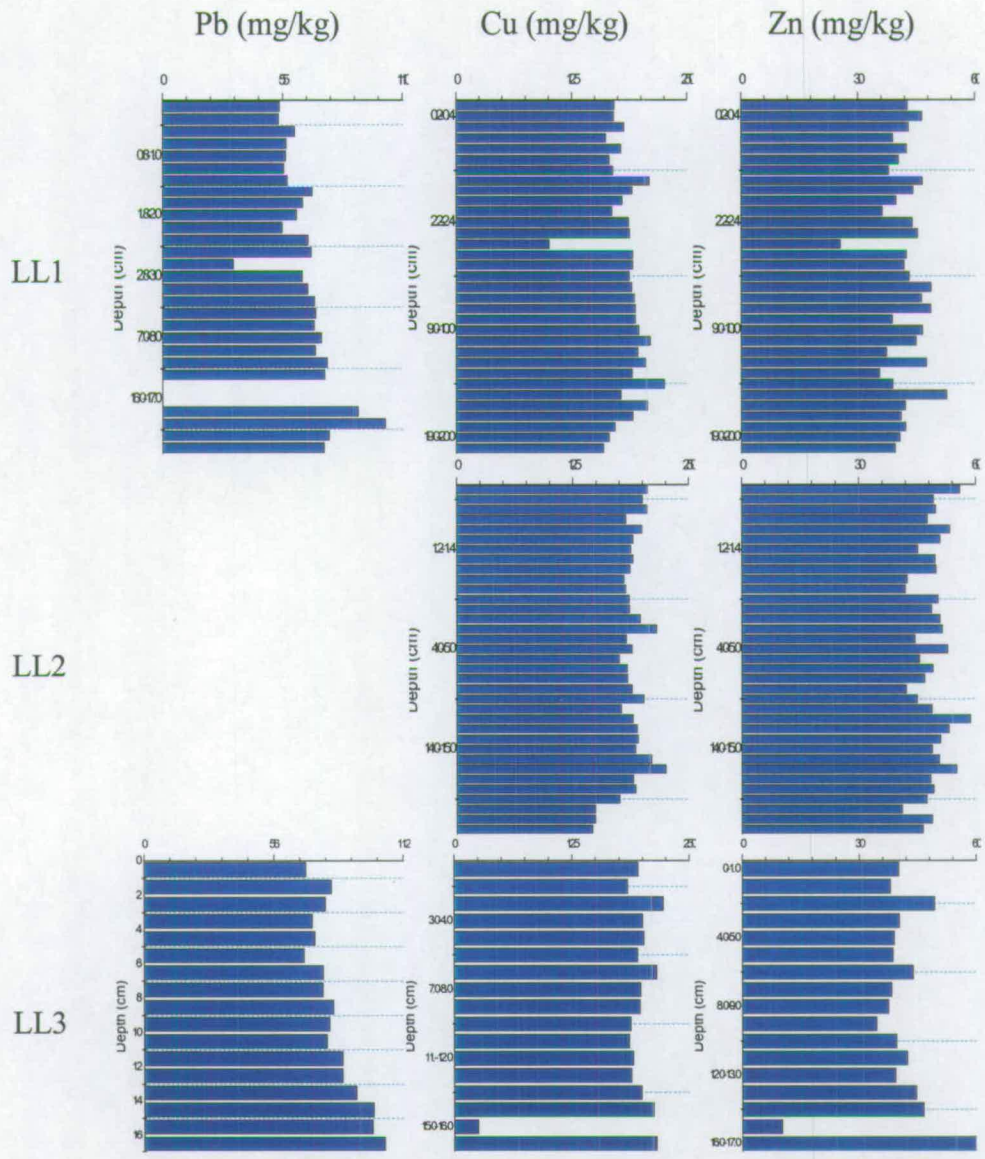

Figure 3.3 Profiles of variation with depth in the sediment of the pseudo-total concentrations of Pb, Cu and Zn in Loch Leven cores, LL1-3, expressed as mg/kg

3.4.1 Redox active elements, Fe and Mn

Figure 3.4 shows that generally the readily reducible Fe concentration increases with depth from 0.52 % at 0.5 cm depth in sediment core LL3. The maximum of 1.81 % occurs at 14.5 cm depth. The concentration of readily reducible Mn decreases from the surface peak of 2.33 % to 0.90 % at 16.5 cm.

Fine sectioning of the upper sediment of core LL2, shown in figure 3.4, revealed a decrease of readily reducible Fe with depth from a surface maximum of 4.62 %. The minimum value of 0.63 % was found at 9.5 cm depth. The readily reducible Mn concentration peaks, below the readily reducible Fe maximum, at 0.9 cm and ranges from 3.36 % to 0.81 % in the lowest sediment section.

The sediment core LL1 has a variable Fe profile for the readily reducible fraction with no distinct trend with depth. The concentration ranges from 1.33 % to 3.36 %. The readily reducible Mn concentration on the other hand has a distinct subsurface peak of 4.02 % and decreases steadily with depth. The minimum concentration of 0.63 % occurs at 15.5 cm depth.

The readily reducible concentration of Mn extracted from the Loch Leven sediment represented 80-100 % of the pseudo-total Mn concentration, as shown in figure 3.5. The elevation of some section readily reducible fractions to greater than 100 % can be attributed to the heterogeneity of the sample. The percentage of pseudo-total Mn for core LL3 remained fairly uniform with depth at approximately 100 %. The fine sectioned material of core LL1 showed a slight decrease in the fraction of the total Mn represented by the readily reducible phase with depth but the values still remain near 100 % for the entire core. Sharp elevations were noted at 2.6-2.8 cm depth coinciding with the increased concentration of the pseudo-total Mn giving a constant value of readily reducible element as a percentage of the total elevated concentration. This was observed again at 19-20 cm depth.

A similar correlation between pseudo-total Mn and readily reducible Mn was found in the upper sediments of core LL2 with the percentage of the pseudo-total Mn represented by the readily reducible Mn peaking at 0.8-1.0 cm depth, coinciding with the elevation

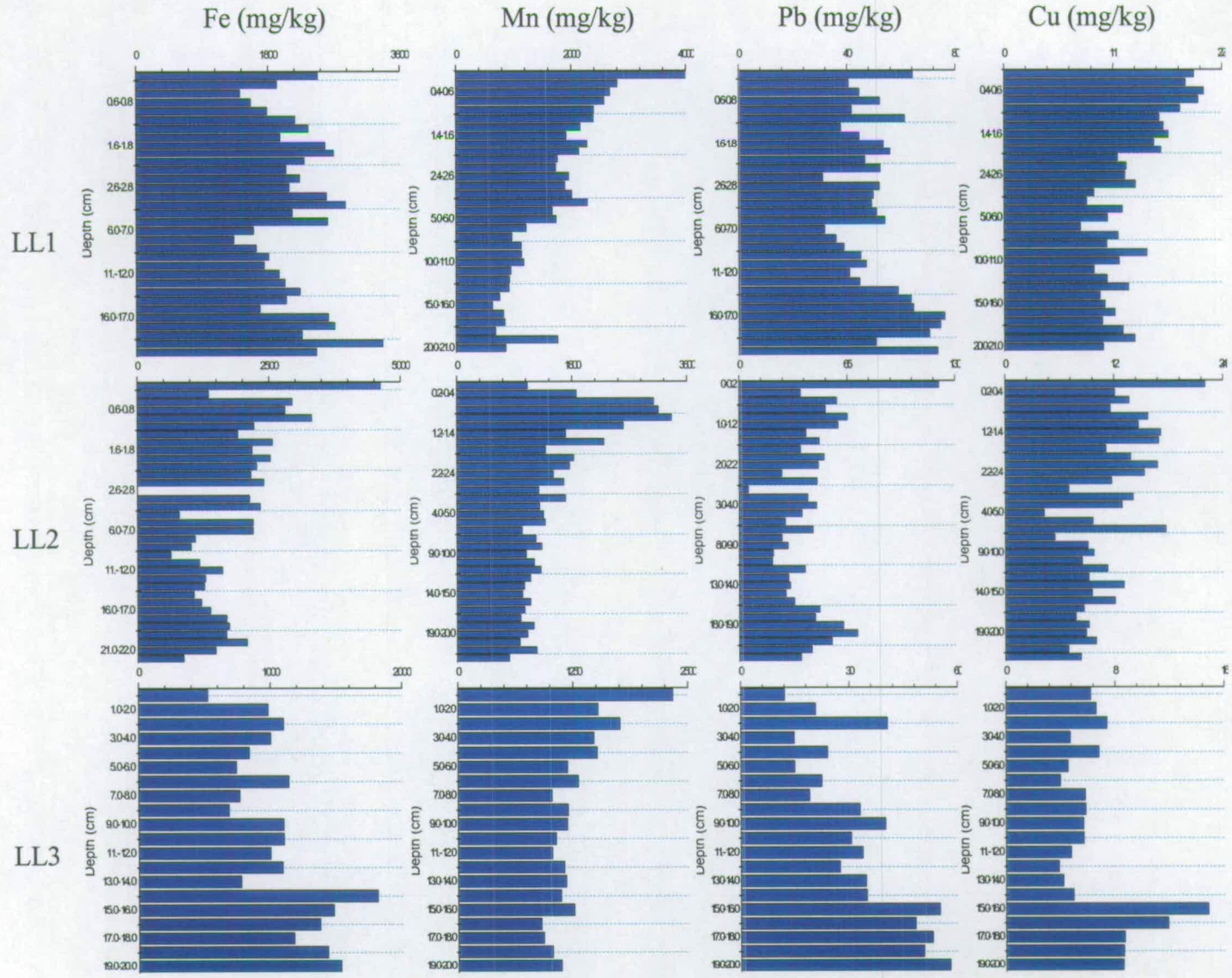

Figure 3.4 Profiles of variation with depth of readily reducible concentrations of Fe, Mn, Pb and Cu in Loch Leven sediments, LL1-3, expressed as mg/kg

in pseudo-total Mn concentration. With depth in the core this relationship broke down as the fraction represented by the readily reducible Mn increased over 16-20 cm depth but no elevation in pseudo-total Mn was found at this point.

3.4.2 Trace heavy elements, Cu and Zn

The profile for readily reducible Cu in sediment core LL3 shown in figure 3.4 shows some similarity to the corresponding Fe profile. The readily reducible Cu concentration remains fairly constant with depth down to 14.5 cm and subsequently peaks at 14.84 mg/kg. The minimum concentration of 3.90 mg/kg was found at 12.5 cm depth. The Pb readily reducible concentration generally increases with depth from 12.15 mg/kg at the interface to 58.0 mg/kg at 20 cm depth with a peak at 3.5 cm. The Zn concentrations were below the limit of detection of the instrument.

The fine sections of sediment core LL2 shown in figure 3.4 display more detail in the upper sediment. The maximum Cu concentration of 22.0 mg/kg was found at the interface, the concentration then decreased with depth and the minimum of 4.3 mg/kg was observed at 4.5 cm depth. The Pb profile also shows a subsurface peak of 120.5 mg/kg at 0.1 cm depth. The concentration then generally decreases with depth until the occurrence of a small peak at 19-20 cm. The minimum concentration of 5.5 mg/kg was found at 2.7 cm.

In the sediment core LL1, shown in figure 3.4, the concentration of readily reducible Cu was found to decrease with depth and had a range of 7.73 mg/kg to 20.2 mg/kg. The readily reducible Pb was very variable with depth but showed no particular trend. The concentration ranged from 31.0 mg/kg to 76.0 mg/kg.

The concentration of Pb in the readily reducible extract of sediments from core LL3, was found to represent 20-60 % of the pseudo-total Pb as shown in figure 3.5. Generally the size of the readily reducible fraction increased with depth from the minimum value at the surface and showed strong correlation with the profile of pseudo-total concentration. A similar picture was found for the fine-sectioned material from core LL1, as shown in figure 3.5. The readily reducible Pb concentrations represented

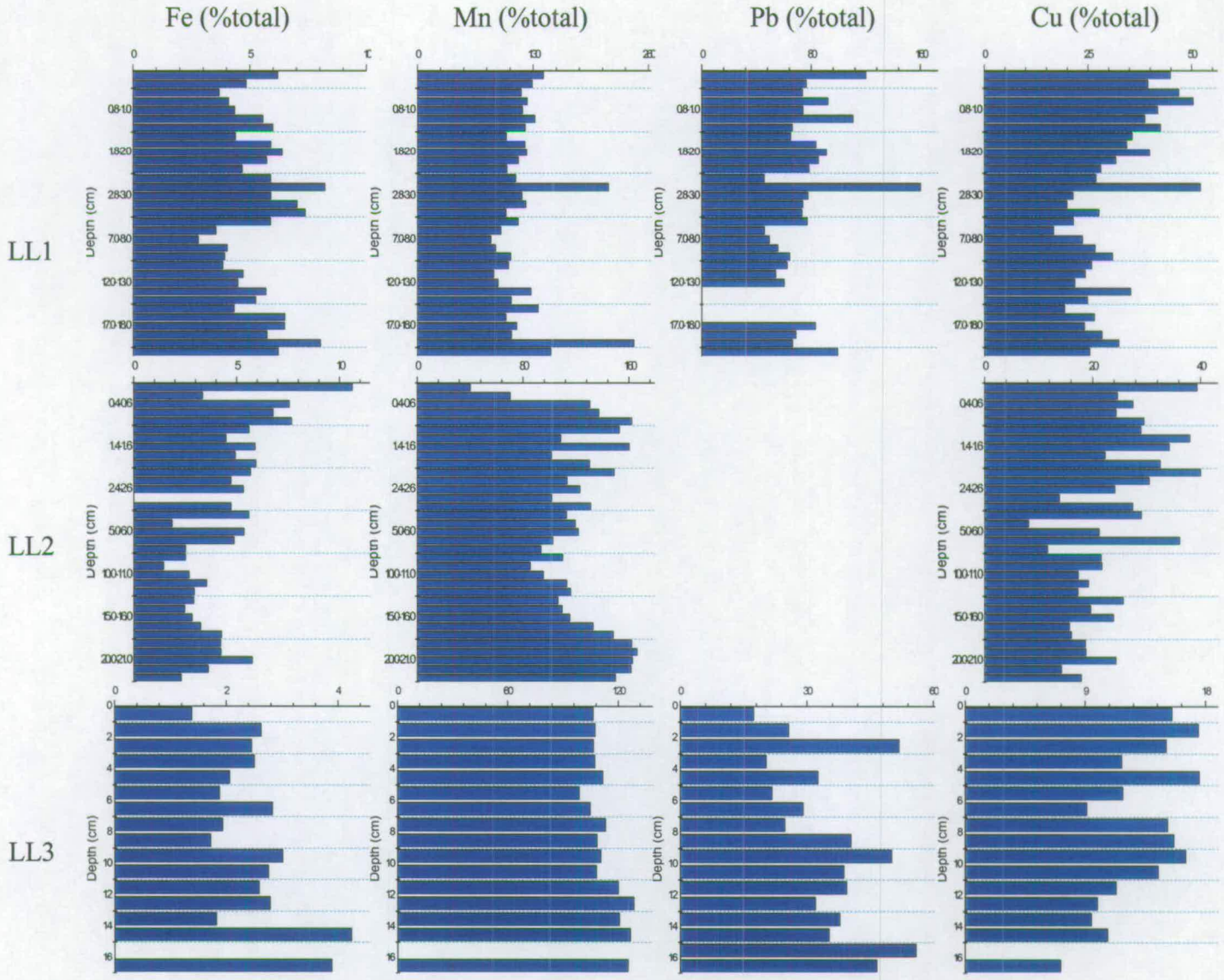

Figure 3.5 Profiles of varition with depth of readily reducible concentrations of Fe, Mn, Pb and Cu in sediments from Loch Leven cores LL1-3, expressed as % total element concentrations

60-100 % of the pseudo-total Pb and the shape of the profile for the readily reducible fraction show strong correlation to the pseudo-total profile.
From the profiles of figure 3.5 it can be noted that the readily reducible Cu concentration found for core LL3 represented 9-18 % of the pseudo-total Cu and the size of the readily reducible fraction decreased with depth. The profiles for LL1 and LL2 had generally similarities, as shown in figure 3.5, with the fraction represented by the readily reducible Cu material decreasing steadily through the fine-sectioned upper sediment. The peaks at 0.6-0.8 cm for LL1 and 1.2-1.4 cm for LL2 correspond to the maximum reducible fractions of 50 % and 40 % respectively and coincide with the elevated concentrations of the pseudo-total profiles.

3.5 Characterisation of pore waters extracted from sediments from Loch Leven, Central Scotland: Organic matter – UV-Visible spectroscopy

The profiles of absorbance at 254 nm and of the E4/E6 ratio for the long cores LL1 and LL2 are shown in figure 3.6. The 254 nm absorbance in general decreased with depth with a sharp peak at 2.6 cm depth and a similar picture can be observed for each core. The profile for LL2 displays an additional broader peak over 7-12 cm depth. A slight elevation in absorbance value can also be noted in core LL1 but is not as distinct as that of LL2.
The profiles of E4/E6 ratio are much more variable in nature although it is possible to distinguish increases in the ratio corresponding to the elevated absorbances at 254 nm for each of the cores.

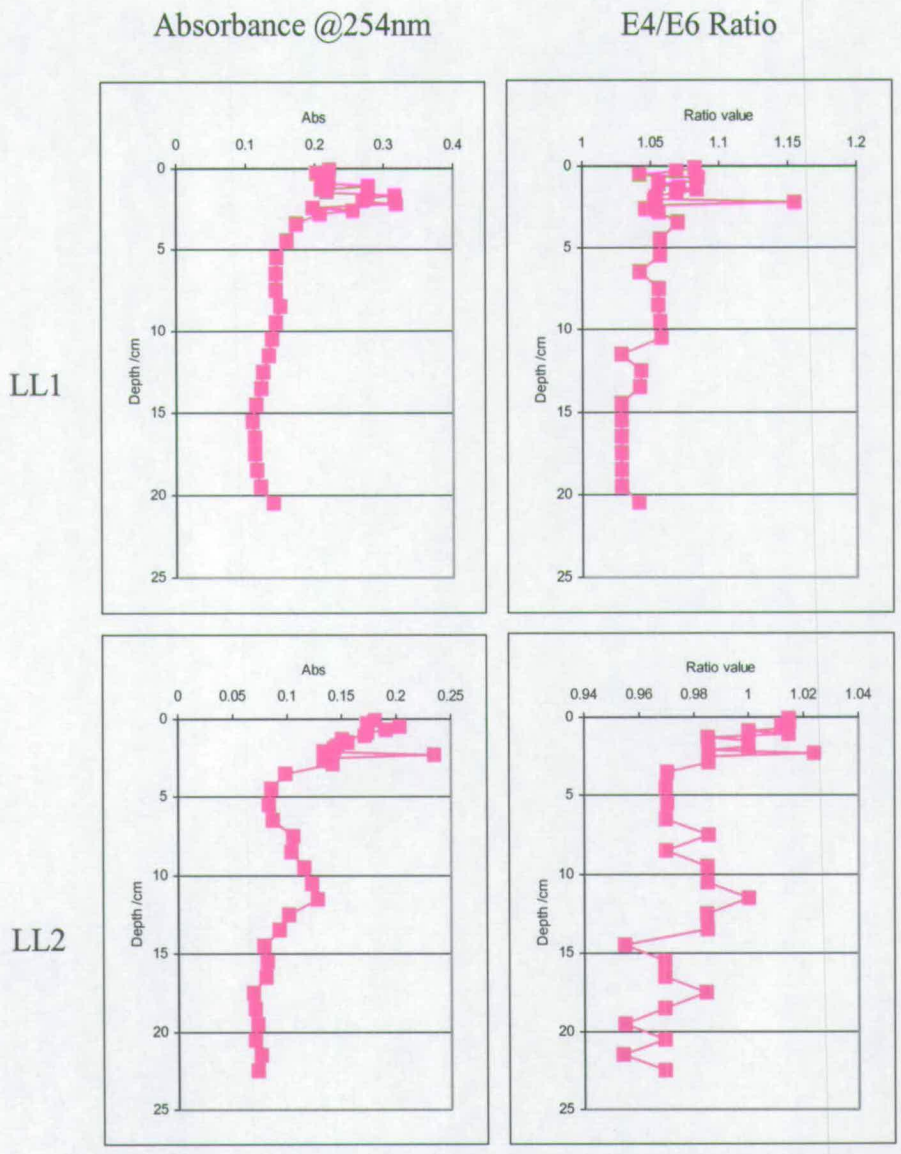

Figure 3.6 Profiles of variation with depth of absorbance values at 254 nm and E4/E6 ratios for porewaters from Loch Leven cores LL1-2

3.6 Total concentrations of elements in pore waters extracted from sediments from Loch Leven, Central Scotland

3.6.1 Redox active elements, Fe and Mn

The pore water concentration of Fe from sediment core LL1 increased steadily with depth, as shown in figure 3.7, from 0.96 mg/l at the interface to 3.22 mg/l at 19.5 cm depth. The concentration of Mn was barely detectable down at 0.02 mg/l to 15.5 cm. It then increased rapidly with depth to 3.71 mg/l at 19.5 cm.

Figure 3.7 also shows the pore water profiles for sediment core LL2, which was sectioned at 0.2 cm intervals over the first 3 cm. The Fe concentration remained very constant throughout the core with a very short range of 3.16 to 3.84 mg/l. The concentration of Mn remained barely detectable with a maximum of 0.008 mg/l down to 17 cm depth. It then increased rapidly to 5.94 mg/l at 21cm depth.

3.6.2 Trace heavy elements, Cu and Zn

The concentration of Cu in the interstitial water was below the detection limit of the instrument. Figure 3.7 shows the concentration of Pb in the pore water of core LL3 increasing from a minimum concentration at the interface of 0.067 mg/l to 0.189 mg/l at a depth of 9.5 cm and then remaining fairly constant with a slight increase in the last 3 cm. The concentration of Zn in the interstitial water was detectable over 5-9 cm and 13-20 cm depth ranging from 0.002 mg/l to 0.17mg/l at depth.

The concentration of Cu remained undetectable for core LL2 pore waters. The concentration of Pb remained constant over the first 3 cm and thereafter increased slowly with depth to 0.296 mg/l at 19.5 cm as shown in figure 3.7. The minimum concentration of 0.162 mg/l is found at 3.5 cm. The fine-sectioned portion of the profile shows more detail in the Zn concentrations near the interface. The concentration

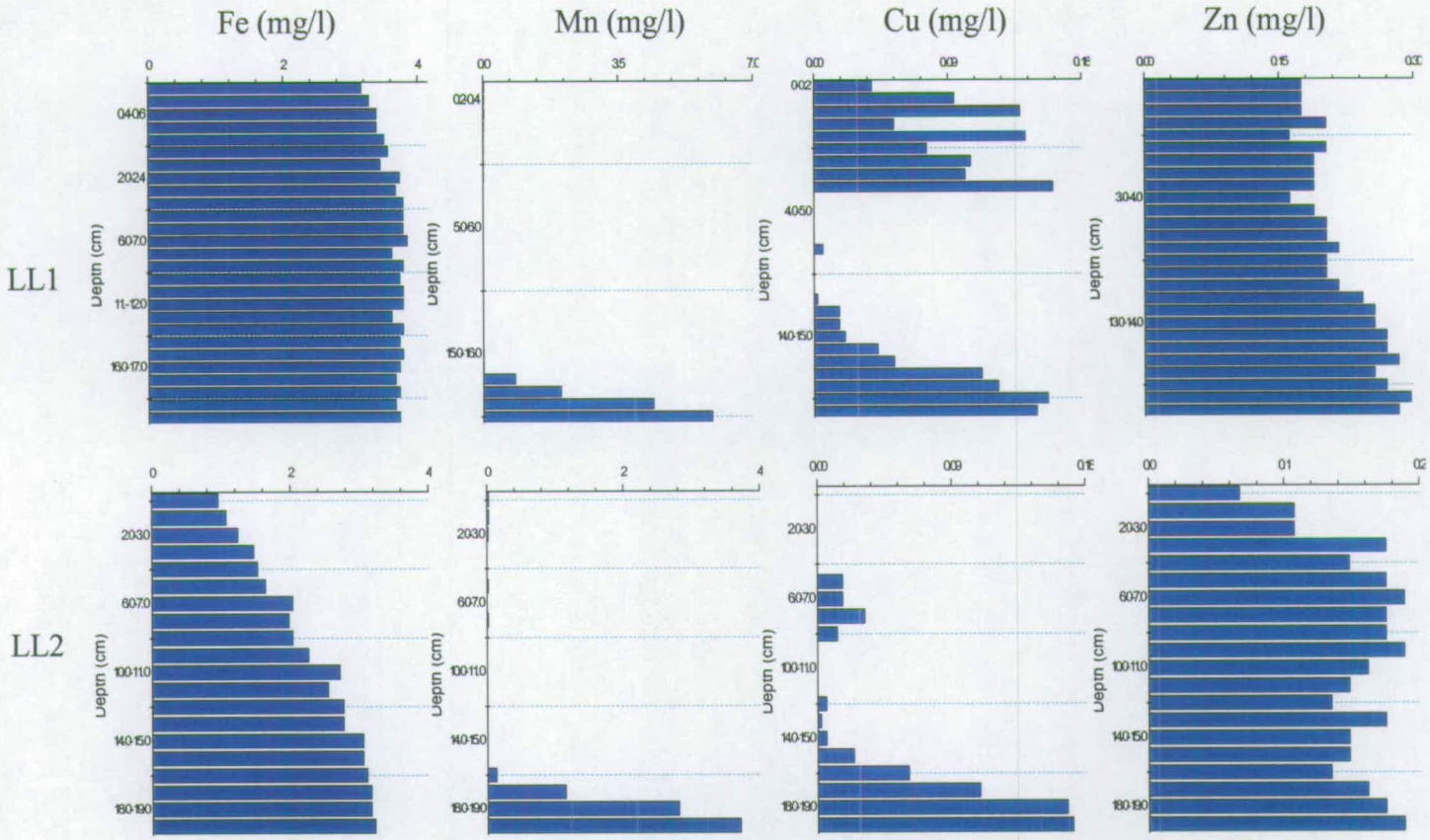

Figure 3.7 Profiles of variation with depth in the sediment of the concentration of Fe, Mn, Cu and Zn in porewaters of Loch Leven cores, LL1-2, expressed as mg/l

increased rapidly from the surface to a maximum of 0.161 mg/l at 2.9 cm. Any Zn present was then barely detectable until 12.5 cm down and from this point it increased rapidly with depth.

Chapter 4: Results – Loch Bradan

4.1 Introduction

This chapter contains the results of the analyses of five cores collected on 10/06/00. Three cores designated LBA1-3 were collected from Site A (Figure 2.6) and two cores designated LBB1-2 were collected from site B (Figure 2.6). Site A was in the middle of the loch centred to the mouth of the main inflow. The water depth at this site was approximately 12 m. Site B was more easterly towards the dam and outflow and the water depth was approximately 15 m.

Section 4.2 describes the characterisation of the sediment sections obtained in each of these cores. This is followed by Sections 4.3-4.4 which contain the pseudo-total and readily reducible elemental concentrations, respectively. Section 4.5 contains the pore water characterisation data whilst Sections 4.6-4.7 contain the elemental concentrations in the total and fractionated pore waters respectively.

4.2 Characterisation of sediments from Loch Bradan, SW Scotland

The water, organic and ash profiles of sediment cores collected from Sites A and B from Loch Bradan are displayed in figure 4.1. Figure 4.2 contains the wet/dry ratio profiles for all four cores.

4.2.1 Percentage water

Site A cores

The percentage water depth profiles for LBA1-3 are displayed in Figure 4.2 The sediment core LBA1 has a water content of ~ 80 % down to 11 cm thereafter the water content decreases rapidly to ~ 40 %. There is a slight minimum in the percentage water profile at 3 cm depth. The percentage water profile for LBA2 follows the same trends as that of LBA1 with a more gradual decrease with depth after 11 cm. A minimum at 3 cm

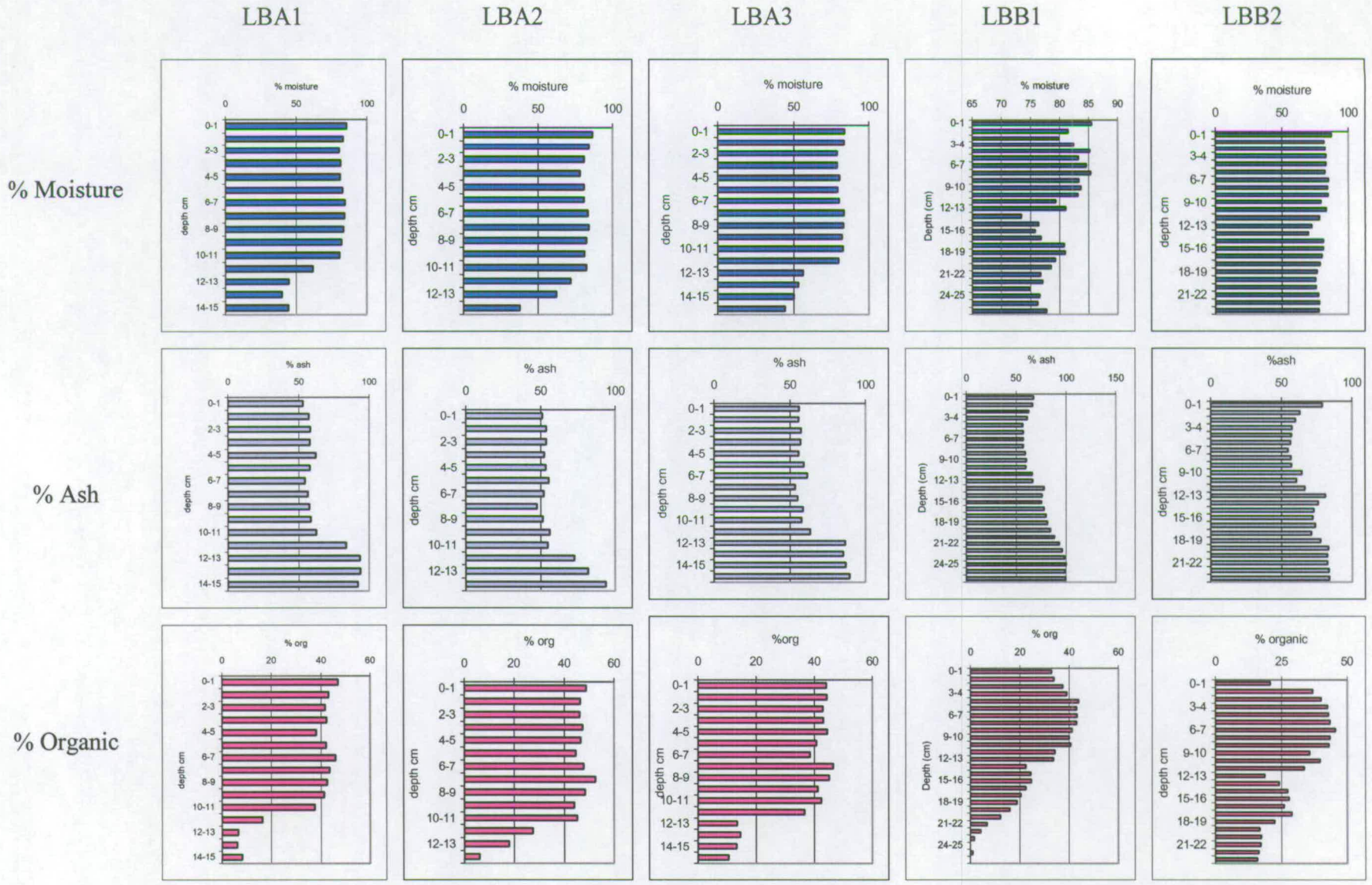

Figure 4.1 Profiles variations with depth in sediment core of moisture (as % total sample), organic and ash content (as %total sediment) of Loch Bradan cores LB site A cores 1-3 and LB site B cores 1-2.

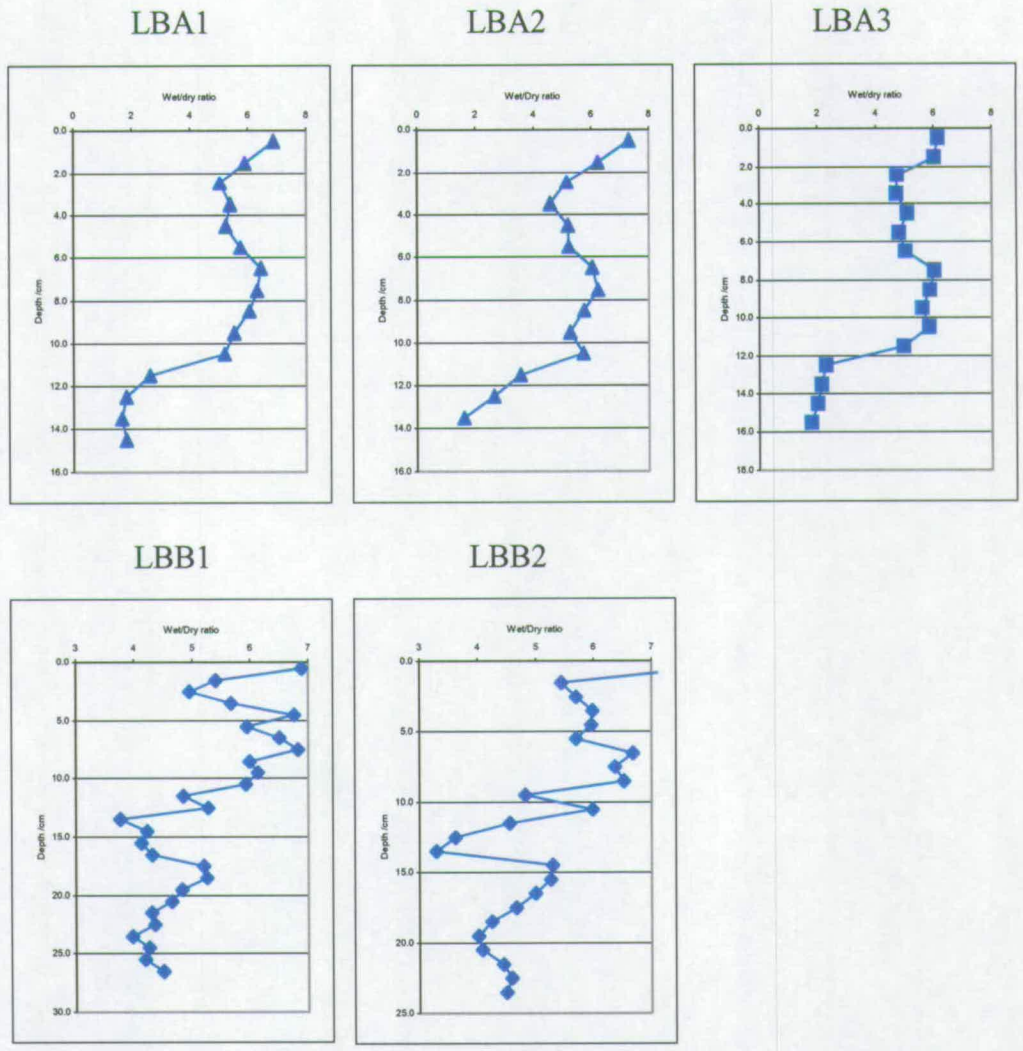

Figure 4.2 Profiles of variation with depth of the wet/dry ratios for sediments of Loch Bradan cores LB site A cores 1-3 and LB site B cores 1-2

depth can again be observed. The sediment core LBA3 has a near surface water content of ~ 80 % down to a depth of 12 cm. The percentage water then decreases rapidly with depth to ~ 40 %. From 3-7 cm depth a broad minimum can be observed in the water content profile.

Site B cores

The water content of the sediment core LBB1 typically displayed values of ~ 80 % with no major decreases with depth. However three minima can be observed at 2-3 cm, 12-16 cm and 23-24 cm depth with corresponding maxima at 0-1 cm, 7-8 cm and 17-19 cm.

The percentage water profile for LBB2 also displays values ~ 80 % with no major decreases towards the bottom of the core. Three minima can again be observed as for LBB1 but the decrease in water content at each point is less than that for the previous core. The minima occur at 2cm, 12-14 cm and 20 cm.

Comparison between the sites

All the cores collected from Loch Bradan have water content values of ~ 80 % in the upper sections of the cores. The pronounced decrease in water content found in the lower sections of the site A cores was absent in the cores from site B. However slight decreases were found in the site B cores at or slightly below the corresponding site A point.

The more discrete features for the different cores collected from the same site occurred at similar depths. Comparison of the cores from different sites shows that the features found occur at similar depths although the magnitude of these features varies.

4.2.2 Wet/dry ratio

Site A cores

The sediment core LBA1, shown in figure 4.2, had maximum in the wet/dry ratio at the surface of 6.1. The broad maximum at 2-5 cm is followed by a broad minimum at

6-9 cm. Below 11 cm the wet/dry ratio decreases sharply to 1.8. The features are similar to those of the water content profile but the changes are more marked.

A similar description of the wet/dry ratio profile is applicable to the LBA2 sediment core with a maximum value at the surface of 7.6. the broad minimum occurs at 3-6 cm and the maximum at 7-10 cm. The decrease noted previously below 11 cm for LBA1 is more gradual for LBA2.

The maximum wet/dry ratio value for the LBA3 sediment core is 6 at 1 cm depth. A broad minimum can be observed at 3-7 cm and a broad maximum over 7-10 cm. Below 12 cm depth the wet/dry ratio drops rapidly to 1.6.

Site B cores

The sediment in core LBB1 at the water interface displays the highest wet/dry ratio with a value of 7 which is followed by a broad minimum at 2-4 cm with a corresponding maximum at 4-11 cm. A second broad minimum follows at 14-17 cm with a slight maximum at 18-20 cm. The ratio then continues to be constant through the remaining sediment sections.

The surface peak in wet/dry ratio for sediment core LBB2 has a slightly higher maximum value that the previous core at 7.8. A sharp decrease follows at 1 cm depth and the value ten increases to a broad maximum at 5-10 cm depth. There is an observable minimum at 12-14 cm and another at 20 cm depth but no overall decrease in the wet/dry ratio towards the bottom of the core.

Comparison between sites

The wet/dry ratio values of the sediments from the two sites are broadly similar with the exception of the lower sediments from each core from site A, which display markedly lower ratios. In all cases the features of the profiles directly correspond with those of the moisture content profiles. There is good agreement between the profiles of the cores collected from the same site as well as between profiles from the different sites.

4.2.3 Organic matter – loss on ignition

Site A cores

The organic matter profile for sediment core LBA1, shown in figure 4.1, shows a surface maximum of 47 %. There is a slight minimum of 38 % at 4.5 cm but with values generally 40-45 % down to 11 cm depth. Below this point the organic matter content of the sediment decreases rapidly to 6-8 %.

A surface maximum can also be observed in the sediment core LBA2 (Figure 4.1) with a value of 49 %. Generally the organic content of the sediment is fairly constant down to 11 cm depth, with a slight maximum of 53 % at 7-8 cm. Below 11 cm depth the organic content decreases dramatically to 6 %.

The sediment core LBA3 (Figure 4.1) has an organic content of 44 % in the surface sediments with little change with depth down to 12 cm. Below 12 cm depth the organic content drops off to 10-15 %.

Site B cores

The organic content of the LBB1 sediments increases from the surface value of 33 % to a broad maximum of 40-43 % at 4-10 cm depth (Figure 4.1). Thereafter the organic concentration in the sediment decreases with increasing depth. A slight dip can be observed at 13-14 cm depth and at the bottom of the core the organic content drops to less than 1 %.

The surface sediments of core LBB2 (Figure 4.1) display lower organic content than those of the previous core at 21 %. The value then increases with depth to a broad maximum of 40-46 % at 4-10 cm. Thereafter the organic content of the sediment decreases with increasing depth with a slight dip at 12-13 cm. The organic content at the bottom of the core is higher than found in the previous core from this site at 15-17 %.

4.2.4 Ash content – mass remaining on ignition

Figure 4.1 contains the profiles of ash content with depth in sediment from both of the Loch Bradan sites. The ash content profiles display the inverse trends of the organic content profiles. Generally the ash content increases with increasing depth in the sediment. The site A sediments have a more distinct transition than the site B sediments from organic rich sediment at the surface to inorganic rich sediment at depth.

4.3 Pseudo-total concentrations of elements in sediments from Loch Bradan, SW Scotland

4.3.1 Site A: redox active elements, Mn and Fe

The pseudo-total Mn concentration in the sediment core LBA1 decreases rapidly with depth from the maximum concentration of 2.25 % at 0-1 cm to a minimum concentration of 0.02% at 14-15 cm depth, as shown in figure 4.3. A broad but slight sub-surface maximum can be observed at 5-10 cm depth. The second core from site A, LBA2, has a very similar profile for Mn concentration with depth. Again the Mn concentration decreases with depth from a slightly lower surface maximum than the previous core of 0.29% (w/w) to min of 0.007% at 13-14 cm depth. The broad peak noted in the previous core is present at 8-9 cm depth and the concentration of Mn decreases more gradually with depth beyond this point. Once again a simliar profile is found for the third core from the sample set, LBA3, with a surface maximum concentration of 3.12% at 0-1 cm and a minimum concentration of 0.19% at 14-15 cm with the broad peak appearing at 7-8 cm depth.

The concentration of pseudo-total Fe in the sediments of core LLA1 (Figure 4.3) decreases with depth from maximum value of 12.0 % (w/w), below the surface Mn peak, at 1-2 cm depth to a minimum concentration of 1.64 % at 14-15 cm. A more pronounced sub-surface peak appears at 6-7 cm depth, compared to the corresponding pseudo-total

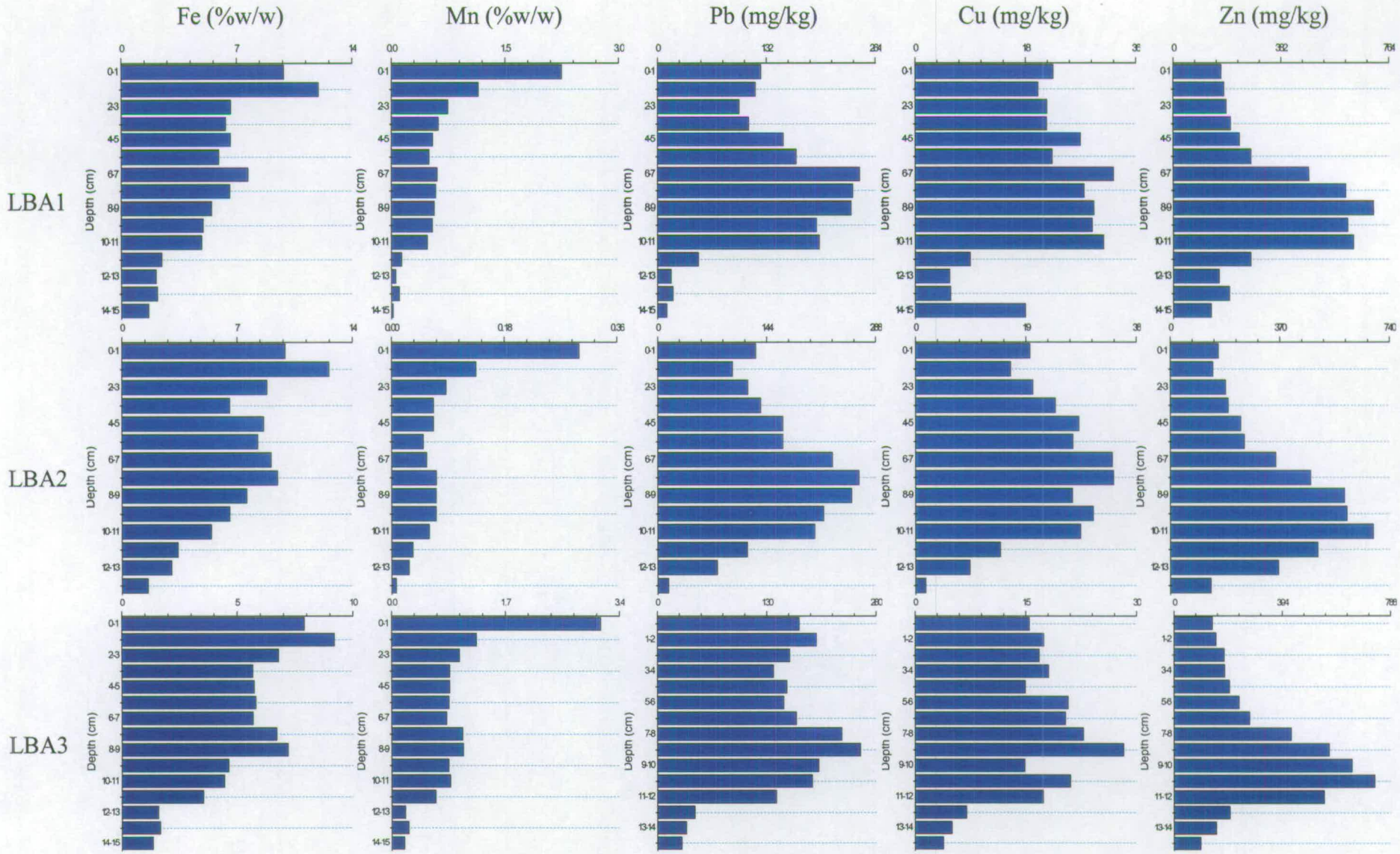

Figure 4.3 Profiles of the variation with depth of the pseudo total metal concentrations of Fe and Mn as % (w/w) and Pb, Cu and Zn in mg/kg for Loch Bradan cores LB site A cores 1-3

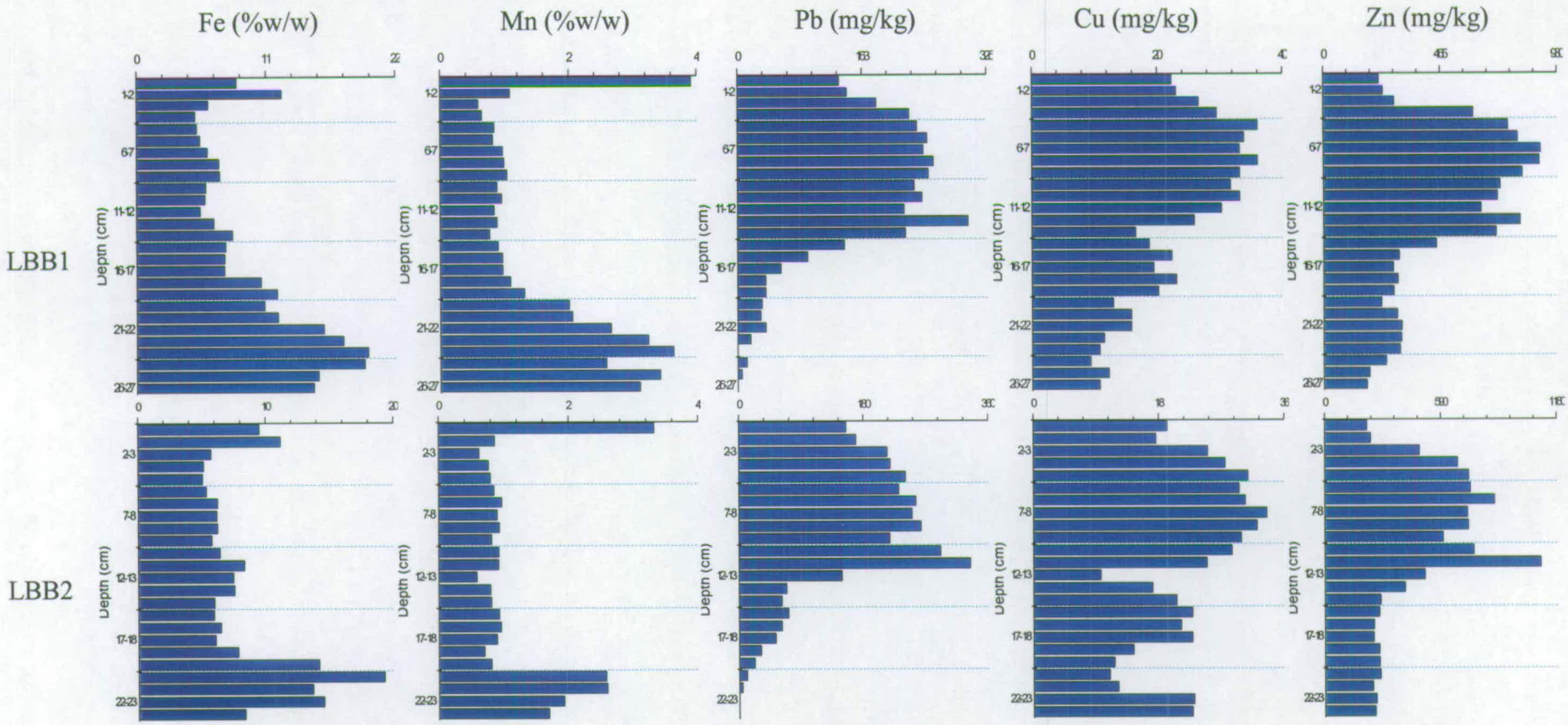

Figure 4.4 Profiles of the variation with depth in the sediment of the pseudo total metal concentrations of Fe and Mn in % (w/w) and Pb, Cu and Zn in mg/kg for Loch Bradan cores LB site B cores 1-2

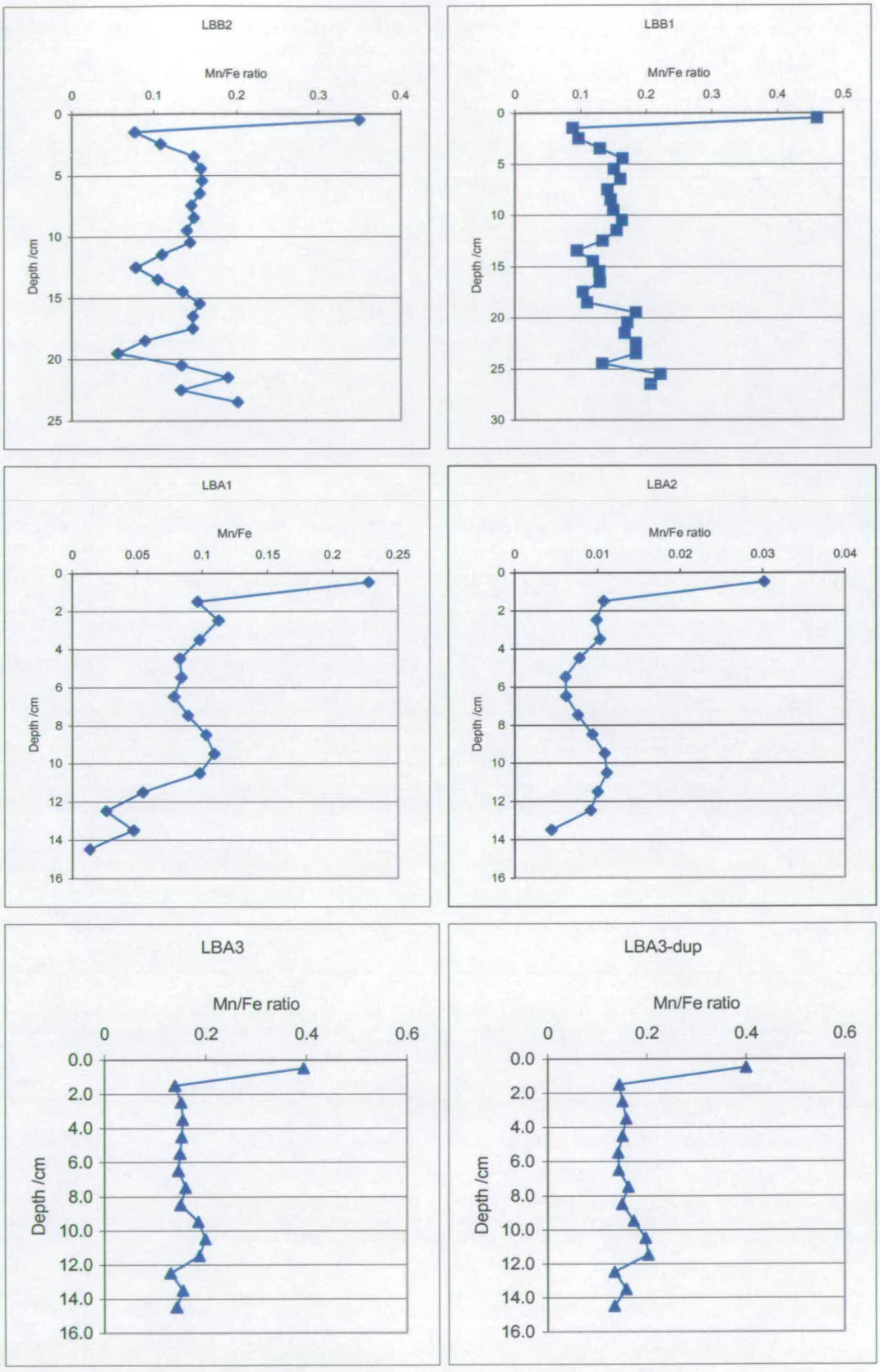

Figure 4.5 Profiles of variation with depth in the sediment of the Mn/Fe ratio for Loch Bradan sediments cores LB site A cores 1-3 and LB site B cores 1-2

Mn profile. The profile for sediment core LBA2 shows the same trends with a maximum concentration of 12.57% (w/w) at depth of 1-2 cm, a broad peak centred at 7-8 cm and a minimum concentration of 1.58% at 13-14 cm. The third core from site A, LBA3, displays similar trends as the previous two cores but the maximum concentration is lower at 9.19% (w/w) and the sub-surface peak in more discrete at 7-9 cm depth.
The profiles of Mn/Fe ratio for the site A sediment cores, shown in figure 4.5, show a sharp change over the first sediment section. A sub-surface maximum occurs at 5-10 cm at the position of the Mn and Fe peaks.

4.3.2 Site B: redox-active elements, Mn and Fe

The pseudo-total concentration of Mn within the sediment core LBB1, shown in figure 4.4, has a maximum value of 3.92 % (w/w) at 0-1 cm depth and then drops rapidly to the minimum concentration of 0.59 % at 2-3 cm depth. A slight sub-surface maximum can be noted at 5-10 cm with the main sub-surface peak at a lower point of 20-27 cm depth. The second core from this site, LBB2, also has a surface maximum concentration of Mn of 3.32% and a minimum value of 0.59% at 2-3 cm. This again is followed by a small, broad sub-surface maximum and a major increase with depth at 19-20 cm.
The profile of pseudo-total Fe for the LBB1 sediment core (Figure 4.4) has a subsurface peak of ~ 12 % at 1-2 cm followed by the minimum concentration of 4.98% at 3-4 cm. A small subsurface maximum can be observed at 5-10 cm depth. Then increases with depth to max of 19.7% (w/w) at 23-24 cm. A similar profile can be observed for the second core at this site, LBB2. The subsurface peak at 1-2 cm depth is again followed by a broad and slight maximum centred at 6-7 cm. The pseudo-total Fe concentration then increases with increasing depth to a maximum of 19.3% (w/w) at 23-24 cm.
The Mn/Fe ratio profiles for the sediment cores from site B both show a sharp decrease over the first two sediment sections, as shown in figure 4.5. Thereafter very little change can be observed.

4.3.3 Comparison between Sites A and B: redox-active elements, Mn and Fe

The longer sediment cores from site B have slightly higher concentrations of pseudo-total Mn over 0-1 cm than those of site A. The rate of decrease in concentration with depth beyond this initial peak is greater for the site B cores. The concentration decreases to lower values at 15 cm depth at site A.

The pseudo-total Fe concentrations found in the second sediment sections, 1-2 cm depth, were slightly higher at site B but the following subsurface maxima, at 5-10 cm, have smaller magnitudes. The concentration of pseudo-total Fe at 15 cm depth is much lower in the sediments of site A.

The values for the Mn/Fe ratio are generally higher in the site B sediment especially in the 0-1 cm section. The site B profile has no sub-surface maximum at 10 cm.

4.3.4 Site A: trace heavy elements, Pb, Cu and Zn

The concentration of pseudo-total Pb, in sediment cores LBA1 and LBA2, increases with increasing depth to maximum values of 244 mg/kg and 266 mg/kg respectively at 6-8 cm (Figure 4.3). The concentrations then decrease rapidly, more markedly for LBA1, with increasing depth to minimum values of 11.2 mg/kg and 14.1 mg/kg respectively at 13-15 cm. Slight sub-surface minima of ~ 99 mg/kg can be observed at 2-3 cm and 1-2 cm respectively. The third core from this site, LBA3, has a slightly different profile. The near surface maximum in pseudo-total Pb concentration occurs at 1-2 cm depth. The slight minimum noted in the two previous cores is present at 3-4 cm depth and the maximum concentration (241 mg/kg) is found at 8-9 cm. The minimum value of 29.1 mg/kg is again found at 14-15 cm depth.

The concentration of pseudo-total Cu in sediment core LBA1 increases from the surface value of 23 mg/kg to the maximum concentration of 32.4 mg/kg 6-7 cm, as shown in figure 4.3. A slight minimum of 20 mg/kg occurs at 1-2 cm. The concentration below the maximum value decreases rapidly with increasing depth and the minimum value of

5.62 mg/kg in reached at 12-13 cm. A similar profile was obtained for sediment core LBA2. The concentration generally increased from the surface value of 20 mg/kg to the maximum concentration of 34.1 mg/kg at 7-8 cm depth. At 1-2 cm depth the concentration decreases slightly to 16 mg/kg. The decrease in concentration with increasing depth below the maximum value is more gradual compared to that of the previous core. The minimum concentration of 1.72 mg/kg occurs at 13-14 cm depth. A similar profile was found for core LBA3 with a slight minimum occurred at 4-5 cm and the maximum concentration was found at 8-9 cm depth.

The pseudo-total Zn concentration within sediment core LBA1 (Figure 4.3) increases gradually, from the surface value of 170 mg/kg, over the upper 5 cm of the core and then increases more sharply to the maximum concentration of 707 mg/kg at 8-9 cm. The concentration then decreases rapidly with depth to the minimum value of 133 mg/kg at 14-15 cm. The profile for the second core taken at this site, LBA2, has the same trends and features. The concentration increases from the surface value of 162 mg/kg to the maximum concentration of 687 mg/kg at 10-11 cm depth. The concentration then decreases rapidly to the minimum of 136 mg/kg at 13-14 cm. The third core also has a similar profile with maximum and minimum concentrations of 731 mg/kg and 96.5 mg/kg at 10-11 cm and 14-15 cm depth respectively.

4.3.5 Site B: trace heavy elements, Pb, Cu and Zn

The pseudo-total concentration of Pb in sediment core LBB1 (Figure 4.4) increases in a broad maximum over the upper 4 cm from the surface concentration of 133 mg/kg up to a value of 256 mg/kg at 7-8 cm. A sharp spike follows at 12-13 cm to a concentration of 302 mg/kg. Thereafter Pb decreases rapidly to a minimum of 5.00 mg/kg at 26-27 cm with occasional drops below the detection limit. The second core from this site, LBB2, has a similar pseudo-total Pb profile. The surface concentration is 155 mg/kg and the maximum value is 335 mg/kg at 11-12 cm. The decrease after the maximum value is more gradual than for the previous core and the minimum concentration is 4.71 mg/kg at 22-23 cm.

The sediment core LBB1 pseudo-total Cu concentration (Figure 4.4) increases with depth, in a broad peak, from the surface concentration of 22 mg/kg to maximum value of 35.8 mg/kg at 5-10 cm. There is no apparent spike in concentration at 12 cm depth as was found for Pb and the decrease with depth after the maximum value is more gradual to a minimum of 12 mg/kg at 19-20 cm. The minimum concentration of 9.36 mg/kg is found at 24-25 cm. The psuedo-total concentration of Cu in the sediment core LBB2 has a similar profile to the previous core. The concentration at the surface is 19 mg/kg and increases gradually with depth to maximum value of 33.5 mg/kg at 7-8 cm. The concentration then decreases to the minimum value of 9.67 mg/kg at 12-13 cm followed by a broad peak centered at 15-16 cm. There a apparently a further peak in the pseudo-total concentration of Cu at 24-25 cm.

The pseudo-total concentration profile of Zn in the sediment core LBB1 has a broad peak centered at 6-7 cm with a maximum value of 862 mg/kg, as shown in figure 4.4. Above this the concentration decreases with decreasing depth to the surface concentration of 221 mg/kg. There is also a small peak, below the broad one, at 12-13 cm. A sharp decrease with increasing depth follows and then the concentration continues at a nearly constant level of ~ 250 mg/kg to the bottom of the core. The LBB2 sediment core has a similar profile with a surface concentration of 214 mg/kg and a maximum concentration of ~ 900 mg/kg. The sharp spike noted in the previous core at 12 cm depth is present again at 11-12 cm. The concentration change at this point is more dramatic than found for the previous core from this site peaking at 1096 mg/kg. Below this the concentration decreases rapidly and then remains constant with depth at ~200 mg/kg.

4.3.6 Comparison between Sites A and B: trace heavy elements, Pb, Cu and Zn

Excluding the difference at the bottom of the core attributable to the difference in the lengths of the cores the main difference between the pseudo-total Pb profiles from sites A and B is the rate of decrease in concentration towards the surface. The rate of decrease is much less and the maximum concentration is greater at site B than at site A.

The pseudo-total Cu profiles at both sites sampled at Loch Bradan are very similar when the concentrations and shapes of the profiles are considered.
The concentration of pseudo-total Zn at site B is greater than that at site A even after excluding consideration of the spike in concentration at ~ 12 cm. The major difference occurs around 3-8 cm with the maximum concentration at site A centred at a greater depth than at site B. The spike in concentration at site B coincides with the broad maximum in concentration at site A.

4.3.7 Quality Assurance - comparison between ICP-OES and AAS results (Mn, Fe, Pb, Cu and Zn) – Site A cores 1 and 2 vs core 3

Comparison of the profiles in figure 4.3 of the site A cores 1 and 2 and the site A core 3 shows good agreement between the ICP-OES and AAS results for Mn, Fe and Zn.

4.3.8 Quality Assurance – comparison of duplicates (Mn, Fe, Pb, Cu and Zn)

The sediment core LBA3 was digested in duplicate and analysed for pseudo-total elemental compositions, shown in figure 4.6. The duplicate data sets, figure 4.3 and 4.6, show excellent agreement when the concentrations and the shape of the profiles are considered.

4.3.9 Site A core 3: additional elements (Al, Si, Ca, Mg, Na, K; S, P; Co)

The profiles of the additional elements for the duplicate analysis of the Loch Bradan core LBA3 are shown in figures 4.7-4.8. The pseudo-total concentration of Al increases gradually, with depth, from a surface concentration of 2.7 % into a broad peak with a maximum concentration of 3.32% (w/w) at 5-6 cm. There is a slight minimum with the concentration dropping to 2.5 % at 1-2 cm depth. After the maximum concentration the

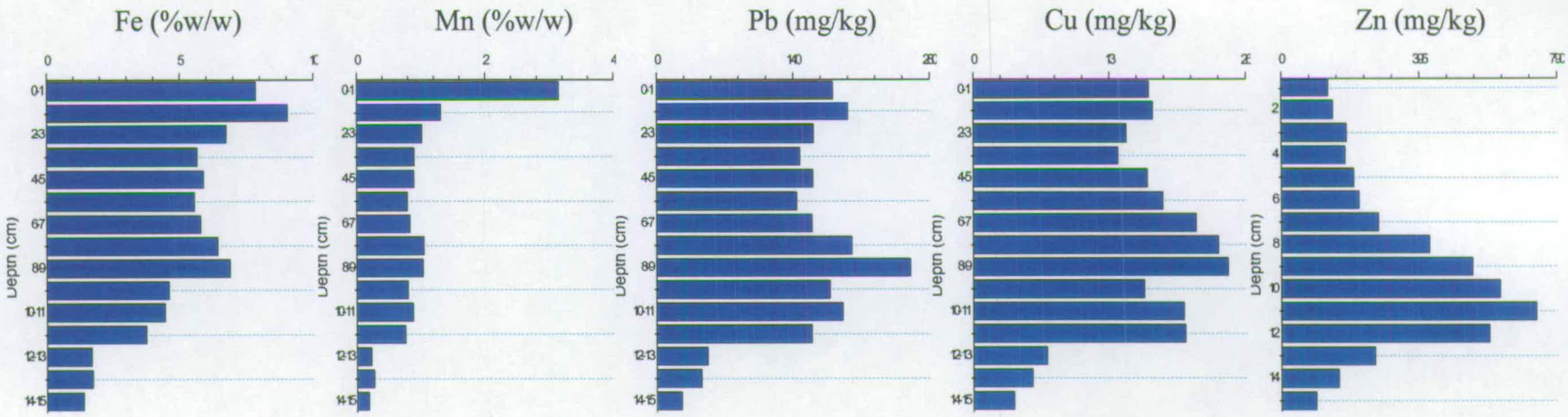

Figure 4.6 Duplicate profiles of the variation with depth in the sediment of the pseudo total metal concentrations of Fe, Mn, Pb, Cu and Zn for Loch Bradan core LB site A core 3

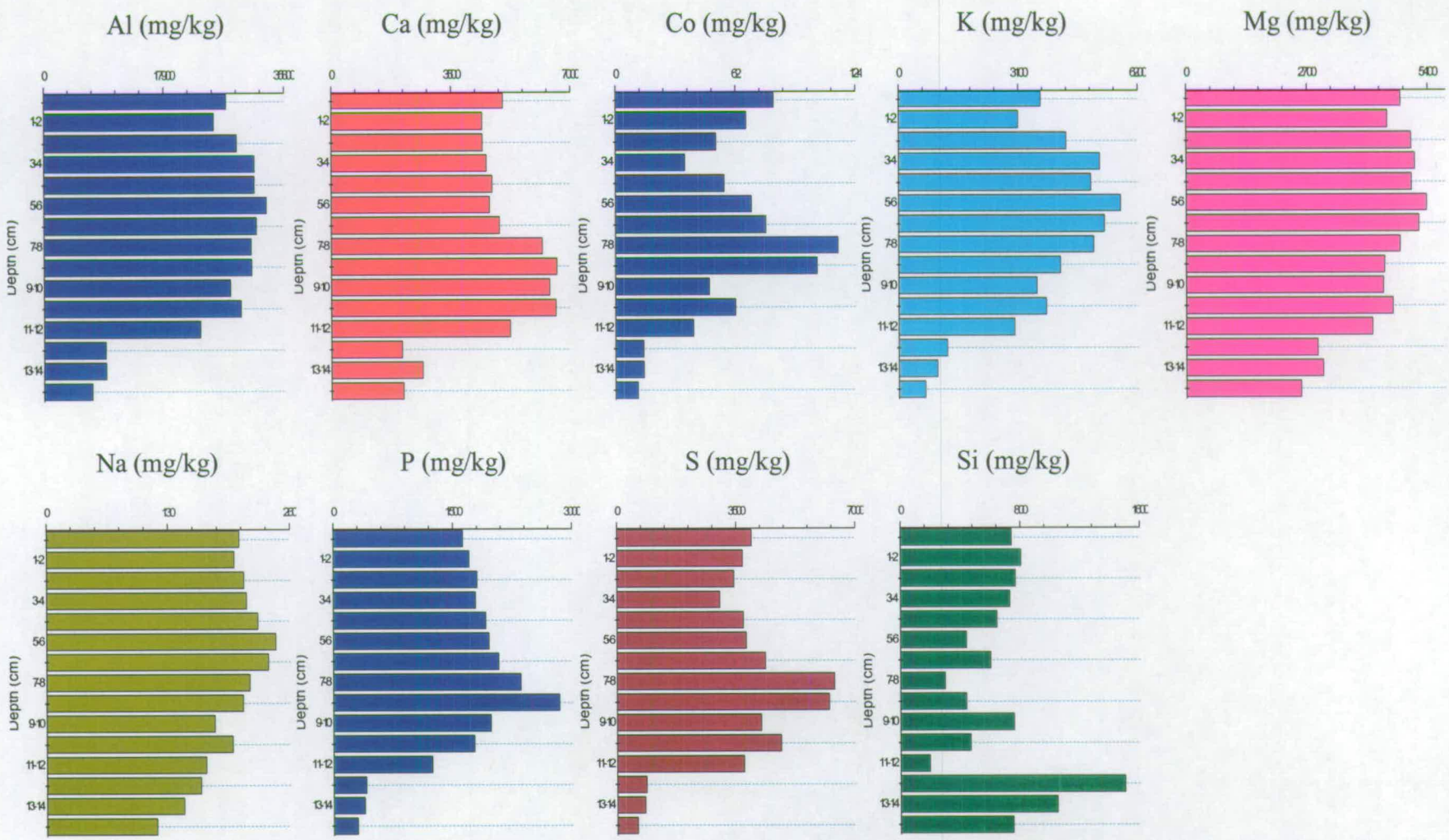

Figure 4.7 Profiles of the variation with depth in the sediment of the pseudo-total concentration for additional elements (Al, Ca, Co, K, Mg, Na, P, S, Si) from Loch Bradan core LB site A core 3 in mg/kg

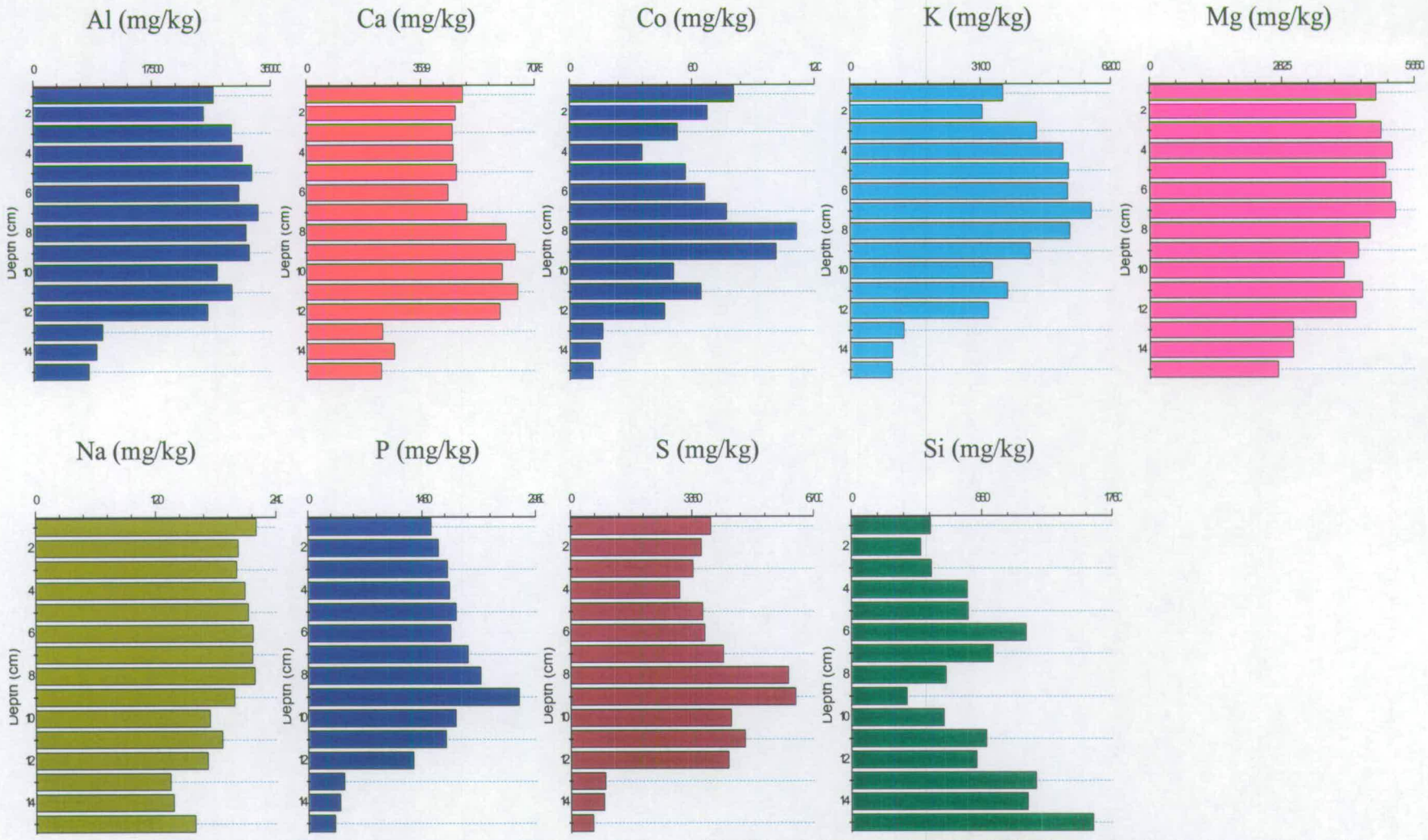

Figure 4.8 Duplicate profiles of pseudo total metal concentrations of additional elements from Loch Bradan core LB site A core 3 in mg/kg

value decreases gradually down to 12 cm and then drops rapidly to the minimum concentration of 0.73% at 14-15 cm.

The concentration of Si in the pseudo-total fraction generally decreases with depth from a surface concentration of 0.07 % down to minimum value of 0.02 % at 11-12 cm. Two small peaks can be noted at 6-7 cm and 9-10 cm and then a sharp peak can be observed to the maximum concentration of 0.15 % at 12-13 cm.

The pseudo-total Ca profile has a slight surface maximum concentration of 0.5 % and is followed by a drop to 0.45 % after which the concentration remains fairly constant. The concentration increases dramatically at 7cm depth to the maximum concentration of 0.66% at 8-9 cm. The concentration then drops rapidly once again to the minimum value of 0.21% at 12-13 cm.

The pseudo-total Mg profile has a slight surface maximum of 0.48 % followed by a slight minimum. The concentration then decreases gradually with depth after maximum concentration of 0.54% (w/w) at 5-6 cm. A slight peak in concentration can be noted at 10-11 cm depth. The minimum concentration of 0.26 % occurs at 14-15 cm.

The concentration profile shape for the pseudo-total fraction of Na is very similar to that of Mg. The near surface minimum noted in the Mg profile is not apparent in the Na profile. The concentration increases from the surface value of 200 mg/kg to the maximum concentration of 245 mg/kg at 5-6 cm. The concentration then decreases gradually with depth to the minimum value of 118 mg/kg at 14-15 cm.

The profile of pseudo-total K is similar to that of Al, Mg and Na with a slight minimum and then the increase in concentration to the maximum value of 0.58% at 5-6 cm following the surface maximum of 0.38%. The concentration then decreases with depth to the minimum value of 0.07% at 14-15 cm. A slight peak in concentration can be noted at 10-11 cm.

The pseudo-total P concentration increases gradually from a surface value of 0.16 % to the maximum concentration of 0.28 % at 8-9 cm. The concentration then decreases gradually with depth but then drops rapidly to the minimum concentration of 0.03 % over 12-15 cm.

The concentration of pseudo-total S decreases from the surface value of 0.4 % to a minimum of 0.3 % at 3-4 cm depth. The concentration then increases to the maximum value of 0.64 % at 7-8 cm. A slight peak at 10-11 cm can be noted and then the concentration drops dramatically to the minimum value of 0.06 % at 14-15 cm.
The pseudo-total Co concentration profile is very similar to that of S but the concentration halves between the surface concentration (of 80 mg/kg at 0-1 cm) to the minimum at 3-4 cm. The concentration then increases again to a maximum of 115 mg/kg at 7-8 cm. Thereafter it decreases with depth until a sharp drop to the minimum of 11.5 mg/kg, which occurs over 12-15cm. A peak can also be noted at 10-11 cm depth.
The duplicates of the pseudo-total digests for the sediment core LBA3 all show good correlation apart from that for Si.

4.4 Concentration of elements in the easily reducible fraction of sediments from Loch Bradan, SW Scotland

The digestion to isolate the easily reducible material from the sediment was then conducted using only the sediment from core LBB1 from Site B. This site yielded longer sediment cores and was near the main inflow therefore presented more information on biogeochemical changes with depth and the potential for a greater understanding of the processes in the loch as influenced by the catchment.

4.4.1 Site B: redox-active elements, Mn and Fe

The profile of readily reducible Fe in core LBB1, as shown in figure 4.9, has a similar shape to that of the pseudo-total Fe profile. The substantial maximum occurs in the surface section, 0-1 cm depth, as opposed to near the surface, at 1-2 cm, as was found for the slight peak in the pseudo-total concentration. The concentration of Fe in the easily reducible form then remains constant until 10-11 cm depth. Thereafter the concentration increases steadily with depth, with a small peak at 15-16 cm depth, until 20-21 cm where another large enrichment is found.

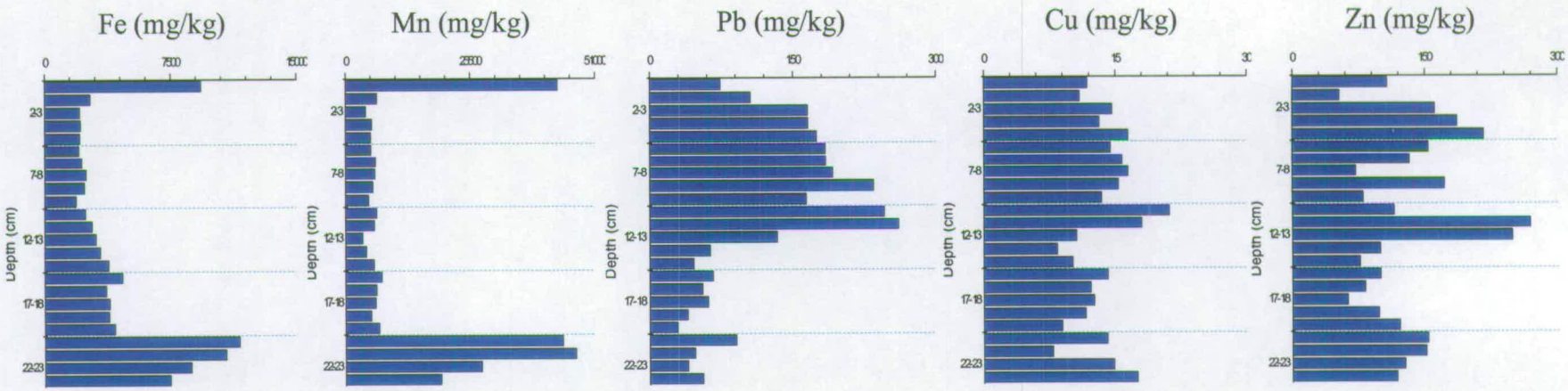

Figure 4.9 Profiles of variation with depth of the readily reducible metal concentrations for Fe, Mn, Pb, Cu and Zn for the Loch Bradan core LB site B core 1

The Mn concentration in the easily reducible fraction (Figure 4.9) also follows similar trends to the pseudo-total profile. A sharp surface maximum can once again be observed followed by low values down to 20 cm depth. The concentration of easily reducible Mn then increases with depth to peak at a maximum of 4 %(w/w) at 22 cm depth and then decreases with depth once again.

4.4.2 Comparison with pseudo-total concentrations of Mn and Fe

The maximum concentration of easily reducible Fe at 0-1 cm corresponds to 10.48 % of the Fe detected in the pseudo-total sample, as shown in figure 4.10. This is followed directly by the minimum value of 3.28 % of the pseudo-total Fe concentration. Thereafter there is very little variation with depth. The concentration of easily reducible Mn is high and sometimes exceeded that of the pseudo-total Mn which can be accounted for by the heterogeneity of the sample. The highest peaks correspond to the surface and sub-surface maxima of the pseudo-total profile. In addition two minor peaks can be observed centered at 4-5 cm and 13-14 cm.

4.4.3 Site B: trace heavy elements, Pb, Cu and Zn

The readily reducible Pb profile (Figure 4.9) resembles that of the pseudo-total Pb profile. The concentration increases with depth in a broad peak. The maximum concentration is found in a sharp enrichment to 261 mg/kg at 11-12 cm. The concentration of readily reducible Pb then decreases and remains constant with depth with the minimum of 29.1 mg/kg at 19-20 cm.

The concentration of Cu in the readily reducible fraction is very variable with depth in the sediment, but the profile bears a general resemblance to the pseudo-total profile. The concentration increases slightly with depth to a maximum of 21.2 mg/kg at 10-11 cm. The minimum concentration of 7.87 mg/kg can be noted at 22-23 cm.

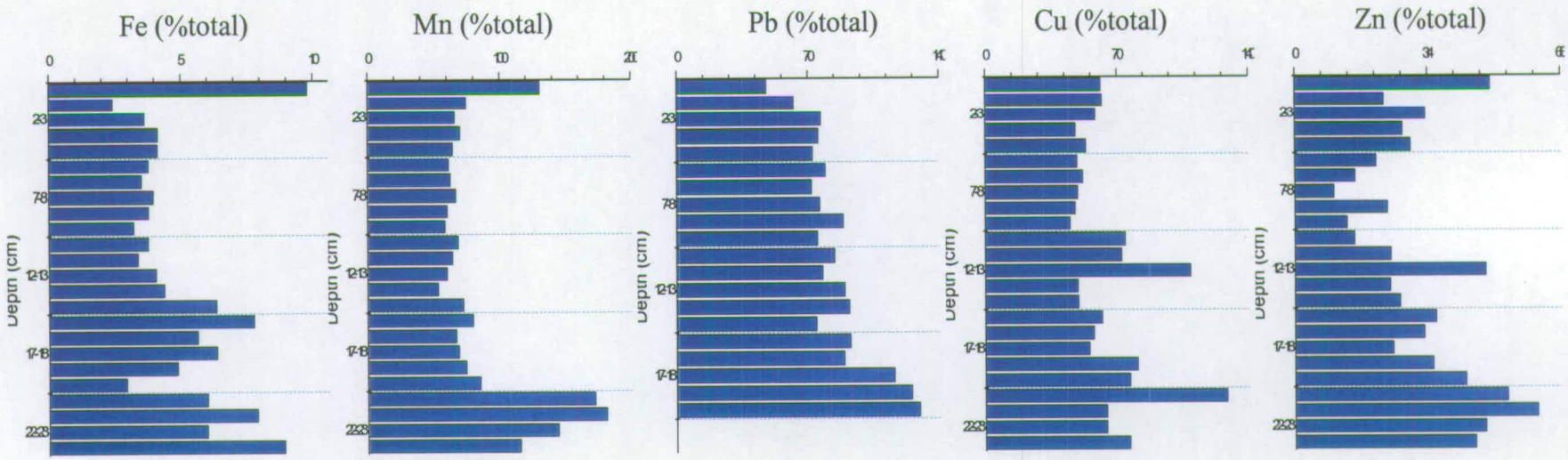

Figure 4.10 Profiles of variation with depth of the elements in the readily reducible fractions of Loch Bradan cores LB site B core 1 expressed as % total concentration

The profile of readily reducible Zn bears little resemblance to the pseudo-total profile as the concentration is highly variable with depth. The minimum concentration of 53.1 mg/kg is near the surface sediment at 1-2 cm. Three broad peaks then dominate the profile centered at 4-5 cm, 11-12 cm and 20-21 cm. The maximum concentration of 269 mg/kg is contained within the sharpest of these enrichments at 11-12 cm depth.

Figure 4.10 contains the concentrations of Pb, Cu and Zn in the Loch Bradan core LBB1 expressed as a percentage of the total concentration. From this it was noted that the fraction of Pb found in the readily reducible fraction increased with depth from 40 % at the surface to nearly 100 % at depth in the core. The fraction of the total concentration of Cu represented by the readily reducible extract was fairly constant through the core at 60-70 %. Elevations to nearly 100 % of the total concentration occurred at 12-13 cm and at 20-21 cm depth. The percentage of the total Zn concentration represented by the readily reducible fraction was very variable with depth in the core with a range of 10-60 %. This fraction was large in the surface sediment and then decreased with depth to the minimum at 7-8 cm. Thereafter the percentage of the total Zn concentration found in the readily reducible fraction increased with depth with sharp peaks at 8-9 cm and 12-13 cm.

4.4.4 Additional elements

None of the easily reducible profiles of the other elements (Figure 4.11) analysed by ICP-OES had any accompanying pseudo-total data. The concentrations cannot therefore be used to aid interpretation. The correlation between these profiles and those of the easily reducible Fe, Mn, Pb, Cu and Zn discussed above may enable understanding of correlations in the pore water phases. As the easily reducible material will be the most labile of the sediment species and thus will be important in illuminating interactions with elements in the pore water.

The profile of Co in the readily reducible fraction is similar to those of Mn and Fe with enrichments at the surface and at the base of the core. The Ca, P, S and, to a lesser

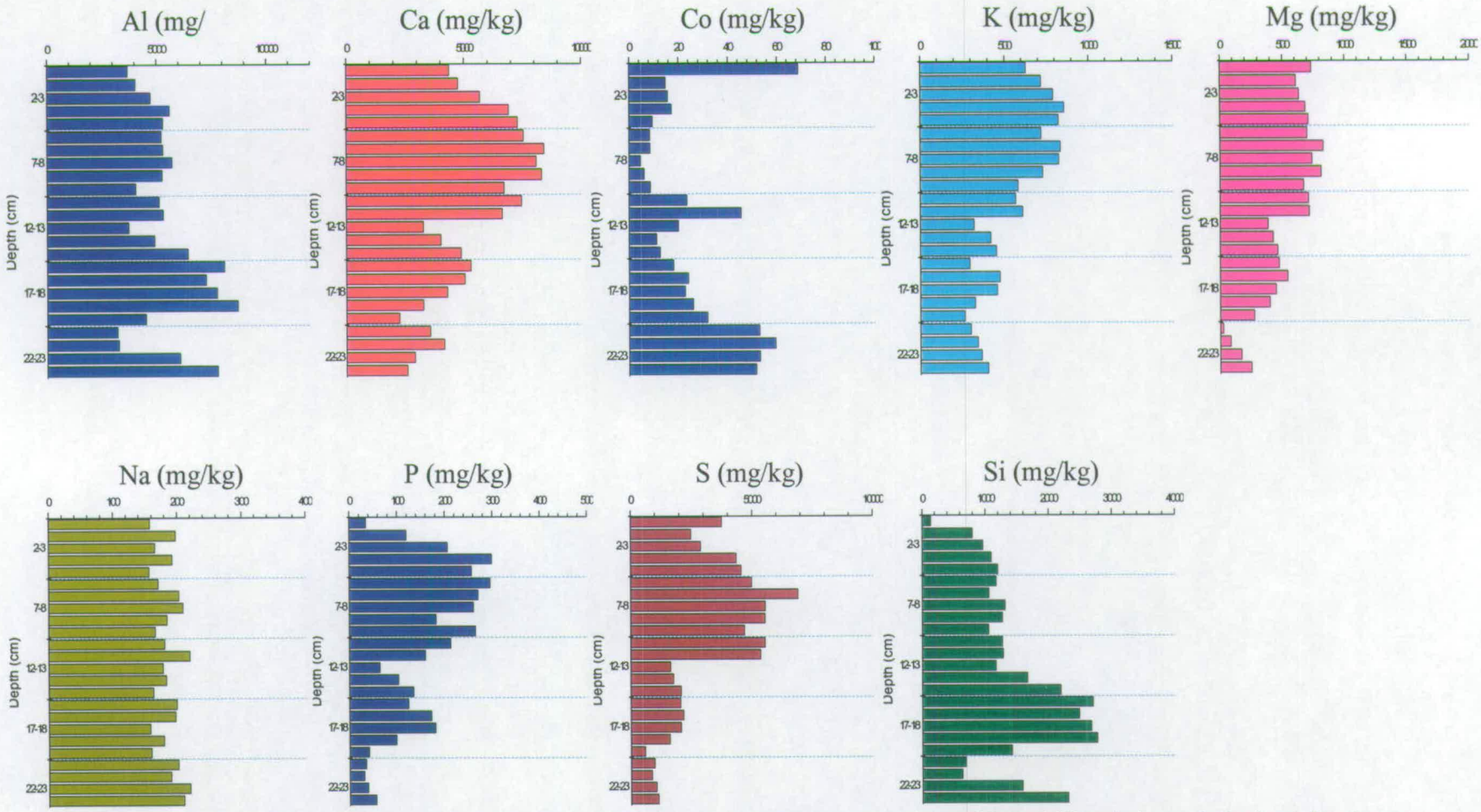

Figure 4.11 Profiles of the variation with depth of the readily reducible metal concentrations of the additional elements for Loch Bradan core LB site B core 1(Al, Ca, Co, K, Mg, Na, P, S, Si)

extent, K and Mg have very similar profiles to the readily reducible Pb and Cu profiles. The profile of Na is featureless with constant concentrations found down the length of the core. A very strong correlation can be observed between the readily reducible Al and Si.

4.5 Characterisation of porewater organic matter- UV-visible

The porewater LBA1-3 and LBB1-2 displaying absorbance at 254 nm and the E4/E6 ratio values with depth in the sediment core are shown in figure 4.12. The absorbance at 254 nm, in core LBA1, generally decreases with depth from the surface peak but peaks sharply again at 3-4 cm depth. The absorbance then remains low down the rest of the core before increasing slightly over 10-15 cm. The profile for LBA2 is different with high absorbance values in the uppermost two sections and the maximum absorbance at 1-2 cm depth. The values then remain low with only slight elevation at 7-8 cm and 12-13 cm depth. The third core from this site has a slightly different profile again with the maximum value at the surface and generally higher values down the rest of the core than found for the previous two cores. Slight peaks can be noted at 3-4, 5-6 and 8-9 cm and the values are elevated over the lowest 4 cm of the core.

Site B, long cores

The absorbance at 254 nm shows no general trend with depth in the LBB1 profile with sharp peaks at 1-2 cm and 13-14 cm and a further broader peak centred at 22-23 cm depth. The profile of LBB2 is very similar with a peak at 1-2 cm, one at 11-12 cm and a slightly sharper peak at 19-20 cm depth.

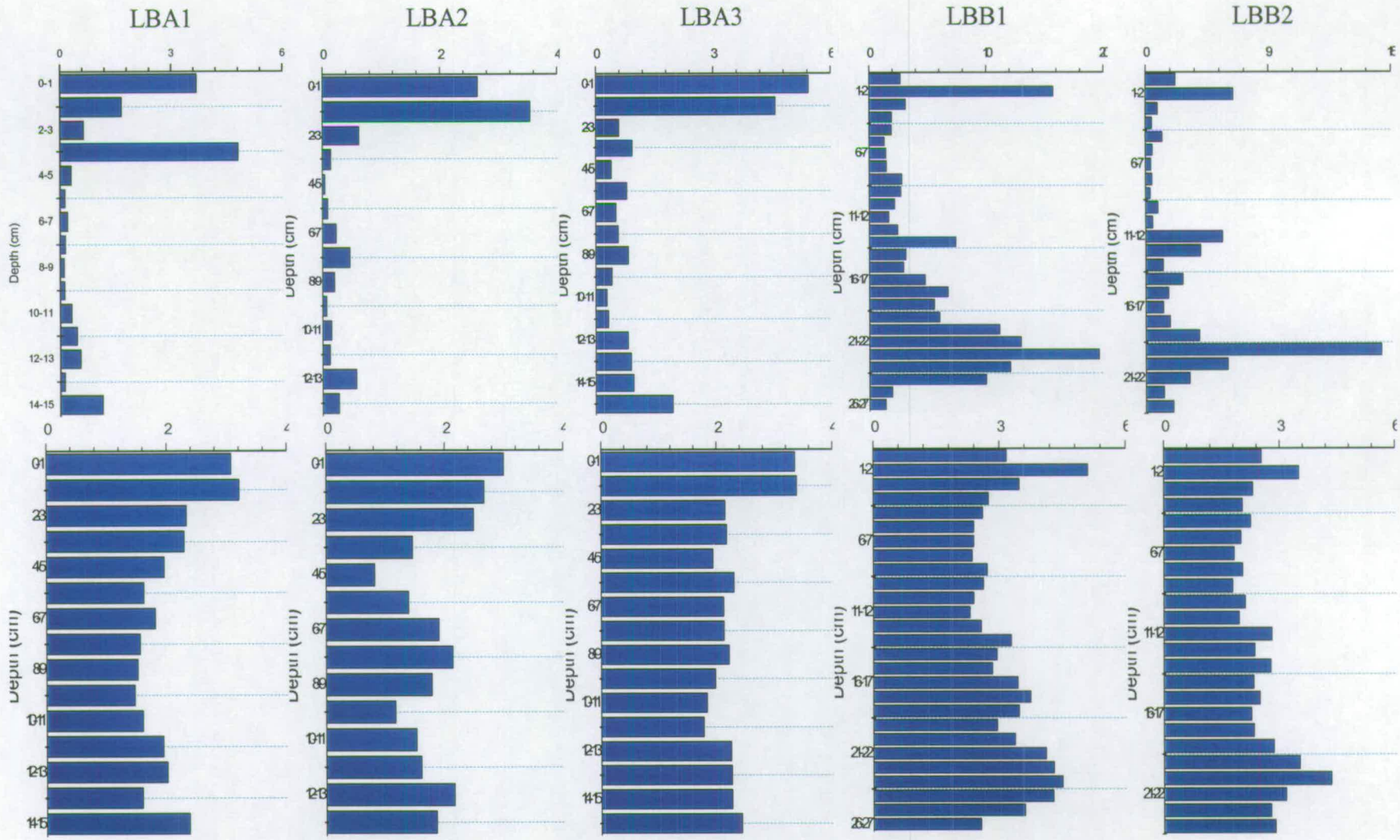

Figure 4.12 Profiles of variation with depth in the sediment of the UV-visible absorbance at 245 nm and E4/E6 ratio for Loch Bradan cores LB site A cores 1-3 and LB site B cores 1-2

4.6 Total concentration of redox active elements in loch sediment interstitial waters

Site A- Mn and Fe

The concentration of Fe in the porewater extracted from core LBA1 ranges from 0.323-17.10 mg/l, as shown in figure 4.13. There is an increase from the surface concentration to the maximum concentration at 3-4 cm depth thereafter the concentration decreases rapidly and then remains fairly constant. The minimum concentration occurred at 9-10 cm. The Mn concentration increases more steadily with depth from a surface minimum of 1.23 mg/l to a maximum of 37.8 mg/l at 5-6 cm. The concentration then decreases with depth once again.

The profile of Fe in the porewater extracted from LBA2 (Figure 4.13) showed a fairly similar picture. The concentration ranged from 0.48 mg/l at the surface to 20.5 mg/l with a sharp peak at 1-2 cm depth. Two other peaks can also be observed at 7-8 cm and 12-13 cm. The concentration of Mn in the porewater increased from a surface minimum of 1.38 mg/l to a maximum of 40.0 mg/l at 5-6 cm depth in a broader peak than that found in core LBA1. Thereafter the concentration decreases with depth but the change with depth is more gradual in comparison to LBA1.

The profile of Fe in LBA3 pore water also generally decreases with depth (Figure 4.13) but the absence of the large subsurface enrichment produces an apparently different profile. The concentration decreases with depth from a small enrichment of 10.7 mg/l at 1-2 cm. Two other peaks, broader than those found in LBA2, can also be distinguished at 6-9 cm and 13-15 cm depth. The minimum concentration occurred at 11-12 cm where the concentration decreased to 0.81 mg/l. The profile of Mn is very similar to the previous Mn profiles described. The surface minimum is 3.38 mg/l and the concentration increases with depth to the maximum of 31.5 mg/l at 7-8 cm before decreasing once again with depth.

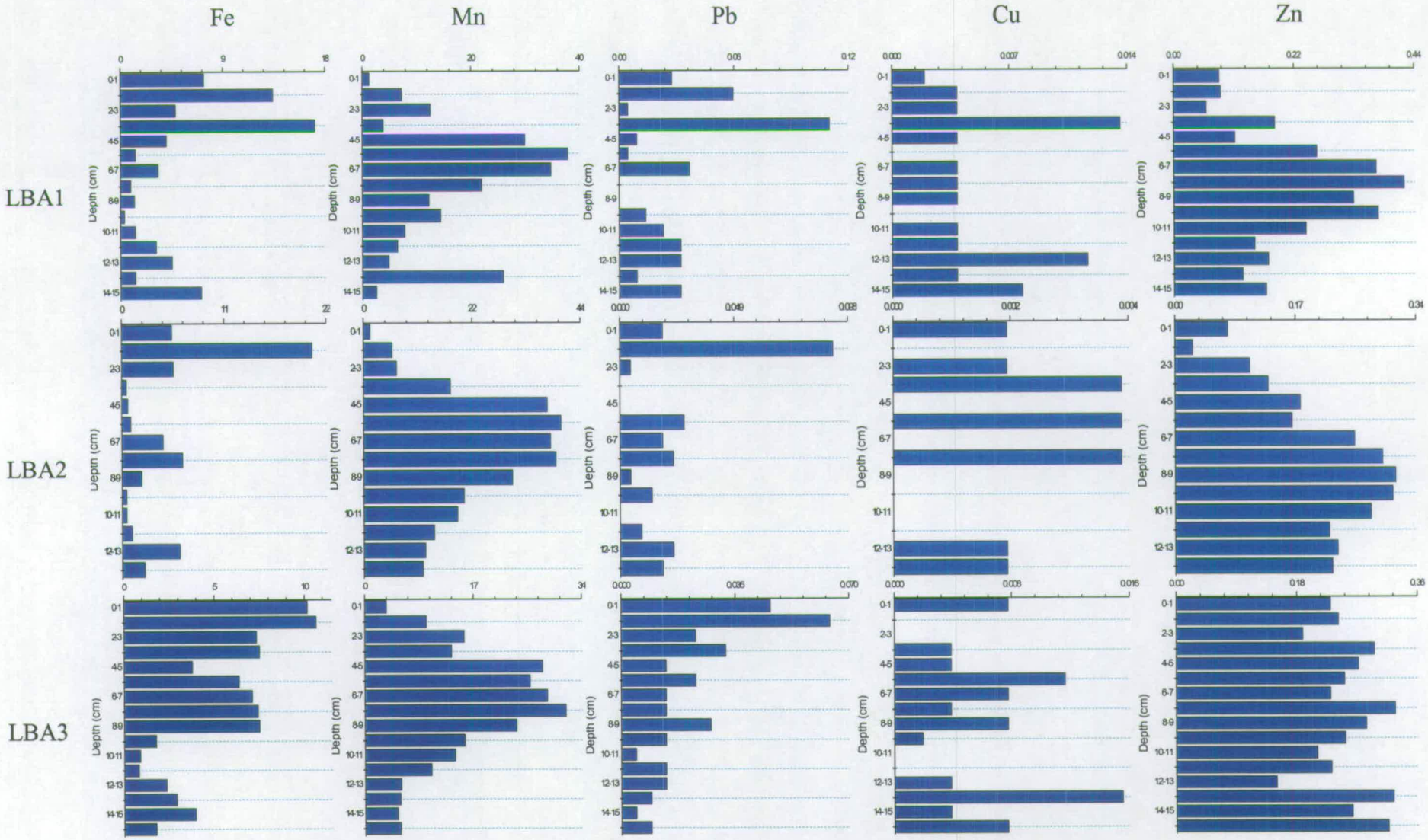

Figure 4.13 Profiles variations with depth in sediment cores of the pore water concentrations of selected metals (Fe, Mn, Pb Cu and Zn) from Loch Bradan LB site A cores 1-3 expressed in mg/l

Site B- Mn and Fe

The profile of Fe extracted in LBB1 pore water (Figure 4.14) contains three peaks centred at 1-2 cm, 13-14 cm and 22-23 cm depth. The concentration ranged from 3.66 mg/l at 5-6 cm depth to 205 mg/l at the enrichment near the base of the core. The Mn porewater concentration increased steadily with depth from the surface minimum of 2.48 mg/l to the maximum of 29.0 mg/l at 22-23 cm. Two subsurface peaks can also be noted at 1-2 cm and 13-14 cm depth.

The concentration profile of Fe in core LBB2 (Figure 4.14) has a similar shape to that of LBB1, but the enrichment at the base of the core is slightly less pronounced in core LBB2. In general the concentrations are also slightly lower ranging from 0.58 mg/l to 178 mg/l. The minimum was noted at 8-9 cm and three peaks were again found at 1-2 cm, 11-12 cm and 19-20 cm depth. The Mn profile is somewhat different to the other core from site B. The concentration again increases from the surface minimum of 0.91 mg/l, but a maximum concentration of 21.5 mg/l was found at 7-8 cm. The concentration then decreased with depth, with a sharp peak at 11-12 cm, before increasing again to peak at 18-19 cm.

4.7 Total concentration of trace elements in loch sediment interstitial waters

Site A

The concentration of Cu found in LBA1 porewater was very low but a detectable peak was found at 3-4 cm depth (Figure 4.13). The Pb profile is similar to that of Fe with a subsurface peak at 1-2 cm and the maximum concentration of 0.11 mg/l at 3-4 cm. The minimum concentration of 0.004mg/l was found at 5-6 cm and there was an area of enrichment in the concentration at depth in the sediment core. The profile of Zn in the porewater has a similar shape to that of Mn but the maximum concentration of 0.42 mg/l was found at a lower depth of 7-8 cm. A slight increase in concentration can be observed at 3-4 cm depth, just below the minimum concentration of 0.06 mg/l.

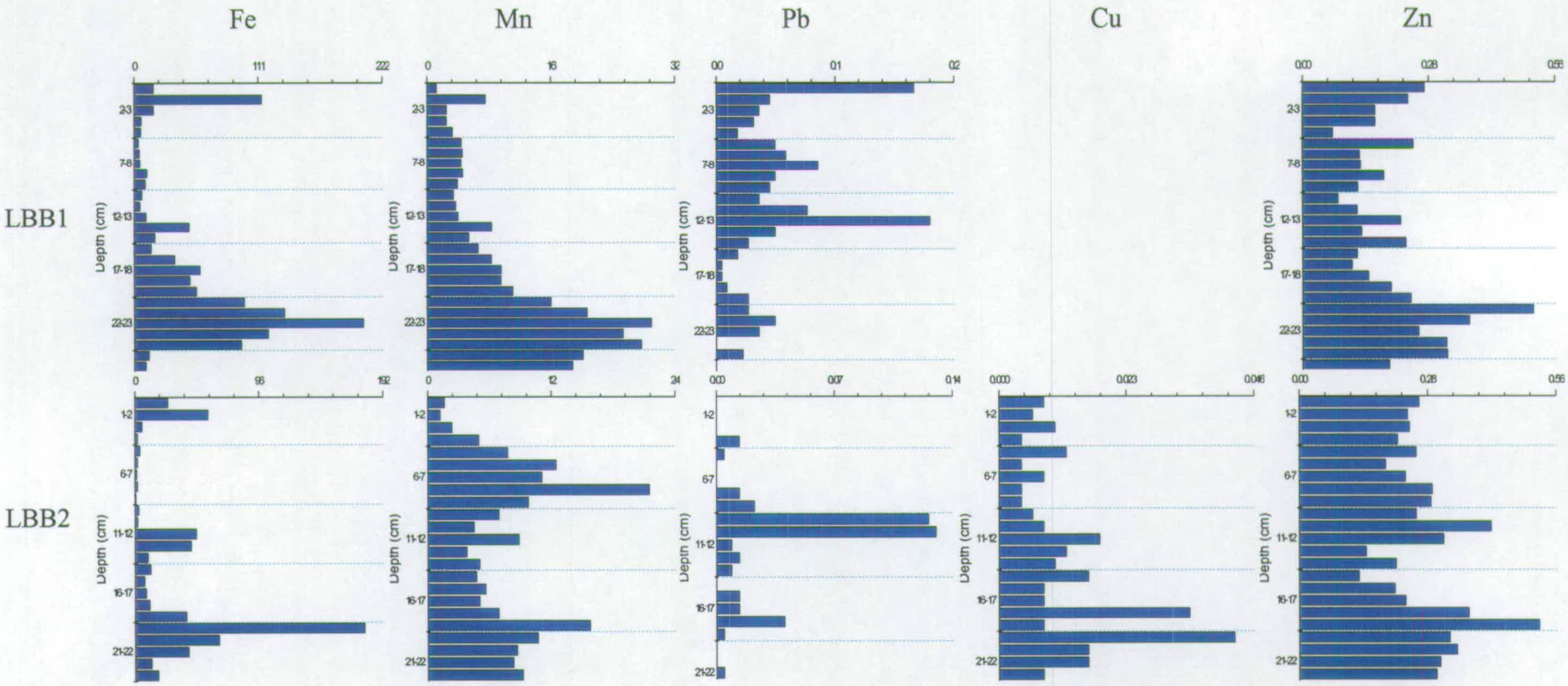

Figure 4.14 Profiles variations with depth in sediment cores of the pore water concentrations of selected metals (Fe, Mn, Pb Cu and Zn) from Loch Bradan LB site B cores 1-2 expressed as mg/l

The concentration of Cu in the LBA2 porewaters (Figure 4.13) was frequently below limit of detection of instrument. No trends with depth or correlation with other profiles were discernable. The Pb concentration ranged from 0.005mg/l to 0.092 mg/l and the profile displayed similar features to the porewater profile of Fe. The maximum concentration was found in the near surface peak at 1-2 cm and minimum concentration was found at 8-9 cm depth. Initially the Zn concentration in the LBA2 pore water decreases from the surface to the minimum value of 0.025 mg/l at 1-2 cm. The concentration then increases with depth in a broad peak resembling that found in the Mn profile, however the peak is centred at a lower section of the core in the Zn profile as the maximum concentration of 0.31 mg/l was found at 8-9 cm depth. The concentration then decreased slightly with depth with a sharper drop over the last 3 cm section of the core.

Several sections of core LBA3 porewater (Figure 4.13) had Cu concentrations that were below the detection limit of the instrument, however there does appear to be an enrichment in Cu at 5-6 cm depth with concentrations peaking at 0.012 mg/l. The profile of Pb is more complete than the previous two cores from this site and shows a subsurface peak with a maximum concentration of 0.064 mg/l at 1-2 cm. The concentration then decreases with depth with a minimum concentration of 0.004 mg/l at 14-15 cm with slight enrichments at 5-6 cm and 8-9 cm. The profile of pore water Zn in the LBA3 core is very different to the previous two cores from this site. The concentration is very variable with no broad peak over the 5-9 cm region and no obvious trend with depth. The concentration ranged from 0.15 mg/l to 0.33 mg/l.

Site B

The concentration of Cu in the LBB1 porewater was below limit of detection of the instruments. The concentration of Pb generally decreases with depth (Figure 4.14) with two major peaks at 0-1 cm and 12-13 cm depth and a further two, more minor, peaks at 7-8 cm and 21-22 cm depth. The maximum concentration of 0.18 mg/l was contained within the major peak at 12-13 cm and the minimum concentration of 0.004 mg/l occurred at 16-17 cm. The concentration of Zn was fairly constant with a slight increase

towards the surface and an enriched area around 20-21 cm depth with a maximum concentration of 0.508 mg/l. The minimum concentration of 0.067 mg/l was found at 4-5 cm.

The concentration of Cu in the pore water extracted from the LBB2 sediment core is barely above limit of detection of the instrument (Figure 4.14). The profile does appear to have peaks at 11-12 cm and at 20-21 cm where the maximum concentration of 0.043 mg/l is located. Overall the concentration of Pb was very low with a detectable peak of 0.13 mg/l at 10-11 cm and peak of ~0.04 mg/l at 17-18 cm. The profile of Zn was fairly constant with depth for the LBB2 porewaters. The concentration ranged from 0.13 mg/l to 0.52 mg/l with sharp peaks at 10-11 cm and 18-19 cm.

4.8 Concentration of elements in fractions of Loch Bradan core LBB1 porewater obtained by centrifugal ultrafiltration

The profiles of Fe, Mn and Zn in the retentate and filtrate fractions obtained by the centrifugal ultrafiltration of Loch Bradan porewater from core LBB1 are displayed in figure 4.15. The recoveries, when compared to the total porewater concentrations, were poor but general trends in the partitioning were noted. The concentration profiles of Mn, Fe and Zn in the retentate were similar with sharp peaks at 1-2 cm , 13-14 cm and 22-23 cm depth. The Mn filtrate concentrations were in a similar range as the retentate profile, without the presence of the large enrichment near the base of the core, but a peak in concentration was noted at 4-5 cm depth. The concentration of Fe in the filtrate was below the detection limit of the instrument and the concentrations of Zn were also very low.

4.9 Loch Bradan Surface Water

Figures 4.16 and 4.17 display the elemental concentration found in the total sample and ultra-filter fractions of waters collected from the sediment-water interface (LBI 1-5) and

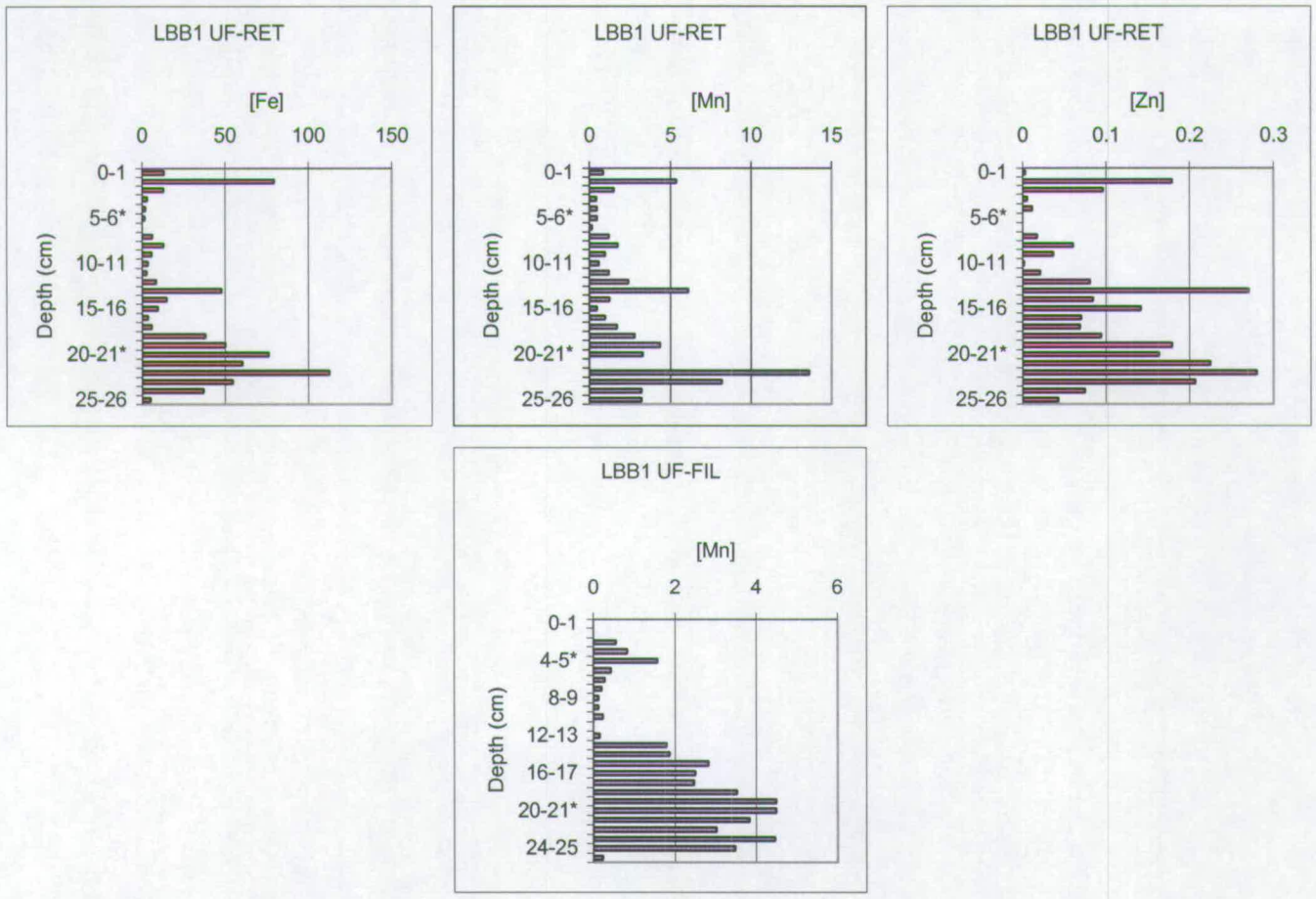

Figure 4.15 Profiles of the variation with depth in the sediment of the concentration of Fe, Mn and Zn in ultrafilter fractions (FIL=filtrate and RET=retentate) of Loch Bradan porewater LB site B core 1 in mg/l

*This sample was made up to the minimum required volume of 5ml with the addition of double-deionised water

Figure 4.16 The total (LTI1-5) and ultrafilter fraction (filtrate LTIF1-5 and retentate LTIR1-5) concentrations of elements in Loch Bradan waters sampled 1cm above the sediment-water interface

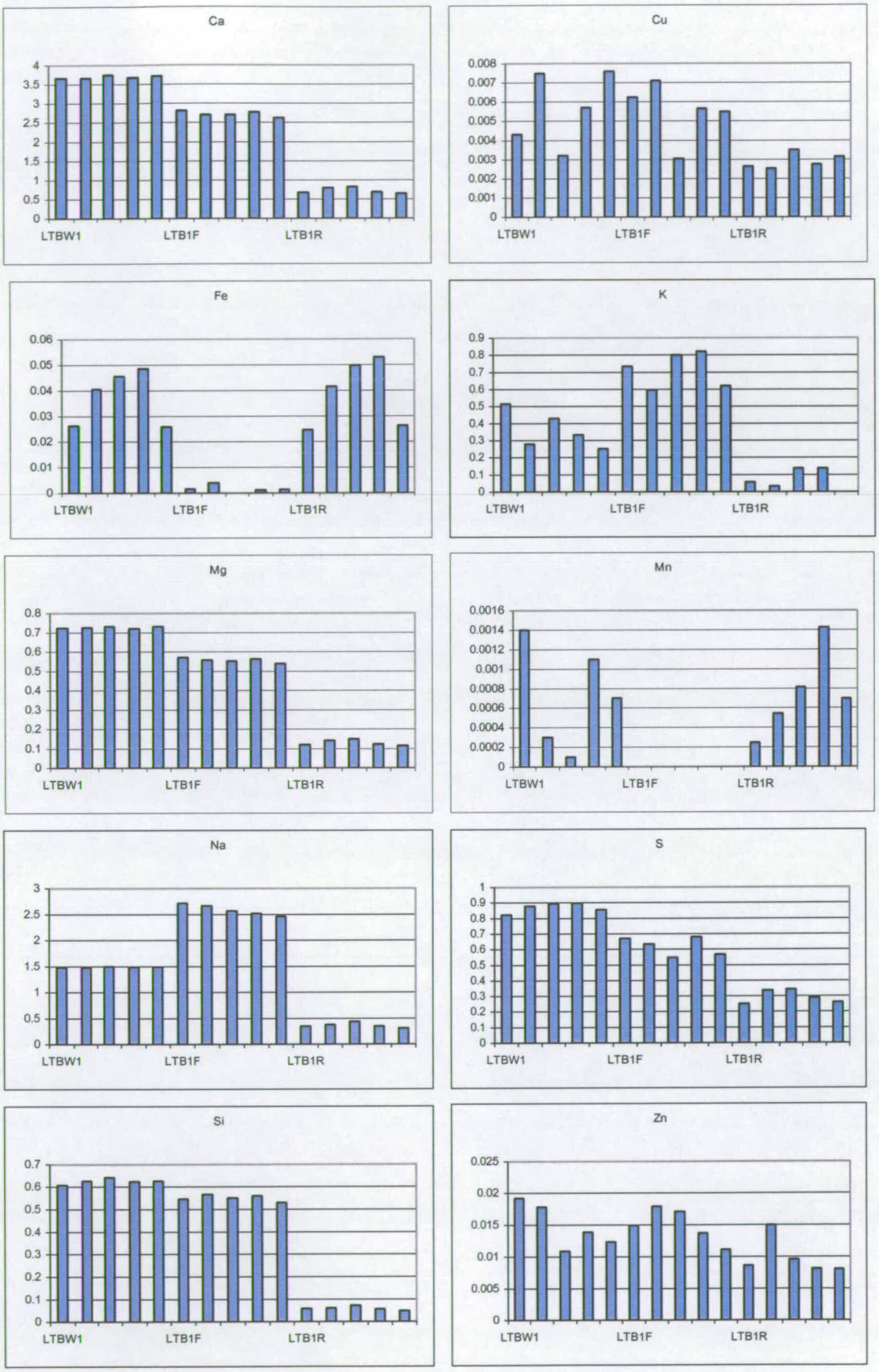

Figure 4.17 The total (LTBW1-5) and ultrafilter fraction (filtrates LTBF1-5 and retentates LTBR1-5) concentrations of elements in Loch Bradan water sampled 10 cm above sediment-water interface

10 cm above the sediment-water interface (LBB 1-5) of Loch Bradan. Overall the concentration of Mn was very low in all of the water samples with a maximum concentration of 0.005 mg/l in sample LBI2. There was poor consistency between replicate samples and no trend could be established on the partitioning of the Mn between the two ultra-filter fractions. The concentration of Fe varied for each of the replicate samples and ranged from 0.026 mg/l to 0.05 mg/l. The concentrations found in each of the retentates corresponded to nearly 100 % of the respective total concentration. The Pb concentrations in these water samples were very low and for the peaks of concentration there was no consistency between the replicate samples and no trend was distinguishable when considering the partitioning between the truly dissolved and colloidal phases. The concentrations of Cu in the total samples were also low. It appears that the Cu is distributed fairly evenly between the truly dissolved and colloidal phases but the mass balance of the two fractions compared to the total sample is poor. Disregarding sample LTI5 the variation in concentration of Zn for the replicate total samples, from 0.005 mg/l to 0.017 mg/l , is reproduced by the ultra-filter filtrates with nearly all of the Zn present in this fraction.
The concentrations of Ca, Mg, S and Si all show good correlation on comparison of the replicates with values of 3.8 mg/l, 0.73 mg/l, 0.8 mg/l and 0.62 mg/l respectively. After ultra-filtration it can be seen that all of these elements are present primarily in the truly dissolved phase.

A similar set of results was obtained for the waters collected from the bottom of Loch Bradan above the interface waters. Generally the concentration were slightly lower than those found nearer the sediment water interface. The Mn concentration ranged from 0.0001 mg/l to 0.001 mg/l in the total water sample. Little or no Mn was detected in the filtrates but the concentrations found in the retentates did not exhibit the same trend as the total concentrations. The mass balance was poor with each sample set producing a large deficit or excess. Only LBB5 has near 100 % recovery of the total Mn in the retentate.

The Fe concentration ranges from 0.025 mg/l to 0.05 mg/l in the total samples and in each case nearly 100 % of the total is present in the colloidal phase, >1kDa.

The Cu concentrations were very variable with concentrations from 0.003 mg/l to 0.007 mg/l in the total samples. In each case the Cu appeared to mainly exist in the filtrate at <1 kDa but the retentate also had a significant concentration and the sum of the fractions was usually greater than the whole. The Zn concentration were a little less variable ranging from 0.01 mg/l to nearly 0.02 mg/l but the concentrations in the fractions were inconsistent in comparison to the totals and no trends were apparent in the data set.

The distributions of Ca, Mg, S and Si were similar to those found in the water sample from the interface with average concentrations of 3.5 mg/l, 0.7 mg/l, 0.85 mg/l and 0.6 mg/l respectively.

Chapter 5. Results - Loch Tay

5.1 Introduction

The following chapter contains the results of the analysis of the four cores collected from Loch Tay on 22/06/01. Section 5.2 describes the sediment characteristics found for each core as a function of depth in the sediment. This is followed by the pseudo-total elemental concentrations and the results of the readily reducible digestion in sections 5.3 and 5.4 respectively. Section 5.5 contains the data from the charaterisation of the porewater followed by the characterisation of the ultrafiltered fractions in section 5.6. The ultrafiltration section leads on to the fractionation of the loch surface water by cross-flow ultrafiltration in section 5.7 and the fractionation of porewater and sediment extracts by electrophoresis in section 5.8.

5.2 Characterisation of sediments from Loch Tay, NE Scotland

The profiles in figure 5.1 show the moisture, ash and organic content of the sediment collected from Loch Tay, LT1-4, and the variation of the composition with depth in the sediment core. The comparison of wet to dry ratio is displayed for each of the cores in figure 5.2.

5.2.1 Percentage water

The variation of moisture content with depth in each sediment core is displayed in figure 5.1. The profile of LT1 shows that the moisture content is highest at the surface section, 0-1 cm depth, and decreases in the underlying sections. Two more slight elevations can be noted at 6-7 cm and 12-13 cm depth though overall the moisture content decreased more gradually with depth after the initial drop. The profiles of LT2 and LT3 have similar trends with depth, with an initial decrease in the moisture content over the near surface sections of sediment. The moisture content ranges from 60 % to 80 %.

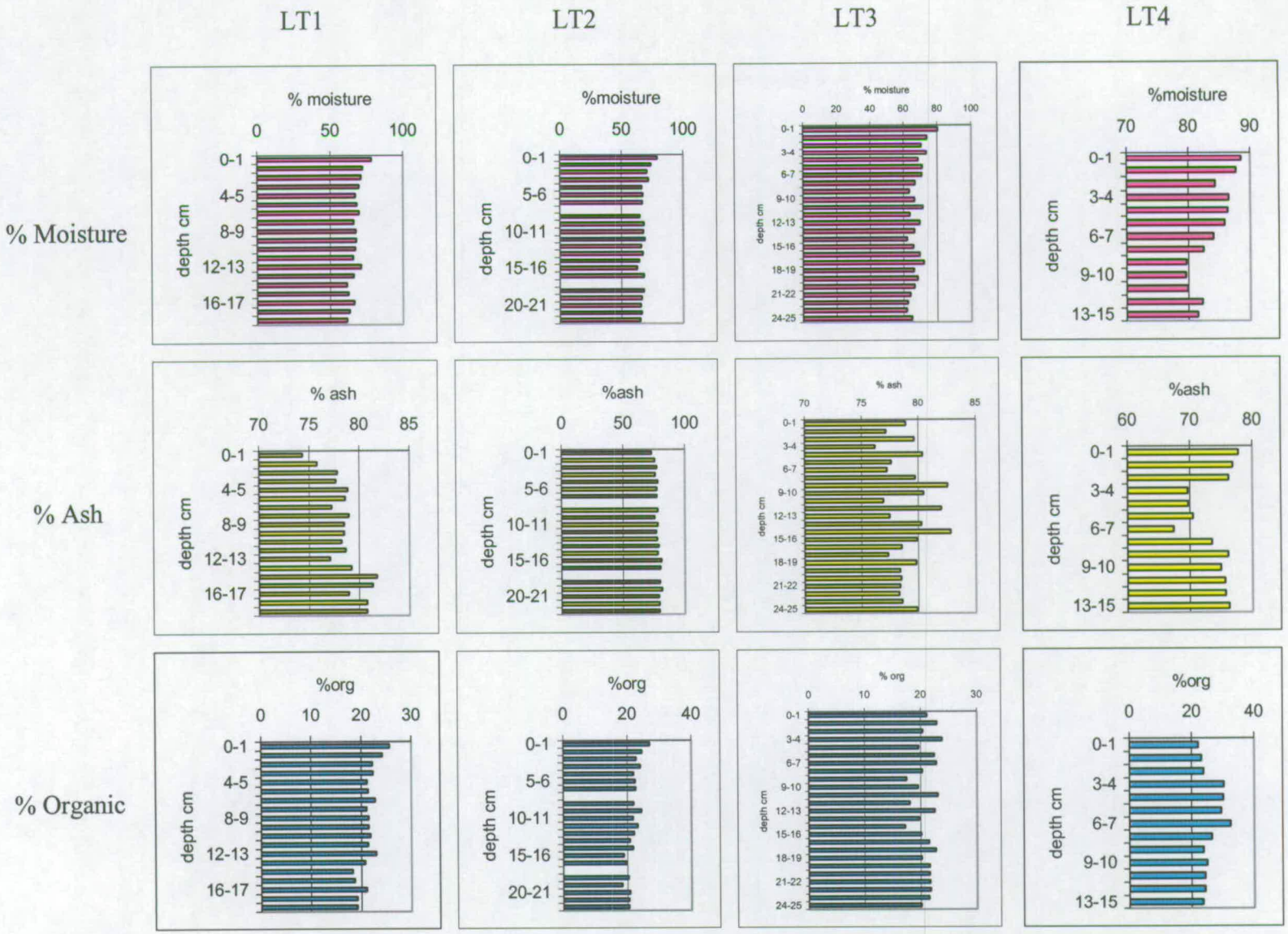

Figure 5.1 Profiles of variation with depth in the sediment of the moisture content as %total sample, organic and ash contents as %dry sediment for Loch Tay cores LT1-4

The fine sectioned, shorter core LT4 shows the decrease in the near surface sections more clearly and with greater resolution, figure 5.1. Decreases from 88 % moisture to 76-79 % occurred rapidly over the 0.0-1.8 cm region. At 2.8 cm depth in the LT4 profile, the moisture content increases slightly once again and an additional broad peak can be observed over 0.8-1.4 cm.

5.2.2 Wet/dry ratio

The depth profiles of wet/dry ratio in the sediment are shown in figure 5.2 and the decrease in moisture content with increasing depth can be clearly observed. The long cores of LT1-3 all had similar profiles with the maximum values of 4.6-5.0 in the surface section. This dropped rapidly with depth, peaking slightly at 6-7 cm. This was followed by a broader shallow peak over 8-11 cm, in the case of LT3 two sharper peaks were found at this point, with a final peak at 17 cm depth.

The shorter core generally had a higher wet/dry ratio value than the longer cores, with a range of 5-9, and the decrease over the upper 3 cm was displayed much more dramatically. The ratio values dipped sharply at 0.5 cm depth before peaking over 0.7-1.1 cm and then decreasing with depth once again to level off at 1.7 cm depth.

5.2.4 Organic matter – loss on ignition

Overall the sediment of the Loch Tay cores consisted of 19-28 % organic material as seen from the diagrams in figure 5.1. The organic component was greatest in the surface section and initially decreased with depth. The amount organic material then appeared to be fairly steady with depth with only slight peaks at 6-7 cm and 12-13 cm depth. At 14-15 cm depth the percentage value for organic material then dropped sharply to 19 %. Similar patterns were seen for LT2 and LT3 sediment cores but the longer cores revealed a slight increase again at depth, to 22% over 20-24 cm depth. Examination of

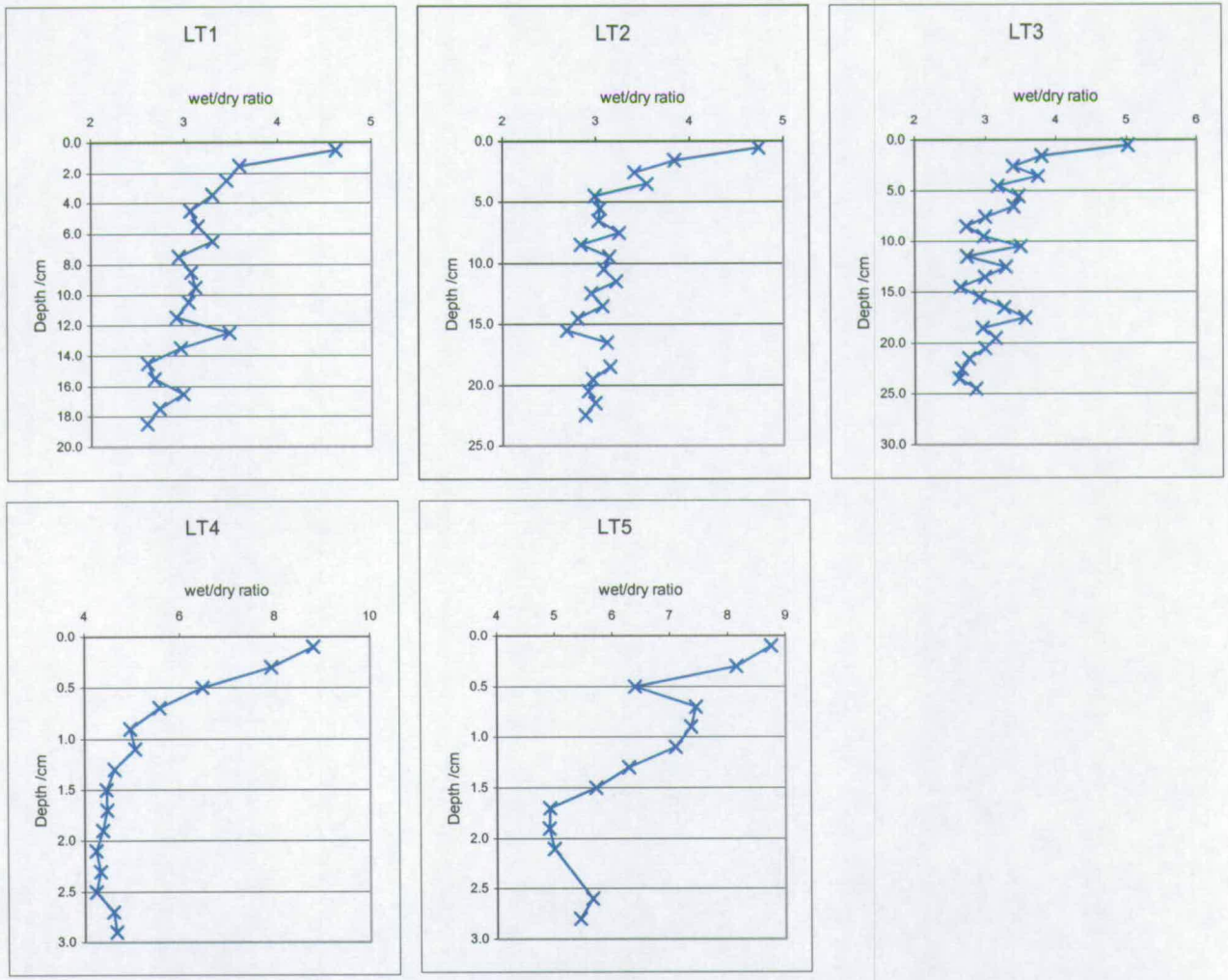

Figure 5.2 Profiles of variation with depth in sediment of the wet/dry ratio values for Loch Tay sediment cores LT1-5

the shorter, fine-sectioned core showed that the organic content of the sediments decreased slightly on approach to the sediment-water interface. In core LT4 the decrease occurs deep in the core and affects more sediment sections ranging from 0.0-0.8 cm depth.

5.3 Pseudo-total concentrations of elements in sediments from Loch Tay, NE Scotland

Figures 5.3-5.7 contain the elemental profiles of redox active elements, trace elements, major cations and non-metallic elements for cores LT1, 2, 3 and the duplicate analysis of LT3.

5.3.1 Long cores: redox active elements, Mn and Fe

Figure 5.3 shows the variation in with depth of pseudo total Fe and Mn in core LT1. The concentration of Fe decreased gradually from 9.66% (w/w) at the surface to a minimum value of 5.04% at a depth of 17-18 cm. The concentration of Mn also decreased with depth but much more dramatically from 1.68% at the surface to 0.15% at a depth of 15-16 cm.

The sediment of LT2 also had a decreasing Fe concentration with depth, as shown in figure 5.4. The maximum value of 8.89% (w/w) was found at the sediment water interface, the concentration then decreased to the minimum value of 4.57 % at 17-18 cm depth. As for the previous core the Mn profile again shows a rapid decrease from the surface maximum of 1.29% (w/w) to the minimum value of 0.10 % at 21-22 cm depth.

Figure 5.5 contains the profiles of redox active elements for core LT3. The concentration of pseudo-total Fe decreased from the surface maximum of 9.46 % (w/w) to the minimum of 4.86% at 22-23 cm depth with an additional peak at 10-11 cm. The Mn concentration decreased rapidly from the surface peak of 1.97 % to a minimum value of 0.13 % at 21-22 cm depth.

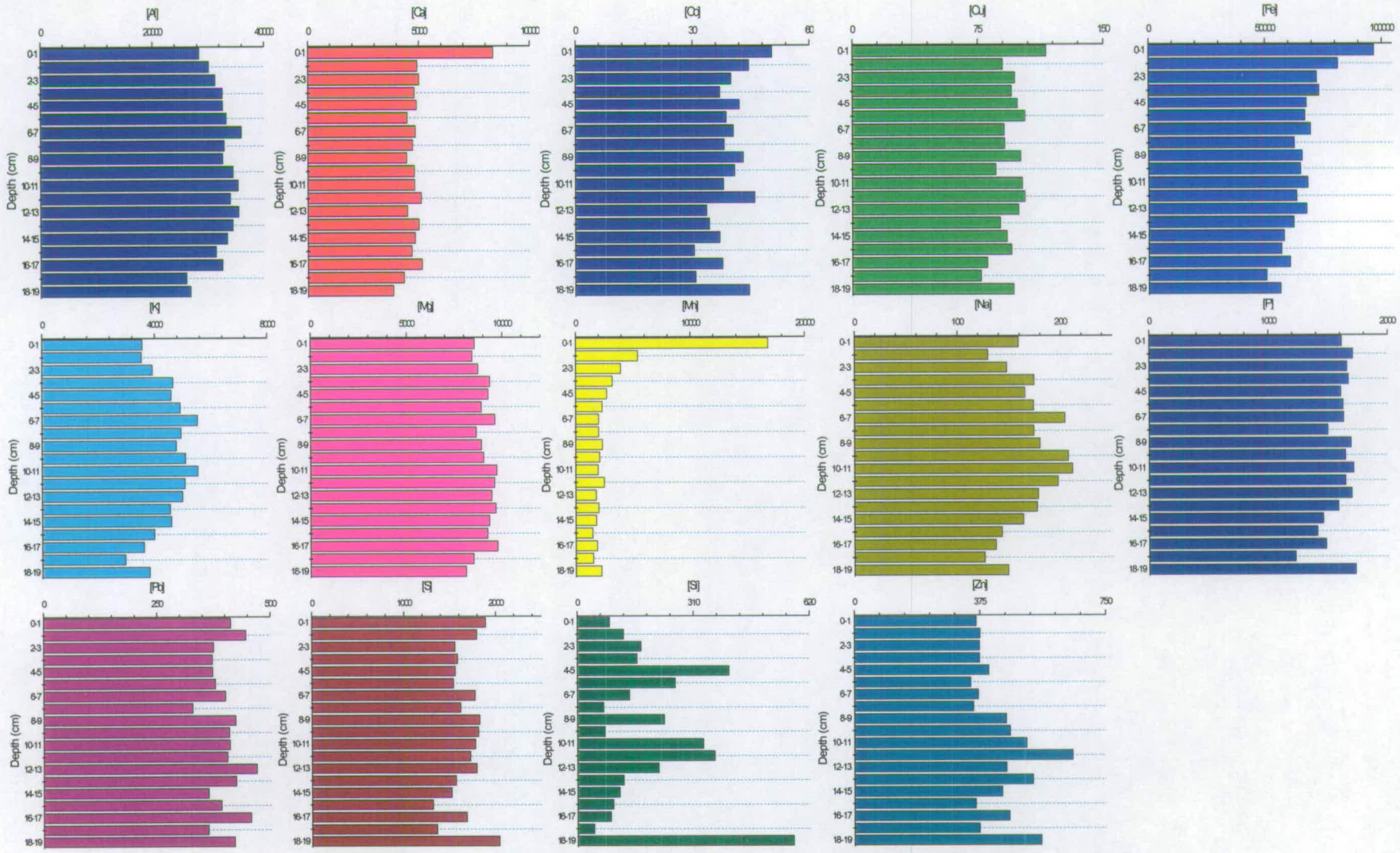

Figure 5.3 Loch Tay core LT1 pseudo total metal concentration with depth in sediment in mg/kg

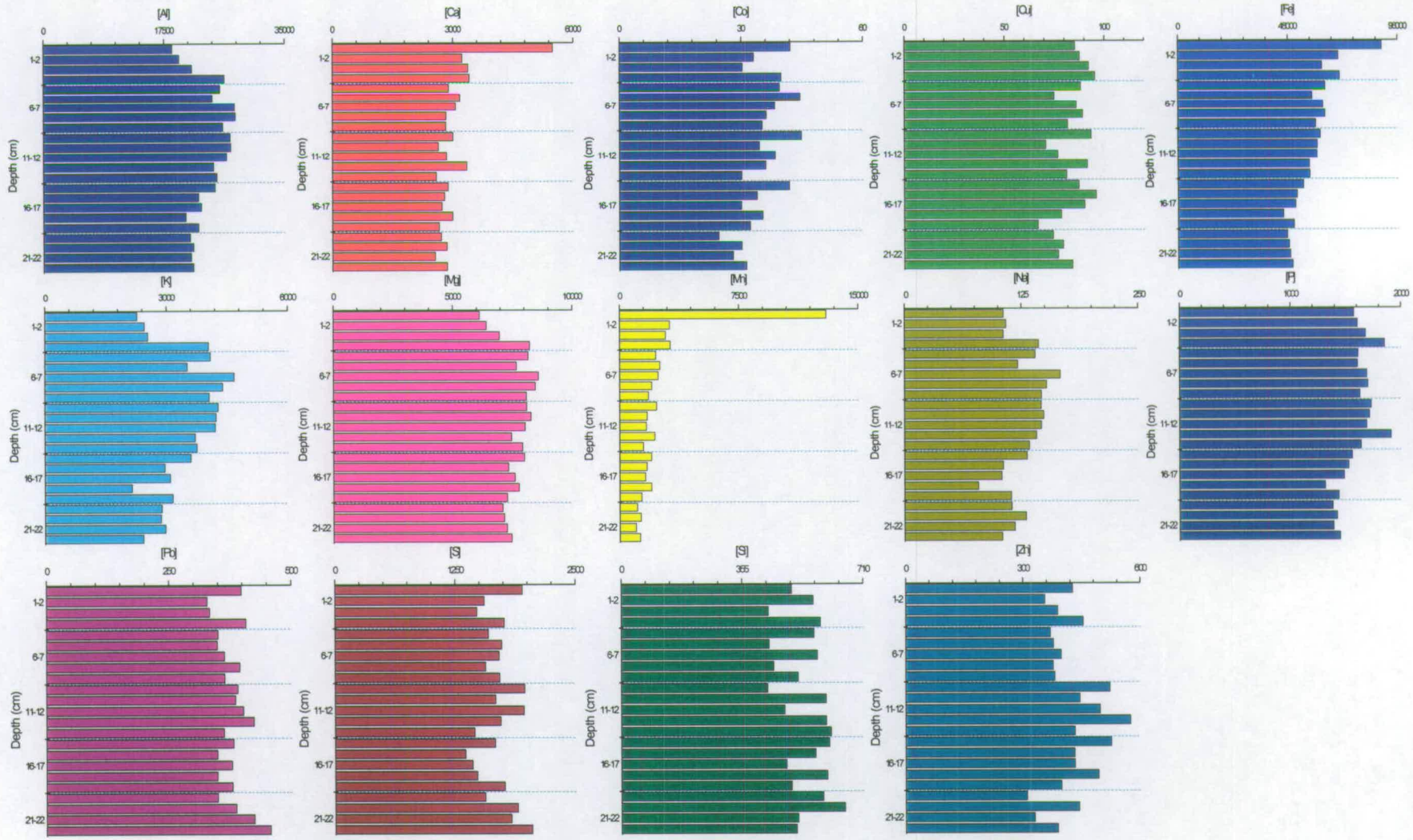

Figure 5.4 Loch Tay core LT2 pseudo total metal concentration with depth in sediment in mg/kg

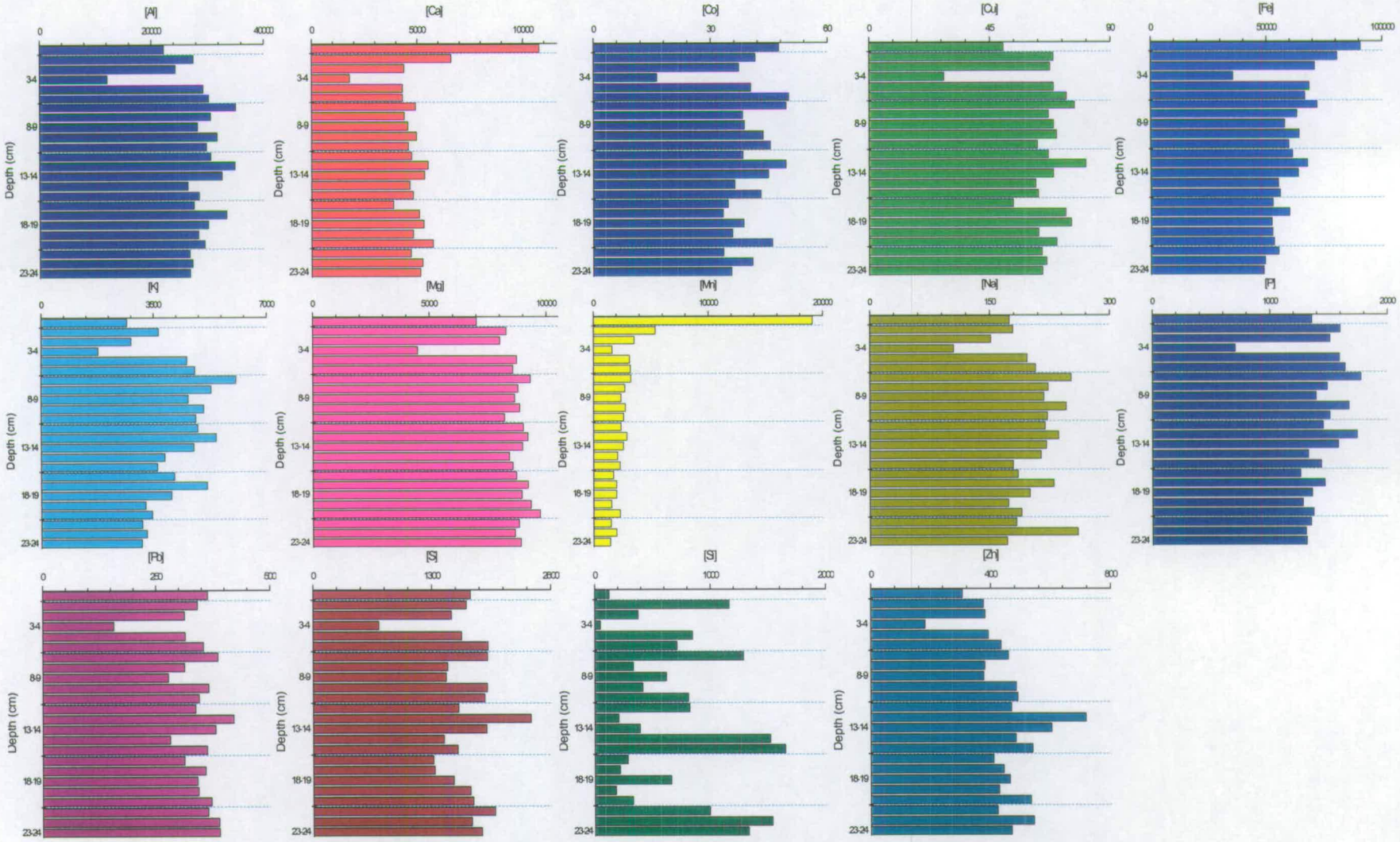

Figure 5.5 Loch Tay core LT3 pseudo total metal concentration with depth in sediment in mg/kg

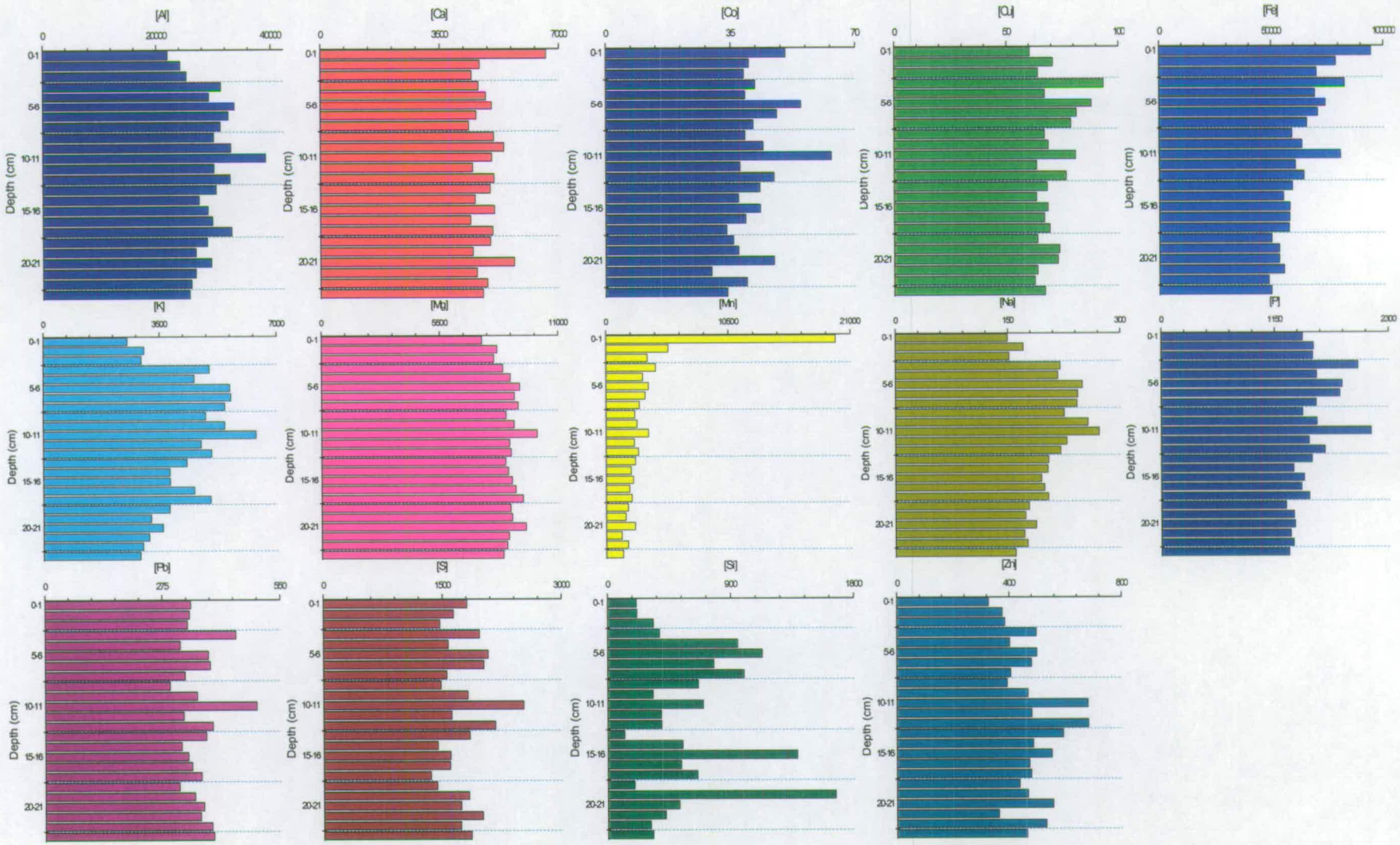

Figure 5.6 Loch Tay core LT3 duplicate pseudo total metal concentration with depth in sediment

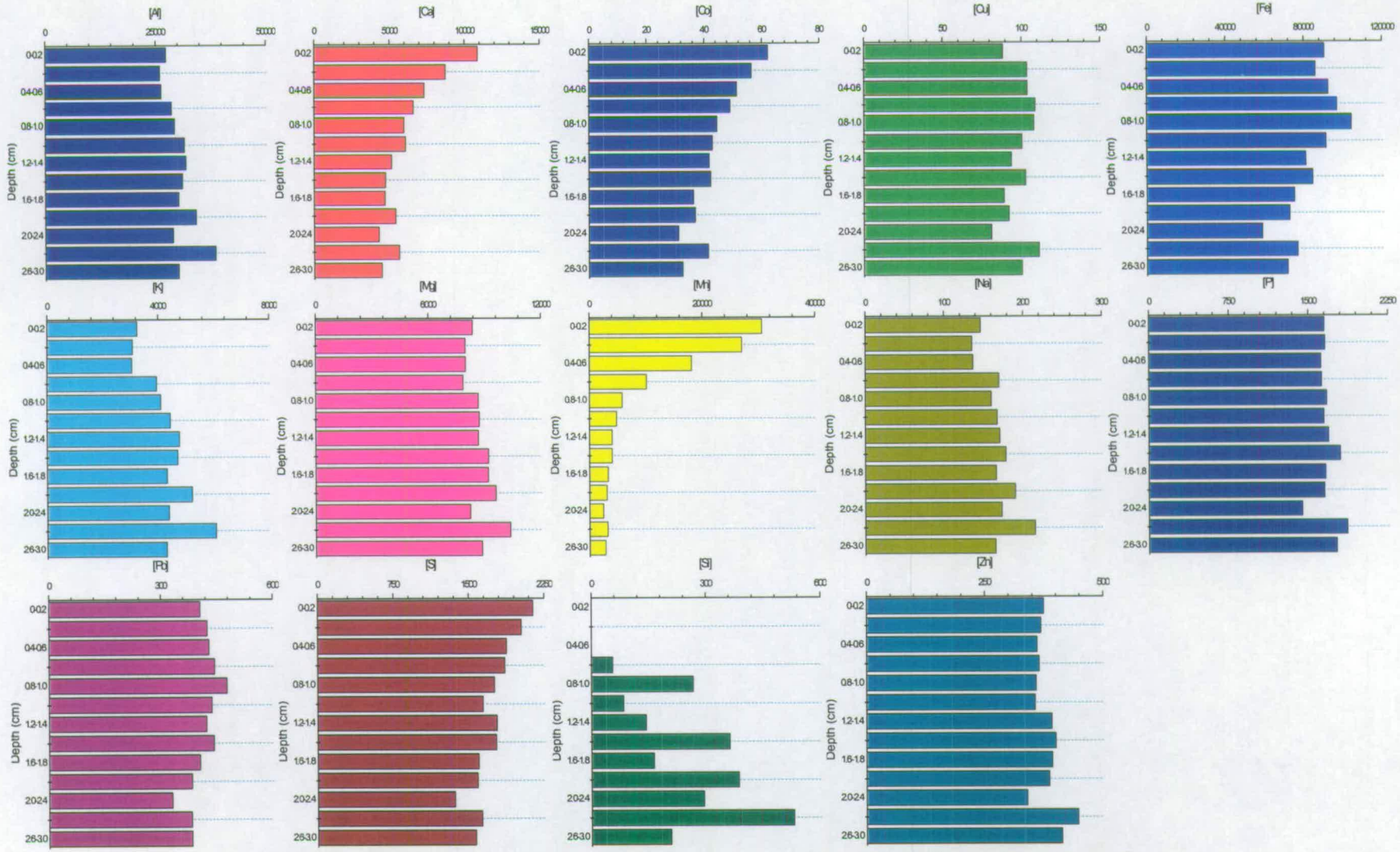

Figure 5.7 Loch Tay core LT4 pseudo total metal concentration with depth in sediment in mg/kg

5.3.2 Short cores: redox-active elements, Mn and Fe

The fine sectioned sediment of core LT4, found in figure 5.7, shows the concentration of Fe increasing from the surface section to a maximum of 10.4% (w/w) at 0.8-1.0 cm and then decreasing with depth. The minimum value of 5.84 % can be seen at 2.0-2.4 cm. The Mn concentration decreased rapidly with depth from the surface maximum of 3.06 % (w/w) to a minimum of 0.24 % at 2.0-2.4 cm.

5.3.3 Long cores: trace heavy elements, Pb, Cu and Zn

The concentration of Pb in the profile of core LT1 remained fairly steady with depth with only slight sub-surface peaks at 1-2 cm, 12-13 cm and 16-17 cm depth. The concentration ranged from 470 mg/kg at 12-13 cm to 328 mg/kg at 7-8 cm depth. The profile of Cu for core LT1, shown in figure 5.3, also shows a fairly steady concentration with depth. The range of concentration found was 116 mg/kg at the surface to 76.9 mg/kg at 17-18 cm depth and slight elevations in concentration were found at 5-6 cm and 10-13 cm. Although remaining fairly constant with depth, the Zn concentration within the sediments of core LT1 was elevated in a broad peak over 8-15 cm with a maximum concentration of 651 mg/kg at 11-12 cm depth. The minimum value for Zn concentration was 347 mg/kg and found at 5-6 cm.

The variation of Pb concentration with depth in LT2 was fairly similar to that of the previous core ranging from the near surface minimum of 328 mg/kg to a maximum of 457 mg/kg at a depth of 22-23 cm. The Cu profile for LT2 is shown in figure 5.4 and it can be seen that the concentration remains fairly constant with depth ranging from 66.8 mg/kg at 18-19 cm to a maximum of 95.8 mg/kg at 15-16 cm depth. The profile overall consists of a series of broad shallow peaks over 0-5 cm, 6-9 cm and 12-16 cm and their respective minima. The Zn concentrations in the pseudo-total fraction of LT2 ranged from 310 mg/kg at 19-20 cm to 575 mg/kg at 12-13 cm. Again the maximum concentration was found in a broad peak at depth in the core.

Figure 5.5 displays the trace element profiles of core LT3. The concentration of Pb was fairly constant with depth ranging from a minimum of 293 mg/kg at 8-9 cm to the maximum value of 495 mg/kg at 10-11 cm. There were also two sharp distinct peaks in Pb concentration at 3-4 cm and 10-11 cm depth accompanied by smaller and broader peaks over 5-7 cm and 12-14 cm depth. The concentration of Cu increased slightly from the surface minimum of 60.5 mg/kg to the maximum of 93.3 mg/kg at 3-4 cm depth and thereafter decreased slightly with depth. A broader secondary peak was also noted at 5-8 cm depth. The concentration of Zn generally increased with depth from the surface minimum of 328 mg/kg to the maximum of 628 mg/kg at 12-13 cm depth.

Al showed a slightly curved profile in core LT1 increasing from the surface to a maximum of 3.59 % (w/w) at 6-7 cm and then decreasing with depth to a minimum of 2.61 % (w/w) at 17-18 cm depth. The concentration of Co generally decreased with depth from a surface maximum of 50.4 mg/kg to a minimum of 30.4 mg/kg at 15-16 cm. The concentration of Al in LT2 increased from the surface minimum of 1.87 %(w/w) to the maximum of 2.78 % at 7-8 cm. The concentration then decreased gradually with depth. The profile of Co showed a general decrease with depth. The maximum of 44.8 mg/kg was found at 9-10 cm and the minimum of 24.4 mg/kg at 19-20 cm depth.
The curved profile of Al in LT3 had a minimum of 2.20% at the sediment water interface and the maximum of 3.91 % at 10-11 cm depth. The concentration of Co decreased slightly with depth. The maximum of 63.3 mg/kg was found at 10-11 cm and the minimum of 29.7 mg/kg at 21-22 cm depth.

5.3.4 Short core: trace heavy elements, Pb, Cu and Zn

The profiles for the core LT4 sediments are shown in figure 5.7. The concentration of Pb remained fairly constant over the top 3 cm with the maximum value, within a very broad peak, of 478 mg/kg at 0.8-1.0 cm and a minimum of 331 mg/kg at 2.0-2.4 cm. The profile of Cu also had a broad fairly shallow peak extending from the surface sediment to 1.2-1.4 cm depth thereafter the Cu concentration decreased with depth to peak to

again at the maximum concentration of 111 mg/kg at 2.4-2.6 cm depth. The minimum concentration of 81.0 mg/kg was found further up in the sediment core at 2.0-2.4 cm. The Zn profile also had the minimum concentration of 340 mg/kg at 2.0-2.4 cm followed directly by the maximum value of 448 mg/kg.

The concentration of Al increased slightly with depth from the minimum value of 2.59 % (w/w) at 0.2-0.4 cm to a maximum of 3.86 % at 2.4-2.6 cm. The Co concentration decreased with depth from a surface maximum of 62.2 mg/kg to a minimum of 31.1 mg/kg at 2.0-2.4 cm.

5.3.5 Long cores: alkali earth metals

The Ca concentration within the sediment of core LT1, show in figure 5.3, decreased from the surface maximum of 8340 mg/kg to a minimum of 3840 mg/kg at a depth of 18-19 cm. The profile of K was curved increasing from the surface to a maximum of 5530 mg/kg at 10-11 cm and then decreasing with depth to a minimum of 2960 mg/kg at 17-18 cm. The concentration of Mg down the sediment core remained fairly constant ranging from 9740 mg/kg to 8090 mg/kg. The Na, like the K profile, also had a curved profile increasing from the surface to a maximum of 211 mg/kg at 10-11 cm and then decreasing with depth to a minimum of 126 mg/kg at 17-18 cm.

The concentration of Ca in the sediment of core LT2 (Figure 5.4) decreased from the surface maximum of 5490 mg/kg to a minimum of 2560 mg/kg with depth. The profile of K had a concentration increasing from the surface to a maximum of 4670 mg/kg at 6-7 cm and then decreasing with depth. The minimum of 2150 mg/kg was found at 17-18 cm depth. The concentration profile of pseudo-total Mg had a surface minimum of 6130 mg/kg and increased to a maximum of 8590 mg/kg at 6-7 cm. The concentration then remained steady with depth. The Na concentration was fairly constant with depth but had a peak, of maximum concentration 166 mg/kg, at 6-7 cm depth and a minimum concentration of 78.8 mg/kg at 17-18 cm.

The concentration of core LT3 Ca ranged from 66.3 mg/kg at the surface to 4350 mg/kg at 7-8 cm, as shown in figure 5.5. The depth profile of K increased from a surface minimum of 2530 mg/kg to a maximum of 6390 mg/kg at 10-11 cm and thereafter decreased with depth. The concentration of Mg increased from a surface minimum of 0.74% and remained fairly constant with depth with a shallow maximum of 1.00% at 10-11 cm depth. The concentration of Na also increased from a surface minimum of 150 mg/kg to the maximum of 272 mg/kg at 10-11 cm but then decreased with depth.

5.3.6 Short core: alkali earth metals

The fine sections of core LT4 (Figure 5.7) show a more gradual decrease of Ca concentration over the top 3 cm. The concentration dropped from the surface maximum of 1.09 % to a minimum of 0.43% at 2.0-2.4 cm depth. Conversely the K concentration increased slightly with depth from a minimum of 3050 mg/kg at 0.4-0.6 cm to a maximum of 6080 mg/kg at 2.4-2.6 cm depth. The concentration of Mg also increased slightly with depth from the minimum value of 0.79% at 0.6-0.8 cm to a maximum of 1.04% at 2.4-2.6 cm. Again the same pattern is seen for Na with a minimum of 135 mg/kg at 0.2-0.4 cm and a maximum of 215 mg/kg at 2.4-2.6 cm depth.

5.3.7 Long cores: non-metal elements

The P concentration of core LT1 sediment, displayed in figure 5.3, remained fairly constant with depth ranging from 1230-1730 mg/kg. The concentration S had a similar profile with depth and ranged from 1310 mg/kg at 15-16 cm to 2040 mg/kg at 18-19 cm depth. The profile of Si was more variable with peaks at 4-5 cm and 11-12 cm depth. The maximum concentration of 577 mg/kg occurred at 18-19 cm and the minimum of 44.1 mg/kg was just above at 17-18 cm.

The profiles of non-metal concentration with depth for core LT2 are shown in figure 5.4. It can be seen that P concentration remained fairly constant with depth peaking slightly at 1910 mg/kg at 12-13 cm and with a minimum value of 1310 mg/kg at 17-18 cm

depth. The concentration of S had a rather variable profile with a minimum of 1360 mg/kg at 15-16 cm and a maximum of 2050 mg/kg 22-23 cm. The concentration of Si was very variable with depth but had no clear trend. The values ranged from 430 mg/kg at 9-10 cm to a maximum of 657 mg/kg at 20-21 cm.

The concentration of P in core 5 sediments, as shown in figure 5.5, was fairly constant with depth. The maximum concentration of 2120 mg/kg occurred at 10-11 cm and the minimum of 1260 mg/kg was at 18-19 cm depth. The S concentrations were variable with depth and the minimum concentration of 1350 mg/kg was at 17-18 cm with the maximum value of 2520 mg/kg occurring higher in the sediment at 10-11 cm. The concentration of Si peaked at 5-6 cm and 15-16 cm and the maximum value of 1670 mg/kg was at 19-20 cm. The minimum value of 122 mg/kg was found at 13-14 cm.

5.3.8 Short cores: non-metal elements

The concentrations of P in the sediments of core LT4 (Figure 5.7) remained fairly constant with depth ranging from 1440-1860 mg/kg. The concentration of S decreased with depth from the surface maximum of 2140 mg/kg to a minimum of 1360 mg/kg at 2.0-2.4 cm depth. Si remained undetectable in the pseudo-total extract until the minimum value of 55.6 mg/kg at 0.6-0.8 cm depth. The concentration then increased rapidly with depth to a maximum of 531 mg/kg at 2.4-2.6 cm.

5.4 Concentrations of elements in the easily reducible fraction of the sediments from Loch Tay, NE Scotland

5.4.1 Long cores redox-active elements, Mn and Fe

Figure 5.8 shows the readily reducible profiles of Fe and Mn for core LT1. The Fe concentration increased with depth from a minimum of 915 mg/kg at 9-10 cm to the maximum concentration of 2400 mg/kg at 18-19 cm. There was also a small peak at

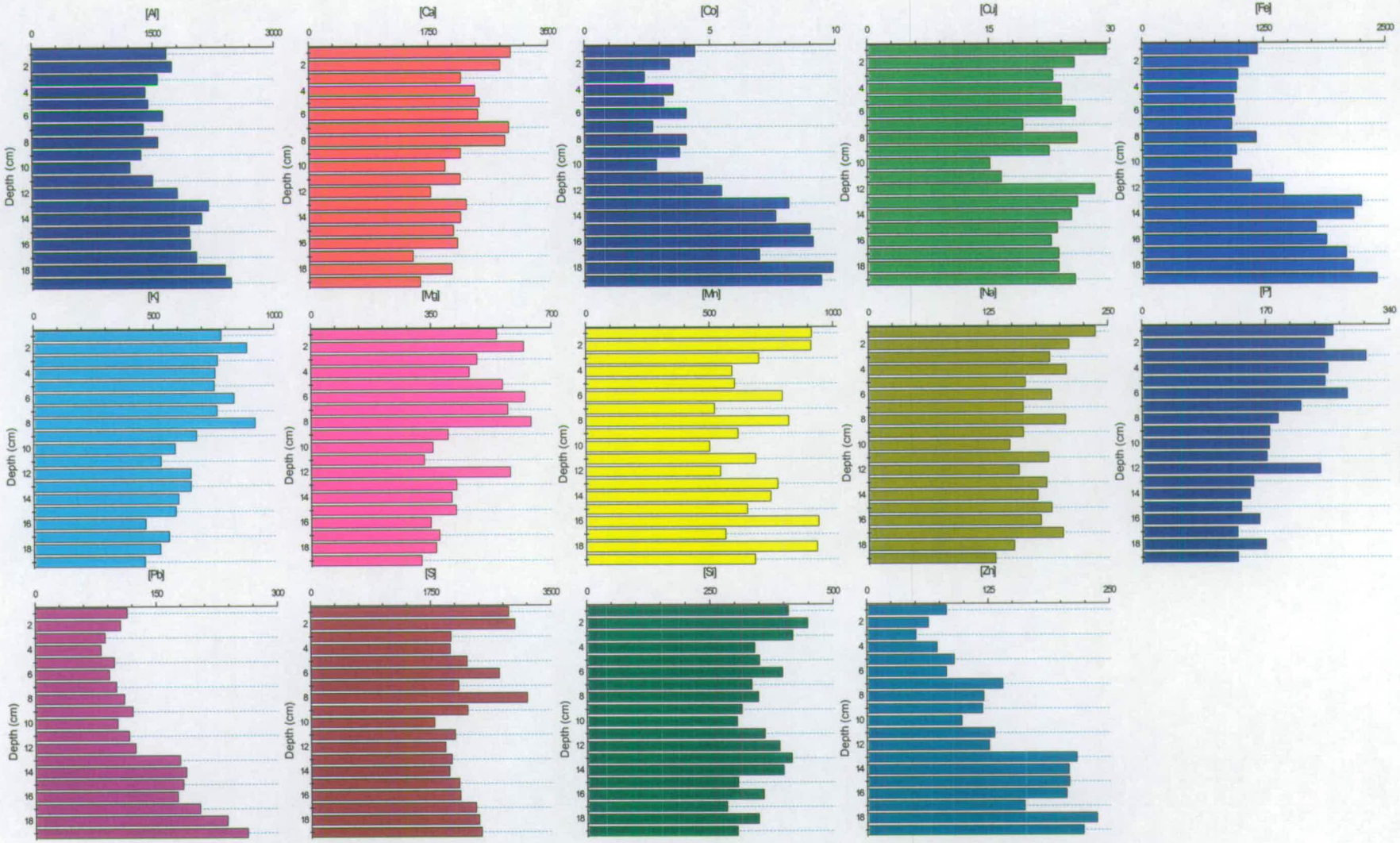

Figure 5.8 Loch Tay core LT1 readily reducible metal concentration with depth in sediment in mg/kg

7-8 cm depth. The Mn concentrations were very variable with depth ranging from 499 mg/kg at 9-10 cm to 941 mg/kg at 15-16 cm but with no clear trends.

The Fe concentration within core LT2 spiked from the surface minimum value of 0.011% to a maximum of 3.47% at 1-2 cm, as shown in figure 5.9. The concentration then dropped rapidly and remained fairly constant with small peaks at 11-12, and 17-18 cm depth. The Mn followed a similar pattern but was offset slightly with the minimum concentration of 0.009% at the surface but the maximum of 1.53% was found at 2-3 cm depth. The two other peaks were found, as for the Fe profile but the positions were slightly different, at 11-12 and 19-20 cm depth.

The concentration of Fe in core LT3 (Figure 5.10) decreased from the surface maximum of 3980 mg/kg to the minimum value of 889 mg/kg at 18-19 cm depth. The concentration then spiked to nearly the maximum value at 19-20 cm and decreased thereafter. The Mn profile follows the same trend with more dramatic decreases with depth. The minimum value of 0.037% occurred at 15-16 cm and the maximum of 1.95% was found at depth at 19-20 cm.

5.4.2 Comparison with pseudo-total concentrations of Mn and Fe

Figure 5.11 contains the profiles of the readily reducible concentrations of Fe, Mn, Pb, Cu and Zn for Loch Tay cores LT1-2 and LT3 expressed as a percentage of the total concentration. The profile for Mn for LT1 shows an increase in the proportion of the readily reducible fraction with increasing depth with values ranging from 5 % to nearly 70 %. The profile of LT2 and LT3 are fairly similar but differ from LT1. Elevations in the percentage value were notable near the surface section and also near the base of the core with values ranging from 20 % to 100 % of the total concentration.

The percentage profiles of Fe for the three cores are all very different. The profile for LT1 remained steady at 1.3 % down to 10-11 cm depth and then increased steadily with depth to 4 % at 18-19 cm. The percentage of total Fe in the readily reducible fraction at the surface of core LT2 was negligible but there was a sudden increase in the section below to 5 %. Thereafter the percentage value remained very low with a sharp peak to

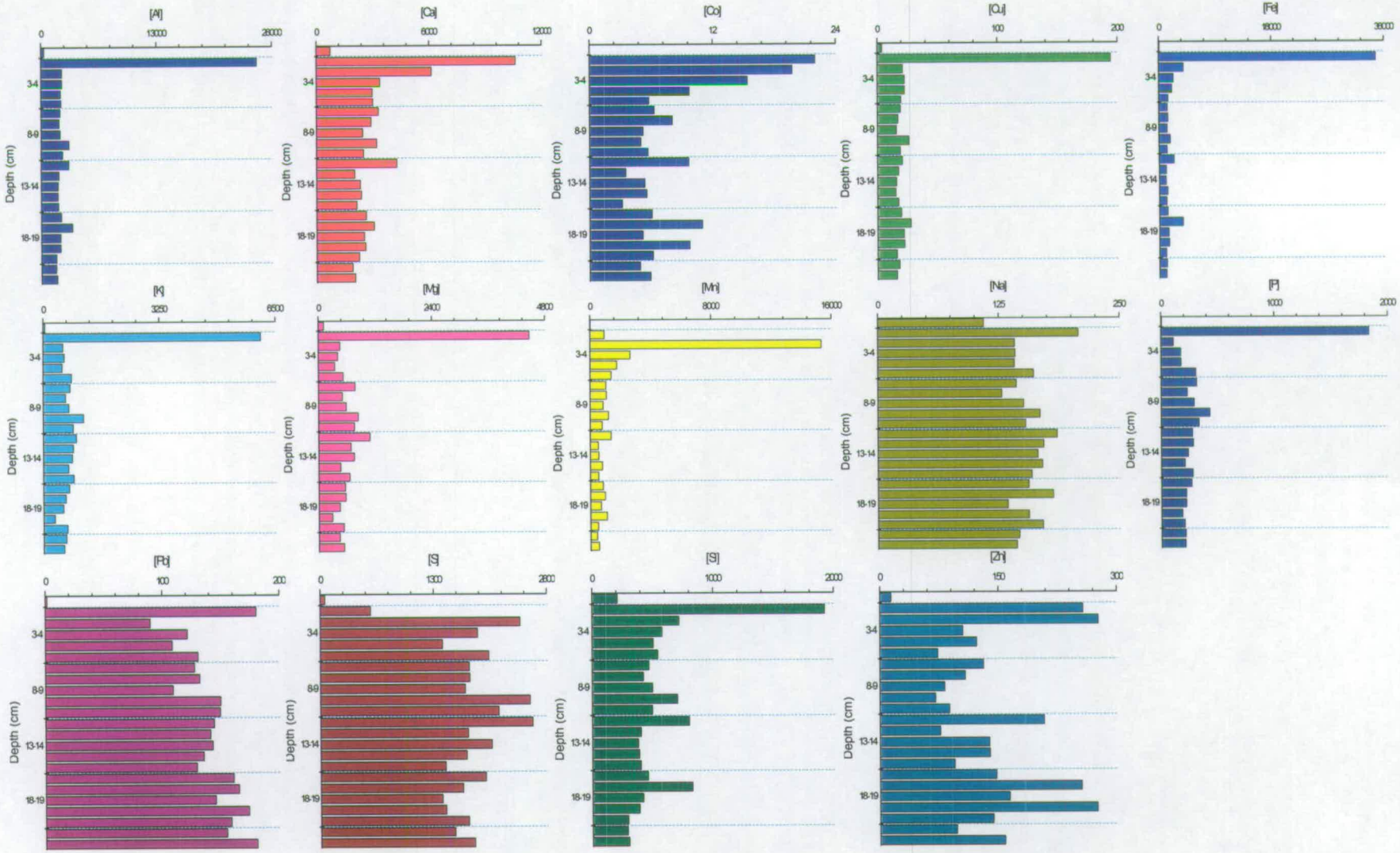

Figure 5.9 Loch Tay core LT2 readily reducible metal concentration with depth in sediment in mg/kg

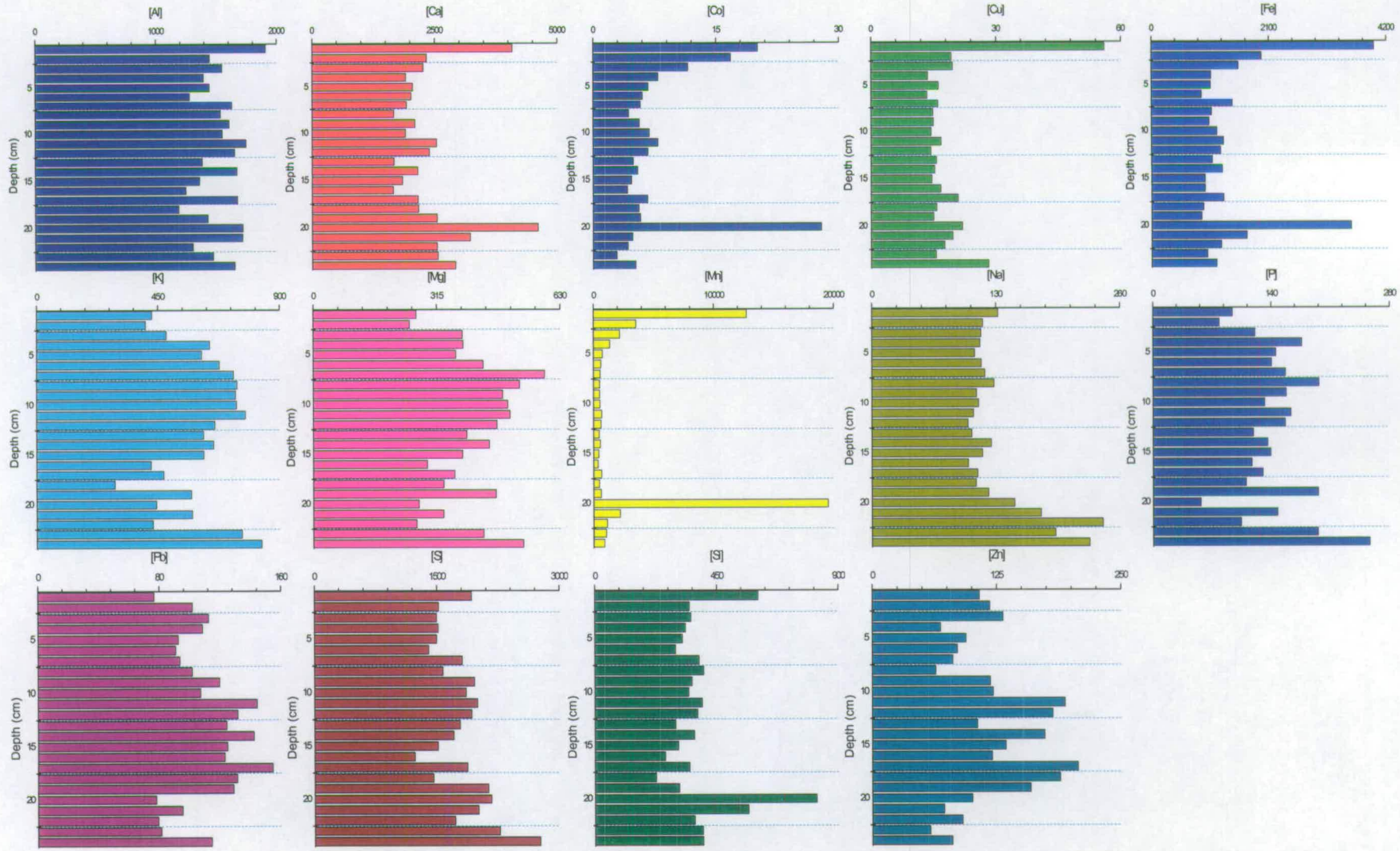

Figure 5.10 Loch Tay core LT3 readily reducible metal concentration with depth in sediment

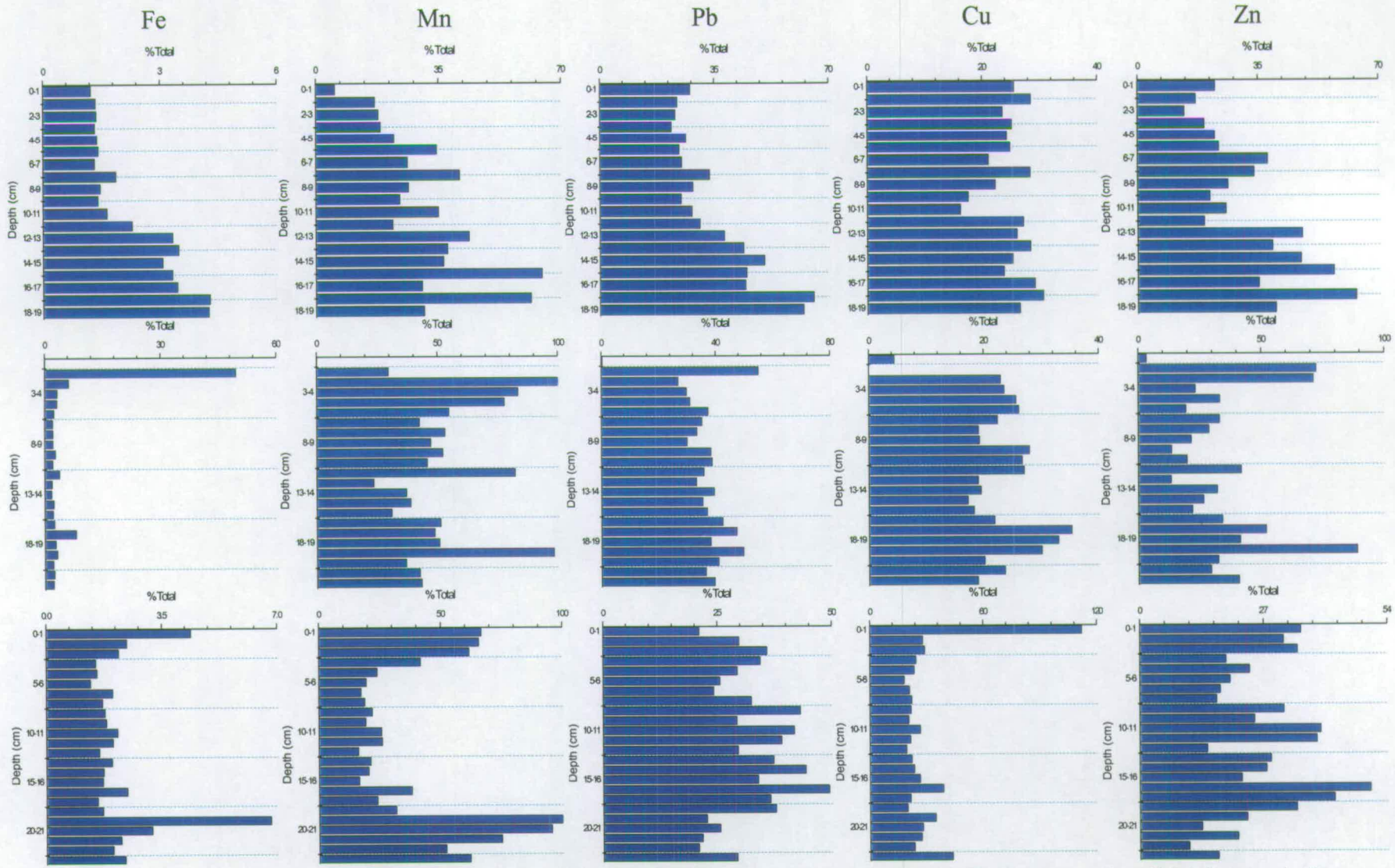

Figure 5.11 Profiles of readily reducible concentration of Fe, Mn, Pb, Cu and Zn for LochTay cores LT1-3 expressed as % total concentration

1 % at 17-18 cm depth. The core LT3 profile showed a surface peak of 4 % followed by a rapid decrease to nearly 2 %. Thereafter the value remained steady apart from a sharp spike to 7 % at 19-20 cm.

5.4.4 Long cores: trace heavy elements Pb, Cu and Zn

The readily reducible concentration of Pb in sediments from LT1 (Figure 5.8) increased with depth down the core from a minimum of 81.5 mg/kg at 3-4 cm to the maximum of 262 mg/kg at 18-19 cm. The concentration of Cu down the sediment core LT1 remained fairly constant with depth with a maximum value of 29.6 mg/kg. There was a significant trough, to a minimum of 15.1 mg/kg, at 9-10 cm. The Zn profile followed a similar pattern with a minimum of 50.6 mg/kg at 2-3 cm and the maximum of 236 mg/kg at 17-18 cm.

The results from core LT2, displayed in figure 5.9, showed that the concentration of Pb was variable with a peak following the surface minimum of 6.02 mg/kg. The maximum concentration of 180.6 mg/kg was found at 24-25 cm. The Cu concentration increased sharply from surface minimum of 3.82 mg/kg to the maximum value of 194.3 mg/kg at 1-2 cm. The concentration then dropped rapidly and steadied out with peaks at 9-10 cm and 17-18 cm depth. The profile of Zn was very variable with the maximum concentration of 277 mg/kg at 2-3 cm and peaks at11-12 cm, 17-18 cm and 19-20 cm depth. The minimum of 14.2 mg/kg occurred at the sediment water interface.

The concentration of Pb, in the readily reducible fraction extracted from LT3 (Figure 5.10), increased from a surface minimum of 76.6 mg/kg to a maximum of 155 mg/kg at 16-17 cm. The concentration then dropped back to near the minimum value. The profile of Cu for core LT3 had a surface spike of 56.0 mg/kg, which was the maximum concentration found in the core. The concentration then remained fairly stable near the minimum value of 13.4 mg/kg which occurred at 5-6 cm depth. A small peak was found at a depth of 23-24 cm. The concentration of Zn generally increased with depth to

maximum of 207 mg/kg at 16-17 cm and then decreased with depth to minimum of 58.2 mg/kg at 22-23 cm.

The concentration of Al in the readily reducible extract from LT1, as shown in figure 5.8, increased only slightly with depth ranging from a minimum value of 1220 mg/kg at 9-10 cm to a maximum of 2460 mg/kg at 18-19 cm. The concentration in the profile of Co increased more significantly with depth from 2.402 mg/kg at 2-3 cm to 9.87 mg/kg at 17-18 cm depth.

The concentration profile of Al, like the Cu in core LT2 (Figure 5.9), had a sharp peak of 2.43% following the surface minimum of 323 mg/kg. The concentration then decreased rapidly with depth with peaks at 9-10cm and 17-18 cm depth. The concentration of Co in the first section remained below the detection limit of the instrument. The maximum concentration of 22.0 mg/kg followed at 1-2 cm and the concentration decreased with depth to a minimum of 3.18 mg/kg at 15-16 cm.

The LT3 readily reducible concentration of Al shown in figure 5.10 was fairly constant with depth ranging from 1190-1910 mg/kg. Co generally decreased from a surface peak to a minimum of 2.89 mg/kg at 22-23 cm. A peak occurred at 10-11 cm depth and there was a maximum of 27.8 mg/kg at 19-20 cm.

5.4.5 Comparison with pseudo-total concentrations of Pb, Cu and Zn

The profiles of readily reducible Pb, Cu and Zn, for cores LT1, 2 and 5, expressed as a percentage of the total concentration are shown in figure 5.11. The similarity of the Pb and Fe percentage profiles for LT1 was clearly observable with the Pb profile remaining fairly constant down to 10-11 cm depth at 23 % and then increasing gradually with depth to nearly 70 % at 17-18 cm. The percentage of the total Cu found in the readily reducible fraction remained fairly constant with depth at 23 % with a drop in value to 16 % at 10-11 cm depth. The profile of Zn was similar to those of Fe and Cu discussed previously, with a generally increasing value with depth and a sharp drop at 9 cm.

The percentage profile of Pb for core LT2 was fairly uniform with depth with a range of 30-40 %. This value was exceeded at 1-2 cm in a sharp peak to 50 %. The profile of Cu was variable with depth with three broad areas of increased value corresponding to the peaks in the Mn profile. The profile of Zn also bore some resemblance to the profile of Mn with elevated values at 1-3 cm, 11-12 cm and 19-20 cm depth. The percentage value for Zn had a broad range with values of 15-90 %.

The profile of Pb for core LT3 expressed as a percentage of the total concentration had a near surface broad peak over 2-6 cm depth with values peaking at 35 %. An additional area of elevated percentage value was found over 8-19 cm with values reaching 50 %. Thereafter the fraction of the total concentration found in the readily reducible extract dropped sharply and remained low. The Cu profile for core LT3 had a large surface elevation in the percentage value to nearly 100 %. Thereafter the fraction of the total Cu found in the readily reducible phase remained fairly low at 24 %. The profile of Zn was very variable with depth, ranging from 13 % to 52 %, with elevated values at 0-3 cm, 9-12 cm and 17-19 cm depth.

5.4.6 Long cores: alkali earth elements

The concentration of Ca in core LT1, shown in figure 5.8, decreased slightly from the surface maximum of 2950 mg/kg to a minimum of 1520 mg/kg at 16-17 cm. The profile of K remained fairly steady until the maximum concentration of 921 mg/kg at 7-8 cm and then decreased to the minimum of 462 mg/kg at 18-19 cm. The LT1 readily reducible Mg concentration generally decreased with depth with a peak at 11-12 cm. The maximum concentration of 640 mg/kg occurred at 7-8 cm and the minimum of 321 mg/kg was at 10-11 cm. The profile of Na decreased from the surface maximum of 237 mg/kg to the minimum of 131.76 mg/kg at 18-19cm.

From figure 5.9 it can be noted that core LT2 had a surface minimum Ca concentration of 0.074% and a maximum of 1.06% at 1-2 cm depth. The concentration then decreased with depth with a peak at 11-12 cm. The K had a similar near surface profile with a minimum of 47.1 mg/kg and a maximum of 6080 mg/kg. A small peak can be observed

at 9-10 cm depth. The Mg surface minimum concentration of 111 mg/kg was also followed by the maximum concentration of 4460 mg/kg. Again the concentration decreased rapidly before peaking slightly at 11-12 cm depth. The concentration of Na remained fairly constant with depth following the minimum value of 109 mg/kg and the maximum of 207 mg/kg in the top two surface sections.

Figure 5.10 shows the core LT3 Ca profile. The concentration decreased from the surface peak to the minimum of 1660 at 15-16 cm and then increased to the maximum of 4800 mg/kg at 19-20 cm depth. The K concentration in the readily reducible fraction had a broadly curved profile over the top 10 cm and decreased to the minimum concentration of 290 mg/kg at 17-18 cm. The concentration then increased with depth to the maximum of 831 mg/kg at 23-24 cm. The concentration of Mg increased from the near surface minimum of 245 mg/kg to the maximum concentration of 590 mg/kg at 6-7 cm depth. The concentration then generally decreased with depth with a slight peak at 23-24 cm. The concentrations of Na remained fairly constant and near minimum value of 100 mg/kg over top 18 cm. The concentration then increased with depth to the maximum of 242 mg/kg at 21-22 cm.

5.4.7 Long cores: non-metals in sediment

In core LT1, shown in figure 5.8, the concentration of P in the readily reducible extract decreased from a near surface maximum of 308 mg/kg to a minimum of 130 mg/kg at 16-17 cm with a peak at 11-12 cm. The concentration of S remained fairly constant with depth with a maximum value of 3150 mg/kg occurring at 7-8 cm and a minimum of 1800 mg/kg at 9-10 cm. The concentration of Si peaked at a maximum value of 448 mg/kg at 1-2cm and a further peak was found at 12-13 cm depth. The minimum of 283 mg/kg occurred at 16-17 cm depth.

The concentration of P in core LT2, shown in figure 5.9, increased rapidly from surface minimum of 5.02 mg/kg to a maximum value of 1840 mg/kg at 1-2 cm. The concentration the dropped as rapidly to peak slightly again at 9-10 cm depth. The concentration of S increased over the top three sections from the surface minimum of

53.9 mg/kg and remained fairly constant with depth. The maximum concentration of 2430 mg/kg occurred at 11-12 cm. The profile of Si concentration increased from surface minimum of 209 mg/kg to a maximum value of 1920 mg/kg at 1-2 cm depth. The concentration then generally decreased with depth with peaks at 9-10, 11-12 and 17-18 cm depth.

The profile of readily reducible P extracted from sediment of core LT3, shown in figure 5.10, generally increased with depth. The concentration ranged from 56.4 mg/kg at 19-20 cm to 256 mg/kg at 23-24 cm depth. The profile of S remained fairly constant with depth. The concentration increased to a maximum of 2760 mg/kg at 23-24 cm the minimum value of 1230 mg/kg occurred at 15-16 cm. The profile of Si decreased from a surface peak to a minimum of 225 mg/kg at 17-18 cm and then increased to the maximum concentration of 820 mg/kg at 19-20 cm depth.

5.5 Characterisation of pore waters extracted from sediments from Loch Tay, NE Scotland

5.5.1 Organic matter UV-Vis

The depth profiles displayed in figure 5.12 contain the absorbance at 254 nm and the E4/E6 ratio for the pore water for the cores, LT3 and LT4 extracted from the Loch Tay sediment.

The absorbance of the porewater at 254 nm for LT3 is shows that the value of absorbance was very variable with depth ranging from 1.8 to 10. The value at the surface was very low, near the minimum value, but increased with decreasing depth to peak at 3-4 cm depth. The absorbance then decreased again before reaching the maximum value 8-9 cm depth. Thereafter the profile generally decreased with depth apart from a small peak at 18-19 cm depth. The E4/E6 ratio generally followed the shape of the absorbance profile with elevated ratio values coinciding with the peaks in absorbance. The magnitude of variation with depth was smaller for the E4/E6 values ranging from 1.4 to 1.8. There was no peak in the E4/E6 value to correspond with the peak at 18-19 cm

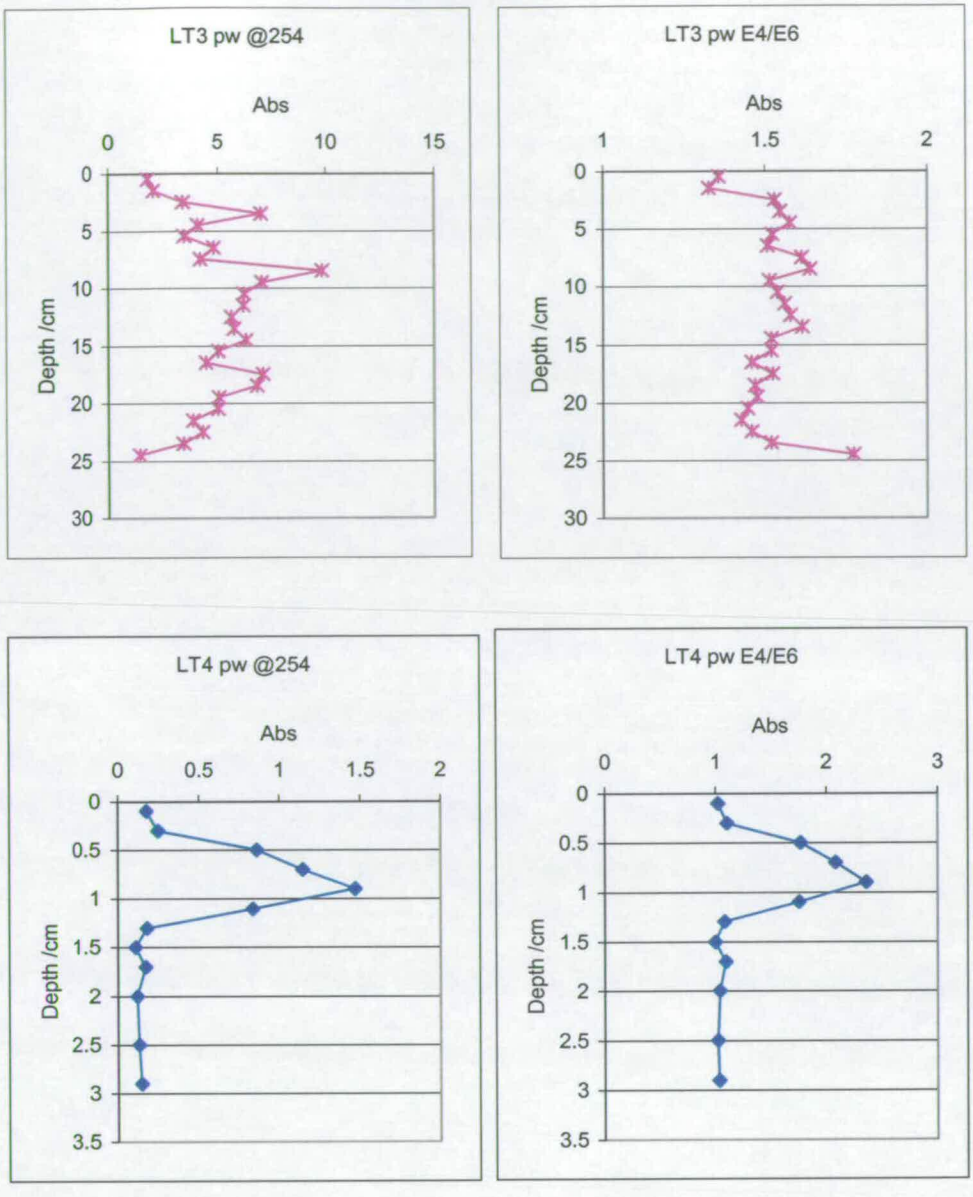

Figure.5.12 Profiles of absorbance at 254 nm and E4/E6 ratio for porewaters from Loch Tay cores LT3-4

depth in the absorbance profile but the ratio value does increase with decreasing depth beyond this point.

The profile of absorbance at 254 nm for the other fine sectioned core, LT4, show a very different picture. A massive near surface peak dominated the profile with a maximum value of 1.55 at 0.8 cm depth. Below this, at 1.5 cm depth, the absorbance value remained low and little variation was noted with decreasing depth. The E4/E6 profile, like that of the previous core, followed the same trend with depth but with a shallower peak.

5.5.2 Redox active elements in pore water

The profile of core LT2, shown in figure 5.13, had an Fe concentration ranging from 0.915 mg/l at 13-14 cm up to 22.8 mg/l at 9-10 cm depth. Overall the profile was slightly curved with a peak at 1-4 cm. The concentration of Mn ranged from the surface minimum of 1.94 mg/l to ~17 mg/l at 11-12 cm depth. Two additional, more broad, peaks in concentration were seen at 4-5 cm and 18-19 cm depth.

Figure 5.13 shows profiles of the porewater metal concentrations of core LT3. Overall the profile of Fe had a very broad curve extending down the length of the core, dotted with sharper peaks in concentration. The concentration ranged from 1.79 mg/l to 52.2 mg/l and three peaks were found at 3-4, 8-9 cm, with the maximum concentration, and 17-18 cm. The concentration of Mn ranged from 0.43 mg/l to 5.90 mg/l. Generally the concentration increased from the surface minimum with two broad peaks at 5-6 and 17-18 and two sharper peaks at 8-9 cm and 24-25 cm depth.

The fine-sectioned detail of core LT4 shows that concentration of Fe increased with depth from the surface minimum of 6.87 mg/l. The maximum value of 25.6 mg/l was found at 0.8-1.0 cm. The concentration of Mn ranged from 0.13 mg/l to 2.53 mg/l at 2.6-3.0 cm depth with two additional sharp peaks at 1.2-1.4 and 1.8-2.2.

The elemental concentrations in porewater extracted from core LT3 were also determined by ICP-OES (Figure 5.14). The concentration of Fe with increasing depth shows a generally curved profile ranging from 13.8 mg/l to 66.4 mg/l. The maximum

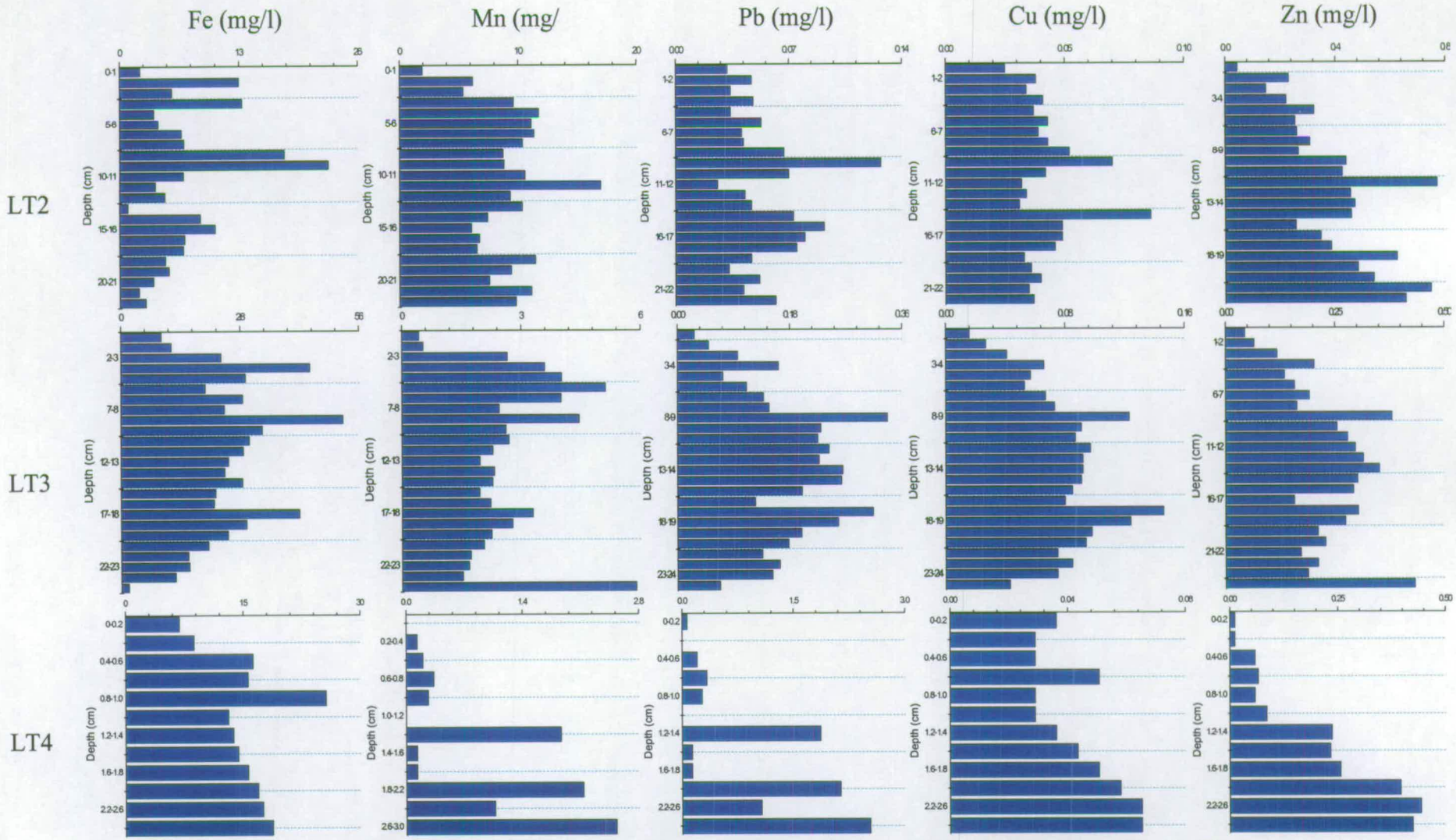

Figure 5.13 Loch Tay cores LT2, LT3 and LT4 pore water total metal concentrations with depth in sediment (Fe, Mn, Pb, Cu and Zn) in mg/l

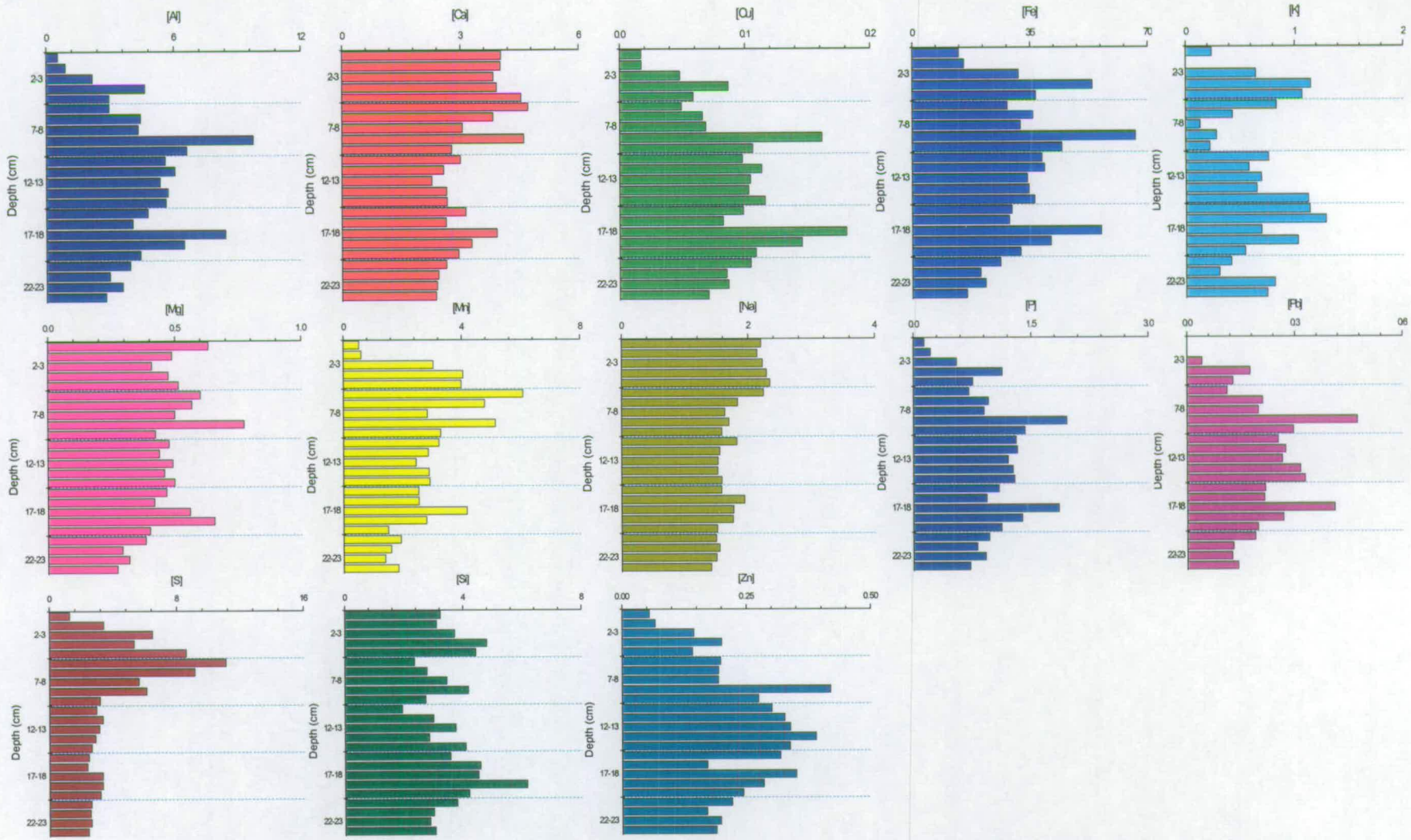

Figure 5.14 Loch Tay core LT3 pore water total metal concentrations with depth in sediment (Al, Ca, Cu, Fe, K, Mg, Mn, Na, P, Pb, S, Si, Zn)

value was found at 8-9 cm with two additional peaks at 3-4 and 17-18 cm depth. The concentration of Mn increased from the surface minimum of 0.527 mg/l to peak at 6.07 mg/l at 5-6 cm depth. The profile then decreased with depth with two further peaks at 8-9 and 17-18 cm.

5.5.3 Trace elements in pore water

Figure 5.13 contains the porewater profiles of trace metals from the LT2 sediment core. The concentration of Pb increased from the surface minimum of 0.026 mg/l and then remained fairly constant with increasing depth. The concentration maximum of 0.127 mg/l was reached at 9-10 cm depth and further peak at 15-16 cm was noted. The concentration of Cu ranged from 0.025 mg/l to 0.086 mg/l within core LT2 pore waters. After the surface minimum the profile was fairly constant with depth apart from the broad peaks at 9-10 cm and 14-15cm, where the maximum concentration was found. The concentration of Zn increased with depth from the surface minimum of 0.044 mg/l and peaked at 0.769 mg/l at 11-12 cm depth.

The concentration profile of Pb, established for the core LT3 porewater (Figure 5.13), had a generally curving profile ranging from 0.027 mg/l at 0-1 cm to 0.337 mg/l at 8-9 cm. Two further smaller peaks were also noted at 3-4 cm and 17-18 cm depth. The concentration of Cu in core LT3 had a very similar distribution to that of Pb with a surface minimum of 0.016 mg/l and the maximum concentration of 0.146 mg/l at 17-18 cm depth. Additional points of elevated concentration were again found at 3-4 cm and 8-9 cm. The distribution of Zn also had a curved profile with a surface minimum of 0.044 mg/l and additional peaks as before but a maximum concentration of 0.432 mg/l was found at 24-25 cm depth.

The fine sections of core LT4 (Figure 5.13) showed that the Pb concentration had a range of 0.067-2.53 mg/l in the porewater and the profile showed strong correlation with that of Mn. The concentration of Cu increased with depth from the surface minimum of 0.029 mg/l to 0.065 mg/l at 2.2-2.6 cm. A strong isolated peak was observed at 0.6-0.8

cm. The Zn concentration increased with decreasing depth from the surface minimum of 0.012 mg/l to the maximum value of 0.443 mg/l at depth of 2.2-2.6 cm.

The ICP-OES data obtained for core LT3, diplayed in figure 5.14, shows that the distribution profile of Pb in the porewater was a gentle curve increasing from the minimum concentration of 0.042 mg/l at 2-3 cm and centred at 13-15 cm depth. The maximum conentration of 0.475 mg/l was found at 8-9 cm and an additional peak was found at 17-18 cm depth. The profile of Cu in the porewater had a very similar shape with increasing concentrations from the surface minimum of 0.0172 mg/l but the maximum value of 0.181 mg/l was at 17-18 cm depth. However there was a sharp elevation of concentration at 8-9 cm as well as at 3-4 cm depth. The shape of the Zn profile was also similar with concentrations ranging from 0.055mg/l at surface to 0.419 mg/l at 8-9 cm.

5.5.4 Additional elements

The profiles of the additional elements analysed by ICP-OES are shown in figure 5.14. The porewater of core LT3 had a Ca profile of decreasing concentration with increasing depth. The maximum value of 4.72 mg/l was found at 5-6 cm and minimum concentration of 2.28 mg/l occurred at 12-13 cm. An additional sharp increase in Ca concentration was noted at 17-18 cm and was followed once again by decreasing concentrations with increasing depth. The concentration of K was very variable, ranging from 0.13 mg/l at 7-8 cm to 1.28 mg/l at 16-17 cm. The maximum conentration was contained within a peak extending over 10-21 cm and was preceded by a sharper peak over 2-7 cm depth. The profile of Mg shows the concentration generally decreasing with depth and ranging from 0.272 mg/l at 23-24 cm to 0.774 mg/l at 8-9 cm. The concentration was slightly elevated at the surface section and an additonal peak was observed at 18-19 cm. The concentration of Na decreased slightly with depth from 2.34 mg/l at 4-5 cm to 1.41 mg/l at 23-24 cm depth.

The distribution of Al with depth in the LT3 porewater produced a curved profile with a surface minimum of 0.537 mg/l and a maximum value of 9.75 mg/l at 8-9 cm. Two additional sharp elevations in concentration were noted at 3-4 cm and 17-18 cm depth. The profile of porewater P concentration curved from the surface minimum of 0.137 mg/l to a maximum of 1.95 mg/l at 8-9 cm and then decreased with depth. Once again additional peaks in concentration were found at 3-4 and 17-18 cm. The S concentration increased rapidly with depth from the surface minimum of 1.25 mg/l to the maximum of 11.1 mg/l at 5-6 cm depth. Thereafter the concentration then decreased with depth. The Si profile was very variable with depth, ranging from 1.941 mg/l at 10-11 mg/l to a maximum of 6.16mg/l at 18-19 cm.

5.6 Loch Tay pore water centrifugal ultrafiltration of LT3

5.6.1 DOC determined by UV-vis spectroscopy for size fractions of Loch Tay porewater LT3

The profile of the DOC concentration in the >30 kDa fraction as determined by the absorbance at 254 nm, is shown in figure 5.15, alongside the profile of the E4/E6 ratio with depth in the sediment core. It can be seen that the absorbance generally decreased with depth from the major peak to a value of 18 at 3-4 cm depth. Additional peaks were noted at 8-9 cm and 18-19 cm and 20-21 cm depth. The trend in the E4/E6 ratio with depth generally followed that of the 254 nm absorbance but the magnitude of change with depth was smaller. Again peaks were observed at 3-4 cm, 8-9 cm and 18-19 cm depth.

5.6.2 Redox-active elements, Mn and Fe in the fractions of porewater from Loch Tay core LT3 after centrifugal ultrafiltration

The concentration of Fe in the >30 kDa fraction generally increased with depth in a broad curve centred at 10-11 cm depth, as shown in figure 5.16. The minimum

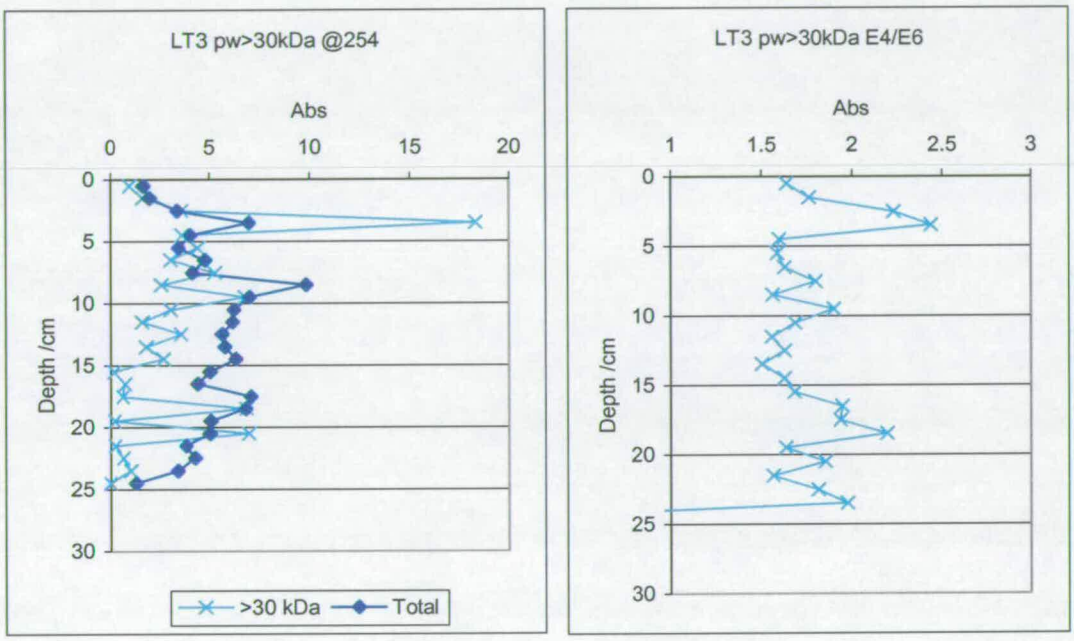

Figure 5.15 Profiles of absorbance at 254 nm and E4/E6 ratio for porewater fraction >30 kDa for Loch Tay core LT3

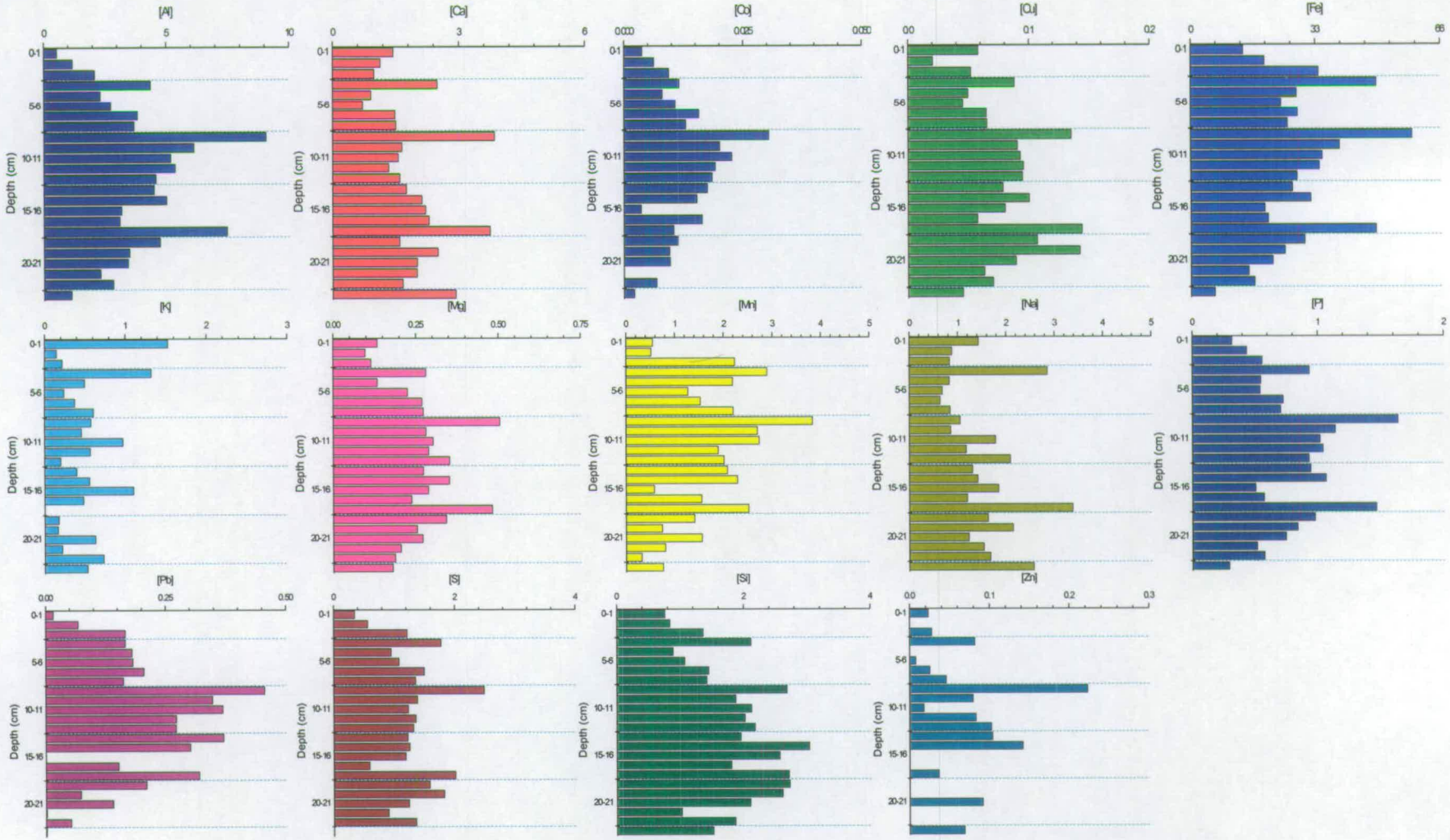

Figure 5.16 Loch Tay core LT5 centrifugal ultrafilter fraction (>30 kDa) metal concentrations with depth in sediment

concentration of ~5 mg/l was found at the base of the core at 23-24 cm depth and the maximum concentration of 58 mg/l occurred at 8-9 cm depth with two additional sharp peaks at 3-4 cm and 18-19 cm depth. The concentration in the 30-1 kDa fraction, shown in figure 5.17, was very low by comparison increasing to ~1 mg/l in a sharp peak at 16-17 cm depth. Thereafter a smaller peak developed at 20-21 cm depth. The concentration of Fe in the <1 kDa fraction (Figure 5.18) was lower still and fairly constant with increasing depth apart from the sharp increase in concentration to ~0.68 mg/l at 7-8 cm depth. The profiles in figure 5.19 show the Fe concentration in each fraction as a percentage of the total porewater Fe concentration as determined in previous experiments. Overall the Fe was primarily found, 60-100 %, in the greater then 30 kDa fraction. The proportion of Fe in the mid size fraction was generally low but increased with depth peaking to 10% at 16-17 cm depth. The truly dissolved Fe decreased from the surface peak of 10 %.

The concentration of Mn in the largest size fraction ranged from 0.5-4.0 mg/l in a profile that was generally curved and centred at 10-11 cm depth, as shown in figure 5.16. Three peaks in the >30 kDa Mn concentration were found at 3-4 cm, 8-9 cm and 17-18 cm depth. The concentration of the Mn in the 30-1 kDa fraction, shown in figure 5.17, was generally low but increased rapidly to ~1.25 mg/l in a peak over 3-7 cm depth. A similar distribution with depth was found in the <1 kDa fraction but the concentrations were much higher, with a maximum of ~4.3 mg/l, at 5-6 cm depth, as shown in figure 5.18. Near the surface of the sediment up-to 100% of Mn was found in the greater than 30 kDa fraction and the percentage of total Mn in this phase decreased with depth. At 5-7 cm depth the percentage found in the largest fraction dropped to 20% and the dissolved Mn peaked at 70% while the mid size range constituted 12% of the total.

5.6.3 Trace elements, Pb, Cu and Zn

Figures 5.16-18 contain the profiles for Pb, Cu and Zn in the three size fractions obtained by ultrafiltration of LT3 porewater and figure 5.19 displays this data as a percentage of the total concentration. The concentration of Pb in the >30 kDa fraction of

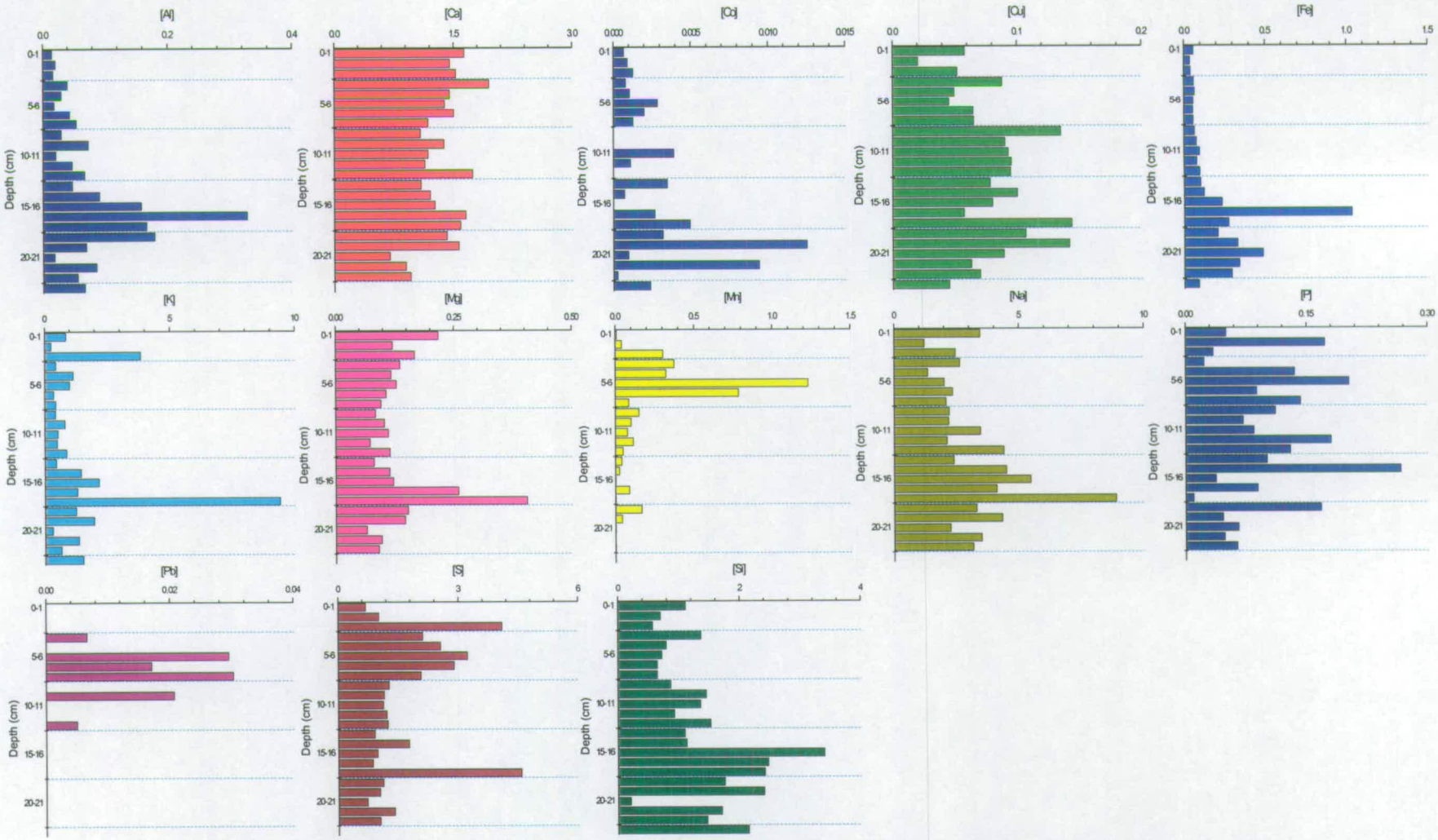

Figure 5.17 Loch Tay core LT5 centrifugal ultrafilter fraction (1 kDa><30 kDa) metal concentrations with depth in sediment

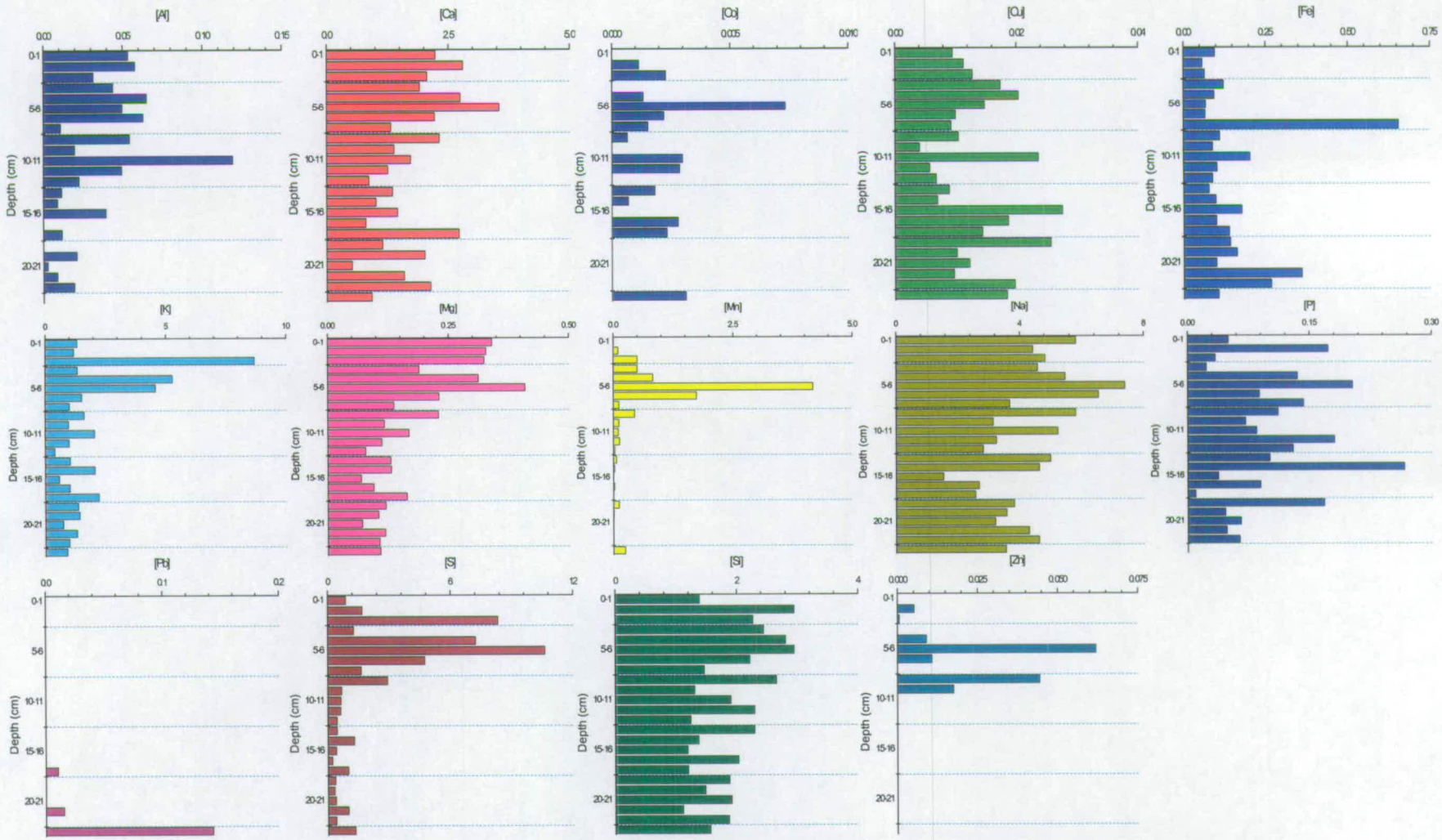

Figure 5.18 Loch Tay core LT5 centrifugal ultrafilter fraction (<1 kDa) metal concentrations with depth in sediment

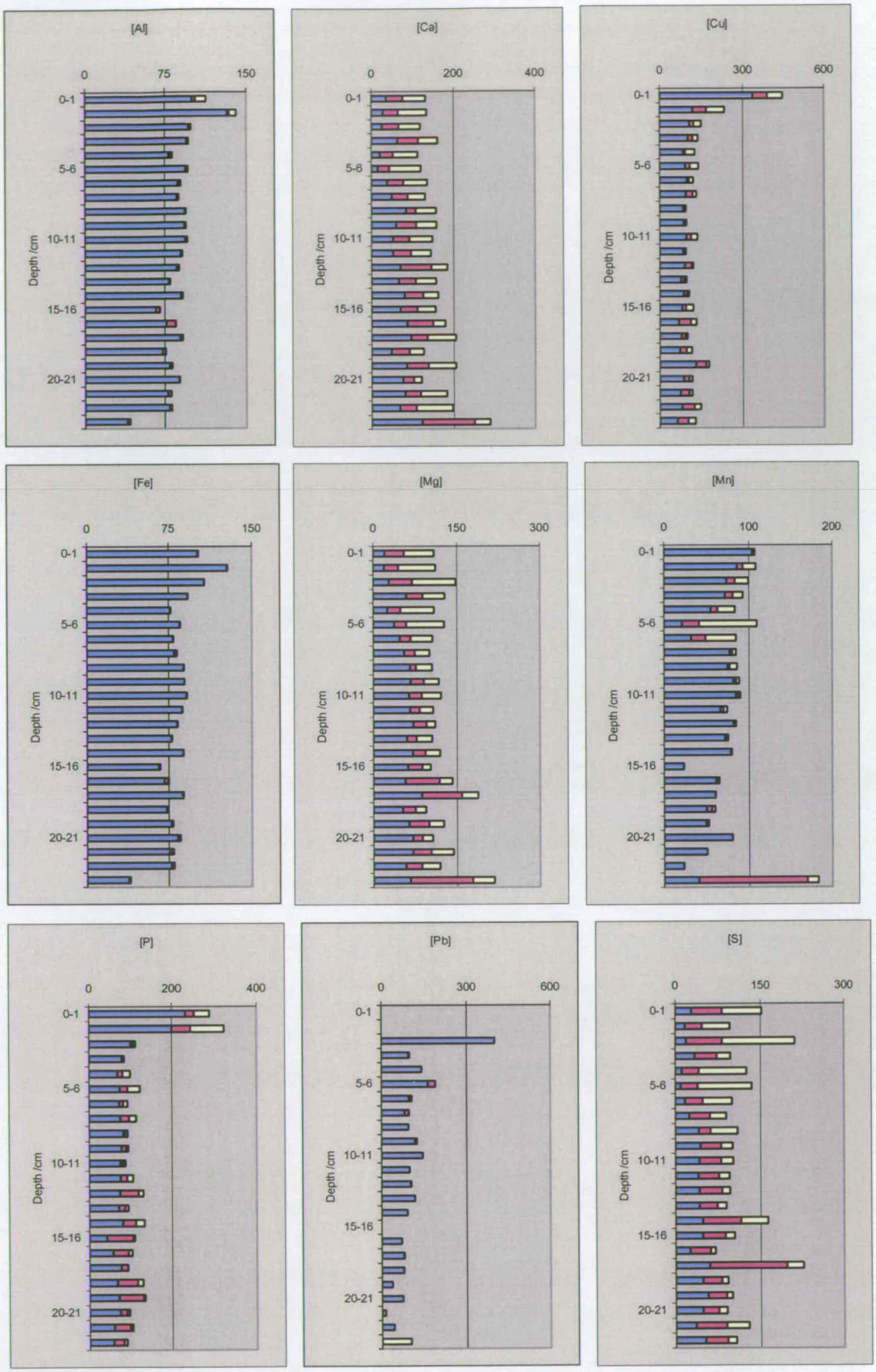

Figure 5.19 Sum of the ultrafilter fractions of Loch Tay porewater LT5 expressed as % total concentration. The blue series represents the greater than 30 kDa fraction, the red seried is the less than 30 kDa and greater than 1 kDa and the yellow series is the less than 1 kDa fraction.

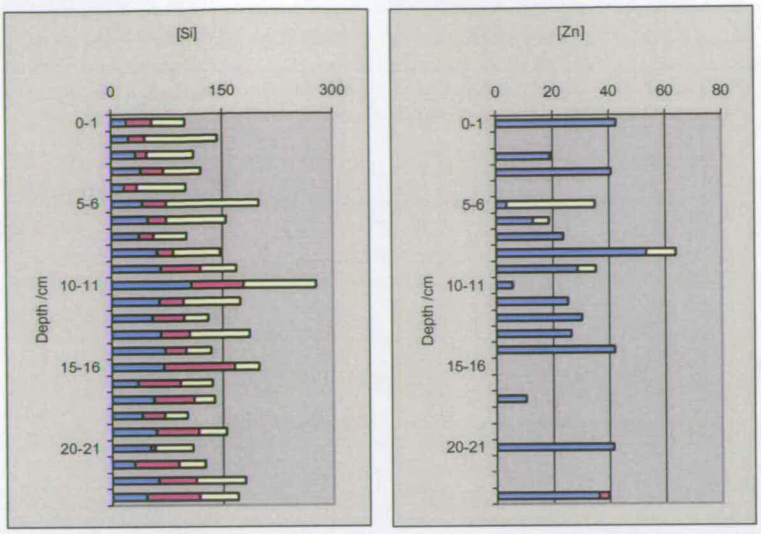

Figure 5.19 Continued

LT3 porewater had a curved profile extending over the length of the core. The concentration ranged from 0.02 mg/l at the surface sample to a maximum of 0.4 mg/l at 8-9 cm depth. A further area of elevated concentration was found at 17-18 cm depth. The concentration of Pb in the 30-1 kDa fraction was very low with detectable value only over 4-13 cm depths. The maximum concentration found was 0.03 mg/l for two peaks at 5-6 cm and 7-8 cm depth. Little or no Pb was found in the truly dissolved phase except for a single peak at the very base of the core with a concentration of 0.15 mg/l. Through most of the core the Pb was found in the largest size fraction, with recovery of 50-100 % of the total Pb from this phase, but at 23-24 cm depth all of the Pb present was in the truly dissolved fraction.

The concentration profile of Cu in the >30 kDa fraction increased from a near surface concentration of 0.02 mg/l in a broad peak centred at 10-11 cm depth. Two sharp peaks in Cu concentration were noted at 3-4 cm and 8-9 cm depth with a broader peak, containing the maximum value of 0.14 mg/l, over 17-20 cm depth. The concentrations found in the 30-1 kDa fraction were lower than for the largest size fraction. The profile of Cu in the <1 kDa size fraction had a very different shape with the concentration peaking at 0.02 mg/l at 4-5 cm before decreasing with depth. An additional sharper peak in concentration was found at 10-11 cm and a broader peak was noted blow this over 15-19 cm depth. Most of the core shows that nearly all of the Cu present in the total sample was found in the greater than 30 kDa fraction. The percentage of total Cu in the mid range fraction although generally low increased with depth, while the dissolved Cu fraction decreased with depth from the surface enrichment. The recovery of Zn in the ultra-filter fractions was very poor with only 50% of the total Zn accounted for. Consideration of the concentration of the fractions on their own showed no clear trends with depth or in comparison to other species.

5.6.4 Additional elements

Figures 5.16-18 contain the distribution with depth of Al in the >30 kDa, 30-1 kDa and <1 kDa fractions of LT3 porewater. The diagram of figure 5.19 contains the profile of

partitioning of Al between the size fractions as a percentage of the total. The concentration initially increased with depth until 10-11 cm and thereafter decreased. The concentration ranged from 0.5 mg/l to 9 mg/l with the maximum concentration in a sharp peak at 8-9 cm and two further peaks at 3-4 cm and 17-18 cm depth. The concentration in the 30-1 kDa fraction was generally lower, ranging from 0.02 mg/l at 0-1 cm depth to the maximum of 0.34 mg/l in a distinct peak over 15-19 cm depth. The concentration of Al was lower again in the <1 kDa fraction with a range of 0.005 mg/l at 20-21 cm to 0.12 mg/l at 10-11 cm. Generally the concentration remained fairly steady over the upper sections, 0-12 cm, and decreased rapidly thereafter. Most of the Al present in the porewater was found in the greater the 30 kDa fraction, 70-100 %, but the sum of the percentage totals for the size fractions exceeded 100%. Though generally low the percentage of the total Al found in the mid-size fraction (30 to 1 kDa) peaked at 16-17 cm depth at about 0.34 %. The less than 1 kDa fraction had a surface peak of 10 % and decreased with depth.

The concentrations of Ca in the fractions of LT3 porewater are shown in figures 5.16-19. Generally the concentrations in the >30kDa size fraction remained at approximately 1.2 mg/l with three peaks at 3-4 cm, 8-9 cm, with the maximum concentration of ~4 mg/l, and 17-18 cm depth. The concentrations in 30-1 kDa fractions were overall slightly higher at around 1.5 mg/l with a decrease in the lower sections to nearer 1 mg/l. Again three peaks were noted but the positions were different at 3-4 cm, 12-13 cm and a broader peak over 16-20 cm depth. The <1 kDa fraction had higher concentrations of Ca again with decreases with depth from the surface value of 2.2 mg/l to nearer 1 mg/l at the base of the core. Near the surface of the core approximately 30 % of the total porewater Ca was found in the large colloidal fraction, 10% was in the mid-size fraction and 60% in dissolved phase. With depth the 30-1 kDa fraction remained fairly constant but the larger size fraction, >30 kDa, becomes more significant with depth as the dissolved fraction decreases.

The profile of Mg concentration in the >30 kDa fraction of the LT3 porewater with depth had a very similar distribution to that of Al as previously discussed. The concentration ranged from 0.1 mg/l at 1-2 cm depth to 0.5 mg/l at the sharp peak at 8-9

cm depth. The profile obtained from the 30-1 kDa material was very different with the concentration decreasing from the surface to 14-15 cm depth where it started to increase to peak at 0.42 mg/l and 17-18 cm depth. The concentration of Mg in the <1 kDa fraction decreased markedly with depth from the surface with a peak to the maximum concentration at 5-6 cm depth. The Mg concentration increased in the greater than 30 kDa fraction from 20% at surface to about 70% at depth and conversely the dissolved fraction decreased from 70% near surface to 20% at depth. The mid-size fraction constituted about 0.2% of the total sample and peaked at 0.4% at 17-18 cm depth.

The profile of P in the >30 kDa profile had the same curved profile as reported previously for other elements. The concentration ranged from 0.3 mg/l at 0-1 cm and the 23-24 cm sections to 1.7 mg/l at 8-9 cm depth. The concentrations in the 30-1 kDa fraction profile were very low and little variation was noted with depth. The same was true for the <1 kDa fraction. Although enriched at the surface section, generally 100% of the total porewater P existed in the greater than 30 kDa phase.

The concentration of S in the largest size fraction generally increased with depth until 2-3 cm and 1.2 mg/l and then remained fairly constant with depth. Two sharp peaks were noted at 3-4 cm and 8-9 cm, and a broader peak was also found over 17-20 cm depth. The concentration range of S in the 30-1 kDa fraction was similar with the concentration increasing from the surface minimum of 0.3 mg/l to a sharp peak at 2-3 cm followed by a broad peak centred at 5-6 cm depth. Thereafter the concentration remained fairly low and constant apart from a small sharp peak at 14-15 cm and a larger sharp peak at 17-18 cm to the maximum concentration of 4.4 mg/l. By comparison the S concentration in the <1 kDa fraction was elevated with a baseline concentration of 0.3 mg/l and a massive peak to 10.4 mg/l over 2-9 cm depth. The concentration of S in the largest size fraction increases with depth representing 10% to 50% of the total S in the LT3 porewater. Mid-size fraction of S in general constituted 20-50% of the total S. At 2-3 cm and 17-18 cm the percentage of the total S found in this fraction was higher but the sum of the fractions at these depths exceeded 100 %. The concentration of S in the truly dissolved phase increased with depth from 70% at the surface to represent nearly 100 % of the total S concentration at 2-3 cm thereafter this fraction decreased with depth.

The concentration of Si in the >30 kDa fraction generally increased with depth from 0.8 mg/l in the 0-1 cm depth porewater to the maximum of 3 mg/l at 14-15 cm. Additional peaks in concentration were noted at 3-4 cm and 8-9 cm depth. The concentrations of Si in the 30-1 kDa fractions were generally lower and mostly remained near 0.8 mg/l. A large elevation in concentration was found at 15-16 cm with a maximum concentration of 3.5 mg/l and thereafter the concentration remained slightly elevated. The profile of Si in the <1 kDa fraction decreases steadily with depth from the near surface maximum of 3 mg/l to the minimum of 1 mg/l at 21-22 cm depth. The mass balance of Si was poor with the sum of the fraction concentrations frequently exceeding the total porewater concentration. Generally near the surface of the core the Si was found predominantly in the <1 kDa fraction but the concentration decreased with depth. Over 8-15 cm depth the Si existed primarily in the largest size fraction of >30 kDa again decreasing with depth so that near the base of the core the 30-1 kDa fraction became most important.

5.7 Loch Tay Cross-flow Filtration of surface waters

Figure 5.20 contains the distributions of elements in the loch and stream waters collected from Loch Tay. The particulate concentrations, total concentrations and the concentrations found in the ultra-filtration fractions are displayed.

Mn was found predominantly in the >0.45um particulate fraction, in both stream and loch water samples, with concentrations up to that of stream 24 at 0.073 mg/l. This was the material removed from the water prior to the determination of the total water concentration. Of the Mn remaining in the water sample the concentration was elevated in streams 13, 18 and 23. Also the Mn rich material in these waters was found predominantly in the < 100 kDa fraction.

The Fe entering the Loch Tay from the streams was predominantly found in the particulate fraction with the highest concentration from stream 24 of 0.58 mg/l. The particulate material was also an important fraction when considering the concentration in the surface water of the loch with concentrations on a par with the total water sample in each case. The total water Fe concentration was elevated for streams 10-14 with a

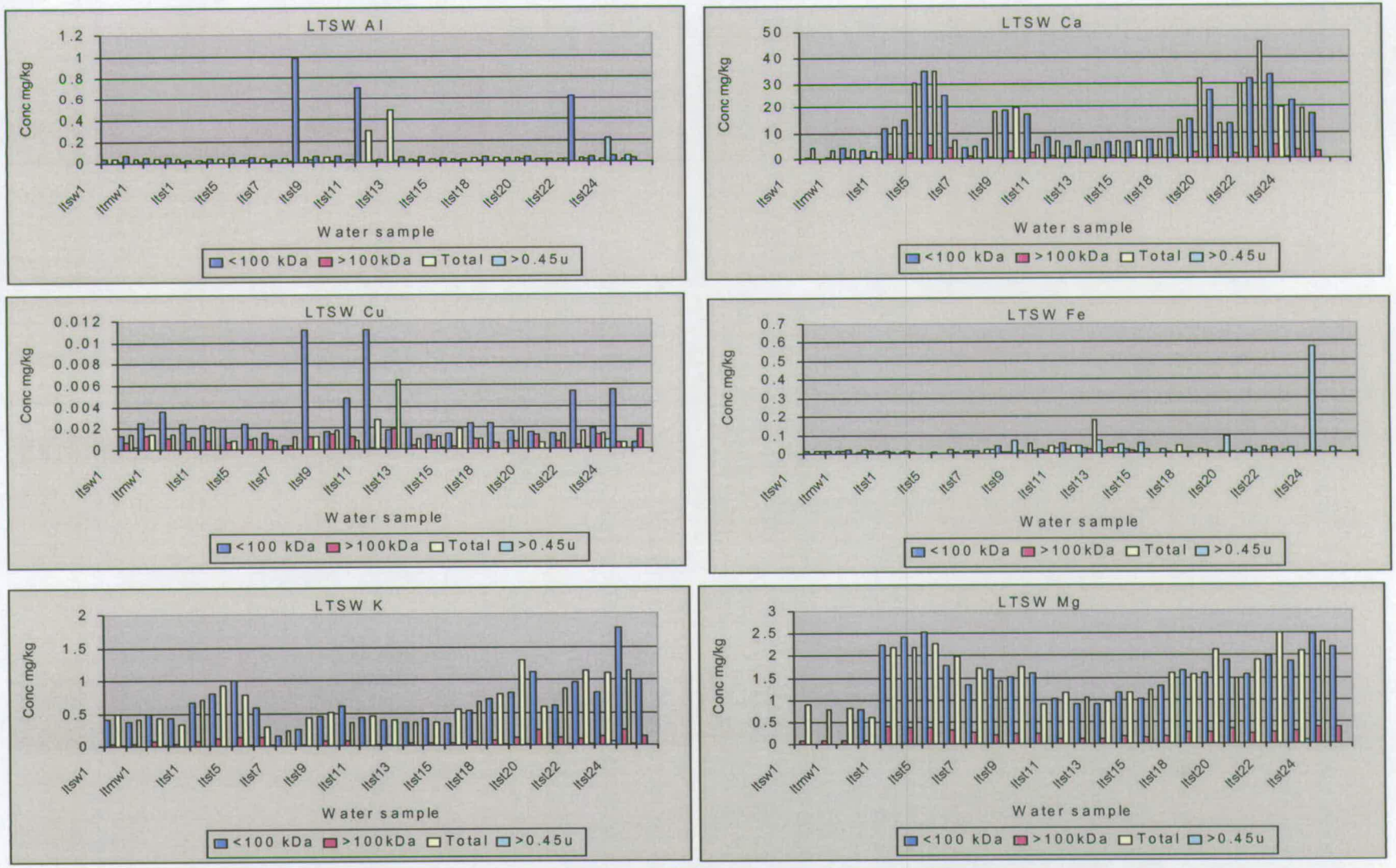

Figure 5.20 Distributions of elements in total samples and cross-flow ultrafilter fractions of surface (SW1, MW1 and MW2) and stream waters of Loch Tay (ST1-26)

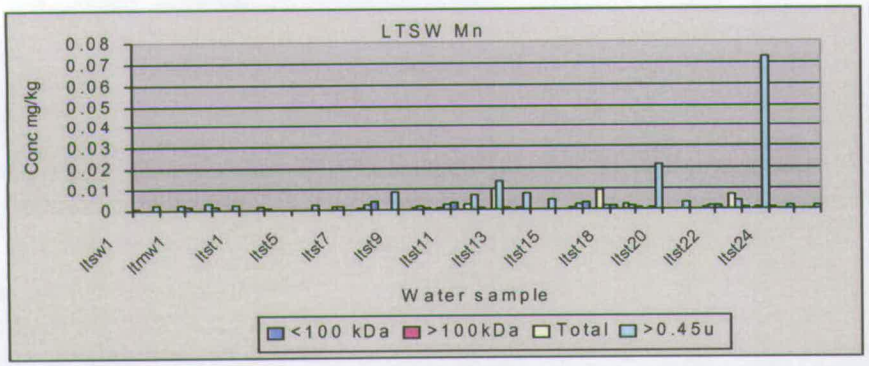

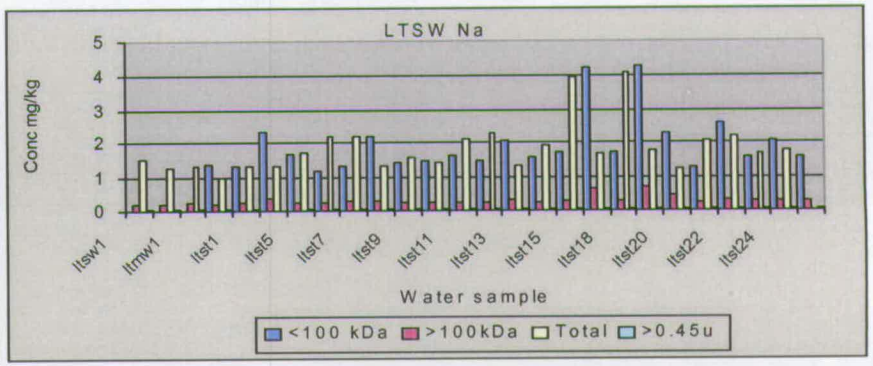

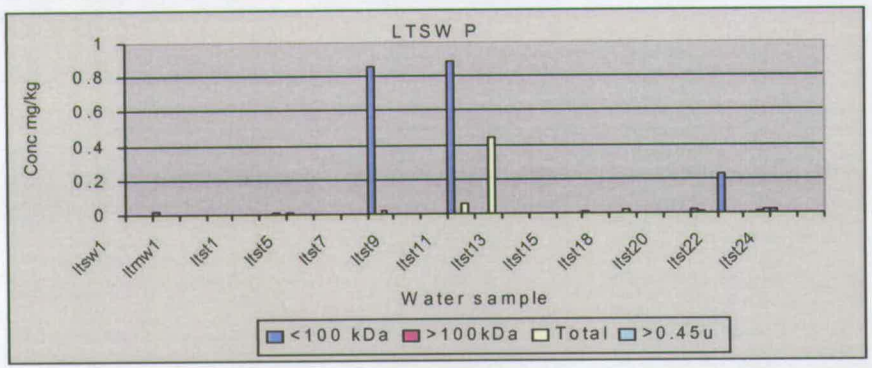

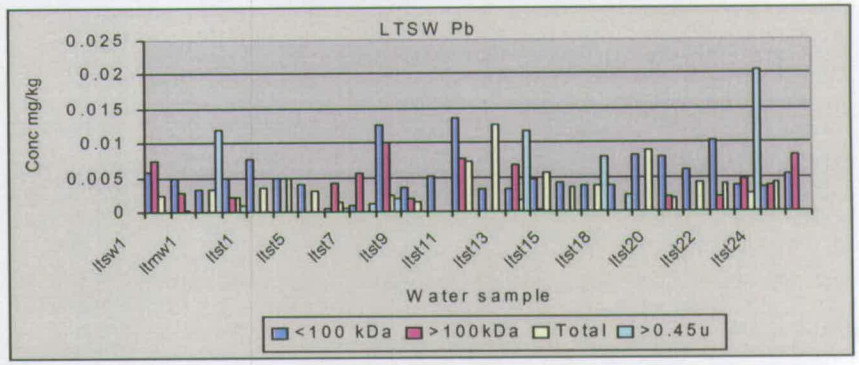

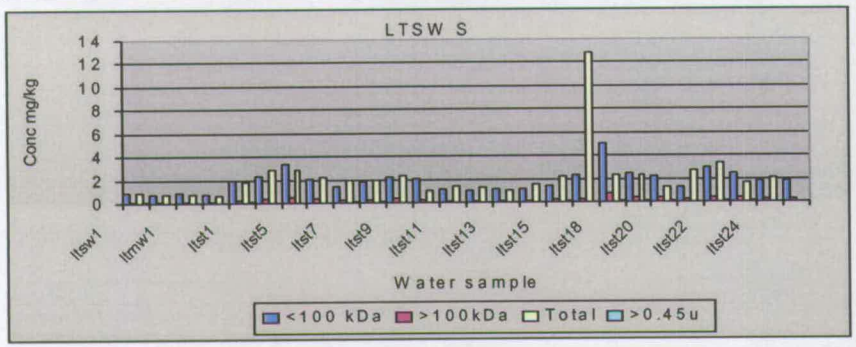

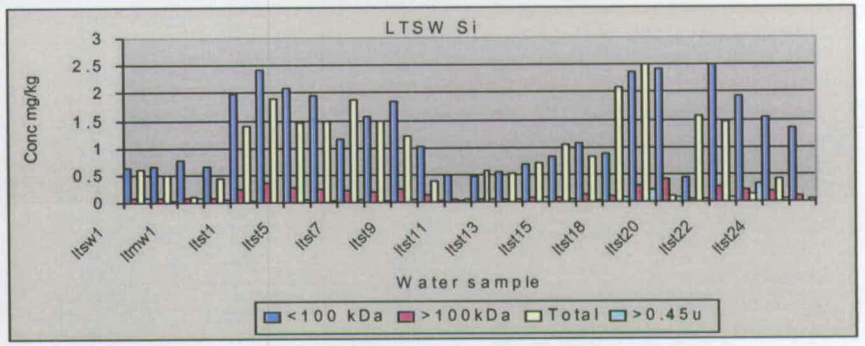

Figure 5.20 continued

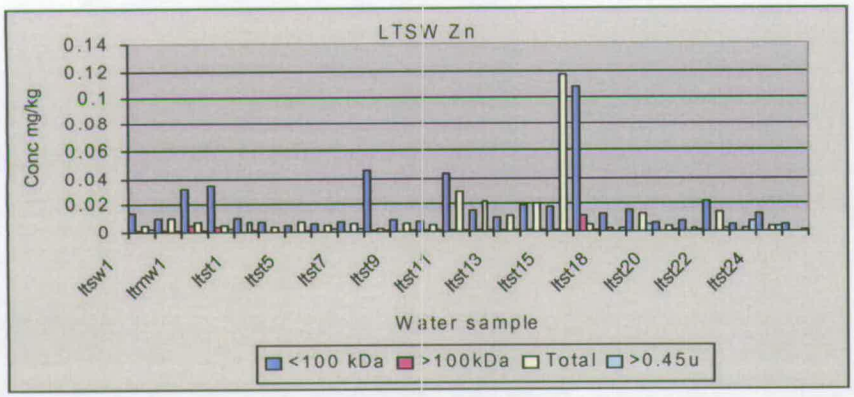

Figure 5.20 continued

concentration approaching 0.2 mg/l for stream 13. Generally the Fe remaining in the surface water was found in the <100 kDa fraction but when the concentration of Fe was elevated in the surface water the >100 kDa fraction became more important.

Overall the concentrations found for Pb in the stream and surface waters were low and the concentration value for the sum of the fractions exceeded that of the total water sample. The importance of the particulate fraction in the stream water can be noted as the >0.45um fraction concentration dominates the chart, especially for streams 14, 18 and 24.

The Cu concentration were very low and generally the mass balance was poor with the sum of the fraction concentrations exceeding the total sample concentration. The particulate material was not rich in Cu and the concentrations barely register on the scale considered here. Of the material in the water sample it appears that the Cu is mainly found in the <100 kDa phase.

The distribution of Zn, both spatially around the catchment and within the fractions of a given sample, generally followed the same pattern previously found for Cu. The particulate material had very low concentrations and the Zn remaining in the water sample was found mainly in the <100 kDa fraction. The mass balance for Zn was better than that for Cu with 50-100 % of Zn recovered from the fractions.

The particulate fraction concentration of Al was only elevated for streams 24 and 25 while streams 12 and 13 had higher concentrations of total sample Al. The Al present for all of the surface and stream water samples was mainly in the < 100 kDa fraction.

The Ca concentration in the particulate fraction was very low and the total water concentrations were elevated for streams 5-7, 10-11 and 20-24. Of the Ca rich material present in the water sample most was found in the < 100 kDa fraction with slightly elevated concentrations in the >100 kDa fraction only for the streams with higher total concentrations noted previously.

The surface waters and streams 8-15 had the lowest concentration of K. Little or no K was found in the particulate fraction and the K rich material in the total sample was

mainly present in the < 100 kDa fraction. The >100 kDa fraction became more significant with increasing total concentration. The distribution of Mg was very similar to that of K.

The Na concentration was fairly consistent for all the samples analysed with elevated total concentrations only in streams 18 and 20. The particulate concentration was low and the Na rich material in the water was mainly in the < 100 kDa fraction.

The concentration of S in the stream waters was generally higher than the concentration in surface and mid-depth loch waters. The particulate fraction concentration was low and the concentrations in the < 100 kDa fraction were near those of the total sample concentrations.

The Si concentrations were lowest in the surface and mid-depth water samples as well as in streams 12-14 and 22. The particulate concentrations of Si were generally low with elevations to near 0.4 mg/l only in streams 20 and 24. The Si remaining on the water sample was mainly present in the < 100 kDa fraction.

5.8 Electrophoretic investigation of humic-metal interactions in LochTay sediments and waters

5.8.1 Electrophoretic extraction of Loch Tay porewaters only from selected depths in the sediment core LT1

The pictures of electrophoretic gels (Figures 5.21-2) and the surface plots in figure 5.23 show the distribution of organic material elements across the agarose gel after the electrophoretic extraction and fractionation of the porewaters from selected depths of the LT1 sediment core. The Mn concentration for most depths and distances across the gel are fairly low and uniform at 0.0-0.5 mg/kg. Elevated concentrations, of up to 0.15 mg/kg, can be noted for 4 cm and 20 cm depths at 0.5-1.0 cm across the gel. The surface plot of Fe shows a similar picture with generally higher concentrations detected. Again the maximum concentration was in the 0.5-1.0 cm gel section from the 4 cm depth.

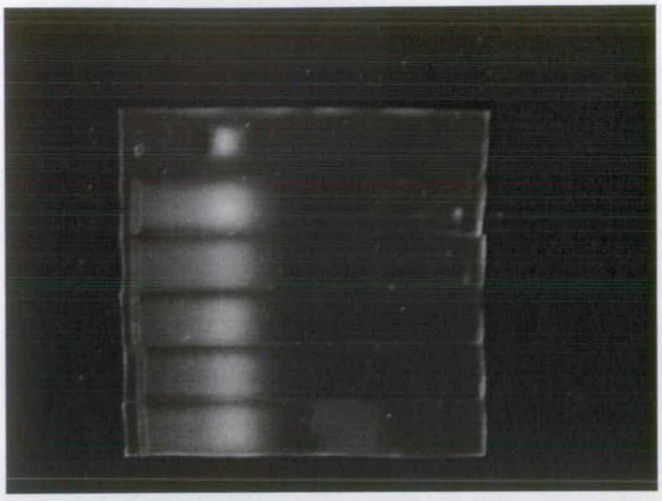

Figure 5.21 Fluorescent electrophoretic pattern of Loch tay pore waters. Top to bottom: Blue ranger, LT core 1 section 4, section 8, section 12, section 17 and section 20 (captured under low UV at Frz=0.2 sec). Sample only run.

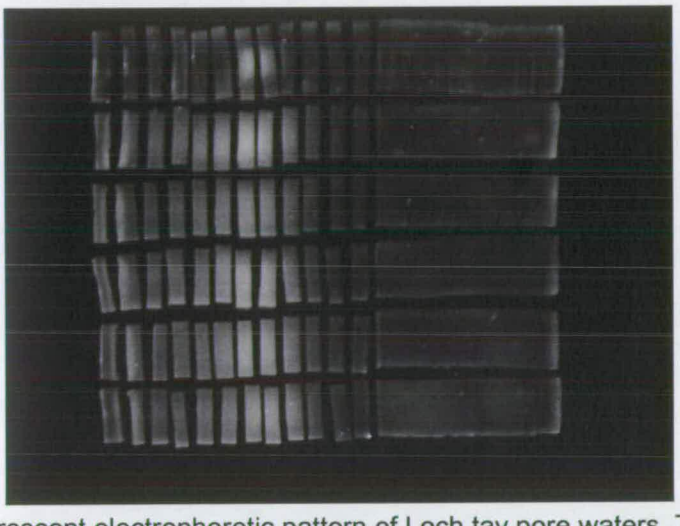

Figure 5.22 Fluorescent electrophoretic pattern of Loch tay pore waters. Top to bottom: Blue ranger, LT core 1 section 4, section 8, section 12, section 17 and section 20 (captured under low UV at Frz=0.2 sec). Sample only run.and sliced into 0.5 cm sections

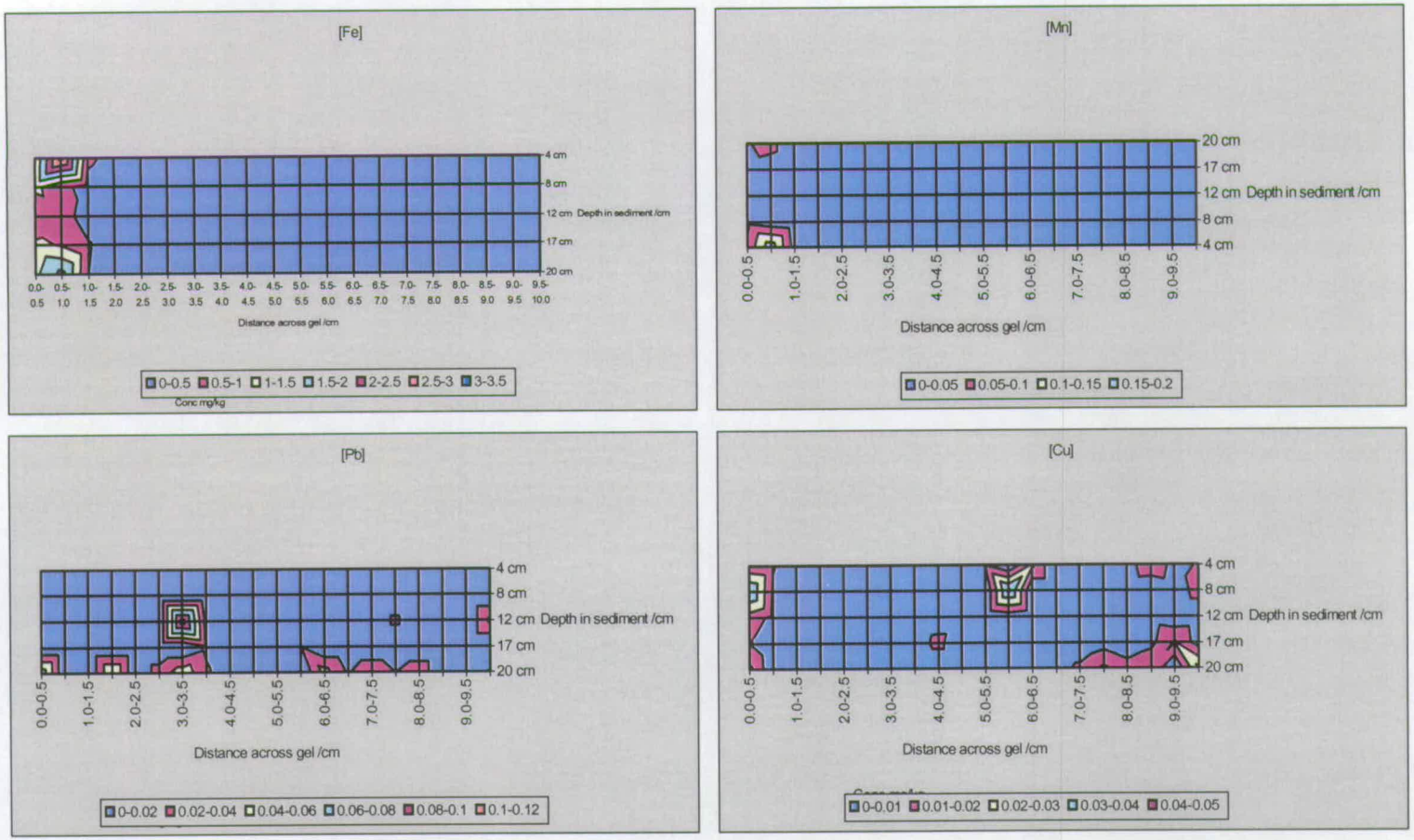

Figure 5.23 Distributions of selected elements across agarose after electrophoretic extraction of LT1 porewater without the addition of running buffer

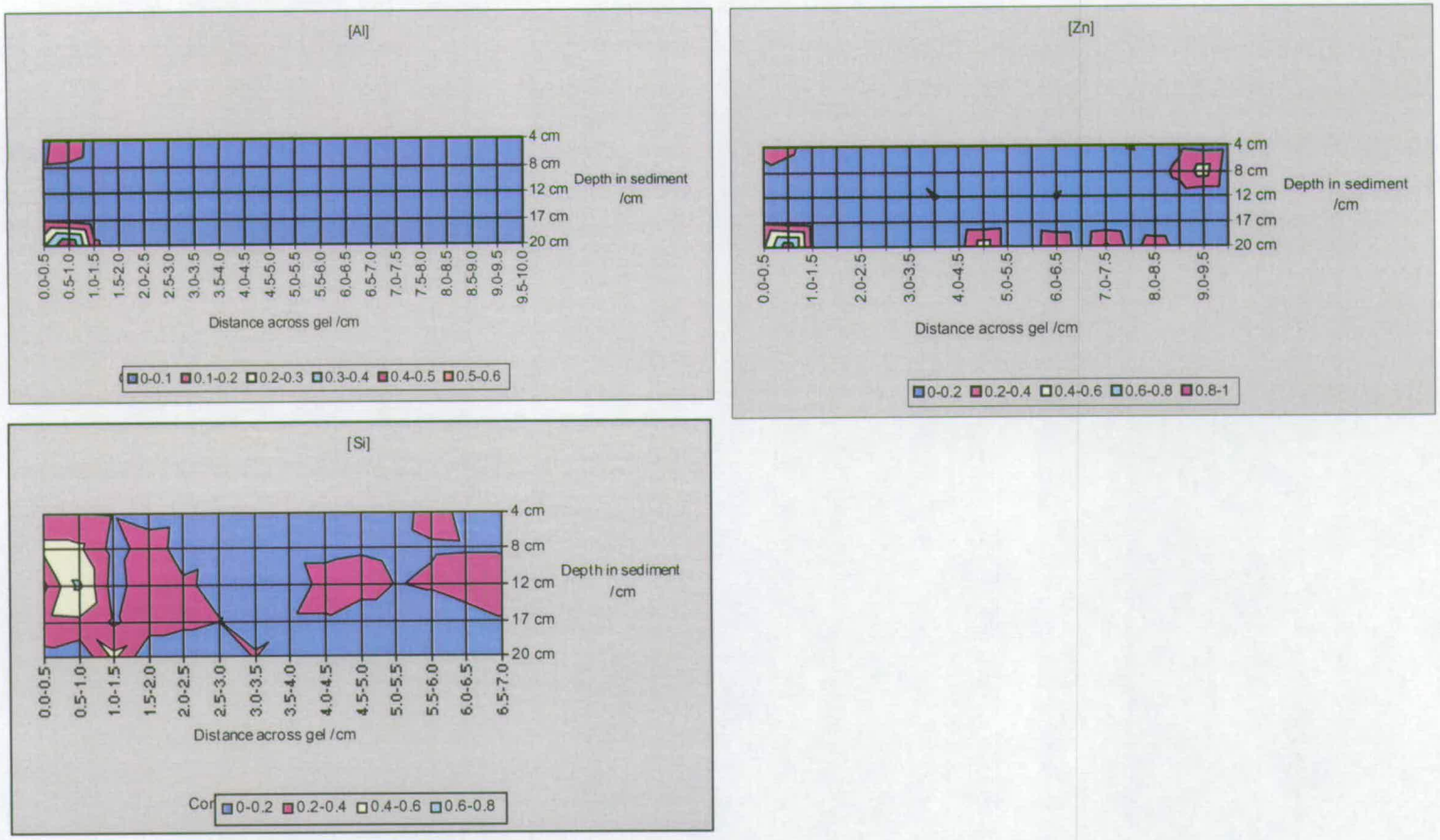

Figure 5.23 Distributions of selected elements across agarose after electrophoretic extraction of LT1 porewater without the addition of running buffer

The baseline concentration of Pb was 0.0-0.2 mg/kg and little Pb rich material was found near the well. The maximum concentration was found at 3.0-3.5 cm across the gel at a depth of 12 cm. The material extracted from the porewater from 20 cm depth showed more mobile Pb rich material extending over 8.5 cm of the gel.
The Cu in these selected porewater samples was divided between the residual fraction remaining in or near the well and the more mobile material. This was particularly evident at 8 cm depth where two distinct areas of equivalent concentration were noted at 0.0-0.5 cm and 5.5-6.0 cm across the gel.
The surface plot of Zn shows a fairly uniform distribution apart from the material from porewater at 20 cm depth. Here the Zn rich material was divided into residual material in the well and five isolated fractions across the gel covering a distance of 8.5 cm.

The Al rich material from the porewater remained entirely in or near the well with no signs of migration. The concentration was greatest in the samples from deeper in the core.
Most of the Si in the 20 cm porewater sample remained in the well but four point of elevated concentration were also noted at 4.5-5.0 cm, 6.0-6.5 cm, 7.0-7.5 cm and 8.0-8.5 cm with decreasing concentrations found for subsequent fractions.

5.8.2 Electrophoretic extraction of porewater from selected depths in Loch Tay core LT1 in the presence of NaOH

Figures 5.24-27 contain the distribution of organic material and elements across the electrophoretic gels for the porewaters of Loch Tay core LT1 in the presence of NaOH.
The concentration of Mn across the gel for the selected depths of porewater was low, not exceeding 0.1 mg/kg, and the Mn found was confined to the well. The concentration of Mn in the residual material in the well was lower for the 12 cm and 17 cm porewaters.

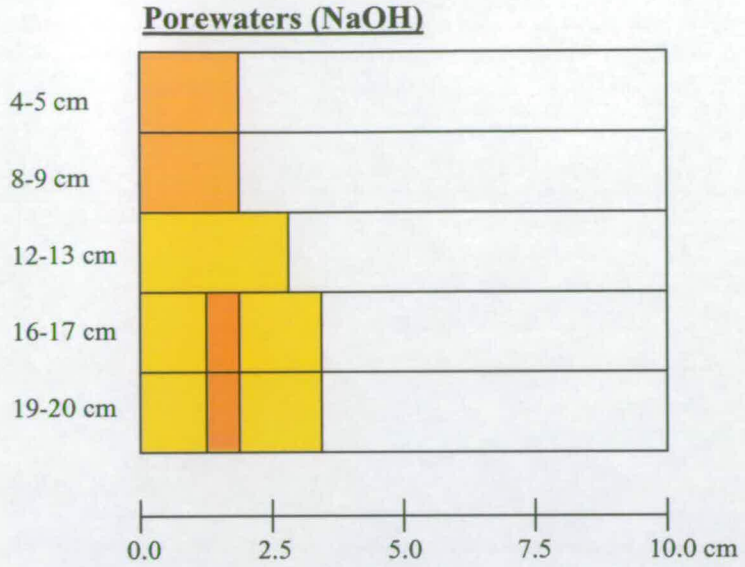

Figure 5.24 Schematic indicating movement of brown humic material through gel for Loch Tay porewater from selected depths in NaOH running buffer

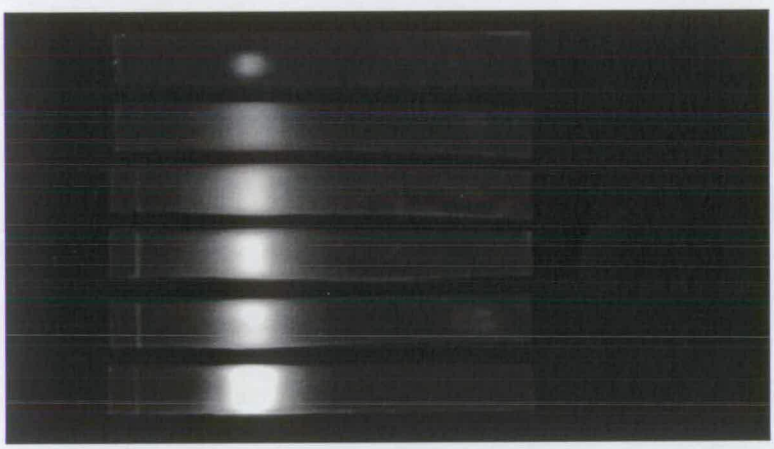

Figure 5.25 Loch Tay pore water in NaOH (0.1M) Fluorescent electrophoretic pattern. Blue ranger, LT core 1 section 4, section 8, section 12, section 17 and section 20. Captured under low UV Frz=2.0 sec

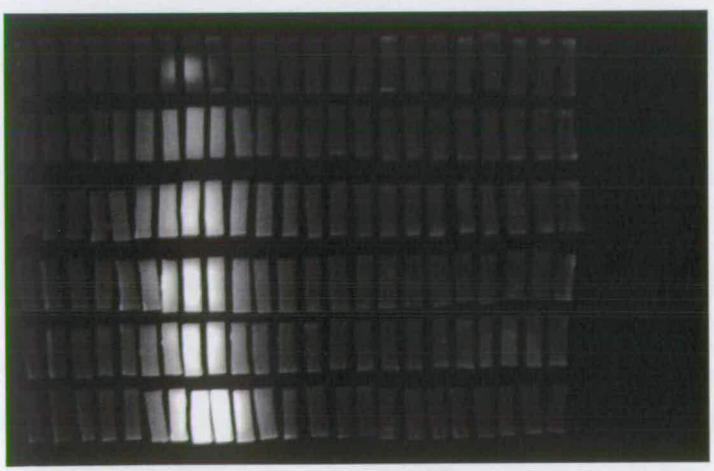

Figure 5.26 Electrophoretic fluorescent pattern of loch tay pore waters in NaOH (0.1 M) Blue ranger, LT core 1 section 4, section 8, section 12, section 17 and section 20. Sectioned at 0.5 cm under low UV FRZ=2.0 sec

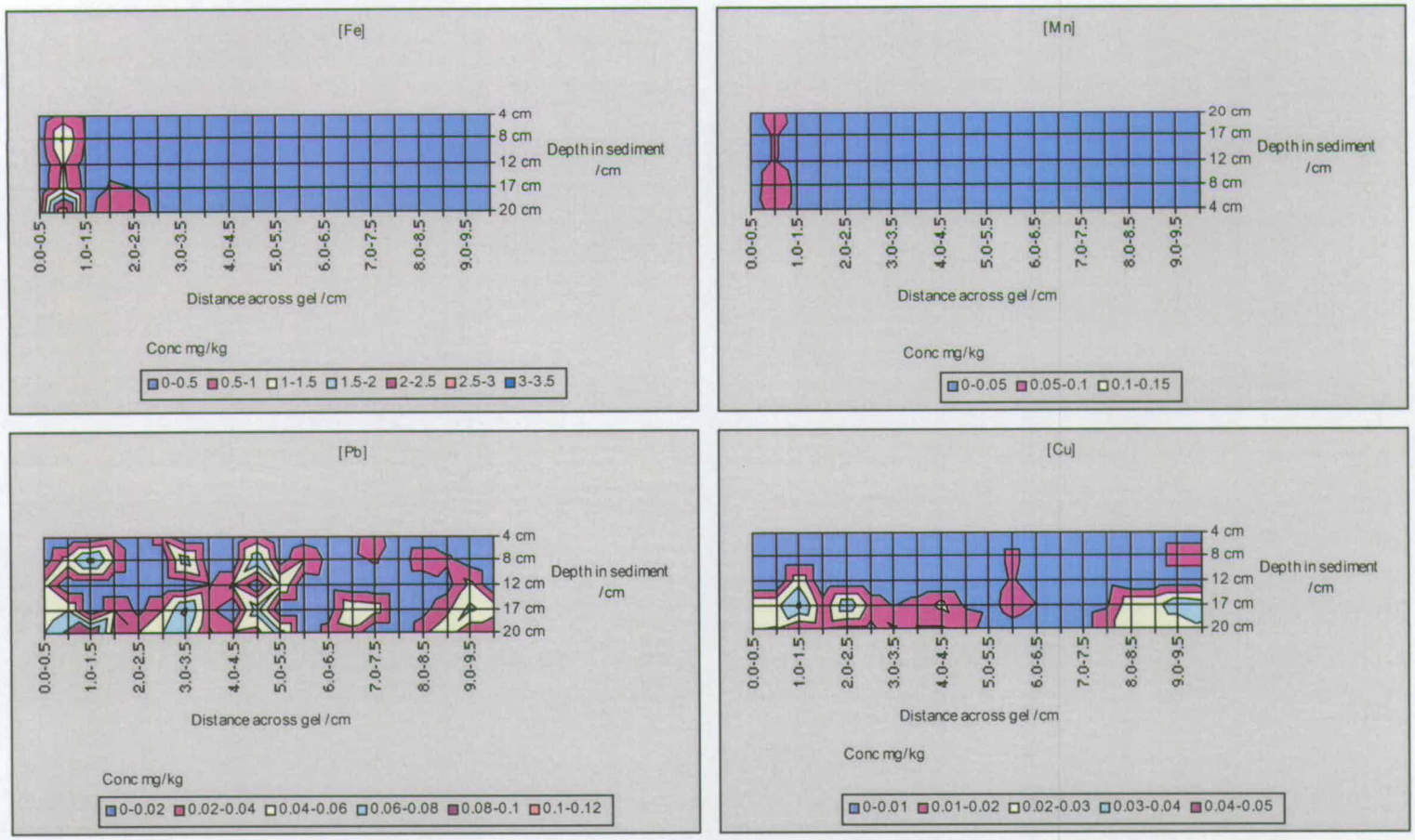

Figure 5.27 Distributions of selected elements across the agarose gel after electrophoretic extraction of LT1 porewater in NaOH

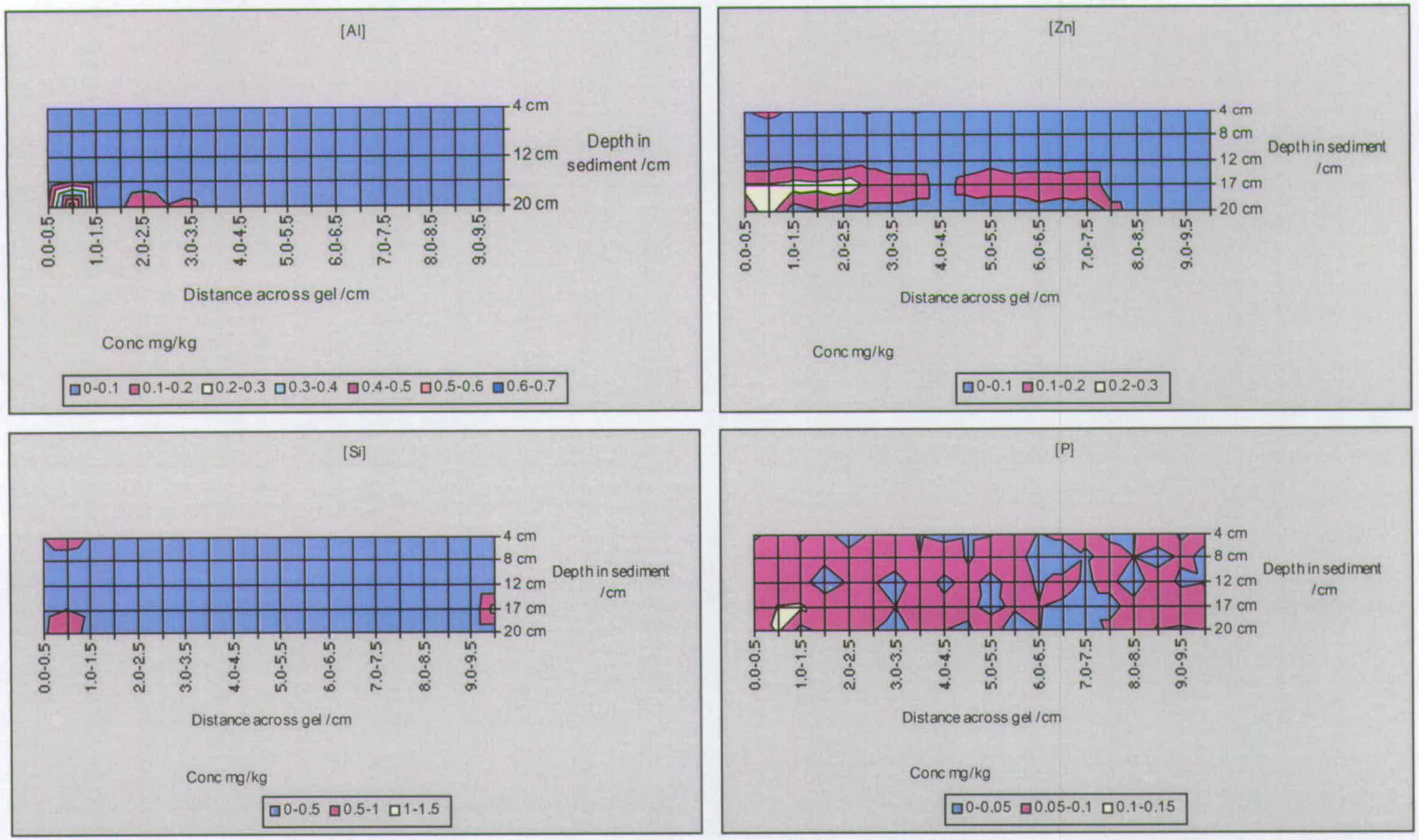

Figure 5.27 Distributions of selected elements across the agarose gel after electrophoretic extraction of LT1 porewater in NaOH

Most of the Fe rich material in the porewater was found in or near the well section with concentration increasing with depth. The material from 20 cm depth in the core also contained a more mobile fraction migrating to 2.0-2.5 cm across the gel.

The Pb was highly mobile across the gel especially for porewaters from 8 cm and 20 cm depth. The highest concentrations were found near the well over 1.0-1.5 cm with additional points of elevation for both sediment depths at 3.0-3.5 cm and 4.5-5.0 cm across the gel. There was a highly mobile fraction from the 20 cm porewater that was found at 9.0-9.5 cm from the start of the gel.
The concentration of Cu and the mobility of the Cu rich material was highest for the 20 cm depth porewater. The highest concentration, like that for Pb, was found in the near well section but points of elevated concentration were also found at 2.0-2.5 cm and 9.0-9.5 cm across the gel.
Zn was prevalent in the material extracted from the porewater isolated at 17 cm depth in the core. The Zn was very mobile in the gel and spread over a large distance with no distinct isolated point of high concentration.

The concentration of Al was only elevated in the material extracted from the porewater at 20 cm depth. The highest concentration was found in the residual material in the well with a small fraction of higher mobility moving to 2-3 cm across the gel.
Overall the Si was evenly distributed across the gel with baseline concentrations of 0.0-0.5 mg/kg and maximum concentrations of 1.0-1.5 mg/kg.

5.8.3 Electrophoretic extraction of porewater from selected depths in core LT1 in the presence of Tris-HCl

The organic and elemental distributions in the gel sections after the electrophoretic extraction of selected depths of core LT1 porewater are shown in figures 5.28-31.

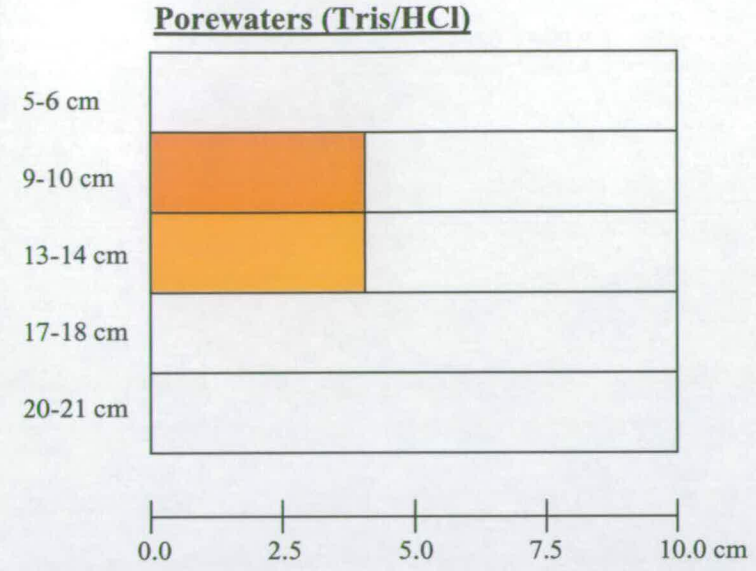

Figure 5.28 Schematic indicating movement of brown humic material through gel for Loch Tay porewater from selected depths in Tris-HCl running buffer

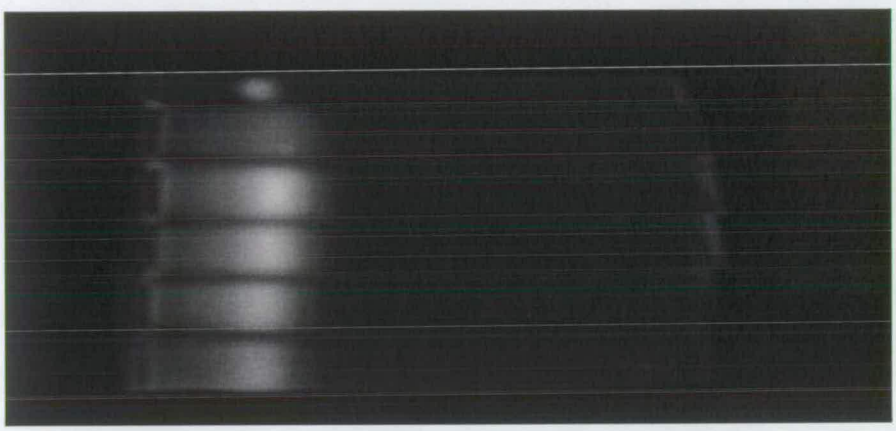

Figure 5.29 Fluorescent electrophoretic pattern of L och Tay porewater in Tris-HCl running buffer. Blue ranger, LT core 1 section 4, section 8, section 12, section 17 and section 20. Captured under low UV Frz=2.0 sec

Figure 5.30 Fluorescent electrophoretic pattern of L och Tay porewater in Tris-HCl running buffer. Blue ranger, LT core 1 section 4, section 8, section 12, section 17 and section 20. Captured under low UV Frz=2.0 sec and sectioned at 0.5 cm intervals

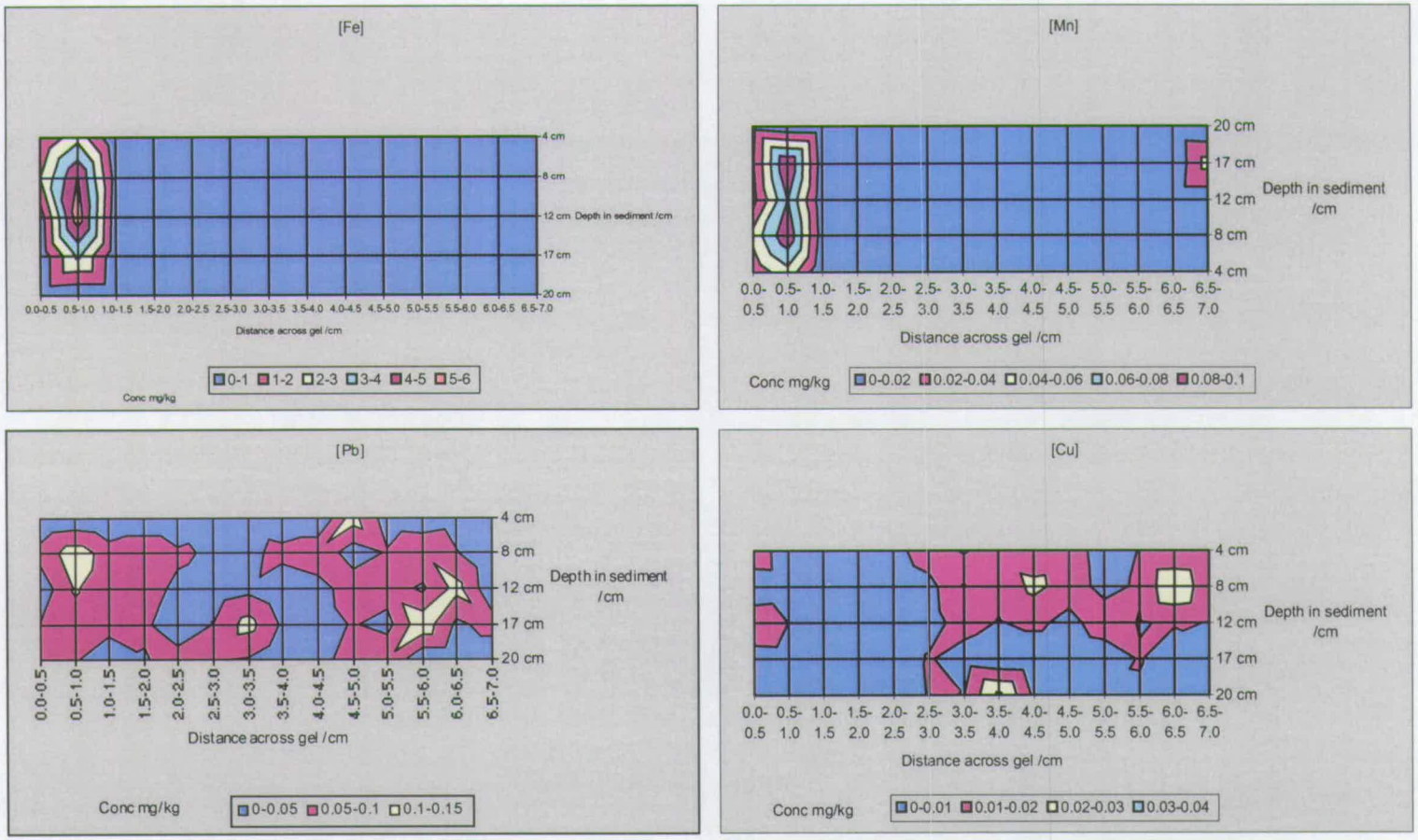

Figure 5.31 Distribution of selected elements across the agarose gel after electrophoretic extraction of LT1 porewater in Tris-HCl running buffer

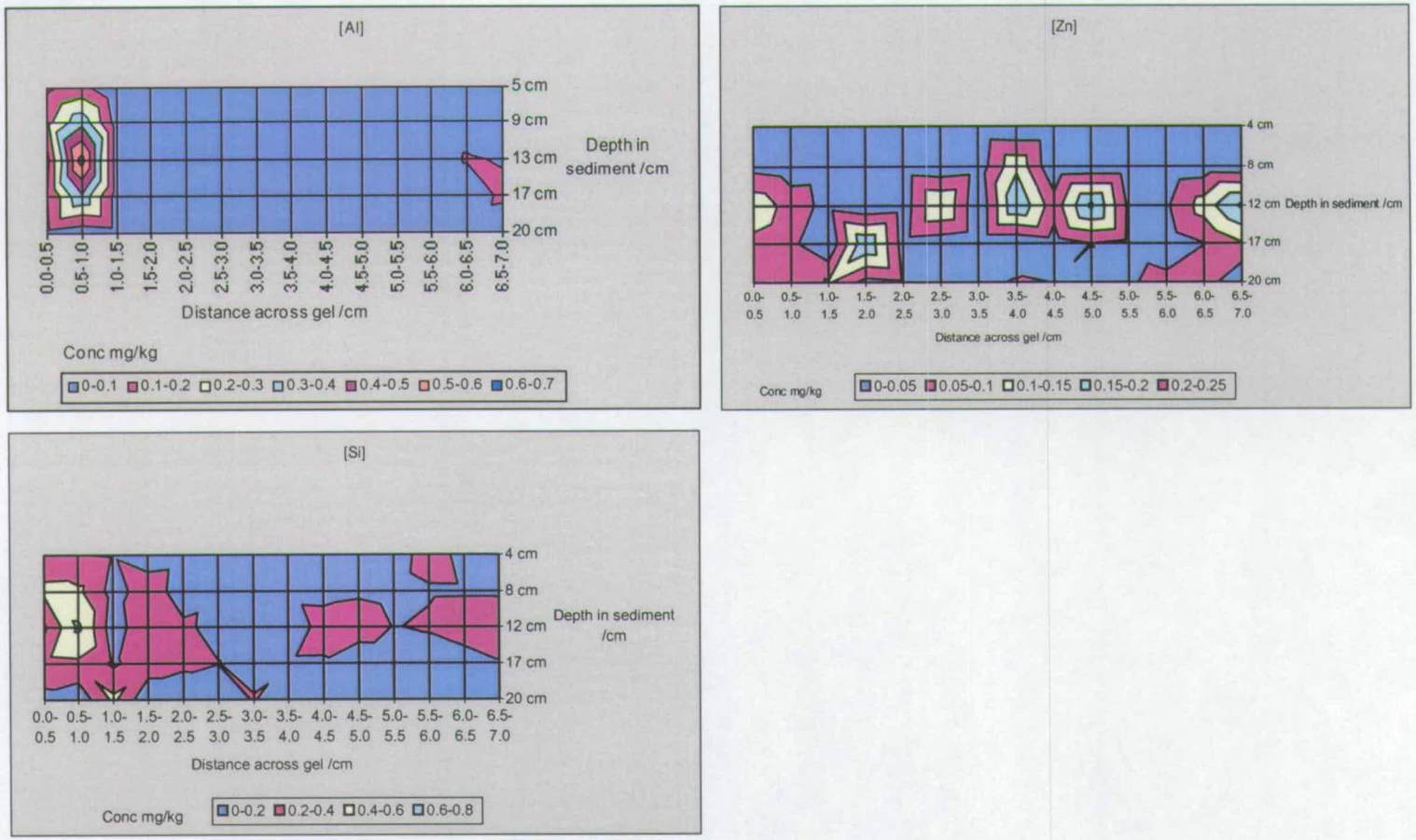

Figure 5.31 Continued.Distribution of selected elements across the agarose gel after electrophoretic extraction of LT1 porewater in Tris-HCl running buffer

The Mn rich material for each core depth was contained within the well and the concentrations were highest for the 8 cm and 17 cm porewaters. A lower concentration of Mn was found in a small highly mobile fraction located at 6.5-7.0 cm across the gel.
The concentration of Fe was also greatest in the well and the 12 cm porewater exhibited the highest concentration of all.

The distribution of Pb across the gel varied from depth to depth. The highest concentration at 4 cm was at 4.5-5.0 cm. The Pb rich material from the porewater at 8 cm depth remained in the well whereas the maximum concentration for 12 cm depth was at 6.0-6.5 cm across the gel. The porewater from 17 cm depth produced two fractions at 30-3.5 cm and 5.5-6.0 cm across the gel.
The Cu rich material was generally highly mobile through the gel and concentrations of Cu were highest in the 8 cm and 20 cm extract. The Cu rich material in the 8 cm porewater extract was divided between two fraction at 4.0-4.5 cm and 6.0-6.5 cm whereas the material from the 20 cm porewater was less mobile and there was no second fraction found.
Five fractions of Zn rich material were isolated from the 12 cm porewater. One fraction was the residual material in the well while the four additional fractions were found at 2.5-3.0 cm, 3.5-4.0 cm, 4.5-5.0 cm and 6.5-7.0 cm across the gel. A single mobile fraction was also found for the material from 17 cm depth which migrated to 1.5-2.0 cm across the gel.

The Al, like the Fe, remained largely in the well and concentrated in the porewater from 13 cm depth.
The Si rich material remained largely in the well and the highest concentration was found for the 12 cm depth porewater extract.

5.8.4 Electrophoretic extraction of sediment from the upper sections of Loch Tay core LT1 in the presence of Tris-HCl

Figures 5.32-35 display the distribution across the gel with sediment depth for the electrophoretic extract of LT1 sediments from the top 5 cm of the core. The Mn concentration had maximum value of 0.55 mg/kg at 0.5-1.0 cm across the gel in the extract from the sediment at 1 cm depth. The concentration then decreased across the gel and with depth in the sediment as did the mobility of the Mn rich material.
The highest concentration of Fe was found in the extract from the sediment at 1 cm depth at 0.5-1.0 cm across the gel. Most of the Fe rich material was contained within the well but a significant fraction, up to 1.5 mg/kg, migrated up to 2.0-2.5 cm. This was most notable for the 1 cm and 3 cm sediment extracts and the concentration and fraction mobility decreased with depth.

Most of the Pb present in the sediment extracts was mobile in the gel. The highest concentration was found for the 1 cm sediment depth at 2.0-2.5 cm across the gel. Generally with depth the mobility of the Pb rich material increased but the overall concentrations decreased.
The concentration of Cu was very low and one point of elevated concentration was noted for the 5 cm depth sample at 3.0-3.5 cm across the gel.
Elevated concentrations of Zn were found over 4.0-5.0 cm and 6.0-6.5 cm for the extract from sediment at 1 cm depth. Two fractions were also found at 2 cm depth at 2.5-3.0 cm and 4.5-5.0 cm. Although the concentration increased with depth the mobility of the Zn rich material decreased. Deeper still in the sediment the Zn concentration decreased and the fractions became less mobile.

The Al enriched material was largely found in the well with increasing concentration with increasing depth in the sediment. A small fraction of Al containing material was mobile and the mobility of this fraction increased with decreasing depth in the core.

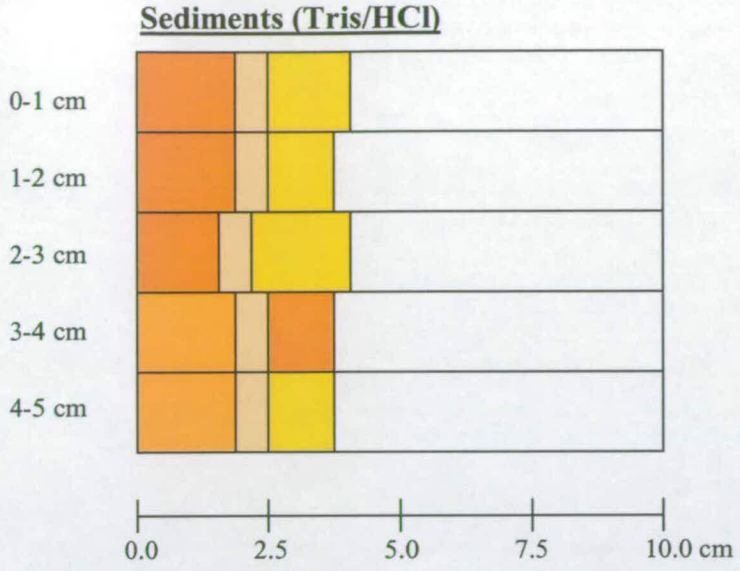

Figure 5.32 Schematic indicating movement of brown humic material through gel for Loch Tay sediments from upper 5 cm in Tris-HCl running buffer

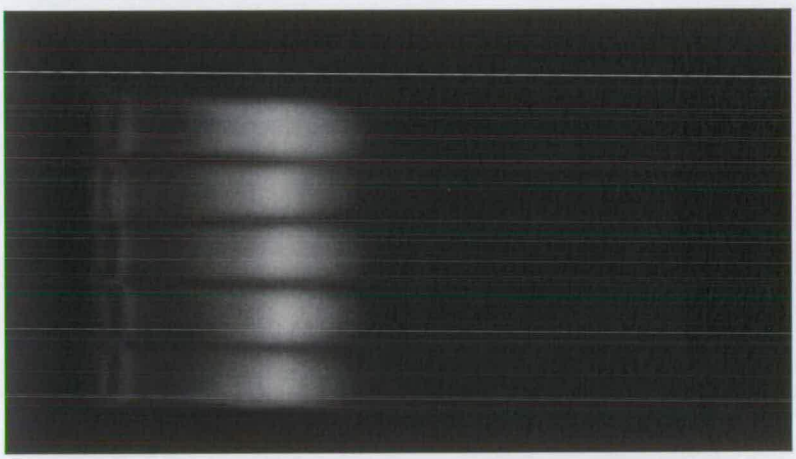

Figure 5.33 Electrophoretic fluorescent pattern of Loch Tay surface sediments core 1 sections 1-5 in Tris-HCl captured under low UV at 3 sec exposure

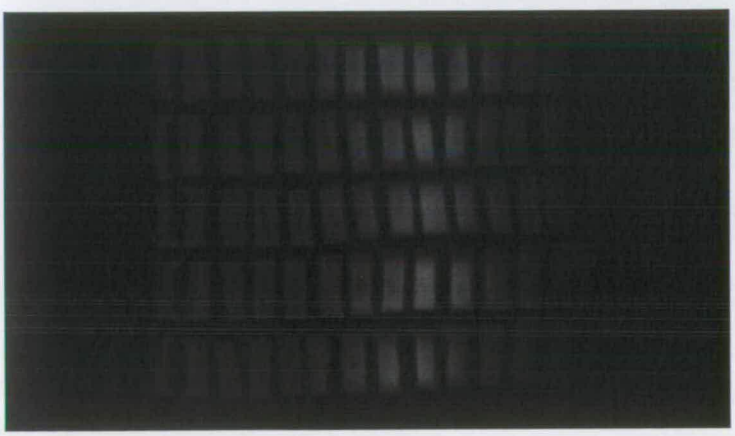

Figure 5.34 Electrophoretic fluorescent pattern of Loch Tay surface sediments core 1 sections 1-5 in Tris-HCl captured under low UV at 3 sec exposure but after sectioning at 0.5 cm

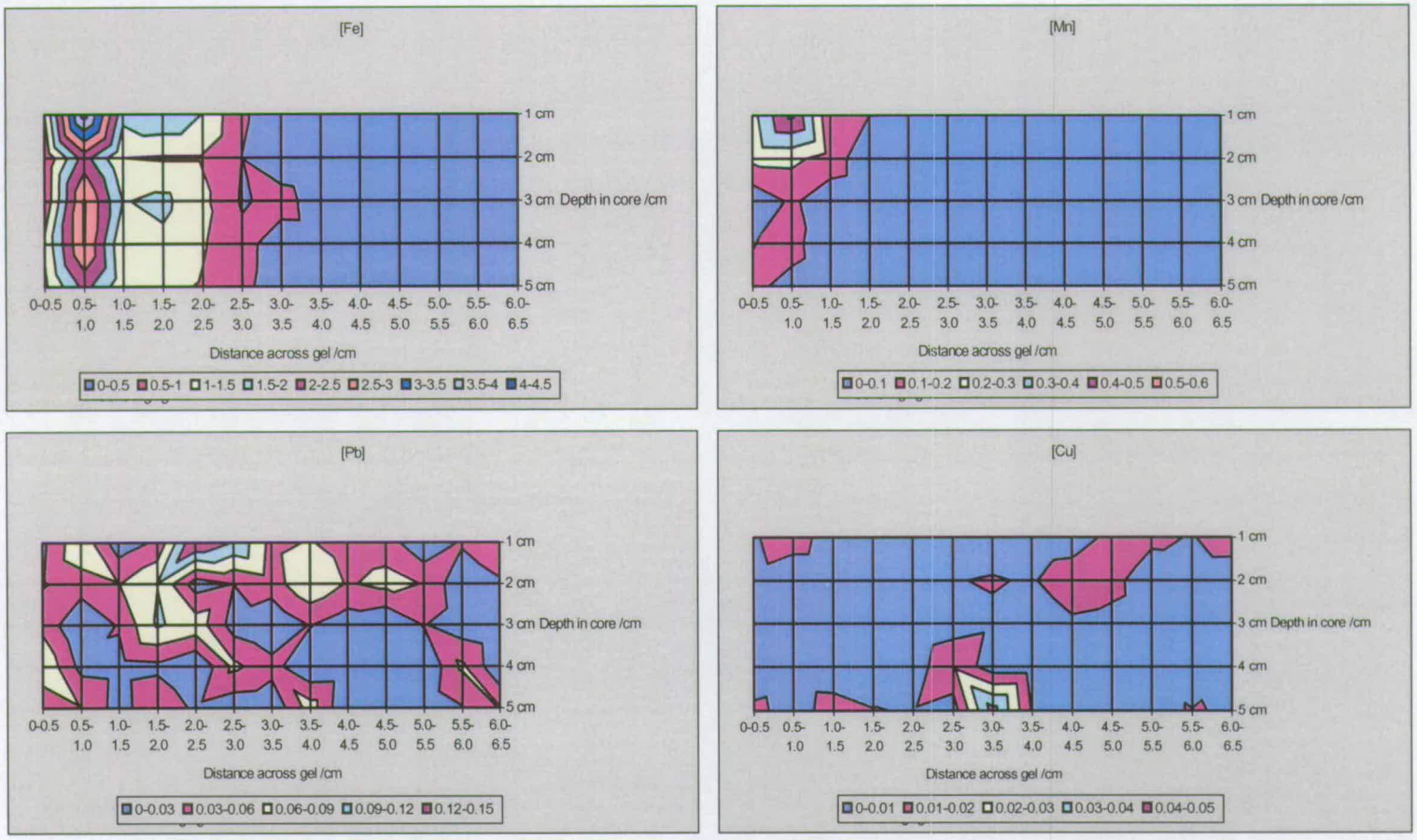

Figure 5.35 Distribution of selected elements across the gel after the electrphoretic extraction of the upper sediments of Loch Tay core LT1

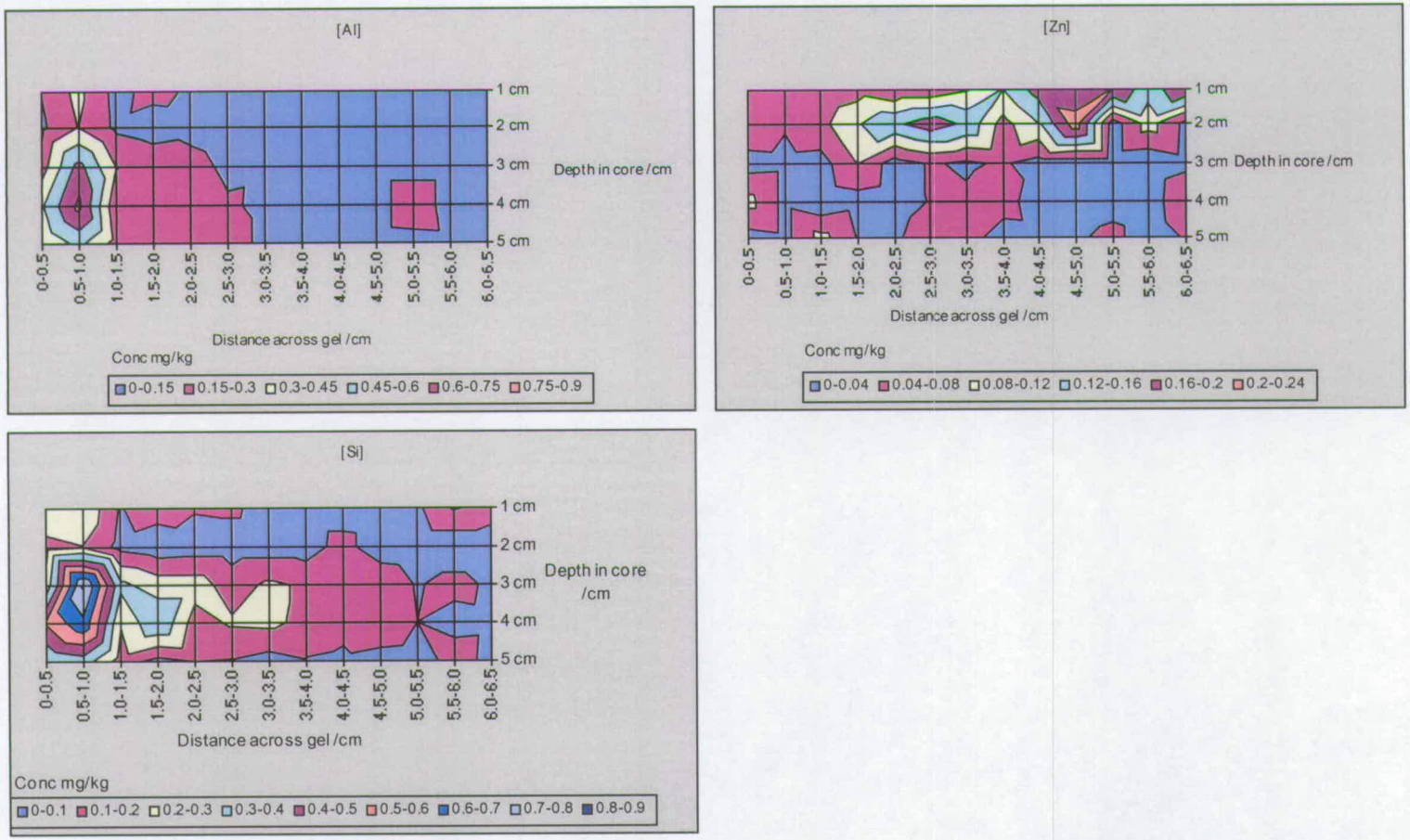

Figure 5.35 continued Distribution of selected elements across the gel after the electrphoretic extraction of the upper sediments of Loch Tay core LT1

The Si concentration at the top of the core was low and the material was not mobile in the gel. With depth the concentration and mobility increased. The highest concentration of Si, 0.8-0.9 mg/kg, was found in the residual material from sediment at 3 cm depth.

5.8.5 Electrophoretic extraction of sediments from selected depths of core LT1 in the presence of Tris-HCl

The surface plots found in figures 5.36-39 show the distribution of elements across a gel after the electrophoretic extraction of sediments from selected depths in core LT1.
Although the highest concentration of Mn was found in the 0.5-1.0 cm section a significant concentration was also found further across the gel. With depth the concentration of Mn decreased, as did the mobility of the fraction moving out of the well. At 8 cm and 12 cm depth the extracted material also comprised of a highly mobile fraction found at 6.0-6.5 cm across the gel.
The distribution of Fe was similar, with concentration in the residual material decreasing with depth and the presence of a highly mobile fraction at 6.0-6.5 cm for depths of 8-17 cm. At 12 cm depth the extraction of the sediment also produced a point of elevated concentration at 2.5-3.0 cm across the gel with values comparable to the highest concentration in the residual material.

The Pb rich material appeared to be highly mobile in the gel with mobility decreasing and concentration increasing with depth. At 4 cm depth two fractions were found at 4.0-4.5 cm and 5.5-6.0 cm. At 8 cm depth a single fraction was found across 2.5-3.5 cm. The sediment from 12 cm depth also had two fractions but the majority of the Pb was found at 1.5-2.0 cm depth. At 17 cm and 20 cm Pb rich material was found in or near the well with a small fraction at 3.5-4.5 cm across the gel.
Generally the Cu concentrations were low with a single point of elevated concentration at 20 cm depth and 4.5-5.0 cm across the gel.

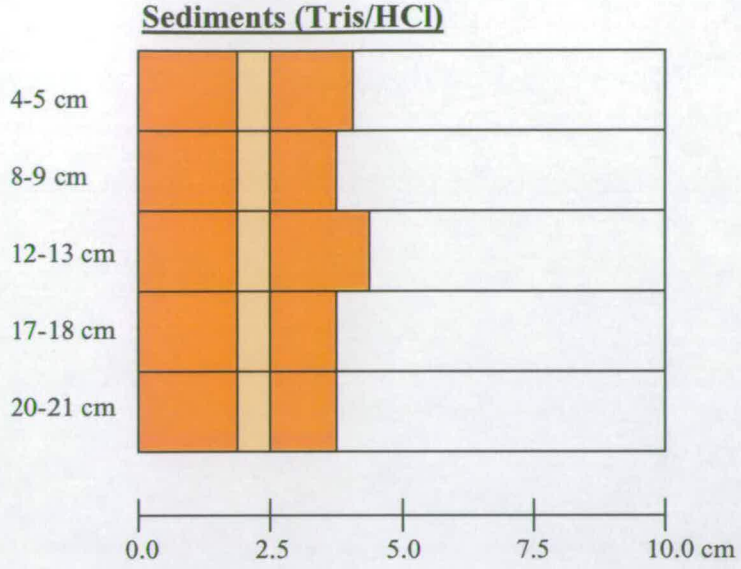

Figure 5.36 Schematic indicating movement of brown humic material through gel for Loch Tay sediments from selected depths in Tris-HCl running buffer

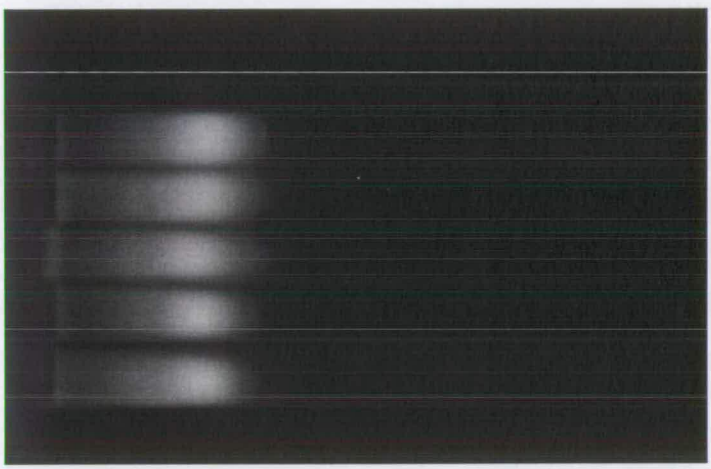

Figure 5.37 Loch Tay sediment from selected depths (LT core 1 section 4, section 8, section 12, section 17 and section 20) in Tris-HCl runing buffer. Captured under UV light, with an exposure of of 3.0 Sec

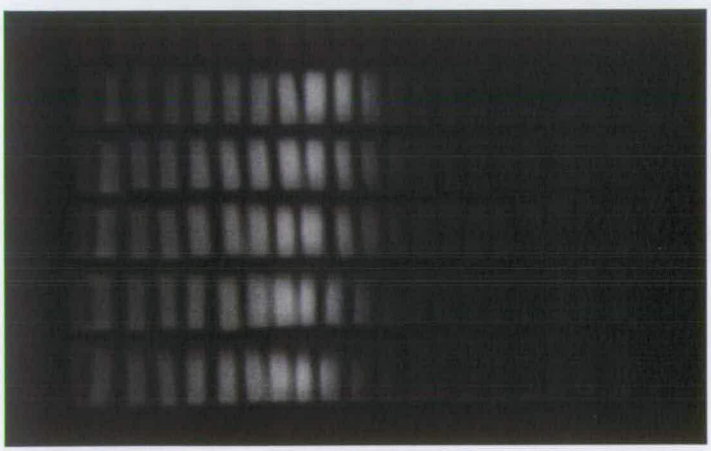

Figure 5.38 Loch Tay sediment from selected depths (LT core 1 section 4, section 8, section 12, section 17 and section 20) in Tris-HCl running buffer. Captured under UV light with 3.0 Sec exposure. Sectioned at 0.5 cm intervals.

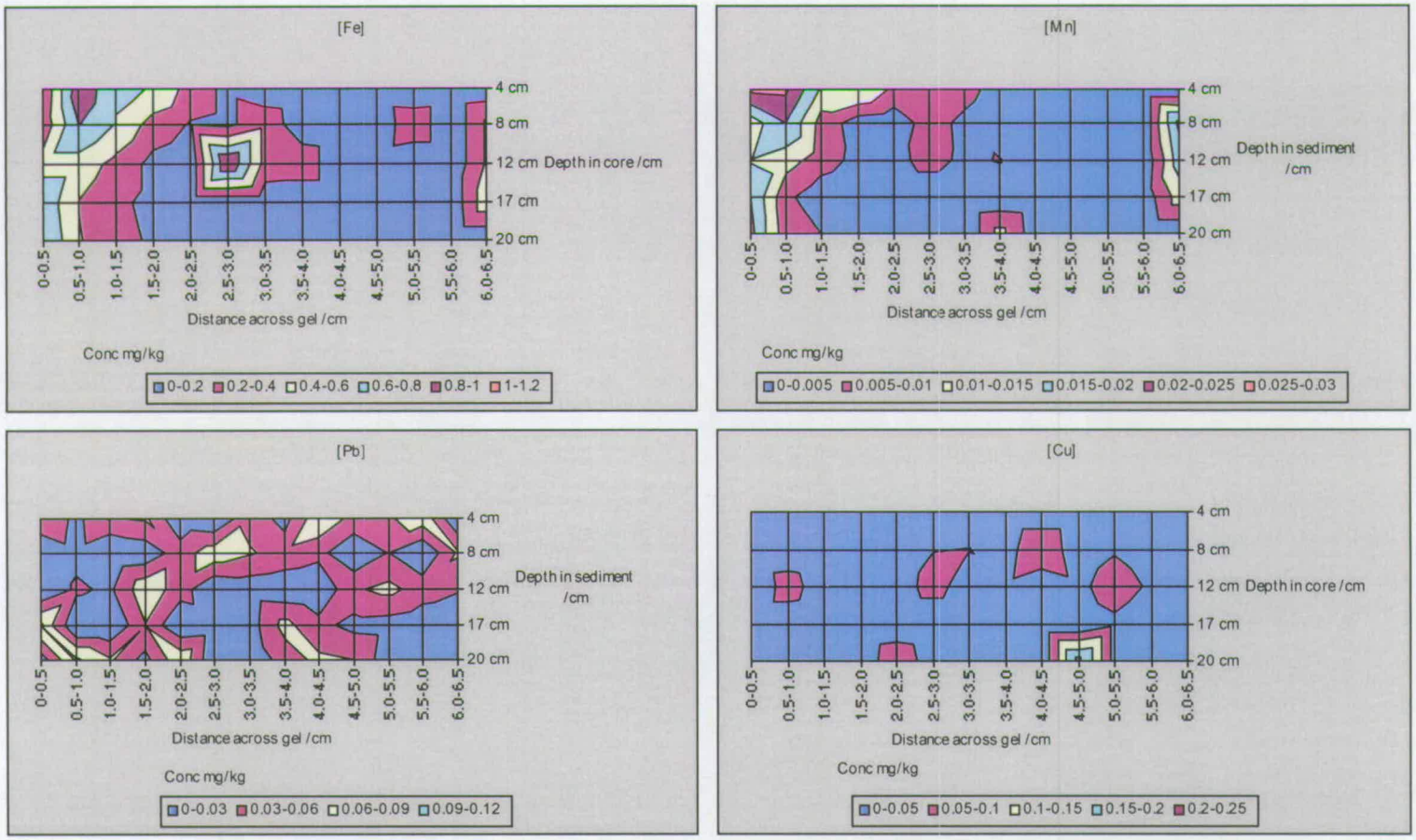

Figure 5.39 Distribution of selected elements across the gel after the electrphoretic extraction of sediments from selected depths of Loch Tay core LT1

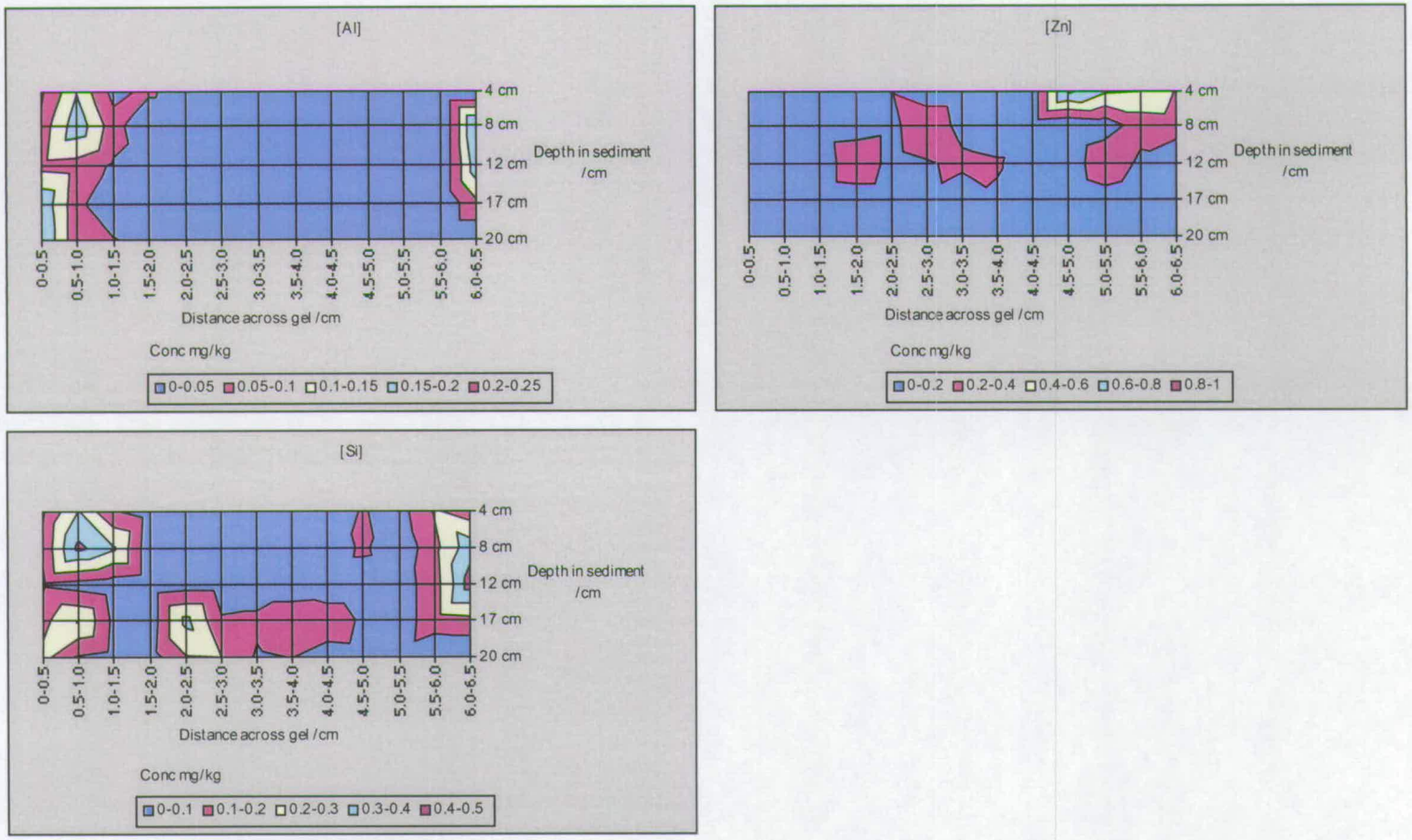

Figure 5.39 continued Distribution of selected elements across the gel after the electrphoretic extraction of sediments from selected depths of Loch Tay core LT1

The mobility and concentration of Zn decreased rapidly with depth in the sediment. At 4 cm depth the maximum concentration was found at 4.5-5.0 cm across the gel.

The Al distribution with distance across the gel and depth in the sediment was similar to that of Fe. A large proportion of the Al rich material remained in or near the well and the mobility of this material decreased with depth. A highly mobile fraction was also found in the extracts from 8 cm and 12 cm depth.

The Si enriched material was found in two fractions for all depths. At 4 cm and 8 cm depth a large portion of the Si rich material was found in the residual material contained in the well. At 12 cm depth the concentration of Si in the residual material was low and the maximum concentration was found at 6.0-6.5 cm across the gel. At 17 cm the mobility of the Si rich material had decreased again with a significant concentration found in the well and the maximum concentration found at 2.0-2.5 cm across the gel.

Chapter 6: Geochemical behaviour of trace metals, Pb, Cu and Zn in Loch Leven bottom sediments

6.1 Introduction

Loch Leven, as described in section 2.1.1, is a eutrophic water body and as such exhibits high levels of primary productivity (Bailey-Watts and Kirika, 1987). This is evident particularly in summer months when mats of blue-green algae frequently cover large areas of the loch surface. As a consequence of the blooms, remains of the algae sink to the bottom of the loch and contribute significantly to the organic matter input to the near-surface bottom sediments. The fate of this organic matter is influenced by microbial decomposition, which may start in the water column, but is an important ongoing process occurring within the sediments. Thus near-surface sediments may be relatively organic-rich whilst deeper sediments may have a significantly lower organic content. In the context of trace metal-organic complexation (section 1.5.2), changes in the organic matter composition and content of the sediments with depth can be an important factor. Decomposition of organic matter, however, often promotes more reducing conditions within sediments and thus also has direct consequences for the stability of heavy metal oxides (HMO) and indirect effects on the mobility of trace metals which may be bound to HMO surfaces (section 1.5.1). Previous work on Loch Leven has shown that, although nutrient-rich, the waters are well-mixed and oxygenated throughout the year and moreover that the porewaters in contact with the sediments may remain oxygenated to a depth of about 15 cm (Kirika, 2002, pers. comm.). The purpose of this study was, therefore, to:

(i) establish the characteristics of the bottom sediments and in particular to quantify the changes in organic matter content with sediment depth

(ii) establish the redox status of the bottom sediments by determining the pseudo-total, readily reducible and porewater vertical profiles for Mn and Fe

(iii) investigate the influence of both organic matter and redox status on the vertical distribution and mobility of trace metals, Pb, Cu and Zn in the bottom sediments.

The moisture content, wet/dry ratio and organic matter content of the depth sections of cores (LL1-3) are in vertical profiles illustrated in Figure 3.1. Similarly the pseudo-total, readily reducible and porewater concentration results for the three cores are illustrated in Figures 3.2-8.

6.2 Characterisation of Loch Leven bottom sediments

The sediments of Loch Leven had moisture contents of approximately 80 % and this value decreased steadily with depth below 2.9 cm. This coincides with a decrease in the wet/dry ratio at this depth and the ratio profiles also show a sharp transition from the upper 3 cm of sediment and the remaining sediment core. The higher water content indicates the presence of coarse textured sediment or of a more open sediment structure. Elevation of the organic content of the sediment would open up the sediment structure and allow more water to be retained. This indeed appears to be the case as the notable decrease in water content at 2.9 cm depth coincides with the decrease of the organic content of the sediment with depth.

The organic content of the Loch Leven sediment typically comprised 12 % of the total sample and increased from the surface composition to peak at 0.7 cm depth. This is followed by a sharp decrease and a gradual increase to another peak at 2.9 cm depth before decreasing steadily with depth. The magnitude of decrease down the core represents 62 % of the maximum organic content of 16 % (w/w). The sediments cannot be classed as organic rich and due to the low organic content the reducing conditions that develop as a result of biodegradation of organic material cannot be expected in this environment.

6.3 Redox cycling of Mn and Fe in Loch Leven bottom sediments

As described in section 3.3.1, there was good agreement between the vertical pseudo-total concentration profiles for Mn. The similarities between the cores are highlighted in Table 6.1.

In each case, there was a large near-surface concentration peak followed by a moderate decrease to about 3 cm and then a rapid decrease in concentration to near-constant values towards the bottom of the core. The position of the maximum concentration of up to ~0.3 % w/w was always in the top 0-1 cm of the sediment. Fine-sectioning, however, revealed that the peak was sometimes much sharper than this and indeed may be positioned in the top 0-0.2 cm (LL1) but in other cases may be as broad as 1 cm (LL2). Thus fine-sectioning is a useful sampling tool for determining the position of concentration peaks with greater accuracy. It should be borne in mind, however, that fine-sectioning also decreases the amount of material available for analysis of a given depth section and may therefore limit the extent of characterisation that can be carried out on a particular sediment core.

From the vertical pseudo-total concentration profiles for Mn and with knowledge of the redox-cycling behaviour of Mn in other freshwater lochs (Bryant *et al*, 1997, Shuttleworth *et al.*, 1999, Williams, 1993, Muller *et al.*, 2002), it would appear that oxic conditions prevail in the near-surface bottom sediments in agreement with previous findings for this relatively shallow loch (section 6.1). On this basis, the sediments should act as a sink for Mn, i.e. Mn should be retained in the near-surface sections in the form of insoluble oxides.

The extraction of Mn using 0.1 M $NH_2OH.HCl$ (pH 2) from each sediment section (LL1-2) showed that most of the Mn at all depths was in a readily reducible form. Typically about 123 ± 29 % of pseudo-total Mn was extracted from the Loch Leven sediments and there was again very good agreement between the profiles for the three cores. High proportions of Mn in a readily reducible form has also been found in other freshwater loch sediments (Chao, 1972, Gavin, 1999, Williams, 1993) and

Depth (cm)	LL1 Mn (% w/w)	LL2 Mn (% w/w)	LL3 Mn (% w/w)
0-1	0.23±0.03*	0.24±0.03*	0.22
2-3	0.15±0.04*	0.13±0.01*	0.17
13-14	0.07	0.10	0.10
16-17	0.07	0.07	0.08

Table 6.1: Comparison of concentrations of Mn at key depth intervals from Loch Leven sediment cores LL1-3 (*mean ± 1 s.d.; LL1 and LL2 fine-sectioned over 0-3 cm interval)

provides strong evidence in support of the potential for redox cycling of Mn within the bottom sediments.

Porewater Mn concentrations provided important additional information about the redox status of the sediments. Concentrations were below the limit of detection (section 2.15) for sections above ~17 cm in porewaters from both LL1 and LL3. Porewater Mn concentrations then increased towards the bottom of each core. This suggested that conditions were not sufficiently reducing to promote reduction of insoluble manganese (IV) to soluble manganese (II) above this depth and would again be consistent with previous observations (Kirika, 2002, pers. comm.) that the porewaters in contact with Loch Leven sediments were oxygenated to a depth of about 15 cm. It is not uncommon to observe redox fronts at depth within sediment cores, e.g. Muller et al. (2002) found that sediments of Lake Baikal were oxygenated to a depth of about 15 cm, but the vertical distance between the increase in porewater manganese (II) concentrations to the solid phase redox enrichment has generally been smaller, e.g. Gavin (1999), Muller et al. (2002), Davison et al. (1982). Specifically for Loch Leven, it is postulated that, with respect to manganese (IV) oxide precipitation/dissolution processes, there are three redox zones within the sediment core defined as:

(i) oxic (~0-3 cm) – precipitation of manganese (IV) oxides
(ii) sub-oxic (~3-17cm) – "metastable" zone where there is no major dissolution of manganese (IV) oxides
(iii) more anoxic (>17 cm) – dissolution of manganese (IV) oxides

Further information about the redox status of loch sediments can usually be obtained from vertical concentration profiles for Fe. The mean pseudo-total concentrations of Fe in LL1-3 were 4.1 ± 0.4%, 4.2 ± 0.2% and 4.0 ± 0.2%, respectively. Clearly, and in strong contrast with the Mn vertical profiles, the concentrations of Fe varied little with depth. There was little evidence of either near-surface or deeper maxima in any of the profiles. Even examination of the fine sectioned cores (LL1-2) did not reveal any enrichment just below the Mn peaks as might have been expected on

thermodynamic grounds (Stumm and Morgan, 1996). Thus, under the conditions prevailing in the Loch Leven sediments, the vertical solid phase pseudo-total concentration profiles for Fe appear unaffected by redox cycling. Other workers have obtained relatively uniform depth profiles for Fe in sediment environments, e.g. riverine estuary sediments (Skowronek et al., 1994). This may be due to sediment mixing but such perturbation is unlikely in the case of the Loch Leven sediments given the sharpness of the Mn enrichments in the solid phase.

The Mn/Fe ratio profiles of all the Loch Leven samples have strong correlations with the corresponding pseudo-total Mn profiles. With the highly uniform nature of the Fe profiles the Mn/Fe ratio is merely reflecting the variation in concentration of Mn with depth.

Very little of the pseudo-total Fe was extracted from the Loch Leven sediments by 0.1 M $NH_2OH.HCl$ (pH 2). Values of ~ 5% of the pseudo-total concentrations were typically obtained for LL1-3. This was not unexpected as the reagent is commonly used specifically to extract readily reducible manganese (IV) oxide phases whilst leaving the more thermodynamically stable and chemically resistant iron (III) phases in the sediment residue (Chao, 1972, Tokaliolu *et al.*, 2000, Laxen *et al.*, 1983). In all cases, however, there was a general slight increase in extractability with increasing depth. Differences between the cores were also evident in that higher proportions of Fe were extracted from the 0-7 cm sediments of LL1 and LL2 compared with LL3 (from direct comparison of extract concentrations but also when reported relative to the pseudo-total). The reasons for the general increase with increasing depth nor the differences between the cores were not immediately apparent.

There were again differences between the vertical porewater concentration profiles for Fe. In contrast with LL1 where, with the exception of the top 0-3 cm, there was almost no change with increasing depth, the Fe concentrations increased fairly uniformly with increasing depth for LL3. Little interpretation can be made from this porewater data as there is no consistent depth trend, correlation to porewater DOC or a link to pseudo-total or readily reducible concentration profiles.

Further work would have been required to establish the underlying reasons for the shape of the Fe porewater profiles. Although no Loch Leven porewater samples remained, modification of the sampling strategy was therefore considered necessary prior to continuation of the overall project.

6.4 Vertical distribution and potential mobility of trace metals, Pb, Cu and Zn in Loch Leven bottom sediments

As summarised in Table 6.2, there was a fair degree of agreement with respect to the mean pseudo-total concentrations of the trace metals, Pb, Cu and Zn, in cores LL1-3. These values, although higher than typical natural background concentrations of these elements, Pb, Cu and Zn which have natural abundances of 14 mg/kg, 50 mg/kg and 75 mg/kg respectively, are not indicative of major anthropogenic contamination of the sediments (Wild, 1993).

There is very little evidence of consistent trends with increasing depth for any of these elements although the near-surface pseudo-total concentrations of all three are sometimes higher than those in the underlying sediments, e.g. in the 0-3 cm sections of LL2. There is recent UK data to support a decrease in anthropogenic emissions particularly of Pb (MacKenzie and Pulford, 2002, Farmer et al., 2000) and this has been reflected in loch sediment profiles (e.g. from Loch Lomond in work by Eades *et al.*, 2002) which have been used as records of historical and recent anthropogenic pollution. Decreases in emissions of Cu and Zn have also occurred in the later part of the 20th Century (Vallius, 1999). With the well-established decline in emissions and given that 0-3 cm is also the position of the redox-controlled enrichments of solid phase Mn it was postulated that manganese (IV) oxide surfaces may be important sinks for Pb, Cu and Zn and that the redox processes giving rise to the solid phase enrichments could also be perturbing the pseudo-total trace metal profiles.

Over the top 0-3 cm sections there appeared to be no relationship between the organic content of the sediment and the Pb concentrations. There was also a slight, negative correlation of Cu and organic matter over the upper 0-3 cm (r^2 = -0.28) as well as with depth in core LL3. The concentration of Zn was also found to have a

Core	Pb mean concentration mg/kg (± 1 s.d.)	Cu mean concentration mg/kg (± 1 s.d.)	Zn mean concentration mg/kg (± 1 s.d.)
LL1	61±21	42±5	183±21
LL2	51±5	48±6	192±11
LL3	83±10	39±8	189±44

Table 6.2: Mean concentrations (± 1 s.d) of Pb, Cu and Zn in cores LL1-3 from Loch Leven

slight negative correlation with organic matter (r^2 = -0.79) in the upper 0-3 cm of core LL3. Generally with increasing depth in core LL3 the ash content increased, as did the Pb, Cu and Zn concentrations suggesting that with time the nature of the material deposited in the loch has changed.

Vertical profiles showing the concentrations of trace metals in the readily reducible extracts do provide some further evidence to support the association between Cu and manganese (IV) oxides in the 0-3 cm part of sediment cores LL1 and LL2. Thereafter, the proportion of Cu extracted decreased and was almost constant to the bottom of the two cores. There was no similar relationship between Pb and Mn in the extracts from the three cores. Instead there was a stronger correlation between Pb and Fe in the readily reducible extracts. Although only about 20% of the total Pb was extracted in this manner, the results suggested some preference for iron (hydr)oxide surfaces and also a contrast between Cu and Zn associations in the Loch Leven sediments. No data was obtained for Zn.

Porewater data was only available for Pb and Zn as the Cu concentrations were always below the limit of detection (section 2.15). Porewater Pb profiles showed no correlation with Mn or Fe porewater data nor with the shape of the pseudo-total Pb profile and so the controls on Pb behaviour in these sediments could not be evaluated further. In contrast, Zn release into the porewaters occurred close to but slightly above the point of Mn release in both LL1 and LL3.
This strongly suggests that Zn on the surface of manganese (IV) oxides is released into the porewater at the point of dissolution of the oxides. The fact that Zn concentrations start to increase in the porewater from sections slightly above Mn could be attributed to a slower removal processes for Zn and thus a greater degree of diffusion away from the point of release. Longer cores would have been beneficial to establish more clearly the shapes of the Mn and Zn porewater profiles. Although the porewater concentrations are low, there is clearly some influence of the redox cycling of Mn on Zn behaviour in the sediments and thus some degree of post-depositional alteration of the vertical distribution of Zn is likely to have occurred.

6.5 Conclusions

6.5.1 Processes occurring within the Loch Leven sediments and their implications for trace heavy metal behaviour

From the vertical pseudo-total concentration profiles, Mn redox cycling was important at all three locations but there was little evidence of Fe cycling. A cold, 0.1 M $NH_2OH.HCl$ (pH2) extraction confirmed that Mn was mainly in a readily reducible form. This reagent extracted only a small proportion of the pseudo-total Fe.

The vertical profiles of trace heavy metal concentrations (Pb, Cu and Zn) were quite uniform and there was little evidence of a major influence of Mn redox cycling. The cold, 0.1 M $NH_2OH.HCl$ (pH2) extraction showed that a greater proportion of pseudo-total Cu was extracted in the top 0-3 cm suggesting a correlation with readily reducible Mn. In contrast, there was a stronger correlation between extractable Pb and extractable Fe indicating a difference in the associations of Pb and Cu within the solid phase of the sediments.

The porewater concentration profiles suggest that point of release of Mn from sediment is ~ 20 cm and that this also results in the release of a small amount of Zn , i.e. a minor influence of Mn cycling on Zn.. The large distance between the redox enrichment in the sediment and the point of release from the porewaters is interesting and indeed unusual and led to the distinction of three zones within the sediment:

(i) oxic (~0-3 cm) – precipitation of manganese (IV) oxides
(ii) sub-oxic (~3-17cm) – "metastable" zone where there is no major dissolution of manganese (IV) oxides
(iii) more anoxic (>17 cm) – dissolution of manganese (IV) oxides

6.5.2 Critical evaluation of the sampling strategy employed at Loch Leven

On the basis of the vertical pseudo-total concentrations profiles for all elements (Mn, Fe, Pb,Cu and Zn) there was a very good degree of agreement between cores. Analysis of replicate cores, therefore, helps to establish the reproducibility of the coring and core cutting techniques employed in this study.

For the readily reducible extraction, although most of the pseudo-total Mn and very little Fe extracted in every case, the agreement between the vertical profiles for Fe was not so good. It is likely that this reflects real environmental differences between the cores and so suggests that, for detailed speciation studies, collection of multiple cores is an essential component of the sampling protocol.

Although the pseudo-total concentration profiles are very similar for each individual element for all cores, this was not always so for the porewater profiles and again points to the collection of multiple cores to establish the generality of observations based on any one individual core.

An additional point was that full interpretation of the porewater profiles could not be made without modification of the sampling to include more detailed examination of associations of elements with different colloidal size ranges within the porewater. This was therefore required for all subsequent work.

The work on Loch Leven was a preliminary investigation and the first application of the sampling/experimental strategy. The vertical uniformity of the heavy metal profiles and requirement for significantly longer cores strongly suggested that the selection of a different freshwater loch might be beneficial.

To this end, Loch Bradan, a drinking water loch with highly-organic rich sediments and previously well-characterised redox-cycling of Mn and Fe in the uppermost sections of the sediments, was chosen for the next part of the work.

7 Geochemical behaviour of trace elements including Pb, Cu and Zn in Loch Bradan bottom sediments

7.1 Introduction

This discussion chapter focuses on Loch Bradan, a freshwater drinking loch in SW Scotland. A full description of the history of the loch and the geology of its locality is contained in section 2.1.2 but there are a several key factors that lead to its inclusion in this study. The bedrock underlying both the loch and its catchment is predominantly Mn-rich greywacke and so the loch sediments have high concentrations of Mn (and indeed Fe) (Gavin, 1999). In contrast with Loch Leven, the waters of Loch Bradan are not as highly productive but the sediments are extremely organic-rich. This is mainly because of inputs of terrigenous organic matter from the peaty catchment soils (section 2.1.2). Thus Loch Bradan was an ideal sampling location for the investigation of the relative importance of organic complexation and redox processes in freshwater lake sediments.

Following on from the sampling and analytical protocols adopted for Loch Leven and on the basis of previous knowledge about Loch Bradan, several important modifications were introduced at this stage.

(i) two locations rather than one were chosen – both were located within the original basin of Loch Bradan (Figure 2.6). Site A was close to the main stream input in the middle of the loch and should therefore be strongly influenced by inputs of organic matter as well as trace and non-trace elements from the catchment. Site B was close to the main output at the eastern end of the loch and should be more strongly influenced by material transported across the loch from west to east (the direction of water flow). Two cores (LBA1-2) were collected from Site A and two (LBB1-2) were collected from Site B. It should also be noted that longer cores were obtained from Site B than from Site A.

(ii) the porewater samples isolated from each sediment section were ultrafiltered using a 1 kD centrifugal ultrafilter to separate colloidal and truly dissolved species.

(iii) multi-element (ICP-OES) analysis was used for selected samples to provide further information about the inorganic composition of the sediments

7.2 Characterisation of Loch Bradan bottom sediments

7.2.1 Site A

Figure 4.1 contains the moisture, ash, OM and wet/dry ratio profiles for LBA1-3. Moisture content in all three cores was constant at ~ 80% to a depth of ~12 cm. Thereafter, the moisture content of sediment decreased rapidly. The OM content (based on loss on ignition) followed a similar pattern and so the inorganic content increased dramatically over the last four sections. The wet/dry ratio also indicated that there was a major change in sediment composition at the same depth consistent with a greater content of unweathered bedrock material. This would explain why short cores (≤17 cm) were obtained at Site A.

The OM content down to depths of ~ 12 cm was significantly greater (~40% dry weight) than that observed at Loch Leven (~15% dry weight) and most likely reflects the amount and different nature of the organic material input at Loch Bradan. Loch Leven sediments receive organic matter inputs mainly from autochthonous sources (primary productivity) and this material is highly susceptible to rapid microbial alteration. Inputs of terrigenous material from the Bradan catchment (covered with woody heather plants and in parts, coniferous forests) are likely to be larger and the material much more resistant to degradation.

7.2.2 Site B

The moisture content again decreased with depth in cores LBB1-2 but a more rapid decrease occurred at 13-14 cm depth. This correlated with an increased ash content. A further correlation of this type was observed at 21-22 cm. From past knowledge of the dam extensions in 1913 and again in 1972, it is feasible that the spikes in the ash content may be present as a result of the imposed changes to the water height. This will be discussed further in the following sections. The organic profile reflects the inundation of inorganic material at these points and decreases at 12-14 cm. This aside the organic profile has a steady decrease with depth consistent with the degradation of organic matter by microbial action.

7.3 Characterisation of the porewaters extracted from Loch Bradan bottom sediments

7.3.1 Site A

Similar DOC profiles were obtained for each of the three cores, as measured by absorbance at 254 nm. The DOC concentration was elevated in the surface section with the maximum value in the upper 4 cm in each case. Thereafter the DOC remained low with a slight elevation, especially notable in LBA2-3, at 7-8 cm and a further slight increase at the base of the core. The surface enrichment of DOC may be due to settling of organic rich material from the overlying water but there was no corresponding elevation in the solid phase organic profile at this point. At the base of the core the DOC increase was accompanied by a distinct decrease in the solid phase organic concentration. This suggests the release at depth of the organic material to the water and that with depth the organic molecules become more soluble. This is generally not considered to hold true as with burial in the sediment and diagenetic alteration the organic molecules become less functional and soluble. The ash content increased at

depth in the core so the elevation of porewater DOC may be from the dissociation of smaller organic molecules from the inorganic surfaces.

7.3.2. Site B

The porewater DOC as measured by absorbance at 254 nm was elevated in three sharp peaks down the core. The cores were comparable, with changes in the position of the elevations attributed to compacting of the core LBB2 as it was extruded from the corer. This would indeed appear to be the case as the distance between the respective peaks increases with depth down the core. The E4/E6 ratio increased with depth with peaks value coinciding with those of the peaks in DOC concentration. This suggests the presence of smaller or less aromatic molecules, which would concur with the elevated solubility of the organic material at these points. The peaks in the porewater concentration of DOC coincide with elevations in the ash content in the sediment and therefore may be attributed to the dissociation of smaller organics from the inorganic surfaces at depth.

7.4 Redox Cycling of Mn and Fe in Loch Bradan bottom sediments

7.4.1 Site A – pseudo-total concentration profiles

In all cases, the maximum concentration of pseudo-total Mn in the 0-1 cm section was followed by a Fe concentration peak in the 1-2 cm section. It is not always possible to find such distinct separations as at a 1-cm resolution the Mn and Fe may appear to coincide in the sediment. Williams (1993), for example, showed that at 1-cm resolution the Mn and Fe near surface enrichments in Loch Dee sediments could not be observed as distinct separated peaks. At Site A, however, even without fine-sectioning, it was possible to observe distinct Mn and Fe peaks in the solid phase of the sediment core and this agreed with the results of previous studies carried out on Loch Bradan (Gavin,

1999). In Lake Baikal sediments, Muller *et al.* (2002) also found an Fe peak located several millimeters below a Mn peak.

Below the redox enrichment, there was a slight broad enhancement in Mn concentrations between 5-10 cm and then a marked decrease in from 12 cm to the bottom of each core. A similar pattern was observed for Fe and indeed the broad enhancement was more distinct. This could be indicative of further redox-related processes occurring under more reducing conditions in the sediments. The marked decrease in Mn and Fe concentrations below 12 cm was observed in all three cores as well and coincided with the major change in the sediment composition discussed in section 7.2.1. The results suggested a transition to unweathered bedrock material that had lower Mn and Fe concentrations than the overlying sediment. It should be noted that the digestion procedure involved hot 8 M HNO_3 rather than stronger reagents such as HF. Thus, incomplete digestion of more resistant phases cannot be ruled out. The main purpose of this study was to investigate the mobile and potentially mobile forms of elements in the sediments and so a pseudo-total digest (hot 8 M HNO_3) was considered to be appropriate.

7.4.2 Site B – pseudo-total concentration profiles

Higher concentrations of Mn were observed in the 0-1 cm sections at site B than at site A. This is consistent with the results of previous studies (Gavin, 1999) involving analyses of cores from a transect across the loch. The concentration of Mn in the near surface enrichment increased from west to east (in the same direction as water flow). Gavin (1999) did not find the same pattern for Fe and, indeed, concentrations occurring at the near-surface maximum in cores from the middle of the loch were similar to those in cores from the eastern end. At Site B in this study, the near surface maximum concentrations again occurred in the 1-2 cm section and were also of similar magnitude to those obtained for Site A. The following explanations may account for these findings. Slow oxidation and removal kinetics for Mn compared with Fe would result in greater

residence times within the water column and thus increase the importance of the water movement. Davison *et al.* (1982) observed that once in the water column, the behaviour of Mn(II) is controlled mainly by comparatively rapid currents rather than the relatively slow oxidation and precipitation processes. Gavin *et al.* (2001) also established that outer-sphere complexation of Mn(II) by humic substances was an important process occurring in the waters of Loch Bradan which can also inhibit the oxidation and precipitation processes.

The Mn and Fe profiles obtained for site B cores (LLB1-2) did not display the enhancement at 5-10 cm nor the decrease in concentration below 12 cm found for LLA1-3 (section 7.4.1). Instead, a small Fe peak at 15 cm depth coincided with a small change in sediment water content as well as colour and texture (section 2.1.2). The Mn concentration increased markedly at 18-20 cm with an increase in Fe concentration at a shallower depth of 17-19 cm. The concentrations of Mn and Fe increased to 4 % w/w and 20 % w/w respectively. These increases did not correlate with changes in water content of the sediment but did coincide with the point where the ash content of the sediment increased and organic content became negligible. The inverse correlation between organic matter content and Fe concentrations (on the weight percent scale) has been observed in the near-surface sections of Loch Bradan sediments (Gavin, 1999) and attributed to the solid phase enrichment process. It is thought that the Mn and Fe peaks at depth in the sediment core are remnants of past redox enrichments with low organic matter content that have been preserved by burial in the sediment and are only slowly changing with time. From these observations, an alternative explanation for the higher Mn concentrations at the eastern end of the loch could be that past enrichments (relic peaks) which are slowly dissolving give rise to an additional source of Mn which may be able to enter the redox cycle in the upper parts of the sediments. Fe, however, is also present at very high concentrations in these relic peaks and so a major difference in the mobility of Mn and Fe within these sediments would have to be established. These points will be discussed further in the following sections.

7.4.3 Site B – readily reducible concentration profiles

The longer cores from site B were extracted using the method for the readily reducible digest (section 2.9) in order to obtain further information about the form of Mn in the near-surface sediments and in the deeper relic peaks as well as the extractability of Fe and the associations of trace elements. Nearly all of the pseudo-total Mn in LBB1 and LBB2 was in a readily reducible form and only approximately 10 % of the pseudo-total Fe was co-extracted The vertical profiles of Mn and Fe in the readily reducible extracts were very similar and indeed the Fe readily reducible profile bears more resemblance to the readily reducible Mn profile (r^2=0.91) than it does to the psuedo-total Fe (r^2=0.62). This is particularly evident from the position of the maximum in the readily reducible Fe profile which is in the 0-1 cm section, the same as that in the readily reducible Mn and pseudo-total Mn profiles. It is proposed, therefore, that the 0.1 M NH_2OH dissolves not only the readily reducible Mn but also sorbed Fe. The relationship between Fe and Mn in the extracts suggests that Mn oxide surfaces have Fe-containing coatings. Although the correlation is quite strong, slightly greater Fe relative to Mn concentrations were extracted in the 15-20 cm zone and so the extent of these coatings is greater at this depth.

This aside, as consequence of the readily reducible extraction results with respect to redox cycling: (i) there is again strong evidence that Mn is present in a readily reducible form but (ii) there is no change in form with increasing depth and in, particular, Mn in the relic peaks is also in a readily reducible form. This latter point is important with respect to demonstrating that the peaks at depth could have been near-surface redox enrichments prior to one of the major extensions of the loch.

7.4.4 Site A – porewater concentration profiles

The Mn porewater profiles from site A could all be interpreted in a classical manner, i.e. Mn(IV) is reduced, dissolution occurs and Mn(II) is released into the porewater below the solid phase maximum. Each profile had a gradual increase to a broad maximum at 5-7 cm followed by a gradual decrease down to 10 cm depth. The broadness of the peak was consistent with diffusion both upwards and downwards from the point of release (Davison, 1985, Stumm and Morgan 1996). The vertical distance between the solid phase and porewater maxima is more typical of that found in other freshwater loch environments (Canfield *et al.*, 1993) than that described in section 6.3 for Loch Leven.

A classical profile was not found for Fe. On thermodynamic grounds, the release of Fe into the porewaters should occur at a greater depth than that of Mn. This was not found to be the case with one or more Fe maxima occurring within the 0-5 cm region, above the Mn maxima. As for Loch Leven, having three cores from the same location helps to establish that this is a general feature of the Loch Bradan porewaters at this sampling location and not just an isolated case or an analytical artifact. It was concluded that a process other than redox cycling must be responsible for the elevated Fe in the porewater from the near-surface sections.

7.4.5 Site B – porewater concentration profiles

In examining the Mn porewater profiles of LBB1-2 (Figure 4.14), it was clear that the classical profile expected from redox cycling of Mn was obtained for LBB2 but not for LBB1. The profile of LBB2 contains a sharp point of release of Mn into the porewater at 8-9 cm depth but there was only a small peak in the 0-1 cm section of LBB1 which coincided with the solid phase enrichment. Both cores had small peaks at 12-14 cm and slightly larger peaks towards the bottom of the core. The peaks at 20 cm depth also

coincided with the elevated concentration of Mn in the solid phase. The similarity in the shapes of the porewater and pseudo-total profiles of Mn, particularly for LBB1, indicates that additional factors are important in controlling Mn behaviour at this location.

Three maxima were evident in the Fe porewater profiles of LBB1-2. The first peak occurred at 1-2 cm depth, the second at 12-13 cm and the major peak towards the bottom of the core (22-23 cm for LBB1 and 19-20 cm for LBB2). All three were coincident with elevated concentrations in the solid phase. The observation that the porewater concentration of Fe appears to be proportional to the solid phase concentrations suggests that solibility of the iron phases is the controlling parameter. The similarity between the Mn and Fe porewater profiles, particularly at LBB1, could be indicative of the initimate association of Mn and Fe in the solid phase and so the solubility of a mixed solid phase is controlling the porewater profiles of both elements.

A highly significant correlation between DOC concentration (as determined by UV/vis measurements – section 2.14) and Fe was found and so the Mn-Fe-containing solubility controlling solid phase is likely to contain organic and, given the brown colouration of the porewaters, humic material. Intimate mixtures of Fe and organic matter have recently been observed in organic-rich lake sediments (P. Andey *et al.*, 2000, Straub *et al.*, 2001, Shaw *et al.*, 2000). The presence of Mn-Fe-humic species in the porewaters would also inhibit (but not necessarily eliminate) redox cycling. Free Fe^{2+} and Mn^{2+} species which would otherwise be the dominant species under anoxic conditions would be subject to upwards diffusion, oxidation and precipitation as previously described.

7.4.6 Summary – importance of redox cycling and DOC

Redox cycling was found to be important in the partitioning and speciation of Mn in the site A cores with a porewater enrichment occurring just below the solid phase enrichment. It was expected that the Fe profiles would produce similar distributions with the elevations ocurring below those of the Mn. This was not found to be the case,

although the sediment profiles did conform to the classical profiles for redox cycling the porewaters did not. Therefore other processes must influence the mobility of Fe in the porewater resulting in the enrichment above that of the Mn. The similarity of the porewater profiles of Fe and DOC suggests the disruption of the redox cycling of the Fe may be due to Fe-humic interactions.

At site B it was noted that of the porewater enrichments were coincident with the solid phase enrichments. The Fe concentrations were found to be elevated at or above the point of Mn enrichment. This is not consistent with redox cycling and therefore additional processes must be considered. A strong correlation was between the porewater Fe concentrations and the DOC profile suggesting the interactions of Fe and humic molecules in the dissolved phase. This was also observed clearly for Mn and DOC profiles of LBB1 but not distinctly for LBB2. Therefore it is likely that the solubility of the mixed solid phase is controlling the porewater concentrations of Mn and Fe and in the porewater association with organic material is disrupting the redox cycling.

7.5 Geochemical behaviour of trace metals, Pb, Cu and Zn in Loch Bradan bottom sediments

7.5.1 Site A – pseudo-total concentration profiles for trace metals, Pb, Cu and Zn

Figure 7.1 summarises the trace metal data obtained for Site A (Fe and Mn profiles are included for comparison purposes).

The concentration profiles for each of the trace elements illustrated good agreement between the cores. There were also some common features for all three metals in that all had lower near-surface concentrations, broad peaks over 5-12 cm depth and a concentration decrease over the bottom three sections of the sediment core. This degree of agreement is not always observed in loch systems as was recently established by Yang *et al.* (2002) who investigated the distribution of some trace metals in Lochnagar,

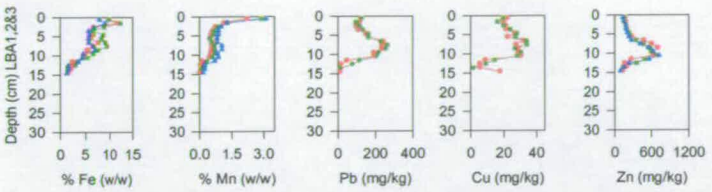

Figure 7.1: The pseudo-total concentrations of Mn, Fe, Pb, Cu and Zn in Loch Bradan bottom sediments (LBA1-3)

a Scottish mountain lake ecosystem, and its catchment. The isolated location of this loch was the main factor leading to its selection. It was thought that the observation of elevated (greater than background) concentrations of trace metals should be attributable to deposition only from the atmosphere (Yang *et al.*, 2002) and thus a reliable record of past pollution could be attained. Some 17 cores were taken across the lake and trace metal analysis revealed a heterogeneity problem. There were variations in the trends found for different metals within a core and for a single metal down different cores. Runoff from a loch catchment can contribute to trace metal concentrations in the loch sediments and this may not occur uniformly across the loch.

At Site A (Loch Bradan), where the cores would have been collected at only a few metres apart, the degree of variability is small. If interpreted as a historical record, the lower near-surface concentrations most likely reflect lower anthropogenic inputs to the loch in recent years. The rapid decrease at 12 cm to the bottom of the core, however, is due to the increased presence of unweathered bedrock material and does not necessarily represent a past pollution trend.

ICP-OES analysis of LBA3 (duplicate sediment sections were digested and analysed), revealed some interesting information about the composition of the sediments. Although the results obtained represent pseudo-total rather than total concentrations, there is strong evidence from the decrease in Al, Ca and Mg concentrations and the increase in Si concentrations of a major change in sediment composition, most probably to silica-rich bedrock material (consistent with the geology of this area). Multi-element analysis also showed that there were S and P peaks close to the positions of the Fe and trace heavy metal peaks previously described. Specifically, the S and P peaks at 7-9 cm coincided exactly with the Fe, Pb and upper part of the Cu peak. Both Cu and S profiles had secondary peaks at 10-12 cm and the Zn peak at 11 cm coincided with the secondary S peak. Processes leading to the release of Fe and other elements into porewaters can often lead to concentrations exceeding the solubility products of certain minerals and precipitation of new solid phases can result. Examples of this include the formation of sulphate minerals and these have been found for Pb, for example in Lake Junin (Martin *et al.*, 2001) and Lake Chevreuil (Huerta-Diaz *et al.*,1998). It is therefore proposed that

the profiles of Pb, Cu and Zn have been perturbed by post-depositional processes involving release into the porewaters and reprecipitation in new phosphate- and sulphate-containing solid phases. These may also contain calcium on the basis of the broad maximum in Ca concentrations at the same depth. The minimum in Si concentrations provides further evidence of a precipitation process that has led to the dilution of the other mineral components comprising the sediment. The formation of maxima just above 12 cm probably also means that downwards diffusion is limited which would be consistent with the silica-rich nature and the low moisture content of the material from 12 cm downwards. These results strongly suggest that historical records could not be obtained from the Pb, Cu and Zn profiles from Site A.

7.5.2 Site B – pseudo-total concentration profiles for trace metals, Pb, Cu and Zn

Figure 7.2 has been included as a summary of the pseudo-total concentration profiles of Pb, Cu and Zn at site B (again Mn and Fe profiles are included for comparison purposes).

In general, the profiles obtained for each of the trace metals in the cores from site B were similar to those from site A. Lower concentrations at the surface were followed by a broad peak extending over 5-15 cm down the core and generally lower concentrations with depth. On a more detailed examination, however, the near surface concentrations were slightly higher at site B (eastern end) compared to site A (middle) (Table 7.3).

More significantly, the small mid-depth peak found for Pb and Zn in the LBB cores coincides with the small Fe peak. Unusually, there was also a minimum in Cu concentration at this depth. Pb and Zn are often associated with Fe phases but the reason for the Cu minimum is not apparent from the other pseudo-total profiles. The same features, however, occur in both cores at almost exactly the same depth. It is possible that sediment from a discrete event and of slightly different origin had been deposited as

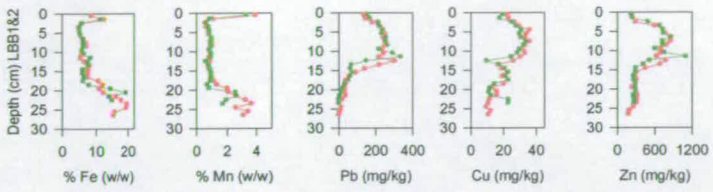

Figure 7.2: The pseudo-total concentrations of Mn, Fe, Pb, Cu and Zn in Loch Bradan bottom sediments (LBB1-2)

Core (0-3 cm data only)	Mean Pb mg/kg (±1 s.d.)	Mean Cu mg/kg (±1 s.d.)	Mean Zn mg/kg (±1 s.d.)
LBA1	114.3±13.7	21.4±1.2	179.1±9.1
LBA2	115.8±15.5	18.8±2.1	164.3±21.2
LBB1	152.8±25.5	24.0±2.3	246.9±31.4
LBB2	179.8±31.2	20.6±3.9	309.7±149.5

Table 7.3 Mean concentration of Pb, Cu and Zn (±1 s.d.) in the 0-3 cm sections of Loch Bradan cores from Sites A and B

the material at this depth was different in texture (section 2.1.2). Alternatively, processes leading to iron enrichment may also have influenced the distribution of the trace metals within the cores.

Below the mid-depth Fe peak the Pb concentrations decreased markedly to almost constant concentrations, Zn concentrations decreased and remained constant at ~ 280 mg/kg whilst the Cu concentrations decreased only slightly to ~20 mg/kg at the bottom of the core. The trace elements are not subject to enrichment at depth as was found previously for Mn and Fe. If these lower concentrations of contaminant metals are indicative of pre-industrial times (pre-1850) then this would date the relic peak much earlier than the first extension of the loch in 1913. On the basis of a previously dated core from Loch Bradan, which gave a sedimentation rate of 12 mg/cm^2/y (Short, 1995), the bottom of the core, however, corresponds to about 1960. This gives a more plausible period for the formation of the Mn and Fe enrichments (now at ~20 cm) which would have been close to the water-sediment interface at approximately 1967-1970. As a consequence, the sediment accumulating since then, with the higher concentrations of Pb, Cu and Zn, has been deposited since about 1970. Transport and deposition of more contaminated material as a result of the second dam extension is inferred. Thus, although there was a good degree of agreement between the trace metal concentrations profiles at Sites A and B, the major perturbations caused by extension of the loch mean that care must be taken in extrapolating these results for Loch Bradan to give a more general picture of past anthropogenic pollution.

7.5.3 Site B – trace heavy metals, Pb, Cu and Zn in readily reducible extracts

Only the concentration of Zn was determined (by AAS) for LBB1 but concentrations of Pb, Cu and Zn were determined (by ICP-OES) for LBB2 (section 2.16). Each of the elements will be discussed in turn using the LBB2 data for Pb and Cu and both the LBB1 and LBB2 data for Zn.

The vertical concentration profile for 0.1 M $NH_2OH.HCl$ (pH2)-extractable Pb closely resembles the pseudo-total concentration Pb profile. Thus a fairly constant proportion of about 50% of the Pb was extracted. This could either be Pb bound to the Mn oxide surface or it may be Pb associated with the Fe bound to the Mn oxide surface. If this were the case it would be expected that the Pb profile would bear some resemblance to the Mn or Fe profiles. There was no correlation between Pb and Mn or Fe in the readily reducible extracts. Thus the reagent may remove a certain form of lead which is present as a relatively constant fraction of the total lead present in the sediments. The readily reducible digestion may liberate some Pb from sulphidic or organic material (Williams, 1993).

The readily reducible Cu profile was also similar in many ways to the pseudo-total Cu profile with a broad peak centred at 6-7 cm depth and a slight decrease towards the bottom of the core. As for Pb, about 50 % of the total Cu was generally extracted. A greater amount of Cu (~75% of pseudo-total) was extracted at the minimum in the pseudo-total profile and this coincided with the position of the maximum in both the readily reducible and pseudo-total Pb profiles. It is proposed that the relatively greater extractability of Cu at this depth is indicative of a speciation change that is in some way related to the decrease in concentration of Cu in the sediment at this depth. This will be discussed further in following sections.

In contrast with the Pb and Cu profiles, the vertical profiles (LBB1 and LBB2) for Zn in the readily reducible extracts bore little resemblance to that of the pseudo-total distributions. Although the maxima at 10-15 cm coincided with peaks in the psuedo-total profiles, there was much greater structure, particularly in the 0-10 cm section of each core. Again in contrast with Pb and Cu, at the position of the broad peak dominating the pseudo-total Zn concentration profile, only 25 % of the Zn was extracted. Even at the position of the maxima at 10-15 cm, only ~30-40 % of the pseudo-total Zn was extracted. It is notable that very similar depth profiles were obtained for the two cores.

Although it can be more difficult to obtain Zn data with low analytical uncertainty, the independent analysis of the two cores gives confidence that the patterns obtained represent real variations in Zn associations with the sediment. Clearly, the geochemical behaviour of Zn is complicated and requires greater evaluation. ICP-OES analysis enabled simultaneous determination of other elements and further discussion of potential associations of Zn (and Pb and Cu) can be found in section 7.5.4.

7.5.4 Site B – other elements (Al, Si, Ca, P, S) in the readily reducible extracts

The shape of the readily reducible Pb profile bears a strong resemblance to the P and the particularly S profiles especially over 0-12 cm, where the broad enrichment occurs. The Ca profile is also quite similar to the profile of Pb. This suggests that about 50% of the psuedo-total Pb is in the form of sulphates or phosphates (with calcium). Under reducing conditions Guo *et al.* (1997) found that sulphide, carbonate and humic complexes controlled Pb behaviour in sediment. Less strong correlations are observed for the other trace elements although there is some similarity between the Zn and S profiles in the upper parts of the sediments. Additionally, the peaks in the 10-13 cm section of the Pb, Cu and Zn profiles are evident but to a lesser extent in the P and S profiles.

A further point of interest is that below the peak at 10-13 cm there was a minimum in the profiles of Al, Ca, Mg, P, S. The minimum marks the position of the enrichment of Fe in the solid phase and there is indeed another minimum in the Al and Si profiles at the position of the deeper solid phase Mn and Fe enrichments. This gives further support to the interpretation of the Mn and Fe peaks as relic peaks, i.e. past redox enrichments of (hydr)oxide phases which have been preserved in the sediment.

7.5.5 Site A – Porewater profiles for trace heavy metals, Pb, Zn and Cu

Pb pore water concentrations showed strong correlation to Fe content at each depth and for all three cores from Site A. In particular, the sharper near-surface peaks coincided with those for Fe as did the broader peaks at greater depth. Cu concentration were generally often very low and close to the limit of detection (section 2.15) but the peak at 3-4 cm in LBA1 coincided with that of Fe. Given the strong correlation of the Fe and DOC profiles, it would appear that DOC might also be important in controlling the shape of the Pb and Cu porewater profiles. The role of organic matter required further investigation and is discussed further in section 7.6.

In strong contrast, the Zn profiles are very different from the Pb, Cu and Fe profiles. At first it might appear that the porewater concentrations of Zn and Mn are strongly correlated but the maxima in the Zn profiles occur at greater depth than in the Mn profiles. Instead the porewater Zn maxima match more closely the pseudo-total solid phase maxima and thus the solubility of the Zn phases present in the sediment appears to be the controlling factor. The differences observed in the porewater profiles help to account for the slight differences observed in the solid phase profiles of Pb, Cu and Zn and reflect the unique geochemical behaviour of each element.

7.5.6 Site B – Porewater profiles for trace heavy metals, Pb, Zn and Cu

As at Site A, the position of the porewater Pb peaks generally coincided with those of Fe. The most important appeared to be at 1-2 cm and 13-14 cm in LBB1 and at 1-2 cm and at 11-13 cm in LBB2. The position of the small maximum in psuedo-total Fe is also at 13-14 cm in LBB1 and at 11-13 cm in LBB2. In both cases, however, the position of the pseudo-total Pb peak is one section closer to the surface than the porewater Pb and Fe peaks. This strongly suggests that Pb released into the porewater along with Fe (from the small relic peak – not due to current cycling) is quickly removed from the porewater as it diffuses upwards (but any moving downwards is not immediately removed). This

explains the presence of the Pb enrichments in the pseudo-total solid phase and is consistent with the high particle affinity of Pb. The porewater concentrations for Cu are again extremely low but, on the basis of the interpretation of the Pb profiles, it is now possible to account for the minimum in the solid phase Cu profile. Release of Cu into the porewater occurs at the position of the relic peak and Cu diffuses away from this point but is not subject to rapid removal to the solid phase. The greater extractability (0.1 M $NH_2OH.HCl$(pH2)) of Cu at this depth also indicates that Cu is in a more available form at this depth and so the result of this post-depositional alteration is a minimum in the solid phase profile. Although the overall porewater profile of Zn is quite different from those of Fe and Pb, there is some correlation between Zn and Fe particularly at greater depth and again there is some evidence supporting removal of Zn to the solid phase close to and slightly above the position of the porewater maximum.

From this, there are clearly some processes occurring that are common to both locations – redox cycling of Mn, DOC complexation of Fe, the importance of sulphate and phosphate phases for Pb, but there are also some that are particular to each individual location – behaviour of Zn and solubility controlling solid phase at Site A – the relic peaks and release of Fe and trace elements and immobilisation of Pb and, to a lesser extent, Zn, at Site B.

7.6 Site B – LBB2 - total concentrations and concentrations in <1 kDa and >1 kDa fractions of Mn, Fe, Pb, Cu and Zn in the sediment porewaters

Figures 4.14 and 4.15 display both the total concentrations and the concentrations found in the <1 kDa and > 1 kDa size fraction obtained from the porewaters of LBB2 by centrifugal ultrafiltration. LBB2 was chosen because, not only was DOC thought to be important for Fe and Pb speciation, but also because this was the only core where the classical Mn profile was not obtained. Although a satisfactory mass balance was not obtained for this first attempt at ultrafiltration, it clearly provided evidence to support the presence of Fe, Mn and Pb in the > 1 kDa fraction. The strong brown coloured organic

material was also retained in the > 1 kDa fraction and the peaks in colour (from visual and UV/vis observations) again matched the positions of the elemental peaks. The results, therefore, do not contradict the interpretation of the porewater data and do indeed suggest that dissolved humic material plays an important role in the porewater geochemistry of Fe, Mn and Pb. Further improvements to the protocols adopted for ultrafiltration were required to obtain a mass balance for all elements.

7.7 Conclusions

7.7.1 Processes occurring within the Loch Bradan sediments and their implications for trace heavy metal behaviour

There were redox enrichments in the 0-1 cm and 1-2 cm for Mn and Fe respectively for all cores at both locations. Shorter cores were obtained at Site A because of bedrock encountered towards the bottom of the core. The longer cores from Site B had relic peaks of past redox enrichments of Mn and Fe. Their occurrence was attributed to perturbations resulting from the major extensions that were made to the loch in the past. The relic peaks at the bottom of the Site B cores were tentatively linked to the extension occurring in 1972 as previous work had shown further Mn/Fe enrichments at depths of 40-45 cm which may have been due to the 1913 extension.

Broad peaks in the vertical pseudo-total concentration profiles for Fe, Pb, Cu and Zn were observed and the possible influence of post-depositional alteration processes was considered. Multi-element analysis (ICP-OES) of the pseudo-total digests and readily reducible extracts strongly suggested that, with increasing depth below the near-surface solid phase enrichments of Mn and Fe, release of Fe and associated heavy metals had occurred and new solid phases had formed. These are probably sulphate and phosphate-containing phases (with time the sulphate may become sulphide). It was further postulated that, at Site A, downwards diffusion of elements in porewaters was inhibited

by bedrock material with low moisture content and that this led to formation of maxima by precipitation of new phases at and above the zone of release.

The coincidence of porewater metal and DOC (particularly brown dissolved humic material) peaks suggested that humic material was involved in release processes and in controlling the shape of the vertical porewater profiles. Association of metals with > 1 kD species (i.e. not truly dissolved) and the presence of the brown humic material in this size fraction was confirmed by analysis of ultrafiltered porewaters but the exact nature of the role of humic material was not established.

Clearly the heavy metal profiles cannot be interpreted as historical records but a much better understanding of important phases and metal speciation within the sediments and the sediment porewaters has been achieved.

7.7.2 Critical evaluation of the sampling strategy employed at Loch Bradan

Collection of cores from two locations at Loch Bradan was particularly useful because of the extensions that had been made to the loch. This enabled the distinction of features in the profiles that were due to the extensions and those that were due to natural geochemical processes.

Ultrafiltration was used to separate truly dissolved and colloidal species within the porewater and provided confirmatory evidence in support of the interpretation of the porewater profiles. Further information, however, could be obtained by using several ultrafilters to distinguish between truly dissolved, small and large colloidal species. A mass balance must also be obtained to improve confidence in results obtained.

A further technique is required to investigate more fully the interactions between metals (Mn and Fe as well as Pb, Cu and Zn) with humic material in both the sediments and the

porewaters. Gel electrophoresis, which fractionates humic materials on the basis of size and/or charge, can be used for this purpose.

8 Geochemical behaviour of trace elements including Pb, Cu and Zn in Loch Tay bottom sediments

8.1 Introduction

Loch Tay is a deep, oligotrophic water body that has high trace metal inventories fed by an extensively mined catchment. High loading of the loch with trace metals would saturate the system and allows otherwise undetectable association within the sediments and waters to be revealed. The water depth results in thermal stratification and may lead to anoxic conditions forming in the bottom waters thus the theories developed over the previous two chapters can be tested for a water system with a very different trophic nature under high metal loading conditions.

The sampling and analytical procedures developed through the work of the previous two chapters were extended again in the sampling and analysis of Loch Tay. Four cores were collected and one was fine-sectioned as before. Samples from the surrounding catchment were also collected to determine the sources in trace metals to the loch and the partitioning of these metals between the particulate, large colloidal and small colloidal phase prior to entering the water body.

For a more cohesive picture of the intimate relationships between trace metal mobility/partitioning, organic content/nature and redox cycling one core from Loch Tay, LT3 was processed to completion. This included fractionation of the porewater through two separate ultrafilters with 30 kDa and 1 kDa cut-offs in order to establish metal partitioning and mobility in the sediment column, and electrophoretic extraction of porewaters and sediments. The electrophoretic extraction and subsequent fractionation of humic material was used to elucidate the role of humic-metal interactions in trace metal mobility. As one core was carried through all of these methods and the established regime of primary analysis no inferences have to be made as to how different cores from a given site relate to one another.

8.2 Characterisation of Loch Tay bottom sediments

8.2.1 Long cores (LT1-3)

The moisture profiles of all three long cores were consistent. The moisture content at the surface was in the region of 80 % and with depth this value declined, but only slightly compared to the profiles obtained for the other lochs, to 60 % at the base of the core. The slight fluctuations in the moisture profiles, that are difficult to distinguish, are highlighted by the wet/dry ratio profiles. In particular features were found at 6 cm, 13 cm and 17cm for each of the cores. These coincide with the slight elevations found for the organic content profiles and the corresponding decreases in the ash profiles. The relative elevation of organic content of the sediments at these points would produce a more open sediment structure and thus the sediments would retain more water.

The concentration of organic matter in the sediments decreased with depth. This can be more clearly determined for cores LT1 and LT2 with the maximum concentration of 25-27 % in surface section and a concentration of 19-20 % at the base of the core. There was a slight increase in organic content of both of these cores, again correlating with a slight increase in water content, over 8-13 cm. The organic content of core LT3 was generally lower with maximum of 24 %. The profile did not exhibit the relatively smooth changes with depth of the other two cores.

8.2.2 Short core (LT4)

The moisture content of the fine-sectioned short core LT4 decreased markedly with depth from 88 % in the surface section to 80 % near the base of the core. The water content appeared to dip at 0.4-0.6 cm and then increase to a broad peak over 0.6-14 cm. This broad peak coincides with a decrease in the ash content, and subsequent increase in the organic content, which is the only feature of an otherwise uniform profile. Apart from this feature the organic content of the short core remains at 23 % with only a slight decrease towards the very surface sections. As observed previously the increase of

organic matter content was accompanied by the increase in the water content of the sediments.

8.3 Characterisation of the porewaters extracted from Loch Tay bottom sediments

8.3.1 Long cores (LT2-3)

The absorbance of the porewater samples, from core LT3, at 254 nm had three distinct peaks at 4cm, 9 cm and 17-18 cm depth corresponding to slighter and broader increases in the E4/E6 ratio. The E4/E6 ratio has been inversely correlated to both molecular size and aromaticity, as discussed in section 1.8.1, thus the higher concentration of DOC as determined by the absorbance at 254 nm corresponds to a relative increase in the concentration of smaller or less aromatic organic molecules.

The Mn concentrations found for the porewaters were not consistent for all both of the cores, with concentrations of 2-17 mg/l for LT2 and 0.5-5 mg/l for LT3. The Mn profiles of the long cores, LT2 and LT3, have broad sub-surface peaks over 4-8 cm with sharp peaks below at 8-9 cm and elevation in concentration near the base of the cores at 17-19 cm. These profiles are not typical of Mn redox cycling which is often characterised by sharp points of elevated Mn concentration near the surface and continuously decreasing concentrations with increasing depth.

If the broad Mn peaks found are redox enrichments it would be expected that the Fe profile would be influenced by the same processes and thus have a similar profile with a sub-surface peak below that of the Mn. This was not found to be the case with the Fe concentration peaking sharply above the area of Mn enrichment. Both of the long cores, but particularly LT3, show a good correlation between the Fe concentration and the DOC profile with elevated concentrations at 4 cm, 9 cm and 18 cm depth. This could be indicative of the well-documented association of Fe and humic substances (Schnitzer and Skinner, 1965, Kerndorff and Schnitzer, 1980) either as Fe bound to humic molecules or humic molecules adsorbed to Fe oxide surfaces. This Fe-organic

association appears to have strong implications for Pb, Cu and Zn partitioning as all of the otherwise rounded profiles of the trace metals, again especially for LT3, have sharp elevations in concentration in the pore water coinciding with those of the Fe and the DOC.

8.3.2 Short core (LT4)

The profile of porewater absorbance at 254 nm for the short fine-sectioned core LT4 was dominated by a large broad peak at 0.8 cm with a value of 1.5. As for the longer cores discussed above the point of elevation in the DOC coincides with a peak, of lesser magnitude, in the E4/E6 ratio, again indicating that the elevated concentration of DOC is attributable to smaller or less aromatic molecules.

The Mn concentrations in the fine section are very low in comparison to the Mn concentrations obtained for the longer cores, with a range of 0.3-2.5 mg/l. At the surface sediments of core LT3 the Mn concentration dropped rapidly to 0.5 mg/l consistent with the concentrations found in the fine-sectioned porewaters. The concentration of Fe in these porewaters increased with depth from 7 mg/l at the surface to 19 mg/l at the base of the core. There is an area of elevated Fe concentration over 0.6-1.0 cm coinciding with the increase in the DOC profile.

The Cu profile also has an elevated concentration at this point, with the concentration increasing rapidly from 0.03 mg/l to 0.05 mg/l. Thereafter the Cu concentration increases steadily with depth in a similar manner to the Fe profile. The Pb concentration profile was very similar to that of Mn when considering the trend with depth, the position of the elevated concentrations and even the relative magnitude of the elevations in concentration. The behaviour of the Zn in the porewaters also appears to be associated with the Mn behaviour with rapidly decreasing concentrations with decreasing depth from the base of the core.

8.4 Distribution of elements in the loch and stream waters

The investigation of the distribution of Mn in the loch and stream waters showed that Mn was predominantly in the particulate (>0.45μm) fraction and that for the Mn remaining in the water sample the <100 kDa fraction was most important. This was also the case for Fe with the >100 kDa fraction increasing in significance only when the Fe total concentration was elevated. The observed partitioning of Fe in to the particulate fraction concurs with the reports of particulate Fe in other freshwater systems (Laxen and Chandler, 1983) and is generally attributed to aggregation of Fe rich material, Fe association with phytoplakton and the formation of Fe oxide coatings on existing particles. Usually Mn is found in the dissolved phase of the water column and in the smaller size fractions (Chiswell *et al.*, 1992, Yagi, 1988). Although in the remaining water sample the distribution of Mn is consistent with these reports there some degree of association of Mn with the larger Fe rich particulate material thus leading to elevations in the concentration of Mn in the particulate fraction.

Pb, like Fe and Mn was, found predominantly in the particulate fraction suggesting the importance of Fe oxide surfaces as binding sites for trace metals. Cu however was not found in the particulate fraction but in the <100 kDa size fraction. This maybe due to the affinity of Cu for the binding sites of humic molecules. Zn also was found in the <100 kDa fraction.

8.5 Redox cycling of Mn and Fe in Loch Tay bottom sediments

8.5.1 Long cores (1-cm sectioning) - pseudo-total concentration profiles

The long core profiles of pseudo-total concentration for Mn and Fe, shown in figures 5.3-6, all showed the same picture with elevated concentrations in the 0-1 cm sections. There was a sharp decrease in Mn concentration from the 0-1 cm to the 1-2 cm section and then a more gradual decrease in concentration to the bottom of the core. Fe concentrations decreased quite rapidly over the first two to three sections and this was

again followed by a more gradual decrease with increasing depth. There was a very slight broad plateau in the Fe concentration profiles at ~7-13 cm but thereafter concentrations again decreased. The magnitude of the overall decrease in concentration from top to bottom was about a factor of 10 for Mn but only a factor of 2 for Fe illustrating the very strong control of redox cycling on Mn geochemistry in these sediments. The extremely good agreement between the cores (for both elements) emphasises the similarity of the redox environment at each of these sampling locations.

8.5.2 Short cores (0.2 cm sectioning) – pseudo-total concentration profiles

On thermodynamic grounds, the Fe enrichment should occur deeper in the sediment than the Mn as discussed previously (section 7.4). This was not apparent in the long cores, as the 1-cm sectioning did not give a high enough resolution of the core. The short 0.2-cm sectioned core, LT4, showed that the Mn maximum does in fact occur above that of the Fe. The Mn maximum concentration was found in the 0-0.2 cm section and the concentration decreased below this to near the minimum value at 1.0-1.2 cm depth. The Fe concentration decreased slightly from the surface concentration before increasing, steadily with depth, to the maximum at 0.8-1.0 cm depth. The Fe concentration then decreased with depth but much less rapidly than for Mn. The concentrations of each element do agree well with those obtained for the 0-3 cm sections of the longer cores. Thus LT1-3 can provide the general picture whilst LT4 can be used to establish in more detail processes occurring in the top 0-3 cm of the sediment.

8.5.3 Long cores (1-cm sectioning) – readily reducible concentration profiles

Given the strong similarity of the Mn profiles (and Fe profiles) for each core, 0.1 M NH_2OH extraction of readily reducible Mn was only carried out on one core, LT3. About 60-70% of the pseudo-total Mn was extracted from the 0-3 cm sections, only about 20% from the 5-20 cm sections and almost all was extracted from the bottom

secitons. Typically less than 5% of the pseudo-total Fe was extracted and most was extracted from the 0-1 cm section, the position of the maximum in the pseudo-total profile. A slight increase in extractability towards the bottom of the core did not correlate with any feature in the pseudo-total profile. These results simply confirm that most of the Mn is able to enter the redox cycle in the near surface sections and that Fe is present in chemically more resistant phases than Mn.

8.5.4 Long cores (1 cm sectioning) – porewater concentration profiles

Porewaters were extracted from LT2 and LT3 only and those from LT3 were analysed by AAS and by ICP-OES. There was very good general agreement between the concentrations obtained by AAS and those obtained by ICP-OES giving additional confidence in the analytical data.

The Mn profiles for both LT2 and LT3 were quite similar in that low concentrations were obtained for the 0-2 cm sections indicative of removal of Mn from the porewater to the solid phase at this depth. Below this, there was a rapid increase to a maximum at 5-6 cm and then a general decrease towards the bottom of the core. Whilst this decrease was relatively smooth for LT2, there was more structure in this part of the LT3 profile. Overall, however, both strongly suggested classical redox cycling with release of Mn into the porewater at around 5-6 cm being followed by diffusion upward and downwards away from this point.

The Fe profiles for LT2 and LT3 are also quite similar in shape although there was much more structure in the LT3 profile (as observed for Mn). The broad picture suggests low concentrations near the surface where Fe is being removed to the solid phase, higher concentrations from 5-20 cm and lower concentrations at the bottom of the core (LT3 only). It is not clear from these profiles alone whether redox controlled dissolution of Fe(III) phases is occurring or the depth at which this process becomes significant. A

strong correlation between the Fe concentrations and DOC concentrations was observed as it was also at Loch Bradan. This will be discussed further in section 8.5.10.

8.5.5 Short cores (0.2 cm sectioning) – porewater concentration profiles

Examination of the 0.2 cm sectioned core, LT4, shows that there was indeed a point of release of Fe into the porewaters and that it occurred at greater depth than that for Mn. Figure 5.7 illustrates that Mn(IV) dissolution leading to release of Mn(II) was occurring at 0.8 cm but that Fe(III) reduction to soluble Fe(II) did not occur until a depth of 1.2 cm. In fact, this also suggests that LT4 is different because quite clearly the point of release of Mn into the porewater in both LT2 an LT3 was at 5-6 cm. Thus, although useful in demonstrating the distinct behaviour of Mn and Fe in LT4, the data do not help in the interpretation of the porewater profiles for the longer cores, LT2-3. Clearly care must be taken in the interpretation of processes occurring on the basis of solid phase information alone. Almost identical solid-phase profiles, therefore, do not necessarily mean identical porewater geochemistry.

8.6 Geochemical behaviour of trace metals, Pb, Cu and Zn in Loch Tay bottom sediments

8.6.1 Long cores (1 cm sectioning) – pseudo-total concentration profiles for trace metals, Pb, Cu and Zn

Figure 8.1 shows the vertical pseudo-total concentration profiles for Pb, Cu and Zn for LT1-3. Mn and Fe profiles are included for comparison.

Pb concentrations were almost constant at all depths and the values obtained for the three cores were very similar. Cu concentrations did not vary significantly with depth either but there was more variation between cores with LT1 having the highest and LT3 having the lowest concentrations. There was much greater agreement between cores for Zn and here there was also some variation with depth. The major feature was a peak in

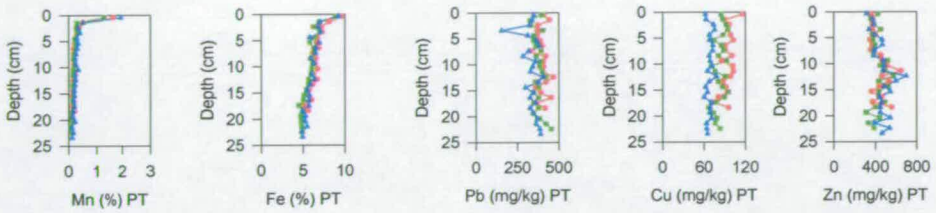

Figure 8.1 Vertical pseudo-total concentration profiles for Pb, Cu and Zn in bottom sediments from Loch Tay (LT1-3)

the 10-15 cm region of all three cores. It is clear, from the consideration of the pseudo-total profiles, that there is little, if any, evidence of an influence of Mn/Fe redox cycling on the Pb, Cu and Zn profiles.

Table 8.2 summarises the mean concentration data for Pb, Cu and Zn in LT1-3 (LT4 also included for discussion in section 8.5.2). This emphasises the similarity in concentration between cores for Pb and for Zn but not for Cu. The larger spread of the Zn data is due to the peak at 10-15 cm described in the previous paragraph. The mean values for each element are also significant. Those for Pb are about 3-3.5 times higher than those observed at Loch Bradan and about 6-8 times higher than those observed at Loch Leven. Similarly Cu concentrations are about 4 and 2 times higher than at Bradan and Leven, respectively. The Zn concentrations were a factor of about 2 greater than at both Bradan and Leven. This is indicative of greater inputs from anthropogenic sources. Although Loch Tay is located further from the major industrial belt in Scotland, past mining activities in the area are well documented and the River Tay as well as the surrounding catchment transport contaminated material into the loch (MacKenzie and Pulford, 2002, Farmer *et al.,* 1996). This is reflected in the significantly higher concentrations of Pb, Cu and Zn. These are also similar to those found in previous studies of Loch Tay (Bryant, 1997). It is notable that there wasn't a significant decrease in the concentrations of these elements in the near surface sections of the sediments and it is therefore suggested that transport and deposition of contaminated material from past activities is still continuing and is the main source of the metals in Loch Tay sediments.

8.6.2 Short core (0.2 cm sectioning) – pseudo-total concentration profiles for trace metals, Pb, Cu and Zn

Figure 8.3 shows the pseudo-total concentration profiles for Pb, Cu and Zn for the fine sectioned core, LT4. Variations in the Pb concentration profile correlate strongly with those in the Fe profile suggesting a post-depositional perturbation of the vertical distribution of Pb. Cu and Zn appear to be unaffected and there is no discernible trend in

Core	Mean Pb conc. mg/kg (± 1 s.d.)	Mean Cu conc. mg/kg (± 1 s.d.)	Mean Zn conc. mg/kg (± 1 s.d.)
LT1	402±35	95±9	434±83
LT2	379±32	84±8	424±65
LT3	341±49	69±5	460±85
LT4	413±37	99±9	381±29

Table 8.2 Mean concentration of Pb, Cu and Zn (±1 s.d.) in bottom sediments from Loch Tay (LT1-4)

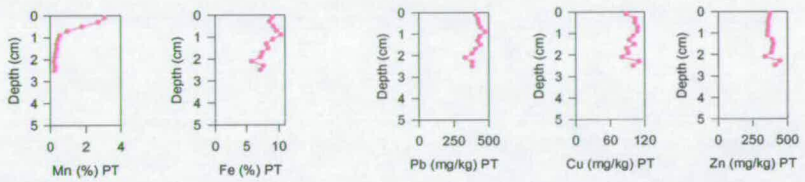

Figure 8.3 Vertical pseudo-total concentration profiles for Pb, Cu and Zn in bottom sediments from Loch Tay (LT4)

the concentration of either of these two elements over the 0-3 cm section of the sediment. The mean concentrations of all three elements (in Table 8.2) were very similar to those obtained for the longer cores, LT1-3, and so a similar extent of contamination was observed.

8.6.3 Long cores – pseudo-total concentration profiles – other elements (Al, Ca, Mg, P, S and Si)

Figure 8.4 shows the concentrations of other elements, Al, Ca, Mg, P, S, Si in Loch Tay cores LT1-3. These were included to provide more information about the composition of the inorganic component of the sediments and particularly, as pseudo-total rather than total concentrations were obtained, to give an indication of major changes occurring with depth. From these profiles, however, there was little evidence of major change in composition. There were some differences between cores and for example concentrations of Al, Mg and P were an order of magnitude lower in LT1 than those in LT2 and LT3. No reason was found for this major difference and so no further interpretation was made on the basis of this data. Using only LT2 and LT3, some other minor features were apparent. For example, the Al concentrations were lower in the uppermost sections of the core indicating a dilution of the other components of the sediment at the position of the solid phase enrichments of Mn and Fe. In contrast, the concentrations of Ca were higher in the same sections suggesting that Ca had been affected by the redox cycling of Mn and Fe.

8.6.4 Short core (0.2 cm sectioned) – pseudo-total concentration profiles – other elements (Al, Ca, Mg, P, S and Si)

Figure 8.5 shows the vertical concentration profiles for Al, Ca, Mg, P, S and Si in the fine sectioned core, LT4. Again, there were generally only small variations in concentration for most elements. Some features were also similar to those observed for the uppermost sections of the long core, LT3, specifically, the decrease in the

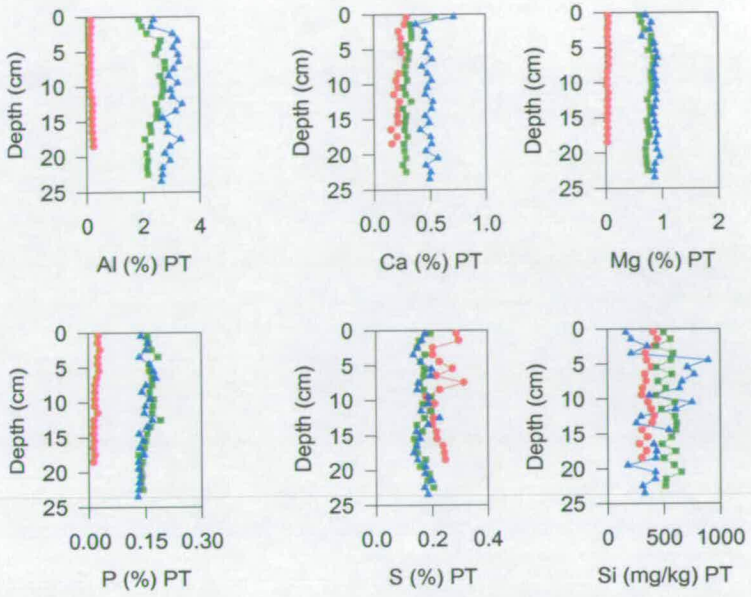

Figure 8.4 Vertical pseudo-total concentration profiles for Al, Ca, Mg, P, S and Si in bottom sediments from Loch Tay (LT1-3)

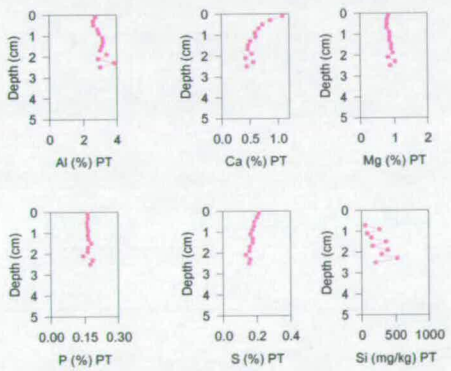

Figure 8.5 Vertical pseudo-total concentration profiles for Al, Ca, Mg, P, S and Si in bottom sediments from Loch Tay (LT1-3)

concentration of Al in the 0-1 cm section and the increase in Ca concentrations towards the surface. The finer sectioning enabled the identification of a much stronger correlation between Ca and Mn than between Ca and Fe concentrations. The shape of the Ca profile did not match precisely that of Mn but the maximum did occur at the same position and which suggests that Ca behaviour is influenced by Mn cycling.

Most of the other elemental profiles were relatively uniform and particularly P and S showed no evidence of involvement in near-surface elemental cycling. The Si concentrations were too variable to be interpreted.

8.6.5. Long core (LT3) – concentrations of trace metals, Pb, Zn and Cu in readily reducible extracts

In comparison with Loch Bradan, Pb and Cu were both present in significantly less extractable forms. About 50% of both Pb and Cu were extracted from Loch Bradan sediments, about 1.5-1.6 times the proportion extracted from the Loch Tay sediments as shown in table 8.6. For Zn, however, the value of 26±10% was closer to the values obtained for Loch Bradan (~25% in the upper parts and ~40% in the deeper parts of the sediment core from Site B). The lower extractability of Pb and Cu could reflect the differing nature of the source of these elements at Loch Tay. Transport of more resistant mineral material, e.g. sulphide ores, rather than deposition from the atmosphere of, for example, sulphates could account for the difference.

The solid phase profile for Zn differed from those of Pb and Cu in that there was a discernible peak at 10-15 cm. There was also a peak in the concentrations of Zn in the readily reducible extracts and in fact a greater proportion of Zn was extracted at this depth indicating a change in association of Zn at this depth.

Core	readily reducible Pb as a % of pseudo total (± 1 s.d.)	readily reducible Cu as a % of pseudo total (± 1 s.d.)	Readily reducible Zn as a % of pseudo total (± 1 s.d.)
LT3	34±11	28±14	26±10

Table 8.6 Mean concentrations of trace metals, Pb, Cu and Zn in readily reducible extracts expressed as a percentage of the pseudo-total concentrations in LT3

8.6.6 Long core (LT3) – concentrations of other elements (Al, Ca, Mg, P, S and Si) in readily reducible extracts

There was little additional information obtained from the vertical concentration profiles for the other elements. Less than 10% of each of pseudo-total Al, Mg and P whilst 50% of Ca and almost all of S was extracted. There was also no apparent correlation between the profiles of these elements and the trace heavy metals, Pb, Cu or Zn. A point of minor importance was that there was a small Ca peak in the 0-1 cm section giving further support to the relationship between Ca and Mn in the uppermost sections of the sediments.

8.6.7 Long cores – porewater concentration profiles for Pb, Cu and Zn

Porewater concentrations of Pb only were obtained for LT2 but all three were determined for LT3 by both AAS and ICP-OES. Very good agreement was observed between the results obtained by these two methods for Pb, Cu and Zn in LT3. There was also some agreement between the shapes of the Pb profiles for the two cores LT2 and LT3 in terms of concentration ranges (up to ~40 ppb) and also the shape of the profiles. Concentrations were lowest in the near surface sections and then increased to a broad maximum down to about 20 cm. Below this the concentrations in LT3 porewaters decreased. As for Mn and Fe, the Pb profile for LT3 had more structure than that for LT2. The peaks at 8-9 cm and 17-18 cm were particularly prominent and coincided with those in the Fe and Mn profiles. Although there was also a peak at 3-4 cm this was relatively less prominent than in the Fe profile. All three peaks were also evident in the Cu porewater profile and just distinguishable in the Zn profile for LT3. The overall shapes of all three trace metal porewater profiles were also similar with the lowest concentrations at the surface, the position of removal of Mn and Fe to the solid phase. A broad maximum in the 10-20 cm region was again followed by lower concentrations in

the bottom sections. There was clearly a very strong relationship between Fe and Pb, Cu but there was a more pronounced peak in Zn concentrations in the 10-15 cm porewaters, the position of the pseudo-total maximum. The importance of DOC concentrations with respect to porewater behaviour of Fe, Pb, Cu and Zn will be discussed further in section 8.6.10.

8.6.8 Short core (0.2 cm sectioned) – porewater concentration profile for Pb

Only Pb data was obtained for LT2 and the analyses were carried out by AAS. The main point of interest here was the correlation between Pb and Fe concentrations down the profile. In particular, the maximum porewater concentration of Pb was found at the point of release of Fe into the porewater (1.2-1.4 cm). This strongly suggests that Fe cycling in the uppermost parts of the sediment is affecting the distribution of Pb. A strong correlation between Pb and Fe was also observed in the solid phase of LT4 and so, although only small amounts of Pb are present in the porewater at any time, the processes controlling Fe cycling in the sediments may also lead to post-depositional perturbation of the Pb profile. Given this relationship between Pb and Fe it is also perhaps not surprising that the amount of Pb extracted by 0.1 M $NH_2OH.HCl$ (pH2) was quite low.

8.6.9 Long core (LT3) – porewater concentrations for other elements (Al, Ca, Mg, P, S, Si)

The additional information available from ICP-OES analysis of the porewaters was very interesting. The Al profile was again similar to that for Fe and there was some similarity between the P and Fe profiles. The peaks were again at the same positions and the general shape of the profiles was similar. The peaks at 3-4 cm, 8-9 cm and 17-18 cm were also visible in the Ca and Mg profiles but the general trend was for a slight but continuous decrease in concentration from top to bottom of the core. The most

interesting profile was that of porewater S concentration which had a major peak at 5-6 cm coinciding with the Mn peak. Below 10 cm S concentrations decreased gradually towards the bottom of the core and there was little evidence of peaks at the positions of those in the Fe profile. The peak at 5-6 cm was intriguing because it suggested that the form of Mn being released might have been S-containing and not simply be Mn(IV)oxide or oxyhydroxide. Further discussion of this can be found in section 8.6.10.

8.6.10 Long core (LT3) – total porewater, >30 kDa, 1-30 kDa and <1 kDa centrifugal ultrafilter fraction concentrations of DOC, Mn, Fe, Pb, Cu and Zn

During ultra-filtration of the LT3 porewaters it was observed that the colour found in the total samples was retained in the >30 kDa fraction. Comparison of the absorbance at 254 nm for the total sample and the largest size fraction showed that over the upper eight sections the organic matter found in the total sample was retained by the 30 kDa filter and that the recovery was very good. With increasing depth, less of the total colour was retained in the largest size fraction but the other fractions were not visibly coloured either. Overall, however, the general trends in DOC concentration with increasing depth for the >30kDa fraction were the same as those found in the unfractionated porewater. Although an "absorbance" balance was not achieved at all depths, difficulties associated with the fractionation process (which results in a high concentration of organic matter in a small volume of liquid and on dilution back to original concentration this material does not always go readily back into solution) were the main reason for any discrepancies between the > 30 kD size fraction and the total porewater values.

The recoveries of Mn and Fe after the ultra-filtration were very good with approximately 70-100 % recovered in most cases. The Mn concentration profiles for the LT3 porewaters are shown in Figure 5.16 The profile obtained for the largest size fraction, >30 kDa, was similar to that of the total profile except that the concentration in the 4-7 cm region was significantly lower than that of the total porewater Mn. Consideration of

the other size fractions showed that a small amount of Mn was present in the 30-1 kDa fraction but a much more significant concentration of Mn was found in the <1 kDa fraction over the 4-7 cm region.

Consideration of the fraction concentrations as a percentage of the total Mn showed the picture more clearly. In general, Mn was found in the >30 kDa fraction with only small concentrations in the other two fractions (0.7-5.9 % in the 30-1 kDa and 0.03-16% in the <1 kDa fraction). At 4-5 cm depth this distribution between the size fractions starts to change with Mn being found predominantly in the <1 kDa fraction. At 5-6 cm depth, the concentration in the truly dissolved fraction (<1 kDa) corresponded to over 60 % of the total porewater Mn. This depth corresponded to the point of release of Mn from the sediment to the porewater at the redox boundary. Thus, as the conditions in the sediment core become more reducing Mn(IV) in the surface sediments become reduced and it has now been shown that it is Mn^{2+} that is released into the pore water and diffuses vertically away from the point of release. As a consequence of the approach taken in this study, the form of Mn at the point of release can clearly be seen as well as the changes in speciation occurring as Mn diffuses upwards and downwards. Above and below this point, Mn is found predominantly in the highly coloured >30 kDa fraction. From previous work, Mn^{2+} formed outer-sphere complexes with humic substances in the organic-rich porewaters and loch waters of Loch Bradan (Gavin et al., 2001). It was shown that this can inhibit but does not prohibit reoxidation and removal of Mn from the porewater under oxic conditions. Thus, observation of a correlation between Mn and DOC in Loch Tay porewaters does not contradict the strong evidence in support of redox cycling of Mn.

The concentration profile of Fe in the >30 kDa fraction showed a very strong correlation to the total porewater Fe profile and the concentrations were comparable. Examination of the concentration profiles of the other two size fractions showed that, although low, the concentration of Fe in the 1-30 kDa fraction increased with depth and peaked sharply at 16-17 cm depth. The concentration of Fe in the truly dissolved phase was very low

and constant with depth apart from the sharp peak at 7-8 cm depth. This occurred just below the enrichment of Mn in the truly dissolved phase and could be attributed to the reduction of Fe oxides and their release into the pore water in a similar manner. The concentrations of Fe in these other size fractions were very low in comparison to the total Fe concentration but their importance should not be underestimated.

Figure 5.19 shows the concentration of Fe in each size fraction calculated as a percentage of the total Fe in the porewater. Fe exists primarily in the largest size fraction with only very small percentage of the total in the other fractions. This is consistent with the known affinity of Fe for large organic molecules (Riise, 1999, Cheshire, 1977). Comparison of the >30 kDa Fe profile and the profile of absorbance at 254 nm provides further support for this theory as the peaks in Fe concentration coincide with peaks in the absorbance at 254 nm. The overall recovery of Fe was very good at 75-100 % of the total.

Comparison of the concentration profile for Cu in the >30 kDa fraction with the profile of total porewater Cu showed that Cu was present almost entirely in the >30 kDa fraction. This is consistent with the high affinity of Cu for binding sites on organic molecules (Tipping and Hurley, 1992, Kerndorff and Shnitzer, 1980). The concentrations of Cu found in the other two size fractions are very small. A very slight increase in concentration in the 1-30 kDa size fraction towards the bottom of the core did coincide with increased Fe concentration in the same size fraction.

The overall distribution of Cu amongst the size fractions can be seen more clearly in the graph of Cu concentration in the fractions as a percentage of the total Cu present in the porewater (Figure 5.19). The >30 kDa fraction accounts for almost 100 % of the Cu in most sections. The recovery for Cu was also very good with the sum of fractions in most sections equaling, and in some cases slightly exceeding, 100 %. The peaks found at 8-9 cm and 17-18 cm in the total Cu profile were also present in the >30 kDa profile and these once again coincide with the peaks in Fe concentration in the >30 kDa fraction.

The concentration profile of Pb in the largest size fraction, shown in figure 5.16, has a similar shape to the total porewater Pb profile (Figure 5.14) and the concentrations were comparable. The 1-30 kDa fraction had a peak in Pb concentration at 5-7 cm depth (close to the position of the Mn peak in the 1-30 kDa size fraction) but the concentration was very small in comparison to the total porewater Pb. The concentrations in the <1 kDa fraction were mainly below the limit of detection. So as for Cu, the main correlation of Pb appears to be with Fe (and DOC) in the > 30 kDa size fraction but there is a smaller correlation between Pb and Mn close to the position of the release of Mn from the solid phase into the porewater. By considering the concentration of Pb in the fractions as a percentage of the total, as shown in figure 5.19, it can be seen that nearly 100 % Pb is present in the largest size fraction.

The fractionation of Zn by this method was less successful with poor recovery rates. Overall, only about 40 % of the total Zn was accounted for in the fractions. The Zn that was recovered, however, was largely in the >30 kDa fraction. It was particularly significant that the maximum concentrations were observed for the porewaters from the 10-15 cm sections. This corresponds to the position of the maximum in the pseudo-total concentration profile for Zn and shows that Zn may be released into the porewater at this point in association with high molecular weight humic material. The nature of the processes controlling Zn distributions with vertical depth in the sediment and the distribution between the sediment and the porewater cannot be further elucidated at this stage. There were two small peaks over 5-10 cm depth interval in the <1 kDa fraction profile, possibly indicative of the release of a small fraction of Zn in conjunction with the release of Mn from the solid phase.

8.6.11 Long core (LT3) – total porewater, >30 kD, 1-30 kD and <1 kD centrifugal ultrafilter fraction concentrations of other elements (Al, Ca, Mg, P, S and Si)

8.6.11.1 Al, Si, Mg and Fe

The profile of Al in the >30 kDa fraction was very similar to that of total porewater Al profile (Figure 5.14). The other two size fractions had small concentrations of Al generally around 0.05 mg/l. The concentration in the 1-30 kDa fraction increased sharply below 15 cm and peaked at 16-17 cm. The concentrations in the < 1 kDa fraction were generally lower but with higher concentrations in the top 0-15 cm sections compared with those lying below this depth. The peak in the 1-30 kDa profile coincides with a peak in the Si profile of the 1-30 kDa fraction indicative of the presence of alumino-silicate clays. There was also a peak in the Fe profile for this size fraction and so there appears to be some relationship between the alumino-silicates and Fe at this depth. Elevated concentrations of Mg in the 1-30 kDa fraction were also observed at this depth.

8.6.11.2 S, Mn, Zn

Comparison of the profiles obtained for the three size fractions for S (Figures 5.14-16) showed that in the upper sediments, especially over the 3-9 cm interval, S was primarily found in the less than 1 kDa fraction. The maximum concentration was coincident with the Mn peak. At the same depth there was also a small broad peak in the 1-30 kDa (again coincident with that in the Mn profile). Over the rest of the core, S was present in both the >30 kDa and 1-30 kDa fractions. There were also peaks in the >30 kDa profile of S at 3-4 cm, 9-8 cm and 17-18 cm that coincided with the Fe peaks in this fraction and in the total Fe profile. These peaks were not apparent in the total S profile due to the presence of the large, broad peak centred at 5-6 cm. When this data is displayed as percentages of the total S it is apparent that, with depth, that the partitioning of the S

changes from the <1 kDa, truly dissolved phase to ~ 50% in the >30 kDa and ~50% in the 1-30 kDa fractions.

From this data, there is a stronger suggestion that S release is in some way linked to Mn release into the pore water. The presence of S in the < 1 kDa size fraction would be consistent with S in the form of either oxidised (SO_4^{2-}) or reduced ions (HS^- or S^{2-}). It would again imply that the Mn containing phase in the sediment was not simply an oxide or hydroxide. The release of Zn at this depth means that some of the Zn in the solid phase was also associated with this phase.

8.7 Elemental associations with electrophoretically fractionated humic substances in porewaters and sediments from LT1

In the following sections, data for Al, Si, P, Mn and Fe as well as Pb, Cu and Zn will be discussed in the context of associations with brown and fluorescent humic materials from the porewaters and sediments from LT1.

8.7.1 Electrophoretic fractionation of humic substances porewaters from selected sections of LT1 (without the addition of loading buffer)

Without the addition of loading buffer, very little of the colour in the porewaters from 3-4 cm, 7-8 cm, 16-17 cm and 19-20 cm sections moved into the gel. There were no visible bands of humic material in the gel. The highest concentrations of Al, Si, Mn and Fe were found close to the gel well (distance travelled < 1.5 cm). This was observed for the samples from all depths. Slight differences between Fe and the other three elements were observed. Although highest concentrations were obtained for the top and bottom sections, Fe was extracted to a greater extent than the other elements from the middle sections. Where detected, Pb and Zn were often found further from the gel well indicating that they were not associated with the Fe, Al, Si and Mn containing material present close to the gel well. Cu, however was detected in the gel at a distance of < 1 cm

from the well. Concentrations were slightly higher in the nearer surface sections than at depth. Some Cu was also found at greater distance from the gel well but, as for Pb and Cu, there was no consistent pattern with porewater sample depth.

8.7.2 Electrophoretic fractionation of humic substances from porewaters from selected sections of LT1 (with the addition of 0.05 M Tris/HCl loading buffer)

The addition of 0.05 M Tris/HCl loading buffer increased the pH of the porewaters to 8.5 and so humic substances from the porewaters should have become more dissociated and had a greater negative charge than in the original porewater samples. The aim was to obtain a more effective electrophoretic extraction and fractionation process. It was immediately apparent that addition of the loading buffer had indeed mobilised more of the humic material from the porewater into the gel. The porewaters from the middle depths of the core gave the most strongly coloured gels. This corresponded to the porewaters with the greatest colour as was previously illustrated by UV/vis characterisation of LT2 and LT3 porewaters and was also consistent with visual examination of the porewaters.

The distance travelled by Al, Mn and Fe was relatively unchanged and these three elements were always found <1.5 cm from the gel well. Greatest concentrations were found for the middle depth sections, i.e. those giving the strongest colour. It is possible that the Al, Mn and Fe travelled in association with very large humic molecules but alternatively, negatively charged inorganic colloidal species may have been able to move within the gel. If the latter, then these are large or have only a small net negative charge. Pb, Zn and P were also detected at this position in the gel for the middle depth porewaters. Pb, Cu and Zn were also associated with material that migrated further in the gel, and in particular, Zn was associated with fluorescent band material, particularly in the 12-13 cm porewaters.

8.7.3 Electrophoretic fractionation of humic substances from porewaters from selected sections of LT1 (with the addition of a small amount of 0.1 M NaOH prior to electrophoretic fractionation)

0.1 M NaOH is commonly used in the extraction and isolation of humic substances from various environmental samples. Increasing the pH to 13 results in major dissociation of acids and the dissolution of a large proportion of humic substances. Removal of humic material from surface coatings of mineral particles is also likely using these relatively harsh conditions. Addition of the a small amount of 0.1 M NaOH to the porewaters was used to dissociate as much as possible of the humic material in the porewaters and to investigate the effect on elemental distributions obtained on electrophoretic fractionation.

The addition of 0.1 M NaOH to the porewater prior to electrophoresis altered the distribution of the humic material, as evidenced by the position of the brown band and the fluorescent material. 0.1 M NaOH was most effective at releasing humic materials from the deeper porewaters as was reflected in the darkest colouration of the gel. The trend with depth does not, however, correlate exactly with the colour of the original porewaters and so it is difficult to relate results obtained directly to porewater composition.

The elemental distributions were also different from those obtained for the original porewaters and where loading buffer had been added. The concentrations of Mn in the NaOH extracted gel were lower than those of the porewater alone and were more uniform with depth. Similarly in the natural porewater samples the Mn did not migrate far across the gel and instead remained in or near the well.

The concentrations of Fe were similar to those for the porewater alone and again most was found < 1.5 cm from the gel well. In addition, however, Fe was detected at the same

position as the dark brown band isolated from the 17-18 cm and 20-21 cm porewaters. This is a first indication of Fe bound to humic material in these porewaters. This was most likely humic material that had been intimately associated with inorganic surfaces in the original porewaters.

Al remained in the gel well for all depths but the bottom section porewater. This suggests that inorganic Al species have been separated from the humic materials and that these are not mobile under the conditions applied. The pattern for Al was similar to that of Fe in the bottom section and the same interpretation is therefore made. It is further postulated that the Al, Mn and Fe present at < 1.5 cm from the gel well is probably indicative of humic-coated mineral colloids which are relatively large and so do not travel a great distance under the conditions applied. At least some of the Al and Fe is truly complexed by the humic molecules.

Generally the Pb concentrations were higher than previously found for the porewater gel sections and the Pb was more mobile through the gel. The highest concentration was found near the well, at 1.0-1.5 cm, for the porewater from the deepest section. There was no consistent pattern with depth and so little further interpretation can be made.

The distribution of Cu was also significantly affected by the addition of 0.1 M NaOH prior to electrophoretic fractionation. The effect on the uppermost sections appears to have been a decrease in the mobility of Cu. Most importantly, though, most Cu was mobilised from the deeper porewaters suggesting an association of Cu with humic substances. A peak in Cu concentration was observed at the position of the dark brown band but Cu was also associated with smaller or more highly negatively charged molecules. A similar but less specific association was also observed for Zn mobilised from the 17-18 cm porewaters.

The addition of NaOH prior to electrophoretic extraction and fractionation appears to yield more information about the associations of trace metals with humic substances and

also extracted more of the organic matter present in the total sample. In comparison to the natural porewater electrophoretic pattern it can be seen that the distributions in the NaOH extracted material are greatly altered, as are the observable associations. Care is therefore needed when interpreting the results. It is suggested that fractionation of the porewaters be carried out both in the presence and absence of chemical reagents in order that observed elemental associations can be extrapolated to real environmental behaviour.

8.7.4 Electrophoretic extraction and fractionation of humic substances from 0-5 cm sections of LT1 (with the addition of 0.05 M Tris/HCl loading buffer)

Extraction and fractionation of humic materials directly from the sediments of core LT1 was also attempted. The sediment was suspended in 0.05 M Tris/HCl loading buffer and placed in the gel well prior to electrophoretic extraction and fractionation. Use of the loading buffer enables direct comparison with the porewater results discussed in section 8.6.2.

Humic material was extracted from the sediment samples at all depths and in each case there appeared to be two main brown bands separated by slightly paler brown material. Ahead of the brown bands, was paler brown fluorescent material which extended to a distance of 5 cm from the gel well. It should be recalled that the 0-1 cm section corresponds to the position of the Mn and Fe enrichments in the solid phase and that Mn concentrations decreased very rapidly below this depth. The magnitude of the decrease in Fe concentration was also smaller than that for Mn.

As was observed in the porewaters, Al, Si, Mn and Fe were found at highest concentration < 1.5 cm from the gel well. Concentrations of Al and Si were greater for the 3-5 cm sediment sections whilst those for Mn were greatest for the 0-1 cm section. Fe concentrations were also greatest for the 0-1 cm section but were also elevated for the

3-5 cm sections. The presence of Mn and Fe, but not Al and Si, at this position in the gel for the 0-1 cm section suggests mobilisation of a small amount of humic-coated Mn/Fe phases that are part of the redox enrichment at this depth. Mn concentrations in the sediment were an order of magnitude lower in the underlying sections and the chemical extractability (0.1 $NH_2OH.HCl$ (pH2) decreased markedly to only about 20% of the pseudo-total below 3 cm. The electrophoretic distribution pattern with increasing depth ties in with these previously discussed results.

Fe complexed by high molecular weight humic material was present at all depths as indicated by the correlation between the brown colour and Fe concentration in the gel. Similar behaviour for Al was only observed for the 3-5 cm sediment sections. It should be noted, however, that sediment concentrations of Al were lower in the uppermost sections of the sediment.

Pb concentrations in the gel were generally very low but there was no correlation with Mn, Fe, Al or Si. Some Pb was extracted in association with humic susbtances from the 0-1 cm sediment. Similarly, Cu concentrations were extremely low and no consistent trends were observed. In contrast with Cu, Zn was extracted in association with humic substances from the 0-2 cm sediment. Zn was associated with the dark brown humic material as well as the paler fluorescent band material. This less specific association was similar to the behaviour observed for Zn in the porewaters (after treatment with 0.1 M NaOH).

8.7.5 Electrophoretic extraction and fractionation of humic substances from selected sections of LT1 (with the addition of 0.05 M Tris/HCl loading buffer)

As in section 8.7.4, the sediments had been suspended in loading buffer prior to electrophoretic extraction and fractionation. As was observed for the 0-5 cm sections,

two dark brown bands separated by a slightly paler band were found at similar distances from the gel well for all sediment depths.

The concentrations of Al, Si, Mn and Fe were generally lower than those obtained for the 0-5 cm sediments. There was also a trend towards smaller migration distances with increasing depth for each of these elements. It would appear that complexation of Al, Mn and Fe by high molecular weight humic materials was greatest at around 3-8 cm but that there was some Fe associated with smaller or more highly charged humic molecules (with the material in the second brown band) from the middle depth sediments. Cu and especially Zn were also associated with this material from the middle depth sediments. It should be recalled that this was the position of the maximum concentrations of porewater DOC and porewater Fe, Mn, Pb, Cu and Zn concentrations. From the electrophoresis results, however, there was an absence of Mn-humic associations at these depths but the predicted outer-sphere associations are generally weak and may not survive under the experimental conditions employed. Bearing this in mind, the electrophoretic distributions described above are broadly consistent with the results discussed in the preceding parts of this chapter.

8.8 Conclusions

8.8.1 Characterisation of Loch Tay sediments and porewaters

At around 20-30 % w/w OM, the sediments of Loch Tay were classified as organic-rich but less so than those of Loch Bradan (~50% w/w OM). A decrease from maximum values in the 0-1 cm section to an almost constant value of ~20 % from 4 cm to the bottom was observed in several of the cores. This was interpreted as rapid degradation of OM accompanying the redox cycling of Mn and Fe.

Porewater DOC concentrations were very low in the near-surface sections where removal of Mn and Fe to the solid phase was a particularly important process. The relatively undegraded nature of the input OM may account for the low DOC

concentrations. Highest DOC concentrations were typically found in the middle part of the core but did not correlate with any feature in the solid phase OM profile.

8.8.2 Geochemical behaviour of Mn and Fe in Loch Tay sediments

The pseudo-total solid phase profiles for Mn and Fe in the long cores (LT1-3; 1-cm sectioned) showed that oxic conditions prevailed at the surface of the sediments but very quickly there was a change to more reducing conditions below 1 cm depth. Fine sectioning of a short core (LT4; 0.2-cm sectioned) enabled the distinction of the depths of Mn and Fe enrichments in the solid phase with the maximum Mn concentration occurring 0.8 cm above that of Fe. These peaks were closer together than observed for Loch Bradan where 1-cm sectioning had been sufficient.

The use of 0.1 M $NH_2OH.HCl$ to establish the form of Mn present in the sediment (LT3) again showed that, particularly in the 0-3 cm sections a large proportion of Mn was in a readily reducible form. Whereas almost all was extracted from Loch Bradan sediments, values of only 60-70% of the pseudo-total, however, were obtained for the 0-3 cm sections of Loch Tay sediments. Below this depth, values of as low as ~20% of the pseudo-total were obtained for the underlying sediment sections indicating a major difference between Tay and Bradan sediments.

For the long cores (LT2-3), the release of Mn(II) into the porewater at ~ 5-6 cm provided further evidence of a change to more reducing conditions with increasing depth. This occurred at a slightly shallower depth in the sediment than was typically observed at Loch Bradan. The point of release of Fe(II) into the porewater could not be identified on the basis of the shape of porewater profiles *per se* and the over-riding control appeared to be DOC concentration.

The porewater profile for the short core (LT4), indicated that more reducing conditions prevailed at this location and that the point of release of Mn(II) into the porewater was at

0.6-0.8 cm. In addition, Fe(II) release into the porewater could be identified at 1.0-1.2 cm. Thus, fine-sectioning can be a very useful tool for studying processes occurring on the millimetre depth scale within the sediment but the results also indicate more geochemical heterogeneity between sampling locations than was observed at Loch Bradan (or Loch Leven).

8.8.3 Geochemical behaviour of Pb, Cu and Zn in Loch Tay sediments

The heavy metal concentrations for Pb and Cu were quite uniform with depth and whilst in the main this was also true for Zn, there was a sub-surface peak at 10-15 cm in all of the long cores (LT1-3). Notably there was no decrease in the concentrations of any of the heavy metals in the near-surface section of the core. Past ore extraction activities in the vicinity are documented and it appears that riverine and catchment run-off transport of heavy metals from these sources into the loch has led to continued contamination of the loch sediments. The surrounding catchment of Loch Bradan has not been affected to any known extent by mining activities and so runoff from the catchment is more strongly influenced by atmospheric inputs.

The results from the readily reducible extraction procedure revealed a much lower extractability of Pb and Cu (but not of Zn) compared to that observed for Bradan sediments. This would be consistent with the difference in source and implied chemical form of Pb and Cu. The relatively constant concentrations of Pb and Cu down the profile along with the lower extractability suggest that post-depositional perturbation processes are less important in the Loch Tay compared with the Loch Bradan sediments. The differences in the geochemical behaviour of Zn compared with Pb and Cu were again evident with Zn being more extractable at the position of the solid phase maximum (10-15 cm). Further information about Zn associations was obtained in the later stages of this study (by ultrafiltration and electrophoresis).

There was a general strong correlation between Pb, Cu, Zn with Fe and DOC in the porewaters from the long cores (LT2-3) but there were some features pertaining only to the porewater profiles of individual elements, e.g. a less pronounced Pb peak in the 0-5 cm sections and a broad peak at 10-15 cm present only in the Zn profile. The information obtained from the readily reducible extractions was not particularly useful in explaining the shapes of the porewater profiles (as it had been to a certain extent for the Loch Bradan samples). The exception to this was that the greater extractability of Zn (0.1 M $NH_2OH.HCl$ (pH2) occurring at 10-15 cm coincided not only with the peak in the pseudo-total concentration profile (as stated in the preceding paragraph) but also with the more pronounced broad peak in the porewater profile.

A limited amount of information was obtained for the porewaters from the short core (LT4) but it showed that, at this location, the release of Fe(II) was accompanied by the release of Pb into the porewaters at 1.0-1.2 cm. The correlation between Pb and Fe concentrations in the porewaters as well as in the solid phase showed that post-depositional mobilisation of Pb was occurring and that this process did indeed lead to a perturbation of the solid phase profile. It is emphasised again that the conditions at this location appeared to be more strongly reducing than at the other sampling locations and so this cannot be generalised as a process affecting the vertical distribution of Pb within Loch Tay sediments.

8.8.4 Geochemical behaviour of other elements (Al, Ca, Mg, P, S and Si) in Loch Tay sediments and implications for behaviour of Mn, Fe, Pb, Cu and Zn

Multi-element analysis of pseudo-total digests and readily reducible extracts did not lead to greater understanding of processes occurring in the Loch Tay sediments. Similar analysis of porewaters, however, produced extremely interesting vertical concentration profiles. Two main groups of elements exhibiting similar profiles were identified. In particular, Al and P (possibly Ca and Mg too) were added to the group of elements with

profiles similar to that of DOC and Fe whilst S and Mn formed the second group. Further distinguishing features obtained from ultrafiltration supported the identification of these groups.

8.8.5 Elemental associations in centrifugal ultrafiltered porewaters

Further work on porewaters involved centrifugal ultrafiltration of the porewaters. The > 30 kDa fraction represented medium and large colloids and contained almost all of the DOC (brown colouration and UV/vis results). The 1-30 kDa and the < 1 kDa size fractions represented smaller colloids and truly dissolved species, respectively. The results from multi-element analysis led to a major breakthrough in understanding of the geochemical processes occurring in the Loch Tay sediments. It also leads to some major areas of importance for future work.

The point of release of Mn^{2+} into the porewaters was identified (5-6 cm) and was consistent with the position of the maximum Mn concentration in the unfractionated porewaters. Slightly more tentatively, the point of release of Fe^{2+} into the porewaters was thought to be at 7-8 cm, at greater depth than that of Mn but further work would be required to demonstrate this more convincingly. S (as SO_4^{2-} or HS^-/S^{2-}) was also released at the same position as Mn and so further work should be carried out to establish the form of Mn in the sediment at this depth. Low concentrations of Zn were also found in the < 1 kDa fraction at ~5-6 cm and so the processes occurring also have implications for Zn mobility.

Although it is Mn^{2+} that is released into the porewater, with time, and as upwards and downwards diffusion occurs, associations with high molecular weight humic substances become important. Changes in association of Mn in porewaters have rarely been documented and so this type of information is extremely valuable.

The correlation between Pb, Cu, Zn, Al, Fe and DOC was reinforced by the occurrence of the highest concentrations of the metals as well as the DOC in the > 30 kDa size fraction. Again the position of the mains peaks in all profiles coincided.

The 1-30 kDa fraction revealed two further groups of elements – those (Pb and S) which had peaks at the position of the Mn peak in this size fraction (5-6 cm) and those (Fe, Si, Al and perhaps Cu and P) which had higher concentrations in the 15-25 cm sections. Often the concentrations in this size fraction were smaller than those in the other two fractions and so the relative importance of the controlling processes may be less. These findings merit further investigation and will help to enhance our understanding of both major and minor processes occurring within sediment systems.

8.8.6 Elemental associations with electrophoretically fractionated humic materials

Gel electrophoresis was employed to fractionate the brown coloured humic material in the porewaters and extract and fractionate humic material from the sediments. Multi-element analysis was then used to establish the elemental associations with the fractionated humic materials.

Gel electrophoresis was probably the most demanding of the procedures adopted in this study because the small volume and sensitive nature of the porewaters meant that experiments could only be carried out a small number of times and over a relatively short time period after sample collection.

Gel electrophoretic fractionation of the porewater humic substances did further the understanding of element associations. Large colloidal species were present in porewaters and it is proposed that these comprise humic-coated inorganic colloids. There was also evidence of high molecular weight humic complexation of elements

(after 0.1 M NaOH treatment) including Fe and associations of Cu and Zn with either lower molecular weight or more negatively charged humic molecules.

Gel electrophoretic extraction and fractionation of humic material from the sediments provided additional evidence for humic-coated inorganic entities. Given that only 0.05 M Tris/HCl was used to suspend the sediment, these can be mobilised under relatively mild conditions. An additional feature of the electrophoretic data for the sediments was that humic complexation of elements (including Fe, Cu and particularly Zn) was at a maximum in the sediment at the position of the observed maxima in DOC and porewater elemental concentrations. This meant that the electrophoretic data was broadly consistent with the data obtained from the other analyses carried out on these sediment cores.

8.8.7 Critical evaluation of approach of this study

Relatively simple procedures (pseudo-total digestion, readily reducible extractions followed by multi-element analyses) are generally required to build up background information (concentrations, vertical distributions and relative extractability) about metals in sediment cores. The study of Loch Tay sediment cores demonstrated that this alone was not sufficient to account for the porewater geochemistry of Mn , Fe, Pb, Cu and Zn. Multi-element and DOC analysis of the porewaters themselves did give some insight into the likely processes controlling the vertical distributions of the these elements within the porewaters. It was however, the inclusion of centrifugal ultrafiltration to fractionate the species present in the porewaters and electrophoresis to fractionate humic substances from the porewaters and solid phase sediments that lead to the substantial improvement in understanding of the Loch Tay sediment system. Further development of the electrophoretic process is still required but more work in this area is likely to be productive.

Chapter 9. Conclusions

This aim of this work was to investigate of the processes controlling trace heavy metal (Pb,Cu and Zn) mobility in three contrasting Scottish freshwater lochs, Loch Leven, Loch Bradan and Loch Tay. A particular goal was to determine the relative importance of redox processes (involving Mn and Fe) and of organic matter complexation on the vertical distribution of Pb, Cu and Zn in the sediments and associated porewaters of these lochs.

The main distinguishing features about the lochs leading to their selection were:

(i) Loch Leven had organic-rich sediments where the input was predominantly of autochthonous origin;

(ii) Loch Bradan had organic-rich sediments but the input was predominantly of allochthonous origin (peaty catchment); Mn-rich bedrock underlying the catchment and loch also meant that high concentrations of Mn were present in the sediments;

(iii) Loch Tay was similar to Loch Bradan in that the catchment-derived material the major source of the organic matter entering the sediments but anthropogenic inputs from past mining activities meant that elevated concentrations of heavy metals were present in the sediments.

This study adopted traditional digestion (hot 8 M HNO_3) and extraction (0.1 M $NH_2OH.HCl$ (pH2) procedures and single element analysis (AAS) to determine the concentrations and vertical distributions of Mn, Fe, Pb, Cu and Zn in the sediments of each loch. The porewaters were analysed directly by AAS. This provided the baseline information for each loch enabling the results from the more specific investigations to be placed in context.

Sample collection, preparative and analytical procedures were carried out on the sediments and porewaters obtained from each loch in turn and so a critical evaluation of the results obtained for Loch Leven led to modification of procedures adopted for

Loch Bradan. A similar evaluation of the Loch Bradan data led to further improvements in the experimental protocol for Loch Tay sediments and porewaters. From the Loch Leven work, the vertical pseudo-total concentration profiles for all elements (Mn, Fe, Pb, Cu and Zn), there was a very good degree of agreement between cores. Analysis of replicate cores, therefore, helped to establish the reproducibility of the coring and core sectioning techniques employed in this study.

For the readily reducible extraction, although most of the pseudo-total Mn and very little Fe extracted in every case, the agreement between the vertical profiles for Fe was not so good. It is likely that this reflects real environmental differences between the cores and so suggests that, for detailed speciation studies, collection of multiple cores is an essential component of the sampling protocol.

In four of the five cores collected from Loch Bradan, classical redox cycling of Mn was clearly important even in the presence of high concentrations of solid phase and dissolved organic matter. Although there was an enrichment in the 1-2 cm solid phase for Fe, the porewater profiles did not suggest a straightforward interepretation based on reduction of Fe(III) phases and dissolution of Fe(II). Moreover the porewater profiles for Fe as well as Pb, Cu and Zn were similar in shape to that of the DOC (this was also observed for the porewater Mn profile from the final core). The addition of centrifugal ultrafiltration to the experimental procedures enabled further supporting evidence of a relationship between the brown dissolved organic matter and these elements.

Multi-element analysis of pseudo-total digests and readily reducible extracts from Bradan sediments illustrated that selected chemical extraction could be used to demonstrate that Mn was in a readily reducible form and thus able to enter the redox cycle. It also demonstrated, that in this instance, it could also be used to identify likely chemical forms of Pb, Cu and Zn within the sediment. From the results in this study, dissolution of Fe phases under more reducing conditions also led to the release of Pb, Cu and Zn into the porewaters. Concentrations in excess of mineral solubility and formation of new mineral phases are often a result of such a process. It was postulated that this had occurred in the Loch Bradan sediments and that sulphate and phosphate

containing phases were a sink for the heavy metals. The exact shape of the vertical profiles depended strongly on the characteristics of the individual metal.

The more extensive study of Loch Tay sediments and porewaters led some of the most significant results emanating from this study.
From the baseline work, first of all, almost identical profiles for Mn and for Fe from all cores were obtained. There was also good general agreement between the porewater profiles for each of these elements for the longer 1-cm sectioned cores. The short-fine sectioned core revealed sample location-specific evidence of classical Fe cycling and its influence on the vertical distribution of Pb within the sediments and porewaters. The general picture, based on the long cores, however, was of a strong association of Fe with DOC. Indeed, the vertical profiles of Pb, Cu, Zn and several other elements including Al and P, also correlated with the DOM profiles. This behaviour was in agreement with the observations made from the Loch Bradan component of the study.

Modification of the protocol for ultrafiltration enabled the separation of medium/large colloids, small colloids and truly dissolved species. Two main groups of elements were identified on the basis of porewater speciation:

(i) Fe, Al, P, Pb, Cu and Zn;

(ii) Mn, S (& Zn).

The first group showed strong correlations with porewater DOM even after ultrafiltration, i.e. similar vertical profiles and highest concentrations in the > 30 kDa size fraction. The second group were found mainly in the truly dissolved fraction at ~5-6 cm which was then defined as the point of release of Mn^{2+} into the porewaters. 'S' and, to some extent, Zn were also present in the truly dissolved fraction at the point of Mn release but further work is required to completely elucidate the processes occurring here.

Gel electrophoretic fractionation of humic material in sediments and porewaters was also incorporated into the experimental protocol for Loch Tay samples. For the

porewater samples, there were particular difficulties associated with sample size and integrity that meant that experiments had to be carefully designed and carried out over a relatively short time period after sample collection. Three experiments were considered essential for this work. These involved fractionation of:

(i) porewaters (no additions) - for comparison of elemental and colour patterns obtained after addition of chemicals;

(ii) porewaters (0.05 M Tris/HCl buffer) – to dissociate acidic groups on the humic molecules such that they could be electrophoretically separated but without exposure to excessively harsh chemical reagents;

(iii) porewaters (after addition of a small amount of 0.1 M NaOH) – to extensively dissociate acidic groups on the humic molecules with a view to disrupting linkages between humic substances and mineral surfaces prior to electrophoretic extraction.

From this work, it was found that gel electrophoretic fractionation of the porewater humic substances did further the understanding of element associations. Large colloidal species were present in porewaters and it was proposed that these comprised humic-coated inorganic colloids. There was also evidence of high molecular weight humic complexation of elements (after 0.1 M NaOH treatment) including Fe and associations of Cu and Zn with either lower molecular weight or more negatively charged humic molecules. Further work is required, however, to establish the size ranges of these molecules in order that a link between the ultrafiltration and electrophoresis results can be achieved.

From the gel electrophoretic fractionation of sediment humic substances, further supporting evidence for coated colloids and for metal-humic complexation was obtained and the sections of the sediment for which this was most important coincided with those where porewater DOC and elemental concentrations were greatest.

Overall, a much improved understanding of the relative importance of redox processes and of organic matter complexation on the geochemical associations of Pb, Cu and Zn in the sediments and porewaters of freshwater lochs has resulted from this work. This has been due in the main to the approach that has been developed and in particular to the inclusion of ultrafiltration and electrophoresis as tools for the isolation and fractionation of humic materials from both porewaters and sediments.

10. Future Work

To obtain a better geochemical understanding of near-surface sediment/aqueous systems, further research must involve analysis of a range of elements and include those which:

(i) are redox-active (Mn, Fe) and redox-sensitive (e.g. As);

(ii) have an affinity for organic matter (e.g. Cu);

(iii) have an affinity for the solid phase (e.g. Pb);

(iv) are more labile (e.g. Zn).

Examples of environmental research areas that would benefit from utilisation of the new approach include:

(i) the validity of historical records of Pb and other heavy metal pollution using organic-rich soils and sediments;

(ii) the true nature and clean-up of arsenic/iron/humic-rich waters used for human consumption.

The distribution of organic matter amongst colloidal size fractions (from ultrafiltration) *per se* would also be useful in the evaluation of the potential effectiveness of coagulation processes for effluent treatment – more so if organic material is in larger size fractions.

The use of electrophoresis in conjunction with ultrafiltration is also recommended to establish a link between the results obtained by the two approaches. For example, gel electrophoretic fractionation of the more concentrated 30 kDa ultrafilter retentates might be particularly productive. Alternatively, better use of protein markers or other size marker could be adopted but it is difficult to get an exact match for characteristics of humic molecules.

11 References

Aitken G. R.; McKnight D.; Wershaw R. L.; MacCarthy P., 1985, Humic Substances in Soil, Sediment and Water, Wiley, New York

Atkins P. W., Physical Chemistry, 5th edition, Oxford University Press, 1994

Balistrieri L. S., Murray J. W. and Paul B., 1995, Geochim. Cosmochim. Acta, 59, 4845-4861, The geochemical cycling of stable Pb, ^{210}Pb and ^{210}Po in seasonally anoxic Lake Sammamish, Washington, USA

Belzile N., Joly H. A. and Li H., 1997, Canadian J. Chemistry, 75, 14-27, Characterisation of humic substances extracted from Canadian lake sediments

Boulegue, Geochim. Cosmochim. Acta, 1982, 46, 453-464

Bowen H. J. M., 1966, Trace Metals in Biogeochemistry, Academic Press, London

Bryant C. L., Farmer J. G., MacKenzie A. B., Bailey-Watts A. E. and Kirika A., 1997, Limnol. Oceanogr., 42, 918-929, Manganese behaviour in the sediments of diverse Scottish freshwater lochs

Buesseler K. O., Bauer J. E., Chen R. F., Eglinton T. I., Gustafsson O., Landing W., Mopper K., Moran S. B., Santschi P.H., VernonClark R. and Wells M. L., 1996, Mar. Chem., 55, 1-31, An intercomparison of cross-flow filtration techniques use for sampling marine colloids: Overview and organic carbon results

Buffle J., Perret D. and Newman M., 1992, Environmental Particles vol.1, Ch.5, 171-230, Lewis Publishers, Inc., The use of filtration and ultrafiltration for size fractionation of aquatic particles, colloids, and macromolecules

Bunce N. J., 1994, Environmental Chemistry, 2nd Ed., Wuerz Publishing Ltd, Canada

Burba P., Aster B., Nifant'eva T., Shkinev V. and Spivakov B. Y., 1998, Talanta, 45, 977-988, Membrane filtration studies of aquatic humic substances and their metal species: a concise overview Part 1. Analytical fractionation by means of sequential-stage ultrafiltration

Butcher S. S., Charlson R. J., Orians G. H. and Wolfe G. V. (eds.), 1994, Global Biogeochemical Cycles, Academic Press, London

Canfield D. E., Thadrup B., Hansen J. W.,1993, Geochim. Cosmchim. Acta, 57, 3867-3883, The anaerobic degradation of organic matter in the Danish coastal sediments: iron reduction, manganese reduction and sulfate reduction

Canfield D. E., Green W. J. and Nixon P., Geochim. Cosmochim. Acta, 1995, 59(12), 2459-2468, ^{210}Pb and stable lead through the redox transition zone of an antartic lake

Carignan R. and Flett R. J., 1981, Limnol. Oceanogr., 26, 361-366, Post depositional mobility of phosphorus in lake sediment

Carignan and Nriagu, 1985, Geochim. Cosmochim. Acta, 49, 1753-1764, Trace metal deposition and mobility in the sediments of two lakes near Sudbury, Ontario

Cheshire M. V., Berrow M. L., Goodman B. A., Mundie C. M., 1977, Geo Cosmo Acta, 41, 1131-1138, Metal distribution and nature of some cu, Mn and V complexes in humic and fulvic acid fractions of soil organic matter

Chin Y. P. and Gschwend P. M., 1991, Geochim. Cosmochim. Acta, 55, 1309-1317, The abundance, distribution, and configuration of porewater organic colloids in recent sediments

Chin Y. P., Traina S. J. and Swank C. R., 1998, Limnol. Oceanogr., 43, 1287-1296, Abundance and properties of dissolved organic matter in pore waters of a freshwater wetland

Chiswell B., Dixon D. R., Hamilton G., Sly L. I., White T. D., 1992, Chemistry in Australia, Aquatic and environmental supplement, 400-402, Manganese speciation in surface waters

Ciavatta C., Govi M., Sitti L. and Gessa C., 1995, Commun. Soil Sci. Plant Analysis, 26, 3305-3313, Capillary electrophoresis of humic acid fractions

Cidu R., 1996, Atomic Spectro., 17, 155-162, Comparison of ICP-MS and ICP-OES in the determination of trace elements in water

Dai M., Martin J. M and Cauwet G., Marine chem, 1995, 51, 159-175, The significant role of colloids in the transport and transformation of organic carbon and associated trace metals (Cd, Cu and Ni) in the Rhone Delta, France

Dai M., Buesseler K. O., Riple P., Andrews J., Belastock R. A., Gustafsson O. and Bradley Moran S., 1998, Mar. Chem, 62, 117-136, Evaluation of two cross-flow ultrafiltration membranes for isolating marine organic colloids

Davison W., 1985, Conceptual models for transport in a redox boundary. In Chemical process in lakes, Stumm W. Ed., Wiley-Interscience, New York

De Nobili M., Bragato G., Alcaniz J. M., Puigbo A. and Comellas L., 1990, Soil Sci., 150, 763-770, Characterisation of electrophoretic fractions of humic substances with different electrofocusing behaviour

Dunkelog R., Ruttinger H. H. and Peisker K., 1997, J. Chromatogr., 777, 355-362, A comparative study for the separation of aquatic humic substances by electrophoresis

Eades L. J., Farmer J. G., MacKenzie A. B., Kirika A. and Bailey-Watts A. E., 2002, Science of the total Environment, 292(1-2), 55-67, Stable lead isotopic characterisation of the historical record of environmental lead contamination in dated freshwater lake sediment cores from northern and central Scotland

Emerson S, 1976, Geochim. Cosmochim. Acta, 40, 925-934, Early diagenesis in aerobic lake sediments: Chemical equilibria in interstitial water

Farmer J. G. *et al.*,1994, Aquatic Conserv.: Marine And Freshwater Ecosystems, 4, 45-56, Phosphorus fractionation and mobility in Loch Leven sediments

Farmer J. G., Eades L. J., Graham M. C and Bacon J. R., 2000, J. Environ. Monitoring, 2(1), 49-57, The changing nature of the 206Pb/207Pb isotopic ratio of lead in rainwater, atmospheric particulates, pine needles and leaded petrol in Scotland

Fujitake N., Kusumoto A., Tsukamoto M., Kawahigashi M., Suzuki T. and Otsuka H., 1998, Soil Sci. Plant. Nutr., 44, 253-260, Properties of soil humic substances in fractions obtained by sequential extraction with pyrophosphate solutions at different pHs

Gaffney J. S. *et al.*, ACS Symp. Series 165, 1996, 2-16, humic and fulvic acids and organic colloidal materials in the environment

Gaffney J. S., Marley N. A. and Orlandini K. A., 1996, ACS Symp. Series 165, 26-39, The use of hollow fibre ultrafilters for the isolation of natural humic and fulvic acids

Garrison A. W., Schmitt P. and Kettrup A., 1995, Wat. Res., 29, 2149-2159, Capillary electrophoresis for the characterisation of humic substances

Gavin K. G., Farmer J. G., Graham M. C., Kirika A. and Britton A., Submitted to 9th IHSS, Manganese-humic interactions in the catchment, water and sediment of Loch Bradan, S.W. Scotland

Guo L. and Santschi P. H., 1996, Mar. Chem., 55, 113-127, A critical evaluation of the cross-flow ultrafiltration technique for sampling colloidal organic carbon in seawater

Gustafsson O., Buesseler K. O. and Gschwend P. M., 1996, Mar. Chem., 55, 93-111, On the integrity of cross-flow filtration for collecting marine organic colloids

Gustafsson O., Gschwend P. M., 1997, Limnol. Oceanogr., 42(3), 519-528, Aquatic colloids: Concepts, definitions, and current challenges

Hamilton W. R., Woolley A. R., Bishop A. C., 1998, Hamlyn Guide: Minerals, rocks and fossils, Reed international books ltd

Hamilton-Taylor J., Davison W., and Morfett K., 1996, Limnol. Oceanogr., 41, 408-418, The biogeochemical cycling of Zn, Cu, Fe, Mn and dissolved organic C in a seasonally anoxic lake

Hayes M. B. H., MacCarthy P., Malcolm R. L. and Swift R. S. (eds.), 1989, Humic Susbtances II In Search of Structure, John Wiley & Sons Ltd

Hongve D., 1997, Limnol. Oceanogr., 42(4), 635-647, Cycling of iron, manganese and phosphate in a meromitic lake

Horowitz, Env. Sci. Tech, 1996, 30, 954-963

Huerta-Diaz M. A., Tessier A., Carignan R., 1998, Applied Geochem., 13, 213-233, Geochemistry of trace metals associated with reduced sulfur in freshwater sediments.

Jackson T. A. and Bistricki T., 1995, J Geochem. Exploration, 52, 97-125 the selective scavenging of Cu, Zn, Pb and As by Fe and Mn oxyhydroxide coatings on plankton in lakes polluted with mine and smelter wastes: results of energy dispersive X-ray micro-analysis.

Kawahigashi M., Fujitake N. and Takahashi T., 1996, Soil Sci. Plant Nutr., 42, 355-360, Structural information obtained from spectral analysis (UV-VIS, IR, ^{1}H NMR) of particle size fractions in two humic acids

Kerndorff H. and Schnitzer M., 1980, Geo. Cosmo. Acta, 44, 1701-1708, Sorption of metals on humic acid

Korshin G. V., Li C. and Benjamin M. M., 1997, Water Res., 31, 1787-1795, Monitoring the properties of natural organic matter through UV spectroscopy: a consistent theory

Kirika, 2002, personal communication

Laxen D. P. H. and Chandler I. M. , Geochim. Cosmochim. Acta, 1983, 47, 731-741, Size distribution of iron and manganese species in freshwater

Leppard G. G., 1992, Environmental Particles vol.1, J. Buffle and H. P. van Leeuwen (eds.), Ch.6, 246-270, Lewis Publishers, Inc.,

Linda May, CEH website, 2002

Macalady D. L. ed., 1998, Perspectives in Environmental Chemistry, Oxford University Press

MacKenzie A. B., Pulford I. D., 2002, Applied Geochemistry, 17(8), 1093-1103 Investigation of contaminant metal dispersal from a disused mine at Tyndrum, Scotland, using concentration gradients

Marley N. A., Gaffney J. S., Orlandini K. A. and Dugue C. P., 1991, Hydrol. Proc., 5, 291-299, An evaluation of an automated hollow-fibre ultrafiltration apparatus for the isolation of colloidal materials in natural waters

Marley N. A., Gaffney J. S., Orlandini K. A., Picel K. C. and Choppin G. R., 1992, Sci. Total Env., 113, 159-177, Chemical characterisation of size-fractionated humic and fulvic materials in aqueous samples

Martin A. J., McNee J. J., Pedersen T. F., 2001, Journal of Geochem Exploration, 74(1-3), 175-187, The reactivity of sediments impacted by metal-mining in Lago Junin, Peru

May, 2002

Mester Z., Cremisini C., Ghiara E. and Morabito R, 1998, Analytica Chimica Acta, 359(1-2), 133-142, Comparison of two sequential extraction procedures for metal fractionation in sediment samples

MLURI, 2002, website info

Mortimer C. H., Limnol. Oceanogr., 1971, 16(2), 387, Chemical exchanges between sediments and water in the great lakes- speculations on probable regulatory mechanisms

Muller B., Granina L., Schaller T., Ulrich A and Wehrli B., 2002, 36, 411-420, P, As, Sb, Mo and other elements in sedimentary Fe/Mn layers of Lake Baikal

Murray J. W., 1975, Geo. Cosmo. Acta, 39, 505-519. The interaction of metal ions at the manganese dioxide-solution interface

Neal C, J. Geolog. Sci, 1986, 143, 635-648

Pandey A. K., Pandey S. D., Misra V., 2000, Ecotoxicology and Environmental Safety, 47(2), 195-200, stability constants of metal-humic acid complexes and its role in environmental detoxification

Peuravuori J. and Pihlaja K., 1997, Anal. Chim. Acta, 337, 133-149, Isolation and characterisation of natural organic matter from lake water: comparison of isolation with solid adsorption and tangential membrane filtration

Pham M. K. and Garnier J. M., 1998, Environ. Sci. Technol., 32, 440-449, Distribution of trace elements associated with dissolved compounds (<0.45 μm-1 nm) in freshwater using coupled (frontal cascade) ultrafiltration and chromatographic separations

Pompe S., Heise K. H. and Nitsche H., 1996, J. Chromatogr. A, 723, 215-218, Capillary electrophoresis for a "finger-print" characterisation of fulvic and humic acids

Rate A. W., McLaren R. G. and Swift R. S., 1993, Environ. Sci. Technol., 27, 1408-1414, Response of copper (II)-humic acid dissociation kinetics to factors influencing complex stability and macromolecular conformation

Riise G., 1999, Environ. International, 25(2/3), 325-334. Transport of NOM and trace metals through macropores in the lake Skjervatjern catchment

Rimstidt J. D., Balog A. and Webb J., 1998, Geo Cosmo Acta, 62, 11, 1851-1863. Distribution of trace elements between carbonate minerals and aqueous solutions

Ross J. M. and Sherrell R. M., 1999, Limnol. Oceanogr., 44, 1019-1034, The role of colloids in trace metal transport and adsorption behaviour in New Jersey Pinelands streams

Schlemmer G., 1996, Atomic Spectroscopy, 17, 15-21, Graphite furnace AAS for complex samples: detection limits, precision, long term stability,

Sahuquillo A., Lopez-Sanchez J. F., Rubio R., Rauret G., Thomas R. P., Davidson C. M. and Ure A. M, 1999, Analytica Chimica Acta, 382(3), 317-327, Use of a certified reference material for extractable trace metals to assess sources of uncertainty in the BCR three-stage sequential extraction procedure

Schmitt-Kopplin P. H., Hertkorn N., Garrison A. W., Frietag D. and Kettrup A., 1998, Anal. Chem. 70, 3798-3808, Influence of borate buffers on the electrophoretic behaviour of humic substances in capillary zone electrophoresis

Schnitzer M and Skinner S. I. M., 1965, Soil science, 99(4), 278-284, Organo-metallic interaction in the soil: 4. Carbonyl and hydroxyl groups in organic matter and metal retention

Schnitzer M., 1972, Humic Substances in the Environment, Decker, New York

Schnitzer M., 1991, Soil Sci., 151, 41-58, Soil organic matter-the next 75 years

SEPA, website, 2002

Shaw P. J., Jones R. I., De Haan H., 2000, Freshwater Biology, 45(4), 383-393, The influence of humic substances on the molecular weight distributions of phosphate and iron in epilimnetic lake waters

Shuttleworth S. M., Davison W., Hamilton-Taylor J., 1999, Environ. Sci. Technol., 33, 4169-4175, Two-dimensional and fine structure in the concentrations of iron and manganese in sediment and porewaters

Soil survey of scotland, 1982

Stepanov A. A., Zharkova L. V. and Stepanov E. A., 1997, Eurasian Soil Sci., 30, 173-177, Application of ^{1}H-NMR spectroscopy for the characterisation of humic substances

Stevenson F. J. and Goh K. M., 1971, Geochim. Cosmochim. Acta, 35, 471-483, Infrared spectra of humic acids and related substances

Stevenson F. J., 1994, Humus Chemistry, 2nd Ed., John Wiley & Sons Inc.

Straub K. L., Benz M., Schink B., 2001, Fems Microbiology Ecology, 34(4), 181-186, Iron metabolism in anoxic environments at near neutral pH

Stumm W. and Morgan J., 1996, Aquatic Chemistry: chemical equilibria and rates in natural waters, 3rd Ed., Wiley-Interscience

Summer R. S., Cornel P. K. and Roberts P. V., 1987, Sci. Total Environ., 62, 27-37, Molecular size distribution and spectroscopic characterisation of humic substances,

Sun L., Perdue E. M., Meyer J. L. and Weis J., 1997, Limnol. Oceanogr., 42, 714-721, Use of elemental composition to predict bioavailability of dissolved organic matter in a Georgia river

Sun T. 1991, Interpretation of Protein and Isoenzyme Patterns in Body Fluids, Igaku-Shoin Medical Publishers

Taillefert M., Gaillard J. F., 2002, J. Hydrology, 256(1-2), 16-34, Reactive transport modeling of trace elements in the water column of a stratified lake: iron cycling and metal scavenging

Tessier A., Environmental Particles vol.1, Ch.11, 425-453, 1992, Lewis Publishers, Inc., Sorption of trace elements on natural particles in oxic environments

Thimsen C. A. and Keil R. G., 1998, Mar. Chem., 62, 65-72, Potential interactions between sedimentary dissolved organic matter and mineral surfaces

Thurman E. A. and Malcolm R. L., 1981, Environ. Sci. Technol., 15, 463-466, Preparative isolation of aquatic humic substances

Tipping E., Hurley M. A., 1992, Geo. Cosmo. Acta, 56, 3627-3641. A unifying model of cation binding by humic subtances

Tokaliolu, Kartal and Elci, 2000, Anal. Chima Acta, 413(1-2), 33-40, Determination of heavy metals and their speciation in lake sediments by flame atomic absorption spectrometry after a four stage sequential extraction procedure

Tomikawa A. and Oba Y., 1991, Soil Sci. Plant Nutr., 37, 211-221, Characteristics of soil humic substances fractionated in relation to particle weight. Part VI Particle weight distribution, optical properties, and infrared absorption spectra of fractions of humic acids with different particle weights

Trubetskaya O. A., Kudryavtseva L. Y. and Shirshova L. T., 1994, Eurasian Soil Sci., 26, 104-109, Fractionation of soil humic substances by electrophoresis in polyacrylamide gel in the presence of denaturing agents

Trubetskoj O. A., Trubetskaya O. E., Afanas'eva G. V. and Reznikova O. I., 1995, Biol. Bulletin, 22, 400-405, Combination of gel chromatography and PAAG electrophoresis for preparative accumulation of humic acid fractions

Trubetskoj O. A., Trubetskaya O. E., Afanas'eva G. V., Reznikova O. I. and Saiz-Jimenez C., 1997, J. Chromatogr. A, 767, 285-292, Polyacrylamide gel electrophoresis of soil humic acid fractionated by size-exclusion chromatography and ultrafiltration

Trubetskoj O. A., Trubetskaya O. E., Markov L. F. and Muranova T. A., 1994, Environ. Int., 20, 387-390, Comparison of amino-acid compositions and E4/E6 ratios of soil and water humic substances fractions obtained by polyacrylamide gel electrophoresis,

Turner D. R., 1995, SCOPE (Lead, Mercury, Cadmium and Arsenic in the Environment), Ch.12, 175-186, 1987, John Wiley & Sons Ltd, Speciation and cycling of arsenic, cadmium, lead and mercury in natural waters

Vallius H., 1999, Chemosphere, 38(9), 1959-1972, Heavy metal deposition and variation in sedimentation rate within a sedimentary basin in the central gulf of Finland

Vermeer A.W. P., Mcculloch J. K., Van Riemsdijk W. H., Koopal L. K., 1999, environ. Sci. Technol., 33, 3892-3897. Metal ion adsorption to complexes of humic acid and metal oxides: deviations from the additivity rule

Vinogradoff S., Farmer J. G., Graham M. C., 1997, The influence of microbial alteration of humic macromolecules on humic-actinide binding: implications for actinide mobility in soils, unpublished Ph. D. report

Wen L. S., Santschi P., Gill G. and Paternostro C., 1999, Mar. Chem., 63, 185-212 Esturine trace metal distributions in Galveston Bay: importance of colloidal forms in the speciation of the dissolved phase

Wild A., 1993, Soils and the Environment: an introduction, Canbridge University Press

Williams M. R., millard G. E., Nimmo M. and Fones G., 1998, Marine Pollution Bulletin, 36, 366-375, Fluxes of Cu, Pb and Mn to the North-Eastern Irish Sea: the importance of sedimental and atmospheric inputs

Wolf R. E. and Grosser Z. A., 1997, Atomic Spectro., 18, 145-151, Overview and comparison of ICP-MS methods for environmental analyses

Williams T. M., 1993, Environ. Geolog., 21, 62-69, Particulate metal speciation in the surficial sediments from Loch Dee, southwest Scotland, UK

Wilson W. S., 1991, Advances in Soil Organic Matter Research: the impact on agriculture and the environment, The Royal Society of Chemistry, Cambridge

Yagi A., 1988, J. Limnology, 19(3), 149-156, Dissolved organic manganese in the anoxic hypolimnion of Lake Fukami-ike

Yonebayashi K. and Hattori T., 1988, Soil Sci. Plant Nutr., 34, 571-584, Chemical of elemental and functional groups of humic acids

Appendix 1: Results from LL1

LL1				
Depth /cm	% moisture	%organic	%ash	wet:dry
0.1	82.5	14.4	85.6	5.7
0.3	78.6	12.7	87.3	4.7
0.5	78.5	12.5	87.5	4.6
0.7	79.7	13.9	86.1	4.9
0.9	78.2	13.2	86.8	4.6
1.1	79.3	13.4	86.6	4.8
1.3	78.6	13.4	86.6	4.7
1.5	79.4	14.5	85.5	4.9
1.7	80.5	14.9	85.1	5.1
1.9	79.6	15.2	84.8	4.9
2.1	79.8	15.0	85.0	4.9
2.3	79.2	14.3	85.7	4.8
2.5	78.5	15.1	84.9	4.7
2.7	78.6	15.2	84.8	4.7
2.9	79.3	15.5	84.5	4.8
3.5	72.3	15.0	85.0	3.6
4.5	71.5	15.2	84.8	3.5
5.5	74.3	15.3	84.7	3.9
6.5	72.9	15.3	84.7	3.7
7.5	74.3	14.9	85.1	3.9
8.5	76.0	14.8	85.2	4.2
9.5	72.2	15.2	84.8	3.6
10.5	74.9	14.8	85.2	4.0
11.5	72.8	14.7	85.3	3.7
12.5	73.4	14.5	85.5	3.8
13.5	73.3	14.4	85.6	3.7
14.5	70.3	14.0	86.0	3.4
15.5	71.9	13.5	86.5	3.6
16.5	71.8	13.3	86.7	3.5
17.5	71.0	12.2	87.8	3.5
18.5	66.1	11.1	88.9	2.9
19.5	66.3	10.2	89.8	3.0
20.5	64.5	10.5	89.5	2.8

Water content of sediment, organic matter, ash content and wet:dry ratio in LL1

Depth (cm)	rrdFe mg/ kg	tsdFe mg/ kg	rrd Fe /%	rrd Mn mg/kg	tsd Mn mg/kg	rrd Mn /%	Mn/Fe
0.1	2479.0	39988.8	6.20	4026.0	2840.1	141.8	0.07
0.3	1920.9	39670.4	4.84	2799.7	2170.6	129.0	0.05
0.5	1419.0	38401.5	3.70	2671.0	2291.0	116.6	0.06
0.7	1564.2	38141.5	4.10	2572.3	2083.7	123.4	0.05
0.9	1782.9	40877.8	4.36	2389.9	2023.2	118.1	0.05
1.1	2165.8	38897.0	5.57	2386.4	1808.0	132.0	0.05
1.3	2347.1	39216.8	5.98	2154.5	1776.5	121.3	0.05
1.5	1964.8	44773.7	4.39	1911.9	1913.4	99.9	0.04
1.7	2579.2	43693.5	5.90	2277.7	1883.6	120.9	0.04
1.9	2697.8	42222.9	6.39	2131.7	1734.9	122.9	0.04
2.1	2294.1	40074.0	5.72	1760.3	1549.2	113.6	0.04
2.3	2049.3	43774.3	4.68	1730.2	1720.5	100.6	0.04
2.5	2233.2	37913.6	5.89	1954.9	1769.3	110.5	0.05
2.7	2087.1	25378.1	8.22	1888.1	878.7	214.9	0.03
2.9	2600.6	44038.1	5.91	2009.6	1710.3	117.5	0.04
3.5	2855.6	40583.0	7.04	2281.0	1871.4	121.9	0.05
4.5	2131.0	28911.3	7.37	1672.4	1673.9	99.9	0.06
5.5	2615.0	44331.0	5.90	1735.5	1531.4	113.3	0.03
6.5	1601.6	45010.5	3.56	1214.7	1292.2	94.0	0.03
7.5	1333.3	47623.3	2.80	969.7	1170.4	82.8	0.02
8.5	1637.5	40588.5	4.03	1130.2	1283.1	88.1	0.03
9.5	1808.8	45972.1	3.93	1136.4	1083.5	104.9	0.02
10.5	1748.5	45429.7	3.85	1176.0	1146.8	102.5	0.03
11.5	1950.5	41331.6	4.72	951.0	1106.6	85.9	0.03
12.5	2030.1	45180.4	4.49	922.8	1017.3	90.7	0.02
13.5	2236.5	39241.6	5.70	918.1	718.9	127.7	0.02
14.5	2046.5	38912.3	5.26	756.3	716.8	105.5	0.02
15.5	1686.6	38960.1	4.33	627.5	462.2	135.8	0.01
16.5	2621.4	40263.3	6.51	820.8	822.7	99.8	0.02
17.5	2707.9	41676.1	6.50	846.4	757.7	111.7	0.02
18.5	2261.0	39409.4	5.74	681.8	643.0	106.0	0.02
19.5	3364.0	41894.3	8.03	1761.4	723.3	243.5	0.02
20.5	2455.2	39460.0	6.22	859.7	572.7	150.1	0.01

Readily reducible Fe, pseudo-total Fe, readily reducible Fe expressed as % total, readily reducible Mn, pseudo-total Mn, readily reducible Mn expressed as % total and Mn/Fe ratio for LL1

Depth (cm)	rrdPb mg/kg	tsdPb mg/kg	rrd Pb / %	rrd Cu mg/kg	tsd Cu mg/kg	rrd Cu /%	tsd zn
0-0.2	64.2	53.5	120.0	19.2	42.7	44.9	171.1
0.2-0.4	40.6	53.1	76.4	18.3	46.5	39.4	170.3
0.4-0.6	44.5	60.5	73.5	20.2	43.0	46.9	181.5
0.6-0.8	52.1	56.6	92.1	19.6	38.9	50.4	161.7
0.8-1.0	41.7	56.4	74.0	17.8	42.5	41.9	178.2
1.0-1.2	61.3	55.4	110.6	15.7	40.5	38.8	165.5
1.2-1.4	37.8	57.1	66.1	16.1	37.9	42.5	169.3
1.4-1.6	44.5	68.5	64.9	16.6	46.5	35.7	208.9
1.6-1.8	53.4	64.1	83.3	15.2	44.2	34.4	190.0
1.8-2.0	55.8	61.3	91.0	15.9	39.8	39.9	179.3
2.0-2.2	46.6	54.7	85.2	11.5	36.3	31.7	168.3
2.2-2.4	52.2	66.6	78.4	12.4	44.0	28.1	186.4
2.4-2.6	31.0	68.0	45.6	12.2	45.2	27.0	187.5
2.6-2.8	51.9	32.4	159.9	13.3	25.5	52.0	100.6
2.8-3.0	49.7	64.0	77.6	9.1	42.4	21.4	190.8
3.0-4.0	49.1	66.5	73.7	8.4	41.9	20.0	190.9
4.0-5.0	50.9	69.5	73.2	11.9	43.2	27.6	186.9
5.0-6.0	54.0	70.2	76.9	10.5	48.7	21.5	189.7
6.0-7.0	31.7	69.4	45.7	7.7	46.3	16.7	192.6
7.0-8.0	36.0	72.8	49.4	11.5	48.6	23.7	193.5
8.0-10.0	38.9	70.0	55.5	10.4	38.8	26.7	193.5
10.0-12.0	45.0	70.0	64.2	14.4	46.5	30.9	197.2
12.0-14.0	47.0	75.5	62.3	11.6	44.9	25.8	210.0
15.0-16.0	40.8	75.5	54.1	9.1	37.3	24.3	196.3
16.0-17.0	44.6	74.2	60.1	10.4	47.5	21.8	204.8
17.0-18.0	58.8	0.0	N/A	12.5	35.6	35.2	190.0
18.0-19.0	63.5	0.0	N/A	9.7	38.9	24.9	225.0
19.0-20.0	64.5	0.0	N/A	10.2	52.7	19.3	178.0
20.0-21.0	76.0	0.0	N/A	11.2	42.1	26.5	206.6

Readily reducible Pb, pseudo-total Pb, readily reducible Pb expressed as % total, readily reducible Cu, pseudo-total Cu, readily reducible Cu expressed as % total and pseudo-total Zn for LL1

Depth /cm	@254	E4/E6	Fe mg/l	Mn mg/l	Pb mg/l	Zn mg/l
0.1	0.221	1.08	3.16	0.025	0.175	0.039
0.3	0.202	1.07	3.28	0.025	0.175	0.094
0.5	0.212	1.04	3.39	0.025	0.175	0.138
0.7	0.211	1.08	3.39	0.017	0.202	0.054
0.9	0.22	1.08	3.50	0.008	0.162	0.142
1.1	0.277	1.06	3.56	0.008	0.202	0.076
1.3	0.209	1.07	3.45	0.008	0.189	0.105
1.5	0.217	1.08	3.73	0.008	0.189	0.102
1.7	0.315	1.07	3.67	N/A	0.189	0.161
1.9	0.276	1.05	3.79	N/A	0.162	N/A
2.1	0.269	1.05	3.79	N/A	0.189	N/A
2.3	0.317	1.15	3.79	N/A	0.202	N/A
2.5	0.197	1.05	3.84	N/A	0.202	N/A
2.7	0.255	1.05	3.62	N/A	0.216	0.006
2.9	0.207	1.06	3.79	N/A	0.202	N/A
3.5	0.173	1.07	3.73	N/A	0.202	N/A
4.5	0.159	1.06	3.79	N/A	0.216	N/A
5.5	0.144	1.06	3.79	N/A	0.243	0.002
6.5	0.143	1.04	3.62	N/A	0.256	0.017
7.5	0.143	1.06	3.79	N/A	0.256	0.017
8.5	0.15	1.05	3.73	N/A	0.270	0.021
9.5	0.143	1.06	3.79	0.008	0.270	0.043
10.5	0.138	1.06	3.73	0.008	0.283	0.054
11.5	0.133	1.03	3.67	0.830	0.256	0.113
12.5	0.125	1.04	3.73	2.020	0.270	0.124
13.5	0.122	1.04	3.67	4.417	0.296	0.157
14.5	0.115	1.03	3.73	5.943	0.283	0.150

Absorbance at 254 nm, E4/E6 ratio,and concentrations of Fe, Mn, Pb and Zn in porewater from core LL1

Appendix 2: Results from LL2

LL2				
Depth cm	%moisture	%organic	%ash	wet:dry
0.1	81.9	16.0	84.0	5.5
0.3	81.1	15.3	84.7	5.3
0.5	81.0	14.0	86.0	5.3
0.7	79.2	15.8	84.2	4.8
0.9	79.7	15.4	84.6	4.9
1.1	80.1	14.5	85.5	5.0
1.3	78.9	14.9	85.1	4.7
1.5	79.5	15.4	84.6	4.9
1.7	78.6	15.6	84.4	4.7
1.9	78.7	15.7	84.3	4.7
2.1	79.4	15.6	84.4	4.9
2.3	76.5	15.5	84.5	4.2
2.5	79.1	16.0	84.0	4.8
2.7	78.6	16.6	83.4	4.7
2.9	79.2	15.9	84.1	4.8
3.5	73.7	16.3	83.7	3.8
4.5	74.7	16.3	83.7	3.9
5.5	75.2	16.5	83.5	4.0
6.5	74.8	16.5	83.5	4.0
7.5	73.3	15.5	84.5	3.8
8.5	73.4	15.3	84.7	3.8
9.5	73.5	15.3	84.7	3.8
10.5	73.6	15.1	84.9	3.8
11.5	73.0	15.1	84.9	3.7
12.5	72.3	14.9	85.1	3.6
13.5	72.5	14.9	85.1	3.6
14.5	72.0	14.9	85.1	3.6
15.5	70.4	14.6	85.4	3.4
16.5	71.8	13.3	86.7	3.5
17.5	68.8	12.9	87.1	3.2
18.5	66.7	11.9	88.1	3.0
19.5	65.3	11.0	89.0	2.9
20.5	66.1	9.5	90.5	2.9
21.5	65.6	9.5	90.5	2.9
22.5	65.4	9.4	90.6	2.9

Water content of sediment, organic matter, ash content and wet:dry ratio in LL2

Depth (cm)	rrdFe mg/ kg	tsdFe mg/ kg	rrd Fe /%	rrd Mn mg/kg	tsd Mn mg/kg	rrd Mn /%	Mn/Fe
0-0.2	4618.3	43478.4	10.62	1102.5	2737.1	40.3	0.06
0.2-0.4	1356.0	40409.9	3.36	1866.0	2646.4	70.5	0.07
0.4-0.6	2935.4	38860.2	7.55	3078.3	2361.8	130.3	0.06
0.6-0.8	2800.9	41401.6	6.77	3152.6	2296.3	137.3	0.06
0.8-1.0	3306.5	43155.4	7.66	3358.9	2072.6	162.1	0.05
1.0-1.2	2216.1	39563.0	5.60	2600.4	1703.1	152.7	0.04
1.2-1.4	1904.0	42521.8	4.48	1698.6	1565.2	108.5	0.04
1.4-1.6	2563.5	43504.1	5.89	2296.7	1434.6	160.1	0.03
1.6-1.8	2177.4	44148.0	4.93	1385.6	1366.7	101.4	0.03
1.8-2.0	2523.5	42553.4	5.93	1827.3	1403.4	130.2	0.03
2.0-2.2	2261.0	39910.9	5.67	1761.4	1183.6	148.8	0.03
2.2-2.4	2151.3	45536.8	4.72	1506.5	1330.6	113.2	0.03
2.4-2.6	2395.0	45013.9	5.32	1669.8	1358.2	122.9	0.03
2.6-2.8	0.0	43456.0	0.00	1280.1	1259.2	101.7	0.03
2.8-3.0	2124.8	45053.1	4.72	1697.6	1296.4	130.9	0.03
3.0-4.0	2327.6	41640.9	5.59	1293.1	1146.7	112.8	0.03
4.0-5.0	791.6	42585.6	1.86	1350.9	1131.1	119.4	0.03
5.0-6.0	2193.5	40976.3	5.35	1376.4	1131.6	121.6	0.03
6.0-7.0	2191.3	44956.0	4.87	1019.0	995.1	102.4	0.02
7.0-8.0	1092.4	43411.8	2.52	1233.8	1318.5	93.6	0.03
8.0-9.0	1013.4	40277.0	2.52	1323.1	1203.1	110.0	0.03
9.0-10.0	632.6	43536.2	1.45	1080.6	1264.4	85.5	0.03
10.0-11.0	1170.3	43679.1	2.68	1205.7	1263.4	95.4	0.03
11.-12.0	1609.0	45498.3	3.54	1310.2	1158.1	113.1	0.03
12.0-13.0	1288.2	43893.1	2.93	1145.5	988.7	115.8	0.02
13.0-14.0	1263.4	43386.2	2.91	1053.7	990.6	106.4	0.02
14.0-15.0	1066.2	43141.6	2.47	1022.7	934.6	109.4	0.02
15.0-16.0	1207.4	42675.8	2.83	1148.3	995.8	115.3	0.02
16.0-17.0	1381.8	42669.6	3.24	1054.9	794.1	132.8	0.02
17.0-18.0	1689.9	39750.6	4.25	993.8	670.2	148.3	0.02
18.0-19.0	1736.5	41221.8	4.21	1200.0	740.4	162.1	0.02
19.0-20.0	1682.6	39812.5	4.23	1099.4	661.7	166.1	0.02
20.0-21.0	2071.6	36063.1	5.74	978.3	601.4	162.7	0.02
21.0-22.0	1479.5	40917.8	3.62	1239.7	767.0	161.6	0.02
22.0-23.0	869.6	37740.0	2.30	810.3	540.9	149.8	0.01

Readily reducible Fe, pseudo-total Fe, readily reducible Fe expressed as % total, readily reducible Mn, pseudo-total Mn, readily reducible Mn expressed as % total and Mn/Fe ratio for LL2

Depth (cm)	rrd Cu mg/kg	tsd Cu mg/kg	rrd Cu /%	tsd zn mg/ kg
0-0.2	22.0	55.9	39.4	205.4
0.2-0.4	12.1	49.2	24.6	199.8
0.4-0.6	13.7	49.7	27.5	204.9
0.6-0.8	11.6	47.6	24.4	182.1
0.8-1.0	15.7	53.3	29.5	199.2
1.0-1.2	14.7	50.8	29.0	189.8
1.2-1.4	17.2	45.1	38.0	187.3
1.4-1.6	17.0	49.6	34.2	189.6
1.6-1.8	11.1	49.8	22.3	186.7
1.8-2.0	13.8	42.5	32.5	179.9
2.0-2.2	16.8	41.9	40.0	181.9
2.2-2.4	15.3	50.3	30.5	185.6
2.4-2.6	11.7	48.6	24.1	186.0
2.6-2.8	7.0	50.8	13.9	197.6
2.8-3.0	14.1	51.3	27.4	215.2
3.0-4.0	12.9	44.4	29.0	182.4
4.0-5.0	4.3	52.7	8.2	188.6
5.0-6.0	9.7	45.5	21.3	175.0
6.0-7.0	17.7	49.0	36.1	183.5
7.0-8.0	5.5	46.8	11.7	183.9
8.0-9.0	9.1	42.1	21.6	188.8
9.0-10.0	9.8	44.9	21.7	201.3
10.0-11.0	8.5	48.7	17.4	176.9
11.-12.0	11.3	58.6	19.2	189.6
12.0-13.0	9.2	53.1	17.3	193.9
13.0-14.0	13.1	50.9	25.7	195.1
14.0-15.0	9.6	48.8	19.6	192.5
15.0-16.0	12.1	50.6	23.9	209.5
16.0-17.0	8.7	55.0	15.8	225.1
17.0-18.0	7.8	48.4	16.1	190.0
18.0-19.0	9.2	49.2	18.7	192.5
19.0-20.0	8.9	47.4	18.8	175.0
20.0-21.0	10.0	41.1	24.3	149.0
21.0-22.0	7.0	48.8	14.3	148.9
22.0-23.0	8.3	46.5	17.9	146.0

Readily reducible Cu, pseudo-total Cu, readily reducible Cu expressed as % total and pseudo-total Zn for LL2

Depth /cm	@254	E4/E6	Fe mg/l	Mn mg/l	Pb mg/l	Zn mg/l
0.1	0.18	1.01	3.16	0.025	0.175	0.039
0.3	0.173	1.01	3.28	0.025	0.175	0.094
0.5	0.203	1.01	3.39	0.025	0.175	0.138
0.7	0.19	1.01	3.39	0.017	0.202	0.054
0.9	0.173	1.00	3.45	0.008	0.162	0.142
1.1	0.171	1.01	3.56	0.008	0.202	0.076
1.3	0.15	0.99	3.45	0.008	0.189	0.105
1.5	0.155	1.00	3.73	N/A	0.189	0.102
1.7	0.145	1.00	3.67	N/A	0.189	0.161
1.9	0.142	1.00	3.79	N/A	0.162	N/A
2.1	0.133	0.99	3.79	N/A	0.189	N/A
2.3	0.234	1.02	3.79	N/A	0.202	N/A
2.5	0.133	0.99	3.84	N/A	0.202	N/A
2.7	0.133	0.99	3.62	N/A	0.216	0.006
2.9	0.141	0.99	3.79	N/A	0.202	N/A
3.5	0.098	0.97	3.73	N/A	0.202	N/A
4.5	0.085	0.97	3.79	N/A	0.216	N/A
5.5	0.083	0.97	3.79	N/A	0.243	0.002
6.5	0.086	0.97	3.62	N/A	0.256	0.017
7.5	0.105	0.99	3.79	N/A	0.256	0.017
8.5	0.103	0.97	3.73	N/A	0.270	0.021
9.5	0.115	0.98	3.79	0.008	0.270	0.043
10.5	0.122	0.98	3.73	0.008	0.283	0.054
11.5	0.127	1.00	3.67	0.830	0.256	0.113
12.5	0.101	0.98	3.73	2.020	0.270	0.124
13.5	0.092	0.98	3.67	4.417	0.296	0.157
14.5	0.078	0.95	3.73	5.943	0.283	0.150

Absorbance at 254 nm, E4/E6 ratio,and concentrations of Fe, Mn, Pb and Zn in porewater from core LL2

Appendix 3: Results from LL3

LL3				
Depth cm	%moisture	%org	%ash	wet:dry
0.5	74.1	15.1	84.9	3.9
1.5	75.8	15.8	84.2	4.1
2.5	74.0	14.6	85.4	3.8
3.5	74.2	14.5	85.5	3.9
4.5	73.7	14.5	85.5	3.8
5.5	71.9	18.0	82.0	3.6
6.5	75.6	14.4	85.6	4.1
7.5	72.5	14.4	85.6	3.6
8.5	74.3	14.2	85.8	3.9
9.5	74.6	13.6	86.4	3.9
10.5	73.9	13.6	86.4	3.8
11.5	72.8	13.2	86.8	3.7
12.5	72.8	13.3	86.7	3.7
13.5	71.2	12.5	87.5	3.5
14.5	70.2	12.7	87.3	3.4
15.5	70.0	12.9	87.1	3.3
16.5	67.7	12.4	87.6	3.1
17.5	65.9	11.7	88.3	2.9
18.5	64.8	10.7	89.3	2.8
19.5	62.2	9.8	90.2	2.6

Water content of sediment, organic matter, ash content and wet:dry ratio in LL3

Depth cm	rrdFe mg/ kg	tsdFe mg/ kg	rrd Fe /%	rrd Mn mg/kg	tsd Mn mg/kg	rrd Mn /%	Mn/Fe
0.5	524.6	37984.8	1.38	2334.2	2192.9	106.44	0.06
1.5	984.2	37498.4	2.62	1521.0	1415.6	107.45	0.04
2.5	1100.6	44930.5	2.45	1759.5	1652.6	106.47	0.04
3.5	1003.2	40090.2	2.50	1475.7	1375.6	107.27	0.03
4.5	838.7	40711.5	2.06	1512.2	1355.9	111.52	0.03
5.5	742.3	39571.9	1.88	1190.5	1205.1	98.78	0.03
6.5	1139.7	40373.9	2.82	1306.8	1247.9	104.72	0.03
7.5	766.5	39672.5	1.93	1019.3	901.6	113.05	0.02
8.5	684.3	39885.1	1.72	1196.7	1103.5	108.44	0.03
9.5	1100.8	36644.3	3.00	1188.1	1074.7	110.55	0.03
10.5	1101.4	40045.2	2.75	1063.8	983.2	108.20	0.02
11.5	1000.0	38677.3	2.59	1022.7	852.0	120.04	0.02
12.5	1091.7	39246.9	2.78	1155.6	899.1	128.53	0.02
13.5	777.1	42717.3	1.82	1176.0	974.1	120.73	0.02
14.5	1815.5	42861.7	4.24	1118.4	883.2	126.63	0.02
15.5	1480.1	1801.3	N/A	N/A	N/A	N/A	0.01
16.5	1375.3	35397.9	3.89	902.8	719.9	125.41	0.02

Readily reducible Fe, pseudo-total Fe, readily reducible Fe expressed as % total, readily reducible Mn, pseudo-total Mn, readily reducible Mn expressed as % total and Mn/Fe ratio for LL3

Depth cm	rrdPb mg/ kg	tsdPb mg/ kg	rr Pb /%	rrd Cu mg/kg	tsd Cu mg/kg	rrd Cu /%	tsd zn mg/ kg
0.5	12.2	69.9	17.4	6.2	40.1	15.5	195.5
1.5	20.8	80.8	25.7	6.6	38.0	17.5	184.1
2.5	40.6	78.3	51.9	7.4	49.3	15.1	222.3
3.5	14.8	72.6	20.4	4.7	40.3	11.7	200.2
4.5	24.0	73.8	32.6	6.8	39.0	17.5	201.4
5.5	15.0	69.0	21.7	4.6	38.6	11.8	194.8
6.5	22.5	77.3	29.1	4.0	43.8	9.1	215.0
7.5	19.1	77.1	24.7	5.8	38.3	15.2	198.1
8.5	33.0	81.7	40.4	5.9	37.5	15.6	197.4
9.5	40.1	80.0	50.1	5.7	34.5	16.5	187.7
10.5	30.6	79.0	38.8	5.7	39.5	14.5	185.8
11.5	33.7	85.6	39.4	4.8	42.4	11.3	190.1
12.5	27.4	85.7	32.0	3.9	39.3	9.9	188.1
13.5	34.7	91.7	37.8	4.2	44.6	9.5	199.1
14.5	34.9	99.1	35.3	5.0	46.5	10.7	212.0
15.5	55.1	98.6	55.9	14.8	10.3		25.2
16.5	48.4	103.9	46.6	11.9	166.3	7.2	215.0

Readily reducible Pb, pseudo-total Pb, readily reducible Pb expressed as % total, readily reducible Cu, pseudo-total Cu, readily reducible Cu expressed as % total and pseudo-total Zn for LL3

Depth cm	Mn mg/l	Pb mg/l	Zn mg/l
0-1.0	0.025147	0.067	N/A
1.0-2.0	0.025147	0.108	N/A
2.0-3.0	0.016764	0.108	N/A
3.0-4.0	N/A	0.175	N/A
4.0-5.0	N/A	0.148	N/A
5.0-6.0	0.016764	0.175	0.017
6.0-7.0	N/A	0.189	0.017
7.0-8.0	0.016764	0.175	0.032
8.0-9.0	N/A	0.175	0.013
9.0-10.0	N/A	0.189	N/A
10.0-11.0	N/A	0.162	N/A
11.-12.0	N/A	0.148	N/A
12.0-13.0	N/A	0.135	0.006
13.0-14.0	N/A	0.175	0.002
14.0-15.0	N/A	0.148	0.006
15.0-16.0	N/A	0.148	0.024
16.0-17.0	0.125733	0.135	0.061
17.0-18.0	1.148365	0.162	0.109
18.0-19.0	2.808047	0.175	0.168
19.0-20.0	3.713328	0.189	0.172

Concentrations of Mn, Pb and Zn in porewater from core LL3

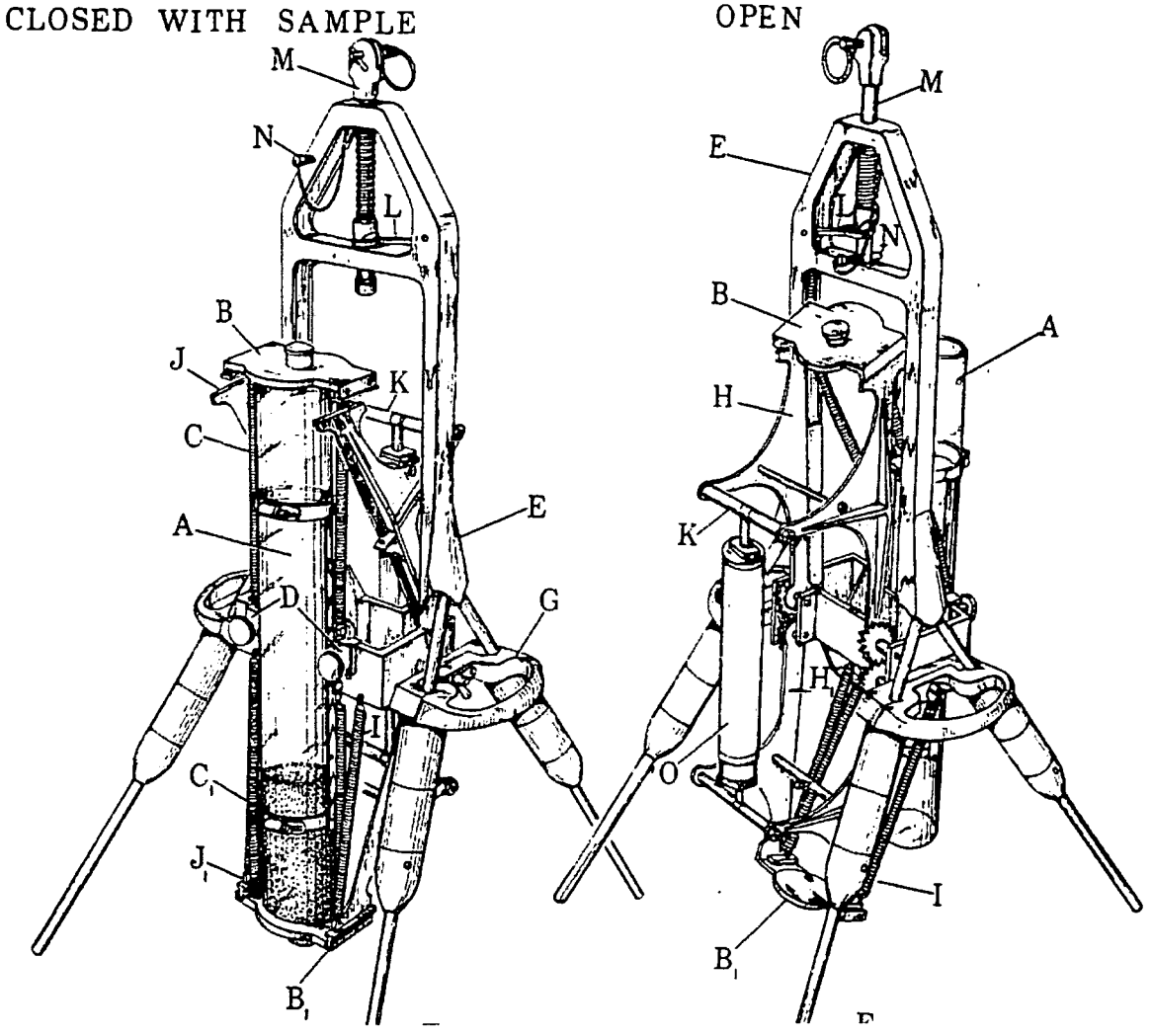

A sampling tube
B and B1 top and bottom lids
C and C1 springs
D harness assembly
E main frame
F legs
G handles
H and H1 arms
I additional springs
J and J1 arms engaging with lids B and B1
K arm assembly pull back from here
L spring loaded release lever
M rod for attachment of cable
N safety pin
O dashpot

Figure 2.15 Diagram of the Jenkin's sub-surface mud sampler (Mortimer, 1971)

Appendix 4: Results from LBA1

LB1				
Depth (cm)	%moisture	%ash	%org	wet/dry
0.5	85.5	53.1	46.9	6.88
1.5	83.0	57.0	43.0	5.88
2.5	80.1	58.3	41.7	5.02
3.5	81.4	57.8	42.2	5.37
4.5	80.9	62.0	38.0	5.23
5.5	82.5	57.9	42.1	5.73
6.5	84.5	54.2	45.8	6.45
7.5	84.2	56.6	43.4	6.31
8.5	83.4	57.5	42.5	6.04
9.5	81.9	58.7	41.3	5.52
10.5	80.7	62.5	37.5	5.19
11.5	61.9	83.6	16.4	2.63
12.5	44.8	93.4	6.6	1.81
13.5	39.9	93.8	6.2	1.66
14.5	44.5	91.9	8.1	1.80

Water content of sediment, organic matter, ash content and wet:dry ratio in LBA1

Depth (cm)	254 nm	E4/E6	Fe mg/l	Mn mg/l	Pb mg/l	Cu mg/l	Zn mg/l
0-1	3.69	3.08	7.34	1.2	0.027	0.0019	0.083
1-2	1.67	3.21	13.39	7.2	0.060	0.0039	0.086
2-3	0.64	2.33	4.84	12.5	0.005	0.0039	0.060
3-4	4.82	2.30	17.10	3.9	0.110	0.0136	0.185
4-5	0.30	1.96	4.03	29.9	0.009	0.0039	0.112
5-6	0.14	1.63	1.29	37.8	0.005	0.0000	0.262
6-7	0.21	1.81	3.31	34.8	0.037	0.0039	0.370
7-8	0.14	1.56	0.89	22.0	0.000	0.0039	0.421
8-9	0.11	1.52	1.21	12.2	0.000	0.0039	0.328
9-10	0.13	1.47	0.32	14.4	0.014	0.0000	0.372
10-11	0.31	1.61	1.29	7.8	0.023	0.0039	0.241
11-12	0.45	1.94	3.15	6.4	0.032	0.0039	0.147
12-13	0.55	2.01	4.52	4.8	0.032	0.0117	0.172
13-14	0.13	1.60	1.29	26.0	0.009	0.0039	0.125
14-15	1.15	2.38	7.10	2.5	0.032	0.0078	0.168

Absorbance at 254 nm, E4/E6 ratio, total concentrations of Fe, Mn, Pb, Cu and Zn in LBA1 porewater

Depth (cm)	Fe % (w/ w)	Mn % (w/ w)	Mn/Fe	Pb mg/kg	Cu mg/kg	Zn mg/kg
0.1	9.87	2.25	0.228	125.1	22.5	169.7
0.3	11.96	1.15	0.096	118.7	20.1	180.0
0.5	6.65	0.75	0.112	98.9	21.5	187.7
0.7	6.35	0.62	0.098	110.3	21.5	202.6
0.9	6.64	0.55	0.082	152.4	27.0	234.4
1.1	5.93	0.50	0.084	167.8	22.4	275.2
1.3	7.70	0.60	0.078	244.8	32.4	478.6
1.5	6.60	0.59	0.089	236.6	27.6	608.8
1.7	5.50	0.57	0.103	234.6	29.2	706.6
1.9	4.98	0.54	0.109	192.4	28.9	616.0
2.1	4.89	0.48	0.098	195.8	30.7	635.9
2.3	2.46	0.13	0.054	49.7	9.0	273.5
2.5	2.11	0.06	0.027	16.5	5.6	160.8
2.7	2.18	0.10	0.047	18.7	5.8	197.7
2.9	1.64	0.02	0.013	11.2	18.0	133.0

pseudo-total Fe, pseudo-total Mn,Mn/Fe ratio, total Pb, total Cu and total Zn for LBA1

Appendix 5: Results from LBA2

LL1				
Depth	%moisture	%ash	%org	wet/dry
0.5	86.3	51.3	48.7	7.32
1.5	84.0	53.7	46.3	6.24
2.5	80.6	53.9	46.1	5.16
3.5	78.2	52.6	47.4	4.59
4.5	80.8	53.5	46.5	5.20
5.5	80.9	55.4	44.6	5.22
6.5	83.4	52.2	47.8	6.03
7.5	84.0	47.4	52.6	6.23
8.5	82.6	51.6	48.4	5.74
9.5	81.0	56.0	44.0	5.27
10.5	82.6	54.9	45.1	5.73
11.5	71.8	72.6	27.4	3.55
12.5	62.3	82.0	18.0	2.65
13.5	37.8	93.8	6.2	1.61

Water content of sediment, organic matter, ash content and wet:dry ratio in LBA2

LB1.2 pw	corrected						
Depth	254 nm	E4/E6	Fe mg/l	Mn mg/l	Pb mg/l	Cu mg/l	Zn mg/l
0-1	2.65	3.00	5.40	1.4	0.0183	0.0019	0.07
1-2	3.54	2.67	20.48	5.8	0.0917	0.0000	0.02
2-3	0.62	2.49	5.56	6.7	0.0046	0.0019	0.11
3-4	0.14	1.46	0.48	17.6		0.0039	0.13
4-5	0.04	0.82	0.65	37.3		0.0000	0.18
5-6	0.09	1.39	0.97	40.0	0.0275	0.0039	0.17
6-7	0.23	1.90	4.44	37.9	0.0183	0.0000	0.25
7-8	0.47	2.13	6.53	39.0	0.0229	0.0039	0.29
8-9	0.20	1.78	2.10	30.2	0.0046	0.0000	0.31
9-10	0.07	1.17	0.48	20.3	0.0137	0.0000	0.31
10-11	0.15	1.52	0.48	19.0	0.0000	0.0000	0.28
11-12	0.13	1.60	1.05	14.3	0.0092	0.0000	0.22
12-13	0.57	2.16	6.21	12.5	0.0229	0.0019	0.23
13-14	0.28	1.86	2.42	11.9	0.0183	0.0019	0.22

Absorbance at 254 nm, E4/E6 ratio, total concentrations of Fe, Mn, Pb, Cu and Zn in LBA2 porewater

Depth (cm)	Fe % (w/w)	Mn % (w/w)	Mn/Fe	Pb mg/kg	Cu mg/kg	Zn mg/kg
0.1	9.91	0.299	0.030	129.4	19.7	162.5
0.3	12.57	0.135	0.011	98.9	16.4	144.0
0.5	8.83	0.087	0.010	119.0	20.2	186.4
0.7	6.55	0.067	0.010	136.0	24.1	195.4
0.9	8.62	0.067	0.008	165.1	28.1	238.0
1.1	8.25	0.051	0.006	165.2	27.1	249.7
1.3	9.07	0.056	0.006	230.8	33.9	355.8
1.5	9.46	0.072	0.008	265.8	34.1	473.5
1.7	7.58	0.071	0.009	256.2	27.0	587.2
1.9	6.55	0.071	0.011	219.0	30.6	595.4
2.1	5.44	0.060	0.011	207.4	28.4	683.7
2.3	3.40	0.034	0.010	118.2	14.6	496.8
2.5	3.02	0.028	0.009	78.5	9.4	364.0
2.7	1.58	0.007	0.004	14.1	1.7	136.3

pseudo-total Fe, pseudo-total Mn,Mn/Fe ratio, total Pb, total Cu and total Zn for LBA2

Appendix 6: Results from LBA3

LL1				
Depth	%moisture	%ash	%org	wet/dry
0.5	83.8	55.9	44.1	6.16
1.5	83.4	55.7	44.3	6.01
2.5	78.9	57.2	42.8	4.74
3.5	78.8	57.0	43.0	4.72
4.5	80.4	55.7	44.3	5.09
5.5	79.2	59.4	40.6	4.80
6.5	80.1	61.5	38.5	5.01
7.5	83.4	53.5	46.5	6.01
8.5	83.0	55.0	45.0	5.87
9.5	82.1	58.8	41.2	5.60
10.5	82.9	57.6	42.4	5.83
11.5	79.9	63.4	36.6	4.97
12.5	56.4	86.6	13.4	2.29
13.5	53.2	85.4	14.6	2.14
14.5	50.0	86.9	13.1	2.00
15.5	44.3	89.5	10.5	1.79

Water content of sediment, organic matter, ash content and wet:dry ratio in LBA3

LB1.3 pw	corrected						
Depth (cm)	254 nm	E4/E6	Fe mg/l	Mn mg/l	Pb mg/l	Cu mg/l	zn mg/l
0-1	5.44	3.36	10.16	3.38	0.0458	0.0078	0.231
1-2	4.59	3.39	10.65	9.64	0.0642	0.0000	0.242
2-3	0.59	2.15	7.34	15.57	0.0229	0.0000	0.189
3-4	0.94	2.18	7.50	13.56	0.0321	0.0039	0.296
4-5	0.40	1.94	3.79	27.84	0.0137	0.0039	0.272
5-6	0.79	2.30	6.37	25.90	0.0229	0.0117	0.251
6-7	0.52	2.13	7.10	28.62	0.0137	0.0078	0.231
7-8	0.57	2.13	7.42	31.53	0.0137	0.0039	0.327
8-9	0.83	2.22	7.50	23.77	0.0275	0.0078	0.284
9-10	0.41	1.98	1.77	15.63	0.0137	0.0019	0.253
10-11	0.29	1.83	0.89	14.13	0.0046	0.0000	0.211
11-12	0.32	1.78	0.81	10.42	0.0137	0.0000	0.232
12-13	0.83	2.25	2.34	5.63	0.0137	0.0039	0.150
13-14	0.90	2.26	2.90	5.51	0.0092	0.0155	0.324
14-15	0.97	2.27	3.95	5.12	0.0046	0.0039	0.263
15-16	1.97	2.44	1.77	5.51	0.0092	0.0078	0.316

Absorbance at 254 nm, E4/E6 ratio, total concentrations of Fe, Mn, Pb, Cu and Zn in LBA3 porewater

sample	Fe %(w/w)	Mn %(w/w)	Mn/Fe	Pb mg/kg	Cu mg/kg	Zn mg/kg
0-1	7.85	3.15	0.40	180.7	16.8	133.7
1-2	9.05	1.31	0.14	196.2	17.1	148.0
2-3	6.75	1.02	0.15	160.8	14.6	186.3
3-4	5.66	0.90	0.16	147.1	13.8	182.1
4-5	5.89	0.89	0.15	160.3	16.6	206.7
5-6	5.56	0.79	0.14	143.9	18.1	221.6
6-7	5.79	0.83	0.14	159.5	21.3	277.1
7-8	6.43	1.05	0.16	200.2	23.4	424.0
8-9	6.88	1.03	0.15	260.4	24.3	547.2
9-10	4.60	0.80	0.17	177.8	16.3	626.5
10-11	4.45	0.88	0.20	191.0	20.1	730.7
11-12	3.74	0.76	0.20	159.1	20.2	596.0
12-13	1.68	0.23	0.13	52.4	7.0	268.4
13-14	1.72	0.27	0.16	46.0	5.7	164.1
14-15	1.38	0.19	0.13	25.9	3.9	99.2

pseudo-total Fe, pseudo-total Mn,Mn/Fe ratio, total Pb, total Cu and total Zn for LBA3

sample	Al mg/kg	Ca mg/kg	Co mg/kg	K mg/kg	Mg mg/kg	Na mg/kg	P mg/kg	S mg/kg	Si mg/kg
0-1	26567.0	4839.2	80.6	3637.0	4833.6	220.1	1596.0	3869.1	535.3
1-2	25117.7	4613.7	67.6	3144.5	4400.4	202.2	1692.1	3607.1	468.8
2-3	29234.0	4514.7	52.9	4440.3	4938.2	200.7	1810.0	3377.7	540.8
3-4	30859.7	4543.8	35.6	5067.9	5169.0	208.8	1836.4	3011.5	781.9
4-5	32231.3	4646.2	56.9	5192.4	5028.3	212.3	1919.8	3641.1	788.0
5-6	30328.8	4383.7	66.4	5169.6	5143.3	216.8	1849.7	3700.4	1180.0
6-7	33142.2	4970.1	77.0	5730.2	5225.1	216.4	2075.0	4212.5	955.0
7-8	31340.0	6187.2	111.1	5219.9	4688.0	218.6	2237.3	5999.4	638.5
8-9	31814.0	6471.0	101.2	4286.3	4437.3	198.2	2740.9	6199.2	373.3
9-10	27066.7	6065.3	50.9	3380.3	4135.8	173.9	1911.7	4422.1	623.4
10-11	29237.2	6553.3	64.3	3734.6	4529.5	186.2	1783.5	4808.2	910.2
11-12	25671.8	5992.4	46.5	3278.8	4390.7	171.6	1361.2	4349.6	843.4
12-13	10196.2	2338.0	16.2	1267.8	3056.7	134.3	463.6	950.9	1246.6
13-14	9323.1	2705.4	15.0	996.5	3057.9	137.4	411.3	915.4	1189.6
14-15	8151.8	2298.4	11.3	987.2	2735.2	158.8	342.5	609.3	1629.6

pseudo-total concentration of Al, Ca, Co, K, Mg, Na, P, S and Si for LBA3

sample	Fe %(w/w)	Mn %(w/w)	Mn/Fe	Pb mg/kg	Cu mg/kg	Zn mg/kg
0-1	7.90	3.12	0.39	168.5	15.5	138.8
1-2	9.19	1.27	0.14	188.9	17.4	152.5
2-3	6.78	1.02	0.15	157.1	16.8	182.0
3-4	5.67	0.87	0.15	138.0	18.1	184.0
4-5	5.73	0.87	0.15	153.6	14.9	201.0
5-6	5.80	0.86	0.15	150.0	20.7	236.0
6-7	5.68	0.83	0.15	165.0	20.4	275.1
7-8	6.70	1.06	0.16	219.1	22.8	426.0
8-9	7.18	1.07	0.15	241.5	28.3	565.0
9-10	4.63	0.86	0.19	191.7	14.9	648.3
10-11	4.44	0.88	0.20	184.0	21.0	730.5
11-12	3.53	0.66	0.19	141.1	17.4	546.2
12-13	1.58	0.20	0.13	44.4	7.0	202.7
13-14	1.66	0.25	0.15	34.4	5.0	152.7
14-15	1.34	0.19	0.14	29.0	3.8	96.5

pseudo-total Fe, pseudo-total Mn,Mn/Fe ratio, total Pb, total Cu and total Zn for LBA3 duplicate sample set

sample	Al mg/kg	Ca mg/kg	Co mg/kg	K mg/kg	Mg mg/kg	Na mg/kg	P mg/kg	S mg/kg	Si mg/kg
0-1	27181.6	5014.5	81.8	3678.9	4790.6	206.0	1625.2	3957.5	741.0
1-2	25343.1	4408.3	67.5	3089.7	4493.6	200.7	1705.1	3694.7	804.9
2-3	28739.6	4414.8	51.9	4337.5	5021.0	211.0	1803.6	3436.7	767.5
3-4	31374.3	4531.3	35.8	5212.9	5100.6	213.7	1782.4	3022.5	730.6
4-5	31382.9	4699.8	56.2	4983.3	5021.3	225.7	1910.8	3712.8	645.4
5-6	33200.3	4624.7	70.2	5750.4	5359.8	244.7	1950.0	3800.1	439.7
6-7	31697.7	4918.9	77.7	5332.8	5185.9	237.0	2072.0	4360.8	603.0
7-8	30918.3	6181.0	115.1	5057.7	4771.5	217.0	2353.2	6395.6	297.3
8-9	30998.8	6609.7	104.2	4187.0	4430.3	210.1	2843.3	6242.1	441.2
9-10	27833.0	6392.2	48.5	3577.8	4408.6	179.9	1973.5	4242.5	758.4
10-11	29385.0	6580.4	61.9	3821.6	4618.8	198.9	1765.2	4821.9	468.9
11-12	23346.1	5233.3	40.2	2992.7	4167.8	170.5	1238.0	3735.8	196.1
12-13	9277.5	2062.3	14.5	1247.9	2939.8	165.0	409.9	862.0	1503.0
13-14	9314.6	2663.9	14.6	1000.3	3061.0	147.0	390.7	821.9	1049.1
14-15	7259.3	2104.5	11.5	687.0	2565.1	118.3	301.2	602.4	753.8

pseudo-total concentration of Al, Ca, Co, K, Mg, Na, P, S and Si for LBA3 duplicate sample set

Appendix 7: Results from LBB1

Depth (cm)	%moisture	%ash	%org	wet/dry
0.5	85.5	67.1	32.9	6.89
1.5	81.5	66.1	33.9	5.40
2.5	79.8	62.6	37.4	4.95
3.5	82.4	61.0	39.0	5.67
4.5	85.2	56.3	43.7	6.76
5.5	83.2	57.1	42.9	5.94
6.5	84.6	56.9	43.1	6.50
7.5	85.3	57.0	43.0	6.82
8.5	83.3	58.9	41.1	5.98
9.5	83.7	60.0	40.0	6.13
10.5	83.1	59.4	40.6	5.92
11.5	79.4	65.8	34.2	4.84
12.5	81.0	66.4	33.6	5.27
13.5	73.4	77.7	22.3	3.76
14.5	76.3	75.6	24.4	4.23
15.5	75.8	75.4	24.6	4.13
16.5	76.8	77.5	22.5	4.31
17.5	80.7	79.7	20.3	5.19
18.5	80.9	81.2	18.8	5.25
19.5	79.2	84.0	16.0	4.82
20.5	78.4	87.9	12.1	4.64
21.5	76.7	93.2	6.8	4.30
22.5	77.0	95.9	4.1	4.35
23.5	74.8	98.4	1.6	3.97
24.5	76.5	99.9	0.1	4.26
25.5	76.1	99.0	1.0	4.19
26.5	77.8	99.7	0.3	4.49

Water content of sediment, organic matter, ash content and wet:dry ratio in LBB1

Depth cm	rr Fe% (w/w)	total Fe% (w/w)	rr Fe% total	rr Mn % (w/w)	total Mn % (w/w)	rr Mn as % total	Mn/Fe
0-1	0.89	8.51	10.48	5.83	3.92	148.9	0.460
1-2	0.40	12.34	3.28	0.71	1.09	65.3	0.088
2-3	0.34	6.09	5.57	0.41	0.59	69.4	0.097
3-4	0.31	4.98	6.28	0.57	0.64	88.8	0.129
4-5	0.34	5.12	6.62	0.73	0.84	87.0	0.164
5-6	0.33	5.40	6.16	0.71	0.82	86.7	0.151
6-7	0.32	6.05	5.21	0.74	0.97	76.2	0.161
7-8	0.27	7.02	3.91	0.64	0.99	64.7	0.142
8-9	0.25	7.07	3.55	0.60	1.04	58.2	0.146
9-10	0.27	5.89	4.56	0.53	0.88	60.5	0.150
10-11	0.28	5.83	4.84	0.45	0.95	47.1	0.163
11-12	0.31	5.41	5.68	0.44	0.84	52.6	0.155
12-13	0.35	6.59	5.27	0.53	0.88	59.6	0.134
13-14	0.38	8.16	4.69	0.45	0.77	58.5	0.094
14-15	0.51	7.59	6.73	0.54	0.90	60.4	0.119
15-16	0.57	7.48	7.59	0.51	0.97	52.3	0.129
16-17	0.66	7.47	8.82	0.41	0.97	42.3	0.130
17-18	0.74	10.58	7.01	0.39	1.09	35.8	0.103
18-19	0.72	11.94	5.99	0.59	1.31	45.3	0.110
19-20	0.87	10.86	8.01	1.67	2.01	83.2	0.185
20-21	0.72	12.02	5.96	1.48	2.06	71.7	0.171
21-22	0.83	15.92	5.20	2.91	2.66	109.4	0.167
22-23	0.89	17.58	5.08	4.44	3.24	137.0	0.185
23-24	0.78	19.68	3.96	3.64	3.64	100.0	0.185
24-25	0.88	19.39	4.52	2.73	2.59	105.6	0.133
25-26	0.75	15.45	4.84	6.81	3.43	198.7	0.222
26-27	1.16	15.05	7.71	5.87	3.11	188.5	0.207

Readily reducible Fe, pseudo-total Fe, readily reducible Fe expressed as % total, readily reducible Mn, pseudo-total Mn, readily reducible Mn expressed as % total and Mn/Fe ratio for LBB1

Depth (cm)	tsd Cu mg/kg	rr Zn mg/ kg	total zn mg/kg	rr Zn as % total
0-0.2	55.9	79.1	221.4	35.7
0.2-0.4	49.2	41.3	237.2	17.4
0.4-0.6	49.7	52.7	282.0	18.7
0.6-0.8	47.6	143.2	595.7	24.0
0.8-1.0	53.3	133.4	735.4	18.1
1.0-1.2	50.8	178.7	772.3	23.1
1.2-1.4	45.1	118.9	861.9	13.8
1.4-1.6	49.6	78.2	856.6	9.1
1.6-1.8	49.8	56.1	788.1	7.1
1.8-2.0	42.5	49.3	701.1	7.0
2.0-2.2	41.9	72.4	690.6	10.5
2.2-2.4	50.3	85.6	624.7	13.7
2.4-2.6	48.6	140.9	780.2	18.1
2.6-2.8	50.8	190.6	685.3	27.8
2.8-3.0	51.3	134.2	448.1	30.0
3.0-4.0	44.4	68.9	300.5	22.9
4.0-5.0	52.7	70.5	276.8	25.5
5.0-6.0	45.5	75.0	295.2	25.4
6.0-7.0	49.0	81.8	279.4	29.3
7.0-8.0	46.8	66.4	229.3	28.9
8.0-9.0	42.1	84.6	292.6	28.9
9.0-10.0	44.9	77.7	311.0	25.0
10.0-11.0	48.7	110.0	308.4	35.7
11.-12.0	58.6	89.4	303.1	29.5
12.0-13.0	53.1	75.4	247.8	30.4
13.0-14.0	50.9	96.1	181.9	52.8
14.0-15.0	48.8	82.2	171.3	48.0

Readily reducible Cu, pseudo-total Cu, readily reducible Cu expressed as % total and pseudo-total Zn for LBB1

LB2.1 pw Depth	corrected 254 nm	E4/E6	Fe mg/l	Mn mg/l	Pb mg/l	Zn mg/l
0-1	2.68	3.18	17.4	1.21	0.027	0.111
1-2	15.73	5.11	113.9	7.55	0.166	0.270
2-3	3.13	3.48	17.4	2.49	0.045	0.234
3-4	1.94	2.74	6.2	2.51	0.036	0.161
4-5	1.90	2.61	5.8	3.26	0.031	0.161
5-6	1.30	2.39	3.7	4.41	0.018	0.067
6-7	1.43	2.39	4.5	4.55	0.049	0.245
7-8	1.48	2.35	5.0	4.40	0.058	0.127
8-9	2.79	2.71	11.3	4.59	0.085	0.128
9-10	2.71	2.63	9.9	3.93	0.049	0.180
10-11	2.17	2.40	6.7	3.40	0.045	0.123
11-12	1.67	2.31	5.2	3.70	0.036	0.079
12-13	2.44	2.57	10.7	4.00	0.076	0.121
13-14	7.40	3.29	49.3	8.33	0.180	0.217
14-15	3.12	2.94	18.4	5.37	0.049	0.130
15-16	2.92	2.83	15.2	6.58	0.027	0.228
16-17	4.77	3.44	36.1	8.29	0.018	0.121
17-18	6.72	3.74	59.1	9.58	0.004	0.109
18-19	5.56	3.47	49.8	9.55	0.004	0.146
19-20	6.02	2.95	55.5	11.08	0.009	0.196
20-21	11.14	3.38	98.4	16.05	0.027	0.240
21-22	12.96	4.11	134.4	20.68	0.027	0.510
22-23	19.62	4.30	204.9	28.97	0.049	0.368
23-24	12.04	4.50	119.9	25.34	0.036	0.257
24-25	9.97	4.29	95.9	27.72	0.000	0.318
25-26	1.96	3.61	13.0	20.16	0.022	0.320
26-27	1.39	2.57	10.3	18.83	0.000	0.192

Absorbance at 254 nm, E4/E6 ratio, total concentrations of Fe, Mn, Pb and Zn in LBB1 porewater

Depth cm	ret Fe mg/l	ret Mn mg/l	fil Mn mg/kg	ret Zn mg/l
0-1	13.0	0.84	0.00	0.003
1-2	79.7	5.36	0.00	0.179
2-3	12.9	1.52	0.55	0.096
3-4*	3.0	0.44	0.82	0.005
4-5*	1.9	0.48	1.56	0.011
5-6*	1.3	0.48	0.43	0.000
6-7*	0.6	0.16	0.27	0.000
7-8	5.9	1.2	0.20	0.017
8-9	12.9	1.76	0.12	0.060
9-10	5.6	0.96	0.12	0.037
10-11	3.4	0.6	0.23	0.001
11-12	2.8	1.2	0.00	0.021
12-13	8.1	2.4	0.16	0.080
13-14	47.4	6.08	1.80	0.270
14-15	14.6	1.24	1.88	0.084
15-16	9.5	0.48	2.81	0.142
16-17	3.3	0.96	2.50	0.070
17-18*	5.7	1.72	2.46	0.068
18-19	37.9	2.8	3.52	0.094
19-20	50.0	4.36	4.49	0.179
20-21*	75.9	3.28	4.49	0.163
21-22*	60.2	0	3.83	0.225
22-23*	112.4	13.6	3.01	0.280
23-24*	54.5	8.16	4.45	0.207
24-25	36.8	3.2	3.48	0.074
25-26	4.8	3.2	0.23	0.043

Fe, Mn and Zn in fraction of porewater retained by 1 kDa ultrafilter and Mn in filtrate for LBB1

Appendix 3: Results from LBB2

Depth (cm)	%moisture	%ash	%org	wet/dry
0.5	87.2	79.2	20.8	7.82
1.5	81.7	63.1	36.9	5.45
2.5	82.4	60.0	40.0	5.70
3.5	83.3	57.5	42.5	5.99
4.5	83.2	57.0	43.0	5.96
5.5	82.5	56.5	43.5	5.70
6.5	85.0	54.4	45.6	6.68
7.5	84.3	56.6	43.4	6.37
8.5	84.7	56.9	43.1	6.52
9.5	79.2	64.3	35.7	4.82
10.5	83.3	60.4	39.6	5.99
11.5	78.0	66.3	33.7	4.55
12.5	72.4	81.3	18.7	3.62
13.5	69.6	75.9	24.1	3.29
14.5	81.1	72.6	27.4	5.29
15.5	81.0	72.1	27.9	5.26
16.5	80.0	73.9	26.1	5.00
17.5	78.5	71.0	29.0	4.66
18.5	76.4	77.5	22.5	4.24
19.5	75.1	83.2	16.8	4.01
20.5	75.5	82.6	17.4	4.08
21.5	77.5	82.7	17.3	4.44
22.5	78.2	83.5	16.5	4.59
23.5	77.8	84.1	15.9	4.50

Water content of sediment, organic matter, ash content and wet:dry ratio in LBB2

Depth cm	Fe % (w/w)	Mn % (w/w)	Mn/Fe	Pb mg/kg	Cu mg/kg	Zn mg/kg
0-1	9.51	3.32	0.35	155.1	19.2	213.9
1-2	11.18	0.86	0.08	169.5	17.6	233.2
2-3	5.74	0.62	0.11	214.9	25.0	482.0
3-4	5.15	0.77	0.15	219.1	27.5	675.6
4-5	5.06	0.80	0.16	240.9	30.8	731.6
5-6	5.36	0.85	0.16	231.5	29.5	739.5
6-7	6.23	0.97	0.16	256.1	30.4	862.9
7-8	6.19	0.90	0.15	250.8	33.5	725.2
8-9	6.25	0.93	0.15	263.5	32.1	728.4
9-10	5.78	0.81	0.14	218.1	29.8	600.3
10-11	6.42	0.92	0.14	291.9	28.5	756.6
11-12	8.35	0.92	0.11	334.5	24.9	1095.6
12-13	7.49	0.59	0.08	148.8	9.7	508.6
13-14	7.56	0.79	0.11	68.6	17.1	407.3
14-15	5.99	0.81	0.13	61.8	20.5	283.1
15-16	5.96	0.93	0.16	71.5	22.8	275.1
16-17	6.49	0.95	0.15	61.8	21.2	248.0
17-18	6.08	0.89	0.15	52.8	22.8	247.8
18-19	7.85	0.70	0.09	31.7	14.4	275.6
19-20	14.17	0.81	0.06	22.4	11.6	276.7
20-21	19.31	2.57	0.13	11.1	10.9	280.6
21-22	13.69	2.60	0.19	4.7	12.2	243.1
22-23	14.55	1.93	0.13	N/A	23.0	260.3
23-24	8.39	1.69	0.20	N/A	22.8	255.5

Pseudo-total Fe, pseudo-total Mn, Mn/Fe ratio, total Pb, total Cu and total Zn for LBB2

LB2.3 pw Depth (cm)	corrected 254 nm	E4/E6	Fe mg/l	Mn mg/l	Pb mg/l	Cu mg/l	Zn mg/l
0-1	2.19	2.54	25.6	0.91	0.0135	0.0000	0.272
1-2	6.43	3.50	56.6	1.61	0.0719	0.0081	0.261
2-3	0.89	2.31	5.5	1.21	0.0000	0.0061	0.237
3-4	0.46	2.04	1.8	2.33	0.0000	0.0101	0.241
4-5	1.23	2.25	3.8	4.94	0.0000	0.0041	0.215
5-6	0.50	2.00	1.8	7.76	0.0135	0.0122	0.255
6-7	0.39	1.82	1.3	12.48	0.0045	0.0041	0.189
7-8	0.47	2.04	2.0	11.09	0.0000	0.0081	0.231
8-9	0.34	1.78	0.6	21.52	0.0000	0.0041	0.290
9-10	0.90	2.10	2.8	9.76	0.0135	0.0041	0.287
10-11	0.50	1.95	2.0	6.91	0.0225	0.0061	0.255
11-12	5.60	2.79	47.5	4.48	0.1258	0.0081	0.419
12-13	4.01	2.35	43.6	8.85	0.1303	0.0182	0.315
13-14	1.27	2.77	10.0	3.79	0.0090	0.0122	0.146
14-15	2.71	2.32	12.1	5.03	0.0135	0.0101	0.211
15-16	1.66	2.48	7.3	4.73	0.0090	0.0162	0.130
16-17	1.28	2.26	8.6	5.61	0.0000	0.0081	0.208
17-18	1.77	2.33	11.3	5.03	0.0135	0.0081	0.231
18-19	3.91	2.85	39.8	6.88	0.0135	0.0344	0.369
19-20	17.26	3.52	177.7	15.76	0.0404	0.0081	0.523
20-21	6.00	4.33	65.0	10.70	0.0045	0.0425	0.328
21-22	3.21	3.16	41.5	8.67	0.0000	0.0162	0.343
22-23	1.32	2.77	12.7	8.30	0.0000	0.0162	0.307
23-24	2.00	2.88	17.8	9.21	0.0045	0.0081	0.299

Absorbance at 254 nm, E4/E6 ratio, total concentrations of Fe, Mn, Pb and Zn in LBB2 porewater

Appendix 9: Results from LT1

Depth (cm)	% moisture	%organic	%ash	wet:dry
0.5	78.4	74.4	25.6	4.62
1.5	72.1	75.8	24.2	3.59
2.5	71.1	77.8	22.2	3.45
3.5	69.8	77.7	22.3	3.31
4.5	67.4	78.8	21.2	3.07
5.5	68.2	78.6	21.4	3.14
6.5	69.7	77.3	22.7	3.30
7.5	66.0	79.0	21.0	2.94
8.5	67.4	78.5	21.5	3.07
9.5	67.9	78.5	21.5	3.12
10.5	67.2	78.2	21.8	3.05
11.5	65.7	78.7	21.3	2.92
12.5	71.2	77.1	22.9	3.48
13.5	66.2	79.2	20.8	2.96
14.5	61.6	81.7	18.3	2.60
15.5	62.6	81.3	18.7	2.67
16.5	66.5	78.9	21.1	2.98
17.5	63.4	80.8	19.2	2.73
18.5	61.5	80.8	19.2	2.60

Water content of sediment, organic matter, ash content and wet:dry ratio in LT1

Depth (cm)	rrdFe mg/kg	tsdFe mg/kg	rrd Fe /%	rrd Mn mg/kg	tsd Mn mg/kg	rrd Mn /%	Mn/Fe
0-1	1187.8	96620.3	1.23	4026.0	16783.6	5.4	0.17
1-2	1093.5	81203.7	1.35	2799.7	5414.3	16.8	0.07
2-3	984.3	72081.8	1.37	2671.0	3926.8	17.8	0.05
3-4	968.5	73046.0	1.33	2572.3	3204.5	18.5	0.04
4-5	938.6	67558.1	1.39	2389.9	2700.3	22.3	0.04
5-6	949.7	66954.5	1.42	2386.4	2304.8	34.5	0.03
6-7	918.9	69364.7	1.32	2154.5	1988.9	26.2	0.03
7-8	1169.8	62355.3	1.88	1911.9	1999.1	41.0	0.03
8-9	963.4	65606.1	1.47	2277.7	2327.1	26.4	0.04
9-10	915.2	64869.6	1.41	2131.7	2085.8	23.9	0.03
10-11	1113.8	67942.8	1.64	1760.3	1961.0	35.0	0.03
11-12	1443.4	63103.6	2.29	1730.2	2479.3	21.9	0.04
12-13	2238.0	67325.0	3.32	1954.9	1771.8	43.7	0.03
13-14	2157.3	61947.4	3.48	1888.1	1988.2	37.5	0.03
14-15	1776.3	57855.7	3.07	2009.6	1792.1	36.4	0.03
15-16	1882.7	56695.4	3.32	2281.0	1458.7	64.5	0.03
16-17	2083.2	60405.7	3.45	1672.4	1859.9	30.3	0.03
17-18	2157.5	50391.0	4.28	1735.5	1522.2	61.4	0.03
18-19	2397.3	56411.6	4.25	1214.7	2210.0	30.9	0.04

Readily reducible Fe, pseudo-total Fe, readily reducible Fe expressed as % total, readily reducible Mn, pseudo-total Mn, readily reducible Mn expressed as % total and Mn/Fe ratio for LT1

Depth (cm)	rrdPb mg/kg	tsdPb mg/kg	rrd Pb /%	rrd Cu mg/kg	tsd Cu mg/kg	rrd Cu /%	rrd Zn mg/kg	tsd zn	rrd Zn / %
0-1	114.0	412.5	27.6	29.6	115.8	25.5	82.0	171.1	22.5
1-2	105.5	446.1	23.7	25.6	89.9	28.5	63.3	170.3	16.9
2-3	86.4	374.9	23.0	22.9	97.3	23.6	50.6	181.5	13.5
3-4	81.5	371.9	21.9	24.0	95.2	25.2	72.3	161.7	19.3
4-5	98.2	372.4	26.4	24.0	98.7	24.3	89.9	178.2	22.4
5-6	91.9	378.9	24.3	25.7	103.3	24.8	81.7	165.5	23.5
6-7	100.5	400.8	25.1	19.2	90.9	21.1	139.8	169.3	37.8
7-8	110.4	328.5	33.6	25.9	91.2	28.4	120.2	208.9	33.8
8-9	120.6	423.3	28.5	22.4	100.6	22.3	118.9	190.0	26.2
9-10	102.0	409.4	24.9	15.1	85.9	17.6	97.4	179.3	20.9
10-11	115.8	410.5	28.2	16.5	101.6	16.2	131.3	168.3	25.5
11-12	123.9	404.9	30.6	28.0	103.0	27.2	125.8	186.4	19.3
12-13	178.9	469.9	38.1	25.9	99.3	26.0	216.0	187.5	47.6
13-14	186.4	424.3	43.9	25.1	88.4	28.4	207.8	100.6	39.0
14-15	182.8	362.9	50.4	23.4	92.3	25.3	208.2	190.8	47.2
15-16	175.8	391.7	44.9	22.6	95.1	23.8	205.4	190.9	56.7
16-17	203.2	456.4	44.5	23.5	80.7	29.1	162.2	186.9	35.1
17-18	237.1	362.5	65.4	23.5	76.9	30.6	236.5	189.7	63.3
18-19	262.0	420.5	62.3	25.5	96.3	26.5	222.8	192.6	40.0

Readily reducible Pb, pseudo-total Pb, readily reducible Pb expressed as % total, readily reducible Cu, pseudo-total Cu, readily reducible Cu expressed as % total and pseudo-total Zn for LT1

Depth	Al mg/	Ca mg/	Co mg/	K mg/	Mg	Na	P mg/	S mg/kg	Si mg/
1	28355.1	8342.6	50.4	3553.9	8536.6	159.1	1615.3	1889.0	86.2
2	30086.7	4909.2	44.5	3535.5	8416.5	129.6	1710.1	1792.1	123.5
3	31240.8	4998.5	39.9	3915.4	8726.9	147.7	1659.4	1556.3	170.4
4	32548.8	4794.2	37.1	4645.8	9353.2	174.1	1671.9	1582.9	159.4
5	32559.6	4875.1	42.1	4581.0	9257.5	165.2	1609.4	1557.1	404.5
6	33227.5	4469.2	38.7	4904.4	8900.3	173.6	1628.6	1539.4	260.7
7	35916.5	4831.4	40.5	5519.2	9615.6	204.0	1631.6	1774.5	139.1
8	32846.2	4707.6	38.1	4931.7	8638.2	174.0	1499.8	1615.4	69.6
9	32590.8	4442.8	43.0	4765.0	8915.6	179.8	1694.0	1822.8	231.5
10	34414.5	4783.7	40.8	5087.5	9022.0	207.0	1647.5	1810.1	73.2
11	35327.9	4796.0	38.0	5525.3	9714.5	211.4	1714.8	1776.3	335.8
12	33939.3	5095.2	46.0	5072.3	9584.2	197.3	1647.5	1720.1	366.6
13	35399.3	4483.9	33.6	4974.5	9447.8	178.1	1697.6	1791.2	217.0
14	34378.3	4993.4	34.3	4539.5	9654.7	177.0	1584.7	1563.6	123.5
15	33394.2	4824.2	37.0	4583.2	9327.0	163.8	1456.5	1518.1	112.5
16	31359.2	4671.5	30.4	3984.6	9221.1	143.1	1407.9	1312.6	95.8
17	32521.9	5137.6	37.7	3609.0	9742.9	137.2	1481.7	1679.3	89.0
18	26055.9	4317.7	30.8	2958.9	8488.6	126.4	1225.5	1357.5	44.1
19	26781.8	3842.4	44.5	3814.9	8092.0	149.0	1728.6	2036.4	577.1

Pseudo-total concentrations of additional elements in sediment from core LT1

Depth /cm	@254	E4/E6
0.1	0.221	1.08
0.3	0.202	1.07
0.5	0.212	1.04
0.7	0.211	1.08
0.9	0.22	1.08
1.1	0.277	1.06
1.3	0.209	1.07
1.5	0.217	1.08
1.7	0.315	1.07
1.9	0.276	1.05
2.1	0.269	1.05
2.3	0.317	1.15
2.5	0.197	1.05
2.7	0.255	1.05
2.9	0.207	1.06
3.5	0.173	1.07
4.5	0.159	1.06
5.5	0.144	1.06
6.5	0.143	1.04
7.5	0.143	1.06
8.5	0.15	1.05
9.5	0.143	1.06
10.5	0.138	1.06
11.5	0.133	1.03
12.5	0.125	1.04
13.5	0.122	1.04
14.5	0.115	1.03
15.5	0.109	1.03
16.5	0.113	1.03
17.5	0.113	1.03
18.5	0.116	1.03
19.5	0.121	1.03
20.5	0.14	1.04

Absorbance at 254 nm, E4/E6 ratio,of porewater for core LT1

Appendix 10: Results from LT2

Depth (cm)	%moisture	%organic	%ash	wet:dry
0.5	78.9	73.0	27.0	4.74
1.5	73.9	75.5	24.5	3.84
2.5	70.7	77.3	22.7	3.41
3.5	71.8	76.0	24.0	3.54
4.5	66.5	78.1	21.9	2.98
5.5	67.1	77.5	22.5	3.04
6.5	67.0	77.5	22.5	3.03
7.5	0.0	0.0	0.0	3.24
8.5	64.7	78.1	21.9	2.84
9.5	68.2	75.7	24.3	3.14
10.5	67.5	78.2	21.8	3.08
11.5	68.8	76.7	23.3	3.21
12.5	66.1	77.8	22.2	2.95
13.5	67.4	79.2	20.8	3.07
14.5	64.3	78.2	21.8	2.80
15.5	62.8	81.1	18.9	2.68
16.5	67.9	80.4	19.6	3.11
17.5	0.0	0.0	0.0	
18.5	68.2	79.7	20.3	3.14
19.5	66.2	81.6	18.4	2.96
20.5	65.7	79.2	20.8	2.92
21.5	66.5	79.5	20.5	2.99
22.5	65.3	79.6	20.4	2.88

Water content of sediment, organic matter, ash content and wet:dry ratio in LT2

Depth (cm)	rrdFe mg/ kg	tsdFe mg/ kg	rrd Fe /%	rrd Mn mg/kg	tsd Mn mg/kg	rrd Mn /%	Mn/Fe
0-1	106.0	88971.4	0.12	9.0	12974.5	0.1	0.15
1-2	34689.3	70049.4	49.52	933.2	3143.3	29.7	0.04
2-3	3915.2	62914.6	6.22	15324.2	2895.2	100.0	0.05
3-4	2301.0	70607.5	3.26	2657.1	3186.1	83.4	0.05
4-5	2053.0	64228.9	3.20	1766.5	2270.6	77.8	0.04
5-6	1428.3	58522.4	2.44	1383.0	2527.8	54.7	0.04
6-7	1327.5	63204.4	2.10	1030.2	2423.7	42.5	0.04
7-8	1394.1	64163.8	2.17	1075.1	2027.1	53.0	0.03
8-9	1280.7	60054.3	2.13	854.4	1811.0	47.2	0.03
9-10	1751.4	62127.9	2.82	1209.9	2322.9	52.1	0.04
10-11	1257.9	60780.4	2.07	790.5	1730.0	45.7	0.03
11-12	2338.5	60570.6	3.86	1374.8	1673.2	82.2	0.03
12-13	1096.8	57115.7	1.92	521.6	2215.6	23.5	0.04
13-14	1032.8	57322.4	1.80	552.8	1492.0	37.0	0.03
14-15	1284.3	54511.9	2.36	778.3	2007.2	38.8	0.04
15-16	1132.3	51726.1	2.19	531.4	1716.6	31.0	0.03
16-17	1278.1	51010.3	2.51	826.0	1612.7	51.2	0.03
17-18	3709.4	45698.0	8.12	977.5	2005.1	48.8	0.04
18-19	1424.3	50333.1	2.83	696.2	1372.2	50.7	0.03
19-20	1523.1	47423.8	3.21	1082.8	1102.8	98.2	0.02
20-21	1049.7	48170.1	2.18	490.4	1331.4	36.8	0.03
21-22	1179.1	48799.5	2.42	435.5	1023.4	42.6	0.02
22-23	1094.8	49737.6	2.20	551.4	1274.8	43.3	0.03

Readily reducible Fe, pseudo-total Fe, readily reducible Fe expressed as % total, readily reducible Mn, pseudo-total Mn, readily reducible Mn expressed as % total and Mn/Fe ratio for LT2

Depth (cm)	rrd Pb mg/kg	tsd Pb mg/kg	rrd Pb %	rrd Cu mg/kg	tsd Cu mg/kg	rrd Cu /%	rrd Zn mg/kg	tsd zn mg/kg	rrd Zn %
0-0.2	1.5	398.0	0.4	3.8	85.2	4.5	14.2	426.5	3.3
0.2-0.4	180.3	328.2	54.9	194.3	87.6	0.0	257.6	356.3	72.3
0.4-0.6	89.7	333.7	26.9	21.2	92.3	22.9	276.9	388.7	71.2
0.6-0.8	121.6	407.6	29.8	22.4	95.3	23.6	105.3	454.0	23.2
0.8-1.0	108.7	350.6	31.0	22.5	88.0	25.6	122.7	369.7	33.2
1.0-1.2	130.6	349.2	37.4	19.5	74.9	26.1	73.1	377.7	19.3
1.2-1.4	127.7	363.5	35.1	19.2	85.9	22.4	131.4	397.2	33.1
1.4-1.6	131.9	395.1	33.4	17.0	89.2	19.1	108.2	376.8	28.7
1.6-1.8	109.3	364.4	30.0	15.7	81.5	19.3	81.9	380.8	21.5
1.8-2.0	149.8	390.9	38.3	26.0	93.3	27.9	70.2	522.1	13.5
2.0-2.2	149.6	385.9	38.8	18.8	70.7	26.6	88.0	445.4	19.7
2.2-2.4	144.3	402.2	35.9	20.7	76.7	27.0	207.9	497.0	41.8
2.4-2.6	141.0	423.9	33.3	17.4	91.4	19.0	76.6	575.0	13.3
2.6-2.8	142.9	362.7	39.4	15.8	81.0	19.5	138.7	432.6	32.1
2.8-3.0	135.2	381.7	35.4	15.0	87.2	17.2	139.5	526.1	26.5
3.0-4.0	129.3	349.3	37.0	17.5	95.7	18.3	94.5	432.3	21.9
4.0-5.0	160.8	378.9	42.4	19.7	90.0	21.9	147.4	432.6	34.1
5.0-6.0	165.2	349.2	47.3	27.6	78.4	35.2	255.6	492.9	51.8
6.0-7.0	145.3	379.9	38.2	22.0	66.8	32.9	164.2	398.0	41.3
7.0-8.0	173.6	349.9	49.6	22.3	74.3	30.1	275.6	310.4	88.8
8.0-9.0	158.4	387.1	40.9	15.9	79.3	20.1	143.7	443.5	32.4
9.0-10.0	154.9	424.1	36.5	18.2	76.8	23.6	96.9	329.6	29.4
10.0-11.0	180.6	457.3	39.5	15.9	83.9	18.9	158.2	388.7	40.7

Readily reducible Pb, pseudo-total Pb, readily reducible Pb as % total, readily reducible Cu, pseudo-total Cu, readily reducible Cu expressed as % total, readily reducible Zn, pseudo-total Zn, readily reducible Zn expressed as % total for LT2

Depth cm	Al mg/ kg	Ca mg/ kg	Co mg/ kg	K mg/ kg	Mg mg/kg	Na mg/kg	P mg/ kg	S mg/kg	Si mg/ kg
0-1	18652.4	5492.9	42.1	2274.8	6125.0	105.7	1575.2	1951.6	500.5
1-2	19673.6	3230.9	33.1	2457.0	6405.1	108.4	1607.2	1554.4	563.8
2-3	21511.3	3378.2	30.3	2540.9	6955.2	105.7	1682.4	1476.8	432.3
3-4	26232.4	3408.6	39.8	4039.6	8223.1	143.2	1852.8	1762.7	584.6
4-5	25610.3	2896.4	39.5	4082.9	8160.7	139.8	1614.1	1597.6	565.6
5-6	24477.2	3173.9	44.5	3510.3	7660.0	121.0	1609.8	1734.6	434.2
6-7	27708.5	3067.3	38.3	4672.5	8588.9	166.2	1692.7	1708.7	575.0
7-8	27824.4	2829.6	36.2	4391.1	8457.4	151.8	1703.3	1567.5	448.0
8-9	25996.8	2822.6	35.2	4056.3	8079.0	146.3	1630.3	1714.5	518.9
9-10	27084.0	3000.9	44.8	4277.5	8089.6	145.9	1732.4	1974.7	430.0
10-11	27157.2	2638.1	34.5	4223.6	8273.9	148.7	1716.1	1671.8	600.8
11-12	26565.2	2845.7	38.4	4208.5	8025.8	146.2	1690.3	1965.7	480.2
12-13	24677.2	3347.6	36.1	3710.7	7457.5	141.0	1912.0	1725.3	601.5
13-14	25169.8	2590.5	30.1	3749.2	7922.0	133.5	1641.1	1453.7	615.8
14-15	24893.3	2880.4	41.8	3603.8	7993.3	130.9	1559.6	1665.8	610.7
15-16	22493.6	2789.8	33.9	2954.7	7336.4	105.4	1527.1	1357.6	570.1
16-17	22886.6	2726.4	30.1	3088.3	7601.5	103.7	1485.4	1432.2	485.2
17-18	20650.1	2998.0	35.3	2148.5	7776.0	78.8	1313.5	1479.7	604.7
18-19	22497.9	2658.3	32.2	3152.9	7276.9	114.0	1436.1	1765.5	500.0
19-20	21272.9	2707.7	24.4	2879.2	7084.1	114.4	1380.7	1561.2	593.0
20-21	21733.3	2846.9	30.1	2862.4	7155.9	129.8	1419.1	1900.2	656.8
21-22	21407.4	2556.2	28.0	2971.4	7272.8	117.8	1387.3	1832.9	519.1
22-23	21743.7	2853.5	31.3	2429.7	7460.6	104.3	1444.9	2048.8	514.3

Pseudo-total concentrations of additional elements in sediment from core LT2

Depth /cm	@254	E4/E6	Fe mg/l	Mn mg/l	Cu mg/l	Pb mg/l	Zn mg/l
0.1	0.18	1.01	2.235	1.939	0.025	0.032	0.044
0.3	0.173	1.01	12.97	6.176	0.038	0.047	0.231
0.5	0.203	1.01	5.71	5.384	0.034	0.034	0.148
0.7	0.19	1.01	13.34	9.628	0.041	0.048	0.222
0.9	0.173	1.00	3.754	11.74	0.037	0.034	0.323
1.1	0.171	1.01	4.215	11.11	0.043	0.053	0.253
1.3	0.15	0.99	6.764	11.34	0.039	0.041	0.26
1.5	0.155	1.00	7.025	10.37	0.043	0.042	0.307
1.7	0.145	1.00	17.94	8.745	0.052	0.067	0.265
1.9	0.142	1.00	22.78	8.834	0.07	0.127	0.438
2.1	0.133	0.99	6.98	10.59	0.042	0.07	0.425
2.3	0.234	1.02	3.911	17	0.032	0.026	0.769
2.5	0.133	0.99	4.936	9.343	0.034	0.043	0.454
2.7	0.133	0.99	0.915	10.35	0.031	0.047	0.469
2.9	0.141	0.99	8.793	7.433	0.086	0.073	0.455
3.5	0.098	0.97	10.42	6.075	0.049	0.092	0.255
4.5	0.085	0.97	7.097	6.738	0.049	0.08	0.345
5.5	0.083	0.97	6.975	6.544	0.046	0.075	0.383
6.5	0.086	0.97	4.998	11.47	0.033	0.047	0.621
7.5	0.105	0.99	5.39	9.426	0.036	0.033	0.48
8.5	0.103	0.97	3.708	7.582	0.04	0.052	0.537
9.5	0.115	0.98	2.101	11.13	0.035	0.042	0.745
10.5	0.122	0.98	2.856	9.834	0.037	0.062	0.654

Absorbance at 254 nm, E4/E6 ratio, Fe, Mn, Pb, Cu and Zn concentrations in porewater for core LT2

Appendix 11: Results from LT3

Depth (cm)	%moisture	%org	%ash	wet:dry
0.5	80.1	78.9	21.1	5.03
1.5	73.7	77.2	22.8	3.80
2.5	70.5	79.6	20.4	3.39
3.5	73.3	76.2	23.8	3.75
4.5	68.5	80.4	19.6	3.17
5.5	71.1	77.6	22.4	3.46
6.5	70.5	77.3	22.7	3.39
7.5	66.6	79.7	20.3	2.99
8.5	63.3	82.5	17.5	2.73
9.5	66.4	80.4	19.6	2.97
10.5	71.4	76.9	23.1	3.50
11.5	63.5	82.0	18.0	2.74
12.5	69.5	77.5	22.5	3.28
13.5	66.5	80.3	19.7	2.98
14.5	62.1	82.8	17.2	2.64
15.5	65.6	79.9	20.1	2.91
16.5	69.3	78.5	21.5	3.26
17.5	71.8	77.3	22.7	3.55
18.5	66.1	79.8	20.2	2.95
19.5	68.1	78.4	21.6	3.14
20.5	66.5	78.5	21.5	2.98
21.5	63.8	78.4	21.6	2.76
22.5	62.4	78.3	21.7	2.66
23.5	61.8	78.6	21.4	2.62
24.5	65.0	79.9	20.1	2.85

Water content of sediment,

Depth cm	rrdFe mg/kg	tsdFe mg/kg	rrd Fe /%	rrd Mn mg/kg	tsd Mn mg/kg	rrd Mn /%	Mn/Fe
0-1	3977.0	90656.6	4.39	12732.1	19080.8	66.7	0.21
1-2	1970.0	80495.3	2.45	3532.5	5375.0	65.7	0.07
2-3	1554.5	70816.8	2.20	2180.6	3537.1	61.6	0.05
3-4	1065.1	70865.4	1.50	1346.6	3227.9	41.7	0.05
4-5	1056.1	68455.9	1.54	752.0	3149.5	23.9	0.05
5-6	894.6	66542.1	1.34	623.3	3210.3	19.4	0.05
6-7	1447.5	71793.5	2.02	562.0	3258.2	17.2	0.05
7-8	1076.8	63061.2	1.71	511.8	2727.0	18.8	0.04
8-9	1031.0	57825.0	1.78	522.8	2386.0	21.9	0.04
9-10	1169.4	64005.1	1.83	533.3	2770.4	19.3	0.04
10-11	1288.0	59567.3	2.16	670.6	2620.2	25.6	0.04
11-12	1233.6	61067.7	2.02	623.3	2398.7	26.0	0.04
12-13	1084.2	67424.2	1.61	467.6	2896.5	16.1	0.04
13-14	1262.9	63324.7	1.99	546.1	2587.6	21.1	0.04
14-15	951.3	54823.2	1.74	424.0	2087.6	20.3	0.04
15-16	952.4	55544.6	1.71	377.9	2293.6	16.5	0.04
16-17	1283.4	52371.1	2.45	659.7	1733.5	38.1	0.03
17-18	926.4	59519.2	1.56	479.0	2003.8	23.9	0.03
18-19	889.4	51949.5	1.71	627.3	1988.1	31.6	0.04
19-20	3553.0	52244.9	6.80	19502.5	1555.6	100.0	0.03
20-21	1694.0	52990.2	3.20	2201.3	2303.7	95.6	0.04
21-22	1243.7	54891.3	2.27	1128.4	1504.9	75.0	0.03
22-23	993.3	49117.6	2.02	1034.8	1986.0	52.1	0.04
23-24	1157.0	48494.9	2.39	897.1	1445.9	62.0	0.03

Readily reducible Fe, pseudo-total Fe, readily reducible Fe expressed as % total, readily reducible Mn, pseudo-total Mn, readily reducible Mn expressed as % total and Mn/Fe ratio for LT3

Depth (cm)	rrdPb mg/kg	tsdPb mg/kg	rrd Pb /%	rrd Cu mg/kg	tsd Cu mg/kg	rrd Cu /%	rrd Zn mg/kg	tsd zn	rrd Zn / %
0-1	76.6	363.4	21.1	56.0	50.0	112.0	107.6	306.1	35.1
1-2	101.6	341.5	29.8	19.3	68.7	28.0	118.1	376.2	31.4
2-3	112.2	313.1	35.8	19.5	67.4	29.0	131.3	381.4	34.4
3-4	108.3	315.0	34.4	13.6	55.9	24.4	68.5	363.4	18.8
4-5	92.3	314.5	29.4	16.1	68.7	23.5	94.0	392.4	23.9
5-6	90.7	354.2	25.6	13.4	73.5	18.2	85.6	434.3	19.7
6-7	93.4	385.9	24.2	16.1	76.6	21.0	80.8	459.2	17.6
7-8	101.5	313.0	32.4	14.8	66.9	22.1	63.7	380.6	16.7
8-9	119.4	277.0	43.1	14.9	68.7	21.7	118.5	376.8	31.5
9-10	107.0	365.8	29.3	14.4	69.9	20.6	121.4	484.7	25.0
10-11	144.2	344.7	41.8	16.7	62.7	26.7	193.5	489.9	39.5
11-12	131.4	336.7	39.0	14.3	66.7	21.5	181.3	469.0	38.7
12-13	124.2	420.2	29.5	15.7	80.7	19.4	105.6	717.4	14.7
13-14	142.0	380.7	37.3	15.2	68.6	22.2	173.2	603.9	28.7
14-15	124.6	281.3	44.3	14.6	62.0	23.5	134.0	483.8	27.7
15-16	122.8	361.9	33.9	16.7	62.9	26.6	120.5	540.3	22.3
16-17	154.5	312.4	49.5	20.9	53.6	38.9	206.7	410.1	50.4
17-18	131.1	358.4	36.6	15.7	73.1	21.5	188.7	443.5	42.5
18-19	128.7	340.6	37.8	15.0	75.2	19.9	159.2	464.0	34.3
19-20	77.8	343.1	22.7	21.9	63.0	34.7	100.4	428.8	23.4
20-21	95.1	371.6	25.6	19.5	69.8	28.0	72.3	534.3	13.5
21-22	79.0	364.4	21.7	17.6	64.3	27.4	90.5	423.4	21.4
22-23	81.1	388.0	20.9	15.5	66.0	23.5	58.2	544.6	10.7
23-24	114.1	389.3	29.3	28.2	64.4	43.7	80.3	469.6	17.1

Readily reducible Pb, pseudo-total Pb, readily reducible Pb as % total, readily reducible Cu, pseudo-total Cu, readily reducible Cu expressed as % total, readily reducible Zn, pseudo-total Zn, readily reducible Zn expressed as % total for LT3

Depth cm	Al mg/kg	Ca mg/kg	Co mg/kg	K mg/kg	Mg mg/kg	Na mg/kg	P mg/kg	S mg/kg	Si mg/kg
1	22224.7	10767.7	47.4	2674.2	7010.1	174.3	1357.8	1724.2	124.1
2	27500.0	6601.4	41.4	3655.7	8280.7	178.6	1598.6	1678.1	1163.7
3	24299.5	4373.8	37.2	2799.5	8007.4	151.1	1511.6	1516.8	376.5
4	24240.4	3587.5	32.5	3536.5	8995.2	209.8	1413.0	1440.4	97.0
5	29240.2	4303.9	40.3	4531.9	8727.9	196.6	1594.6	1626.7	846.3
6	30210.3	4306.1	50.0	4771.0	8560.7	207.0	1642.8	1913.1	711.9
7	35027.2	4913.0	49.4	6048.9	9317.9	251.6	1776.9	1909.5	1286.1
8	30535.7	4387.8	38.2	5275.5	8778.1	222.8	1490.1	1473.0	335.2
9	28225.0	4550.0	38.7	4570.0	8645.0	217.3	1394.5	1457.0	619.5
10	31709.2	4964.3	43.4	5051.0	8854.6	245.3	1674.7	1905.9	415.1
11	29831.7	4572.1	45.3	4802.9	8209.1	222.0	1511.5	1879.6	810.6
12	30572.9	4737.0	38.3	4867.2	9007.8	219.2	1455.7	1591.9	821.9
13	34899.0	5510.1	49.3	5429.3	9207.1	235.9	1744.2	2382.1	206.5
14	32551.5	5350.5	44.8	4737.1	8982.0	220.5	1584.5	1897.2	391.0
15	26489.9	4643.9	36.2	3843.4	8409.1	213.8	1329.0	1432.8	1519.9
16	28490.1	4804.5	42.8	3618.8	8564.4	178.9	1437.9	1582.4	1648.0
17	27577.3	3863.4	34.5	4141.8	8713.9	185.0	1261.1	1316.8	286.1
18	33365.4	5091.3	33.2	5156.3	9216.3	229.9	1466.3	1331.7	217.3
19	30114.7	5311.9	38.5	4045.9	8949.5	199.8	1357.3	1538.1	662.8
20	28367.3	4808.7	35.6	3247.4	9339.3	173.0	1277.8	1720.2	182.0
21	29485.3	5737.7	45.8	3451.0	9730.4	189.4	1370.1	1750.5	328.9
22	26807.1	4692.9	33.3	3146.7	8823.4	183.1	1348.4	1985.9	997.0
23	27303.9	5254.9	40.7	3289.2	8649.5	260.0	1304.7	1734.6	1536.8
24	26887.8	5137.8	35.3	3127.6	8903.1	171.5	1310.5	1843.6	1330.6

Pseudo-total concentrations of additional elements in sediment from core LT3

Depth cm	Al mg/kg	Ca mg/kg	Co mg/kg	K mg/kg	Mg mg/kg	Na mg/kg	P mg/kg	S mg/kg	Si mg/kg
1	1907.7	4084.2	20.08	427.0	262.2	132.0	94.4	1925.3	603.6
2	1443.8	2336.8	16.78	404.0	245.2	116.1	78.8	1521.3	349.0
3	1545.7	2267.2	11.57	480.6	380.1	114.2	121.1	1497.5	354.8
4	1393.0	1909.1	7.92	640.1	382.3	113.2	176.3	1516.4	334.1
5	1441.3	2051.5	6.71	609.9	363.5	107.8	145.6	1495.4	322.4
6	1278.9	2019.6	6.00	675.7	432.8	114.5	140.4	1401.0	297.8
7	1626.5	1924.5	5.74	728.2	590.4	118.3	157.0	1809.6	384.1
8	1533.4	1668.4	4.32	741.3	526.1	127.9	196.6	1575.8	401.3
9	1605.0	2098.0	5.63	735.3	482.8	109.6	157.9	1959.5	358.5
10	1548.2	1907.1	6.84	739.6	496.0	111.7	132.6	1856.8	346.5
11	1745.6	2538.0	7.89	771.9	501.3	106.5	163.3	1995.6	396.1
12	1650.7	2393.1	6.69	658.6	467.9	100.5	156.7	1925.2	378.7
13	1382.4	1674.8	4.88	616.6	391.1	104.5	118.9	1781.9	297.5
14	1668.7	2150.8	5.42	654.2	448.4	124.9	135.8	1705.8	367.1
15	1359.6	1842.2	4.67	618.2	380.1	115.5	139.4	1512.1	307.8
16	1246.7	1659.0	4.17	422.9	290.0	100.7	117.2	1229.5	259.0
17	1673.2	2158.4	6.61	470.0	359.7	110.7	130.2	1871.3	348.9
18	1187.1	2168.6	5.55	290.0	332.4	109.0	110.3	1455.7	225.4
19	1427.8	2545.5	5.76	572.2	465.4	121.9	195.5	2126.0	310.4
20	1716.7	4603.5	27.85	443.2	268.4	149.3	56.4	2165.2	819.9
21	1715.1	3216.1	4.79	574.7	331.8	176.9	147.3	2005.7	567.2
22	1304.2	2546.8	4.24	429.5	262.8	241.8	104.1	1721.1	367.9
23	1473.2	2560.6	2.89	758.8	433.8	192.1	194.9	2264.7	397.7
24	1650.0	2919.3	5.16	831.5	535.4	227.8	255.9	2763.0	398.4

R

Depth cm	@254	E4/E6	Fe mg/l	Mn mg/l	Pb mg/l	Cu mg/l	Zn mg/l
0-1	1.75	1.36	13.8	0.53	N/A	0.017	0.055
1-2	2.04	1.33	15.3	0.60	N/A	0.017	0.067
2-3	3.39	1.53	31.6	3.04	0.042	0.048	0.144
3-4	7.01	1.55	53.5	4.05	0.176	0.087	0.200
4-5	4.08	1.58	36.7	3.98	0.128	0.059	0.142
5-6	3.46	1.52	28.2	6.07	0.112	0.049	0.199
6-7	4.83	1.51	35.9	4.78	0.211	0.066	0.194
7-8	4.19	1.61	32.1	2.84	0.198	0.069	0.194
8-9	9.83	1.64	66.4	5.14	0.475	0.161	0.419
9-10	7.03	1.51	44.5	3.29	0.296	0.106	0.274
10-11	6.23	1.54	38.5	3.23	0.253	0.098	0.301
11-12	6.19	1.56	39.3	2.87	0.274	0.113	0.327
12-13	5.65	1.58	34.2	2.45	0.265	0.104	0.338
13-14	5.78	1.62	34.6	2.89	0.315	0.103	0.390
14-15	6.33	1.52	36.3	2.92	0.328	0.116	0.338
15-16	5.04	1.52	29.6	2.54	0.217	0.099	0.318
16-17	4.46	1.46	28.8	2.55	0.214	0.083	0.172
17-18	7.11	1.52	56.1	4.17	0.410	0.181	0.350
18-19	6.84	1.47	41.1	2.80	0.267	0.145	0.285
19-20	5.08	1.48	32.2	1.51	0.196	0.109	0.244
20-21	5.04	1.45	26.1	1.94	0.188	0.105	0.221
21-22	3.86	1.43	20.2	1.61	0.128	0.085	0.170
22-23	4.31	1.46	21.7	1.40	0.124	0.087	0.198
23-24	3.45	1.52	16.2	1.85	0.140	0.071	0.189

Absorbance at 254 nm, E4/E6 ratio, Fe, Mn, Pb, Cu and Zn concentrations in porewater for core LT3

Depth (cm)	Al mg/l	Ca mg/l	K mg/l	Mg mg/l	Na mg/l	P mg/l	S mg/l	Si mg/l
0-1	0.54	4.03	0.24	0.63	2.20	0.14	1.26	3.24
1-2	0.90	4.01	0.00	0.49	2.14	0.22	3.40	3.11
2-3	2.17	3.83	0.65	0.41	2.23	0.55	6.47	3.72
3-4	4.64	3.92	1.15	0.47	2.29	1.13	5.31	4.80
4-5	2.95	4.54	1.07	0.51	2.34	0.76	8.59	4.44
5-6	2.95	4.72	0.83	0.60	2.24	0.71	11.10	2.36
6-7	4.44	3.83	0.43	0.57	1.84	0.96	9.14	2.78
7-8	4.33	3.06	0.13	0.50	1.63	0.90	5.61	3.45
8-9	9.75	4.61	0.28	0.77	1.70	1.95	6.10	4.19
9-10	6.61	2.78	0.22	0.42	1.58	1.42	3.17	2.73
10-11	5.58	3.00	0.76	0.48	1.82	1.31	2.94	1.94
11-12	6.04	2.58	0.58	0.44	1.55	1.32	3.35	3.00
12-13	5.35	2.28	0.69	0.49	1.52	1.21	3.12	3.75
13-14	5.72	2.65	0.65	0.46	1.52	1.27	2.89	2.86
14-15	5.63	2.67	1.12	0.50	1.59	1.29	2.64	4.09
15-16	4.77	3.14	1.13	0.47	1.58	1.09	2.48	3.58
16-17	4.06	2.64	1.28	0.42	1.94	0.93	2.37	4.58
17-18	8.43	3.93	0.69	0.56	1.77	1.86	3.34	4.52
18-19	6.47	3.29	1.02	0.66	1.76	1.39	3.33	6.16
19-20	4.41	2.95	0.54	0.40	1.51	1.12	3.19	4.20
20-21	3.93	2.64	0.41	0.38	1.49	0.97	2.61	3.80
21-22	2.98	2.44	0.30	0.29	1.55	0.81	2.57	3.00
22-23	3.58	2.41	0.81	0.32	1.50	0.92	2.61	2.88
23-24	2.80	2.38	0.74	0.27	1.41	0.72	2.44	3.05

Total concentrations of additional elements in porewater from core LT3

Appendix 12: Results from LT4

Depth	%moisture	%org	%ash	wet:dry
0.1	88.6	77.8	22.2	8.75
0.3	87.7	76.9	23.1	8.15
0.5	84.3	76.2	23.8	6.39
0.7	86.6	69.7	30.3	7.45
0.9	86.4	69.8	30.2	7.36
1.1	85.9	70.5	29.5	7.09
1.3	84.1	67.4	32.6	6.29
1.5	82.5	73.6	26.4	5.72
1.7	79.7	76.1	23.9	4.92
1.9	79.6	74.9	25.1	4.91
2.1	79.9	75.6	24.4	4.99
2.6	82.3	75.7	24.3	5.65
2.8	81.6	76.3	23.7	5.43

Water content of sediment, organic matter, ash content and wet:dry ratio in LT4

Depth cm	tsdFe mg/	tsd Mn	tsd Pb	tsd Cu	tsd Zm
0-1	90499.0	30583.9	405.7	88.3	374.6
1-2	85927.1	27039.6	425.2	103.7	369.1
2-3	92309.6	18127.6	429.9	103.7	360.8
3-4	96816.1	10122.5	444.8	108.8	365.4
4-5	104110.3	5795.9	478.1	108.0	358.9
5-6	91256.8	4803.9	437.0	100.4	356.7
6-7	80717.7	4003.2	422.7	93.7	392.0
7-8	84089.1	3996.1	442.6	102.6	400.4
8-9	74756.4	3309.3	405.3	88.9	392.8
9-10	72296.4	3048.0	383.4	92.1	386.4
10-11	58427.6	2414.9	330.6	81.0	340.1
11-12	76435.8	3203.3	383.1	110.9	447.7
12-13	71434.0	2774.9	383.4	100.3	413.4

Pseudo-total concentrations of Fe, Mn, Pb, Cu and Zn in sediment from core LT4

Depth cm	tsd Al mg/kg	tsd Ca mg/kg	tsd Co mg/kg	tsd K mg/kg	tsd Mg mg/kg	tsd Na mg/kg	tsd P mg/kg	tsd S mg/kg	tsd Si mg/kg
0-1	27360.5	10877.0	62.2	3244.8	8362.4	146.3	1652.0	2138.4	0.0
1-2	25979.8	8737.5	56.4	3084.0	7974.9	135.4	1660.6	2024.9	0.0
2-3	26295.8	7319.9	51.3	3053.7	7986.0	136.6	1621.9	1876.4	0.0
3-4	28659.0	6590.7	49.0	3949.8	7851.4	169.7	1629.3	1858.5	55.6
4-5	29338.9	5967.3	44.5	4095.3	8652.4	160.1	1676.8	1755.1	267.5
5-6	31527.7	6076.6	42.9	4439.9	8711.1	167.5	1649.2	1641.5	84.0
6-7	31908.0	5149.5	41.7	4763.6	8651.7	170.4	1694.7	1780.7	143.9
7-8	31124.6	4739.9	42.3	4705.6	9192.3	178.4	1803.9	1772.0	362.7
8-9	30226.1	4705.6	36.3	4316.8	9184.2	165.9	1664.3	1597.0	164.0
9-10	34169.1	5406.7	36.8	5223.7	9591.1	190.3	1653.3	1585.9	386.7
10-11	28942.5	4300.7	31.1	4386.6	8226.0	173.2	1442.1	1361.9	295.1
11-12	38595.5	5653.9	41.3	6078.4	10359.8	215.2	1864.9	1628.2	531.0
12-13	30218.1	4478.0	32.5	4302.3	8841.4	165.2	1764.0	1566.2	208.9

Pseudo-total concentrations of additional elements in sediment from core LT4

Depth cm	@254	E4/E6
0.1	0.18	1.03
0.3	0.25	1.11
0.5	0.86	1.77
0.7	1.15	2.08
0.9	1.47	2.36
1.1	0.84	1.76
1.3	0.18	1.08
1.5	0.11	1.00
1.7	0.18	1.10
2	0.12	1.04
2.5	0.14	1.03
2.9	0.15	1.04

Absorbance at 254 nm, E4/E6 ratiofor porewater from core LT4

Appendix 13: Results from LT3 porewater ultrafiltration

Depth ./ cm	Fe mg/l	Mn mg/l	Pb mg/l	Cu mg/l	Zn mg/l
0-1	13.9	0.55	0.016	0.058	0.023
1-2	19.6	0.52	0.068	0.020	N/A
2-3	33.9	2.23	0.166	0.052	0.028
3-4	49.1	2.90	0.166	0.088	0.082
4-5	28.1	2.19	0.180	0.050	N/A
5-6	23.9	1.27	0.182	0.045	0.008
6-7	28.4	1.52	0.205	0.065	0.025
7-8	25.7	2.20	0.163	0.065	0.046
8-9	58.5	3.83	0.456	0.135	0.223
9-10	39.5	2.69	0.347	0.090	0.079
10-11	34.9	2.73	0.369	0.093	0.018
11-12	34.1	1.89	0.273	0.095	0.083
12-13	28.2	2.01	0.272	0.095	0.103
13-14	26.9	2.08	0.370	0.079	0.104
14-15	31.7	2.29	0.302	0.100	0.142
15-16	19.6	0.58	N/A	0.080	N/A
16-17	20.5	1.55	0.152	0.058	N/A
17-18	48.9	2.52	0.320	0.144	0.036
18-19	30.1	1.40	0.210	0.107	N/A
19-20	24.9	0.74	0.073	0.142	N/A
20-21	21.7	1.56	0.141	0.089	0.092
21-22	15.3	0.81	0.002	0.063	N/A
22-23	16.8	0.32	0.053	0.070	N/A
23-24	6.3	0.75	0.001	0.045	0.068

Concentration Fe, Mn, Pb, Cu and Zn in >30 kDA fraction of LT3 porewater

Depth ./ cm	Al mg/l	Ca mg/l	Co mg/l	K mg/l	Mg mg/l	Na mg/l	P mg/l	S mg/l	Si mg/l
0-1	0.54	1.44	0.004	1.53	0.13	1.43	0.32	0.35	0.76
1-2	1.18	1.13	0.006	0.15	0.10	0.88	0.44	0.56	0.84
2-3	2.09	0.98	0.009	0.22	0.11	0.83	0.56	1.21	1.36
3-4	4.37	2.49	0.012	1.32	0.28	2.85	0.94	1.78	2.11
4-5	2.31	0.91	0.008	0.50	0.13	0.83	0.55	0.95	0.89
5-6	2.75	0.71	0.011	0.24	0.22	0.68	0.54	1.08	1.07
6-7	3.83	1.48	0.016	0.37	0.27	0.63	0.73	1.50	1.45
7-8	3.70	1.50	0.013	0.61	0.27	0.84	0.71	1.36	1.42
8-9	9.07	3.84	0.030	0.58	0.50	1.05	1.64	2.49	2.68
9-10	6.13	1.65	0.020	0.46	0.28	0.85	1.14	1.39	1.87
10-11	5.18	1.56	0.023	0.97	0.30	1.78	1.02	1.23	2.12
11-12	5.37	1.33	0.019	0.56	0.29	1.17	1.04	1.36	2.02
12-13	4.58	1.60	0.019	0.20	0.35	2.09	0.93	1.32	2.18
13-14	4.51	1.75	0.017	0.39	0.27	1.31	0.94	1.22	1.95
14-15	5.02	2.12	0.015	0.55	0.35	1.41	1.07	1.26	3.03
15-16	3.18	2.21	0.004	1.10	0.29	1.84	0.50	1.19	2.57
16-17	3.10	2.29	0.016	0.48	0.24	1.20	0.57	0.59	1.80
17-18	7.48	3.74	0.010	N/A	0.48	3.38	1.46	2.01	2.71
18-19	4.74	1.59	0.011	0.17	0.34	1.63	0.98	1.58	2.72
19-20	3.51	2.50	0.010	0.16	0.25	2.14	0.84	1.83	2.61
20-21	3.44	2.01	0.010	0.63	0.27	1.23	0.75	1.24	2.10
21-22	2.32	2.00	N/A	0.21	0.20	1.54	0.52	0.90	1.02
22-23	2.83	1.66	0.007	0.73	0.19	1.67	0.57	1.36	1.87
23-24	1.12	2.92	0.002	0.53	0.18	2.57	0.29	3.56	1.52

Concentration additional elements in >30 kDA fraction of LT3 porewater

Depth ./ cm	Fe mg/l	Mn mg/l	Pb mg/l	Cu mg/l
0-1	0.058	0.009	N/A	0.009
1-2	0.037	0.041	N/A	0.009
2-3	0.039	0.303	N/A	0.008
3-4	0.060	0.375	0.007	0.014
4-5	0.065	0.322	N/A	0.004
5-6	0.056	1.229	0.030	0.009
6-7	0.055	0.785	0.017	0.005
7-8	0.056	0.085	0.030	0.017
8-9	0.065	0.149	N/A	0.006
9-10	0.076	0.100	0.021	0.008
10-11	0.095	0.077	N/A	0.017
11-12	0.077	0.114	N/A	0.006
12-13	0.094	0.048	0.005	0.024
13-14	0.100	0.040	N/A	0.012
14-15	0.121	0.025	N/A	0.014
15-16	0.230	0.002	N/A	0.012
16-17	1.028	0.088	N/A	0.034
17-18	0.272	0.002	N/A	0.022
18-19	0.205	0.167	N/A	0.033
19-20	0.325	0.041	N/A	0.039
20-21	0.483	0.002	N/A	0.021
21-22	0.337	0.000	N/A	0.026
22-23	0.291	0.002	N/A	0.039
23-24	0.089	N/A	N/A	0.027

Concentration Fe, Mn, Pb, Cu and Zn in 30-1 kDA fraction of LT3 porewater

Depth ./ cm	Al mg/l	Ca mg/l	Co mg/l	K mg/l	Mg mg/l	Na mg/l	P mg/l	S mg/l	Si mg/l
0-1	0.015	1.63	0.001	0.85	0.217	3.45	0.030	0.683	1.11
1-2	0.020	1.45	0.001	0.26	0.121	1.21	0.095	1.017	0.70
2-3	0.016	1.53	0.001	3.85	0.167	2.45	0.028	4.094	0.57
3-4	0.039	1.94	0.001	0.44	0.136	2.63	0.024	2.113	1.36
4-5	0.029	1.45	0.001	1.15	0.117	1.35	0.081	2.556	0.79
5-6	0.018	1.39	0.003	1.00	0.128	2.00	0.124	3.227	0.72
6-7	0.043	1.50	0.002	0.36	0.107	2.34	0.080	2.892	0.64
7-8	0.054	1.18	0.001	0.44	0.096	2.08	0.177	2.064	0.65
8-9	0.029	1.08	N/A	0.43	0.084	2.20	0.083	1.270	0.87
9-10	0.073	1.38	N/A	0.81	0.103	2.18	0.143	1.149	1.45
10-11	0.021	1.18	0.004	0.52	0.111	3.46	0.064	1.132	1.35
11-12	0.047	1.14	0.001	0.49	0.072	2.12	0.189	1.214	0.93
12-13	0.067	1.74	N/A	0.87	0.114	4.39	0.509	1.242	1.52
13-14	0.047	1.09	0.003	0.46	0.080	2.39	0.174	0.915	1.10
14-15	0.091	1.21	0.001	1.45	0.114	4.49	0.389	1.770	1.13
15-16	0.158	1.26	N/A	2.16	0.121	5.47	0.665	0.981	3.40
16-17	0.328	1.65	0.003	1.30	0.259	4.10	0.316	0.863	2.47
17-18	0.166	1.59	0.005	9.40	0.405	8.89	0.289	4.579	2.42
18-19	0.179	1.41	0.003	1.25	0.153	3.30	0.640	1.125	1.75
19-20	0.070	1.56	0.013	1.97	0.146	4.33	0.626	1.036	2.40
20-21	0.018	0.70	0.001	0.30	0.065	2.26	0.142	0.727	0.20
21-22	0.086	0.90	0.009	1.36	0.097	3.50	0.290	1.403	1.70
22-23	0.056	0.96	0.000	0.65	0.090	3.17	0.207	1.045	1.46
23-24	0.067	3.04	0.002	1.53	0.303	8.52	6.415	N/A	2.14

Concentration additional elements in 30-1 kDA fraction of LT3 porewater

Depth ./ cm	Fe mg/l	Mn mg/l	Pb mg/l	Cu mg/l	Zn mg/l
0-1	0.096	0.01	N/A	0.009	N/A
1-2	0.057	0.10	N/A	0.011	0.0052
2-3	0.065	0.50	N/A	0.013	0.0005
3-4	0.123	0.50	N/A	0.017	N/A
4-5	0.093	0.82	N/A	0.020	0.0090
5-6	0.068	4.17	N/A	0.015	0.0618
6-7	0.067	1.73	N/A	0.010	0.0108
7-8	0.654	0.11	N/A	0.009	N/A
8-9	0.110	0.44	N/A	0.010	0.0444
9-10	0.089	0.11	N/A	0.004	0.0175
10-11	0.203	0.10	N/A	0.024	N/A
11-12	0.102	0.12	N/A	0.006	N/A
12-13	0.088	0.02	N/A	0.007	N/A
13-14	0.077	0.06	N/A	0.009	N/A
14-15	0.098	0.02	N/A	0.007	N/A
15-16	0.176	N/A	N/A	0.028	N/A
16-17	0.100	0.02	N/A	0.019	N/A
17-18	0.137	0.00	0.010	0.014	N/A
18-19	0.141	0.11	N/A	0.026	N/A
19-20	0.161	0.01	N/A	0.010	N/A
20-21	0.099	0.00	N/A	0.012	N/A
21-22	0.358	0.00	0.015	0.010	N/A
22-23	0.265	0.00	N/A	0.020	N/A
23-24	0.106	0.24	0.143	0.018	N/A

Concentration Fe, Mn, Pb, Cu and Zn in >30 kDA fraction of LT3 porewater

Depth ./ cm	Al mg/l	Ca mg/l	Co mg/l	K mg/l	Mg mg/l	Na mg/l	P mg/l	S mg/l	Si mg/l
0-1	0.053	2.23	N/A	1.32	0.34	5.81	0.05	0.88	1.39
1-2	0.058	2.80	0.001	1.18	0.33	4.43	0.17	1.68	2.94
2-3	0.032	2.06	0.002	8.68	0.32	4.82	0.03	8.32	2.26
3-4	0.044	1.91	N/A	1.34	0.19	4.58	0.02	1.27	2.44
4-5	0.065	2.74	0.001	5.27	0.31	5.46	0.14	7.23	2.80
5-6	0.050	3.54	0.007	4.57	0.41	7.39	0.20	10.62	2.94
6-7	0.063	2.21	0.002	1.52	0.23	6.53	0.09	4.74	2.21
7-8	0.011	1.32	0.002	1.00	0.14	3.67	0.14	1.64	1.46
8-9	0.054	2.31	0.001	1.62	0.23	5.81	0.11	2.93	2.65
9-10	0.020	1.38	N/A	0.96	0.12	3.15	0.07	0.68	1.30
10-11	0.119	1.72	0.003	2.05	0.17	5.23	0.08	0.64	1.90
11-12	0.049	1.25	0.003	0.99	0.11	3.24	0.18	0.63	2.29
12-13	0.022	0.86	N/A	0.39	0.08	2.82	0.13	0.45	1.24
13-14	0.011	1.35	0.002	1.03	0.13	4.99	0.10	0.45	2.29
14-15	0.009	1.01	0.001	2.07	0.13	4.63	0.27	1.30	1.37
15-16	0.039	1.45	N/A	0.58	0.07	1.54	0.04	0.41	1.19
16-17	N/A	0.80	0.003	1.03	0.09	2.68	0.09	0.22	2.02
17-18	0.012	2.72	0.002	2.23	0.16	2.57	0.01	1.00	1.19
18-19	N/A	1.14	N/A	1.37	0.12	3.82	0.17	0.36	1.87
19-20	0.021	2.01	N/A	1.42	0.10	3.58	0.05	0.33	1.48
20-21	0.003	0.51	N/A	0.74	0.07	3.21	0.07	0.39	1.91
21-22	0.009	1.59	N/A	1.31	0.12	4.30	0.05	1.00	1.11
22-23	0.019	2.13	N/A	0.98	0.11	4.62	0.06	0.39	1.86
23-24	N/A	0.92	0.003	0.90	0.11	3.54	N/A	N/A	1.56

Concentration additional elements in <1 kDA fraction of LT3 porewater

Depth ./	Abs at	E4/E6
0-1	1.07	1.64
1-2	1.72	1.76
2-3	3.63	2.23
3-4	18.31	2.44
4-5	3.64	1.60
5-6	4.44	1.59
6-7	3.07	1.63
7-8	5.27	1.80
8-9	2.59	1.56
9-10	6.81	1.90
10-11	3.06	1.68
11-12	1.68	1.56
12-13	3.59	1.63
13-14	1.87	1.50
14-15	2.70	1.63
15-16	0.21	1.68
16-17	0.83	1.95
17-18	0.70	1.94
18-19	6.87	2.20
19-20	0.24	1.64
20-21	7.00	1.85
21-22	0.28	1.56
22-23	0.72	1.81
23-24	1.12	1.98

Absorbance at 254 nm and E4/E6 ratio for >30 kDa fraction of LT3 porewater

Appendix 14: Results from LT surface waters

Sample	Fe mg/l	Pb mg/l	Cu mg/l	Zn mg/l
LTSW1	0.0012	0.0075	0.0008	0.0018
LTSW2	0.0010	0.0029	0.0013	0.0014
LTMW1	0.0016		0.0010	0.0051
LTMW2	0.0011	0.0021	0.0008	0.0038
LTSt 1	0.0008		0.0008	0.0006
LTSt 4	0.0005		0.0008	0.0005
LTst5			0.0010	0.0005
LTst6		0.0042	0.0010	0.0005
Ltst7	0.0028	0.0057	0.0004	0.0006
LTst8	0.0076	0.0100	0.0012	0.0011
LTst9	0.0031	0.0019	0.0014	0.0001
LTst10	0.0119		0.0012	0.0008
LTst11	0.0215	0.0077	0.0002	0.0014
LTst12	0.0195		0.0019	0.0018
LTst13	0.0278	0.0067	0.0003	0.0018
LTst14	0.0129	0.0003	0.0008	0.0014
LTst15	0.0022		0.0003	0.0018
LTst16	0.0008		0.0010	0.0112
LTst18	0.0002		0.0007	0.0019
LTst19	0.0027		0.0007	0.0004
LTst20		0.0021	0.0013	0.0004
LTst21	0.0005		0.0007	0.0005
LTst22		0.0021	0.0003	0.0002
LTst23		0.0047	0.0013	0.0001
LTst24	0.0001	0.0037	0.0006	0.0006
LTst25		0.0083	0.0018	0.0002

Concentrations of Fe, Pb, Cu and Zn in the <100 kDa fraction of surface waters from Loch Tay

Sample	Al mg/l	Ca mg/l	K mg/l	Mg mg/l	Na mg/l	P mg/l	S mg/l	Si mg/l
LTSW1		0.49	0.04	0.10	0.20		0.12	0.07
LTSW2		0.49	0.05	0.10	0.20		0.11	0.07
LTMW1		0.49	0.07	0.09	0.23		0.11	0.07
LTMW2		0.47	0.04	0.09	0.20		0.11	0.07
LTSt 1		2.12	0.08	0.41	0.25	0.0014	0.32	0.25
LTSt 4		2.28	0.12	0.38	0.36		0.34	0.35
LTst5		5.61	0.14	0.39	0.24	0.0017	0.45	0.28
LTst6	0.0030	4.74	0.14	0.31	0.23	0.0007	0.36	0.26
Ltst7		0.92		0.26	0.29		0.26	0.22
LTst8		0.62	0.02	0.21	0.29	0.0010	0.24	0.20
LTst9	0.0002	3.20	0.08	0.24	0.25	0.0003	0.34	0.24
LTst10		2.42	0.07	0.22	0.22		0.27	0.13
LTst11		0.79		0.13	0.24		0.16	0.06
LTst12		0.67	0.01	0.12	0.23		0.14	0.06
LTst13		0.70	0.04	0.13	0.33	0.0045	0.17	0.06
LTst14	0.0010	0.95	0.04	0.16	0.26		0.18	0.08
LTst15		0.99	0.03	0.15	0.29	0.0044	0.21	0.09
LTst16		1.08	0.06	0.18	0.68	0.0022	0.32	0.15
LTst18		1.19	0.08	0.26	0.28		0.74	0.11
LTst19		2.46	0.12	0.26	0.74		0.34	0.30
LTst20	0.0029	5.20	0.23	0.34	0.48	0.0024	0.35	0.41
LTst21		2.14	0.11	0.24	0.21	0.0068	0.20	0.06
LTst22	0.0011	4.63	0.10	0.28	0.32		0.37	0.27
LTst23	0.0005	5.77	0.14	0.30	0.27		0.36	0.22
LTst24		3.37	0.23	0.37	0.31		0.26	0.19
LTst25	0.0019	2.78	0.13	0.37	0.27	0.0001	0.28	0.12

Concentrations of additional elements in the <100 kDa fraction of surface waters from Loch Tay

Sample	Fe mg/l	Mn mg/l	Pb mg/l	Cu mg/l	Zn mg/l
LTSW1	0.0138	0.0007	0.0060	0.0013	0.015
LTSW2	0.0144	0.0004	0.0048	0.0026	0.010
LTMW1	0.0177	0.0014	0.0033	0.0036	0.032
LTMW2	0.0153	0.0019	0.0049	0.0024	0.034
LTSt 1	0.0086	0.0004	0.0076	0.0023	0.010
LTSt 4	0.0091	0.0005	0.0049	0.0021	0.007
LTst5	0.0057	0.0003	0.0039	0.0024	0.005
LTst6	0.0049	0.0003	0.0006	0.0015	0.007
Ltst7	0.0109	0.0003	0.0009	0.0004	0.008
LTst8	0.0427	0.0038	0.0127	0.0111	0.046
LTst9	0.0107	0.0003	0.0035	0.0017	0.009
LTst10	0.0236	0.0005	0.0050	0.0048	0.008
LTst11	0.0571	0.0034	0.0136	0.0112	0.043
LTst12	0.0268	0.0006	0.0032	0.0018	0.016
LTst13	0.0201	0.0005	0.0034	0.0021	0.010
LTst14	0.0198	0.0003	0.0046	0.0014	0.019
LTst15	0.0177	0.0004	0.0042	0.0015	0.017
LTst16	0.0102	0.0029	0.0036	0.0024	0.108
LTst18	0.0061	0.0014	0.0038	0.0024	0.013
LTst19	0.0069	0.0004	0.0082	0.0017	0.015
LTst20	0.0043	0.0003	0.0079	0.0016	0.006
LTst21	0.0113	0.0003	0.0060	0.0014	0.007
LTst22	0.0269	0.0015	0.0102	0.0054	0.022
LTst23	0.0027	0.0004	0.0037	0.0019	0.005
LTst24	0.0083	0.0007	0.0035	0.0055	0.013
LTst25	0.0039	0.0003	0.0055	0.0006	0.005

Concentrations of Fe, Pb, Cu and Zn in the >100 kDa fraction of surface waters from Loch Tay

Sample	Al mg/l	Ca mg/	K mg/l	Mg mg/l	Na mg/l	P mg/l	S mg/l	Si mg/l
LTSW1	0.037	N/A	0.41	N/A	N/A	0.003	0.90	0.63
LTSW2	0.072	N/A	0.37	N/A	N/A	0.021	0.83	0.66
LTMW1	0.053	4.5	0.48	N/a	N/A	0.001	0.97	0.76
LTMW2	0.046	3.8	0.42	0.80	1.38	0.001	0.83	0.67
LTSt 1	0.029	12.3	0.66	2.24	1.35	0.001	1.91	1.97
LTSt 4	0.033	15.0	0.80	2.43	2.32	0.002	2.38	2.43
LTst5	0.049	35.0	1.01	2.53	1.64	0.007	3.31	2.09
LTst6	0.051	25.1	0.58	1.78	1.18	N/A	2.05	1.95
Ltst7	0.022	4.6	0.15	1.34	1.35	N/A	1.40	1.17
LTst8	0.978	8.0	0.25	1.68	2.18	0.859	1.87	1.57
LTst9	0.057	18.9	0.45	1.53	1.41	N/A	2.20	1.83
LTst10	0.066	17.1	0.60	1.59	1.50	0.003	2.08	1.02
LTst11	0.712	8.8	0.44	1.03	1.60	0.889	1.16	0.50
LTst12	0.029	4.8	0.39	0.91	1.46	0.001	1.06	0.48
LTst13	0.043	4.8	0.35	0.89	2.04	0.003	1.12	0.54
LTst14	0.045	6.5	0.42	1.15	1.59	0.003	1.22	0.68
LTst15	0.032	6.4	0.34	1.03	1.69	0.001	1.39	0.81
LTst16	0.028	7.4	0.54	1.31	4.23	0.005	2.32	1.09
LTst18	0.045	7.8	0.70	1.67	1.71	N/A	5.05	0.88
LTst19	0.038	15.1	0.80	1.61	4.27	N/A	2.42	2.37
LTst20	0.049	27.4	1.12	1.90	2.31	0.001	2.14	2.43
LTst21	0.029	13.5	0.60	1.58	1.30	0.021	1.32	0.44
LTst22	0.621	31.6	0.96	1.97	2.62	0.224	2.96	2.51
LTst23	0.047	33.3	0.81	1.87	1.59	N/A	2.51	1.93
LTst24	0.055	22.7	1.79	2.46	2.06	0.014	1.88	1.55
LTst25	0.039	17.0	0.99	2.19	1.59	N/A	1.87	1.35

Concentrations of additional elements in the >100 kDa fraction of surface waters from Loch Tay

Sample	Fe mg/l	Mn mg/l	Pb mg/l	Zn mg/l
LTSW1	0.014	0.002	N/A	0.003
LTSW2	0.014	0.002	N/A	0.001
LTMW1	0.018	0.003	0.012	0.001
LTMW2	0.012	0.002	0.001	0.002
LTSt 1	0.014	0.002	N/A	0.001
LTSt 4	N/A	N/A	N/A	N/A
LTst5	0.020	0.002	N/A	0.001
LTst6	0.015	0.002	0.001	0.003
Ltst7	0.019	0.002	0.001	0.003
LTst8	0.073	0.008	0.002	0.001
LTst9	0.012	0.001	N/A	0.001
LTst10	0.031	0.002	N/A	0.001
LTst11	0.042	0.007	N/A	0.002
LTst12	0.070	0.014	N/A	0.002
LTst13	0.048	0.008	0.012	0.001
LTst14	0.053	0.005	N/A	0.002
LTst15	0.019	0.002	N/A	0.001
LTst16	0.007	0.001	0.008	0.001
LTst18	0.014	0.002	0.002	0.002
LTst19	0.089	0.022	N/A	0.005
LTst20	0.028	0.003	N/A	0.002
LTst21	0.016	0.002	N/A	0.001
LTst22	0.031	0.004	N/A	0.003
LTst23	0.575	0.073	0.021	0.008
LTst24	0.026	0.002	N/A	0.004
LTst25	0.009	0.002	N/A	0.002

Concentrations of Fe, Pb, Cu and Zn in the >0.45u fraction of surface waters from Loch Tay

Sample	Al mg/l	Ca mg/	K mg/l	Mg mg/l	Na mg/l	P mg/l	S mg/l	Si mg/l
LTSW1	0.009	0.040	0.012	0.004	0.036	0.003	0.085	0.073
LTSW2	0.009	0.023	0.008	0.004	0.028	0.003	0.058	0.021
LTMW1	0.009	0.022	0.011	0.004	0.025	0.003	0.058	0.070
LTMW2	0.009	0.034	0.009	0.004	0.029	0.002	0.058	0.058
LTSt 1	0.008	0.027	0.010	0.004	0.031	0.001	0.066	0.037
LTSt 4	N/A	N/A	N/A	N/A	N/A	N/A	N/A	N/A
LTst5	0.021	0.044	0.010	0.005	0.029	0.002	0.063	0.048
LTst6	0.011	0.043	0.011	0.004	0.030	0.002	0.059	0.033
Ltst7	0.016	0.055	0.008	0.005	0.034	0.002	0.068	0.064
LTst8	0.023	0.031	0.008	0.006	0.030	0.002	0.065	0.041
LTst9	0.011	0.028	0.007	0.003	0.030	0.001	0.059	0.058
LTst10	0.020	0.059	0.010	0.005	0.027	0.002	0.057	0.036
LTst11	0.014	0.024	0.011	0.004	0.029	0.002	0.063	0.056
LTst12	0.016	0.029	0.008	0.005	0.029	0.003	0.063	0.048
LTst13	0.009	0.024	0.005	0.004	0.028	0.002	0.059	0.054
LTst14	0.010	0.060	0.008	0.005	0.027	0.003	0.060	0.073
LTst15	0.016	0.034	0.011	0.005	0.039	0.002	0.081	0.059
LTst16	0.006	0.032	0.009	0.003	0.032	0.002	0.056	0.031
LTst18	0.011	0.036	0.012	0.005	0.028	0.002	0.076	0.080
LTst19	0.026	0.068	0.015	0.007	0.040	0.002	0.081	0.209
LTst20	0.024	0.052	0.017	0.007	0.041	0.002	0.081	0.085
LTst21	0.019	0.032	0.010	0.005	0.028	0.002	0.060	0.056
LTst22	0.022	0.056	0.026	0.008	0.041	0.002	0.099	0.092
LTst23	0.225	0.266	0.051	0.076	0.044	0.016	0.114	0.318
LTst24	0.059	0.144	0.021	0.010	0.029	0.003	0.058	0.047
LTst25	0.010	0.049	0.008	0.004	0.027	0.001	0.061	0.044

Concentrations of additional elements in the >0.45u fraction of surface waters from Loch Tay

Appendix 15: Results from LT1 electrophoresis of porewater

Depth in sed					
distance across gel	4 cm	8 cm	12 cm	17 cm	20 cm
0.0-0.5	0.064	0.083	0.071	0.084	0.292
0.5-1.0	0.209	0.070	0.061	0.065	0.523
1.0-1.5	0.035	0.023	N/A	0.025	0.127
1.5-2.0	0.001	0.009	N/A	N/A	0.009
2.0-2.5	N/A	0.006	N/A	0.005	0.051
2.5-3.0	N/A	0.022	0.019	0.006	0.015
3.0-3.5	N/A	0.059	N/A	0.009	0.033
3.5-4.0	N/A	0.010	N/A	0.021	0.010
4.0-4.5	N/A	0.003	N/A	N/A	N/A
4.5-5.0	N/A	0.001	N/A	N/A	N/A
5.0-5.5	0.001	N/A	N/A	N/A	N/A
5.5-6.0	N/A	0.010	N/A	N/A	0.028
6.0-6.5	N/A	N/A	N/A	N/A	N/A
6.5-7.0	N/A	0.029	N/A	N/A	0.001
7.0-7.5	N/A	0.007	N/A	N/A	0.020
7.5-8.0	N/A	N/A	N/A	N/A	0.003
8.0-8.5	N/A	N/A	N/A	N/A	0.018
8.5-9.0	N/A	0.024	N/A	N/A	0.017
9.0-9.5	N/A	0.025	N/A	N/A	N/A
9.5-10.0	N/A	N/A	N/A	N/A	0.006

Concentrations of Al in agarose gel after electrophoretic extraction of porewater from selected depth of LT1

Depth in sed					
distance across gel	4 cm	8 cm	12 cm	17 cm	20 cm
0.0-0.5	0.013	0.040	0.015	0.010	0.022
0.5-1.0	0.010	0.009	0.008	0.000	0.001
1.0-1.5	0.008	0.002	0.004	0.003	0.000
1.5-2.0	0.000	0.000	0.001	0.000	0.000
2.0-2.5	0.000	0.003	0.000	0.000	0.000
2.5-3.0	0.001	0.000	0.003	0.000	0.000
3.0-3.5	0.003	0.001	0.003	0.006	0.004
3.5-4.0	0.000	0.003	0.003	0.005	0.000
4.0-4.5	0.000	0.002	0.004	0.013	0.000
4.5-5.0	0.001	0.001	0.004	0.000	0.000
5.0-5.5	0.010	0.000	0.000	0.007	0.000
5.5-6.0	0.000	0.041	0.004	0.000	0.000
6.0-6.5	0.022	0.000	0.001	0.005	0.000
6.5-7.0	0.000	0.000	0.001	0.000	0.005
7.0-7.5	0.000	0.000	0.000	0.000	0.012
7.5-8.0	0.008	0.000	0.002	0.005	0.022
8.0-8.5	0.005	0.002	0.002	0.000	0.015
8.5-9.0	0.017	0.000	0.004	0.007	0.018
9.0-9.5	0.007	0.004	0.002	0.021	0.000
9.5-10.0	0.011	0.014	0.003	0.005	0.031

Concentrations of Ca in agarose gel after electrophoretic extraction of porewater from selected depth of LT1

Depth in sed					
distance across gel	4 cm	8 cm	12 cm	17 cm	20 cm
0.0-0.5	1.10	1.12	0.58	1.10	1.39
0.5-1.0	3.14	0.62	0.73	0.97	2.17
1.0-1.5	0.60	0.34	0.26	0.54	0.50
1.5-2.0	0.34	0.13	0.15	0.17	0.15
2.0-2.5	0.06	0.11	0.13	0.10	0.15
2.5-3.0	0.12	0.14	0.20	0.08	0.08
3.0-3.5	0.05	0.20	0.11	0.12	0.09
3.5-4.0	0.03	0.09	0.09	0.06	0.08
4.0-4.5	0.01	0.03	0.06	0.06	0.05
4.5-5.0	0.02	0.03	0.05	0.03	0.07
5.0-5.5	0.02	0.02	0.04	0.04	0.06
5.5-6.0	0.03	0.04	0.05	0.05	0.09
6.0-6.5	0.09	0.02	0.04	0.05	0.07
6.5-7.0	0.01	0.03	0.04	0.02	0.03
7.0-7.5	0.01	0.01	0.02	0.02	0.06
7.5-8.0	0.02	0.02	0.25	0.02	0.05
8.0-8.5	0.01	0.01	0.02	0.02	0.06
8.5-9.0	0.02	0.01	0.04	0.03	0.07
9.0-9.5	0.07	0.02	0.02	0.02	0.03
9.5-10.0	0.02	0.01	0.03	0.02	0.03

Concentrations of Fe in agarose gel after electrophoretic extraction of porewater from selected depth of LT1

Depth in sed					
distance across gel	4 cm	8 cm	12 cm	17 cm	20 cm
0.0-0.5	0.066	0.037	0.017	0.033	0.046
0.5-1.0	0.179	0.021	0.016	0.026	0.065
1.0-1.5	0.027	0.011	0.006	0.012	0.014
1.5-2.0	0.017	0.003	0.004	0.003	0.003
2.0-2.5	0.002	0.004	0.003	0.002	0.004
2.5-3.0	0.001	0.004	0.005	0.001	0.002
3.0-3.5	0.001	0.006	0.002	0.002	0.001
3.5-4.0	0.000	0.002	0.002	0.002	0.001
4.0-4.5	0.000	0.000	0.001	0.001	0.001
4.5-5.0	0.000	0.000	0.001	0.003	0.001
5.0-5.5	0.000	0.001	0.001	0.001	0.001
5.5-6.0	0.001	0.001	0.001	0.001	0.001
6.0-6.5	0.001	0.000	0.001	0.001	0.001
6.5-7.0	0.001	0.000	0.001	0.000	0.001
7.0-7.5	0.002	0.000	0.001	0.001	0.001
7.5-8.0	0.017	0.005	0.006	0.002	0.005
8.0-8.5	0.042	0.044	0.018	0.017	0.020
8.5-9.0	0.036	0.036	0.032	0.032	0.028
9.0-9.5	0.023	0.028	0.026	0.026	0.017
9.5-10.0	0.014	0.023	0.018	0.019	0.009

Concentrations of Mn in agarose gel after electrophoretic extraction of porewater from selected depth of LT1

Depth in sed					
distance across gel	4 cm	8 cm	12 cm	17 cm	20 cm
0.0-0.5	0.104	0.090	0.082	0.084	0.126
0.5-1.0	0.167	0.063	0.115	0.080	0.137
1.0-1.5	0.072	0.076	0.052	0.042	0.051
1.5-2.0	0.045	0.041	0.075	0.043	0.057
2.0-2.5	0.075	0.037	0.064	0.055	0.061
2.5-3.0	0.075	0.080	0.076	0.064	0.066
3.0-3.5	0.059	0.087	0.075	0.059	0.095
3.5-4.0	0.055	0.047	0.093	0.060	0.066
4.0-4.5	0.080	0.051	0.084	0.067	0.082
4.5-5.0	0.092	0.088	0.095	0.074	0.079
5.0-5.5	0.078	0.066	0.075	0.078	0.080
5.5-6.0	0.082	0.069	0.065	0.032	0.064
6.0-6.5	0.055	0.055	0.051	0.056	0.072
6.5-7.0	0.035	0.041	0.050	0.061	0.066
7.0-7.5	0.048	0.042	0.055	0.061	0.081
7.5-8.0	0.057	0.029	0.057	0.025	0.077
8.0-8.5	0.040	0.042	0.020	0.049	0.075
8.5-9.0	0.045	0.034	0.050	0.049	0.062
9.0-9.5	0.050	0.018	0.048	0.053	0.053
9.5-10.0	0.065	0.036	0.067	0.036	0.046

Concentrations of P in agarose gel after electrophoretic extraction of porewater from selected depth of LT1

Depth in sed					
distance across gel	4 cm	8 cm	12 cm	17 cm	20 cm
0.0-0.5	N/A	N/A	N/A	N/A	0.074
0.5-1.0	N/A	N/A	N/A	N/A	N/A
1.0-1.5	N/A	N/A	N/A	N/A	N/A
1.5-2.0	N/A	N/A	N/A	N/A	0.062
2.0-2.5	N/A	N/A	N/A	N/A	N/A
2.5-3.0	N/A	N/A	N/A	N/A	0.030
3.0-3.5	N/A	N/A	0.109	N/A	0.052
3.5-4.0	0.003	N/A	0.013	0.015	0.024
4.0-4.5	0.007	N/A	N/A	N/A	N/A
4.5-5.0	N/A	N/A	0.020	N/A	0.011
5.0-5.5	N/A	N/A	N/A	N/A	N/A
5.5-6.0	0.014	N/A	N/A	0.020	N/A
6.0-6.5	N/A	N/A	0.014	N/A	0.047
6.5-7.0	N/A	N/A	N/A	N/A	0.018
7.0-7.5	N/A	N/A	N/A	N/A	0.037
7.5-8.0	N/A	N/A	0.025	N/A	0.020
8.0-8.5	0.012	N/A	N/A	N/A	0.034
8.5-9.0	N/A	N/A	N/A	N/A	N/A
9.0-9.5	N/A	N/A	N/A	N/A	N/A
9.5-10.0	N/A	N/A	0.043	N/A	0.021

Concentrations of Pb in agarose gel after electrophoretic extraction of porewater from selected depth of LT1

Depth in sed					
distance across gel	4 cm	8 cm	12 cm	17 cm	20 cm
0.0-0.5	0.22	0.18	0.15	0.17	0.38
0.5-1.0	0.25	0.11	0.11	0.12	0.95
1.0-1.5	0.11	0.08	0.04	0.10	0.13
1.5-2.0	0.05	0.08	0.14	0.08	0.13
2.0-2.5	0.07	0.08	0.01	0.04	0.20
2.5-3.0	0.03	0.07	0.16	0.06	0.09
3.0-3.5	0.04	0.18	0.01	0.05	0.18
3.5-4.0	0.04	0.06	0.21	0.09	0.08
4.0-4.5	0.03	0.05	0.14	0.05	0.12
4.5-5.0	0.14	0.07	0.20	0.06	0.52
5.0-5.5	0.19	0.04	0.03	0.09	0.07
5.5-6.0	0.15	0.08	0.06	0.08	0.08
6.0-6.5	0.08	0.07	0.21	0.04	0.40
6.5-7.0	0.01	0.16	0.06	0.04	0.07
7.0-7.5	0.05	0.05	0.06	0.07	0.42
7.5-8.0	0.22	0.06	0.04	0.05	0.13
8.0-8.5	0.03	0.11	0.05	0.05	0.30
8.5-9.0	0.14	0.26	0.09	0.05	0.12
9.0-9.5	0.12	0.50	0.04	0.07	0.07
9.5-10.0	0.13	0.07	0.04	0.06	0.05

Concentrations of Si in agarose gel after electrophoretic extraction of porewater from selected depth of LT1

Depth in sed					
distance	4 cm	8 cm	12 cm	17 cm	20 cm
0.0-0.5	0.040	0.070	0.040	0.046	0.190
0.5-1.0	0.055	0.042	0.120	0.028	0.602
1.0-1.5	0.024	0.034	0.082	0.025	0.039
1.5-2.0	0.010	0.024	0.030	0.013	0.023
2.0-2.5	0.023	0.040	0.022	0.027	0.037
2.5-3.0	0.009	0.022	0.020	0.010	0.272
3.0-3.5	0.036	0.052	0.050	0.034	0.052
3.5-4.0	0.015	0.028	0.030	0.094	0.047
4.0-4.5	0.014	0.024	0.031	0.028	0.051
4.5-5.0	0.008	0.022	0.078	0.006	0.221
5.0-5.5	0.008	0.016	0.087	0.013	0.028
5.5-6.0	0.004	0.042	0.073	0.012	0.034
6.0-6.5	0.043	0.017	0.018	0.027	0.229
6.5-7.0	0.004	0.048	0.090	0.016	0.031
7.0-7.5	0.010	0.014	0.023	0.006	0.157
7.5-8.0	0.009	0.013	0.015	0.022	0.060
8.0-8.5	0.005	0.023	0.051	0.014	0.222
8.5-9.0	0.013	0.016	0.107	0.013	0.041
9.0-9.5	0.009	0.019	0.093	0.030	0.040
9.5-10.0	0.016	0.029	0.135	0.051	0.045

Concentrations of Zn in agarose gel after electrophoretic extraction of porewater from selected depth of LT1

Depth in sed					
distance	4 cm	8 cm	12 cm	17 cm	20 cm
0.0-0.5	0.008	0.011	0.008	0.004	0.112
0.5-1.0	0.051	0.053	0.057	0.101	0.672
1.0-1.5	0.005	0.031	0.010	0.041	0.035
1.5-2.0	0.012	0.034	0.017	0.039	0.087
2.0-2.5	0.008	0.016	0.030	0.056	0.162
2.5-3.0	N/A	0.020	0.008	0.046	0.103
3.0-3.5	0.015	N/A	0.020	0.045	0.124
3.5-4.0	0.011	0.011	0.009	0.018	0.026
4.0-4.5	N/A	0.004	N/A	N/A	N/A
4.5-5.0	N/A	N/A	N/A	0.004	0.004
5.0-5.5	0.012	0.012	N/A	0.001	N/A
5.5-6.0	N/A	0.004	N/A	N/A	N/A
6.0-6.5	N/A	0.003	N/A	N/A	N/A
6.5-7.0	N/A	N/A	0.001	N/A	N/A
7.0-7.5	N/A	0.002	0.002	0.002	N/A
7.5-8.0	0.001	0.004	N/A	N/A	N/A
8.0-8.5	N/A	N/A	N/A	N/A	0.004
8.5-9.0	0.011	N/A	0.001	0.008	N/A
9.0-9.5	N/A	0.012	N/A	N/A	N/A
9.5-10.0	0.006	N/A	0.003	0.046	N/A

Concentrations of Al in agarose gel after electrophoretic extraction in NaOH of porewater from selected depth of LT1

Depth in sed					
distance	4 cm	8 cm	12 cm	17 cm	20 cm
0.0-0.5	N/A	N/A	0.000	0.028	0.021
0.5-1.0	N/A	N/A	N/A	0.028	0.019
1.0-1.5	N/A	N/A	0.027	0.042	0.008
1.5-2.0	N/A	N/A	N/A	0.014	0.010
2.0-2.5	N/A	N/A	N/A	0.038	0.006
2.5-3.0	N/A	N/A	N/A	0.017	0.006
3.0-3.5	N/A	N/A	N/A	0.009	0.021
3.5-4.0	N/A	N/A	N/A	0.014	0.009
4.0-4.5	N/A	N/A	N/A	0.022	0.008
4.5-5.0	N/A	0.002	N/A	0.008	0.016
5.0-5.5	N/A	N/A	N/A	0.008	0.005
5.5-6.0	N/A	0.014	0.012	0.013	0.008
6.0-6.5	N/A	N/A	N/A	0.010	0.006
6.5-7.0	N/A	N/A	N/A	0.008	0.008
7.0-7.5	N/A	N/A	N/A	0.007	0.006
7.5-8.0	N/A	N/A	0.004	0.009	0.017
8.0-8.5	N/A	N/A	N/A	0.027	0.028
8.5-9.0	N/A	0.000	N/A	0.027	0.021
9.0-9.5	N/A	0.019	N/A	0.037	0.021
9.5-10.0	N/A	0.019	N/A	0.036	0.028

Concentrations of Cu in agarose gel after electrophoretic extraction in NaOH of porewater from selected depth of LT1

	Depth in sed				
distance	4 cm	8 cm	12 cm	17 cm	20 cm
0.0-0.5	0.05	0.11	0.07	0.08	0.31
0.5-1.0	0.72	1.56	1.05	1.13	3.08
1.0-1.5	0.32	0.44	0.24	0.32	0.35
1.5-2.0	0.42	0.45	0.45	0.52	0.77
2.0-2.5	0.12	0.30	0.26	0.50	1.08
2.5-3.0	0.03	0.05	0.04	0.14	0.26
3.0-3.5	0.02	0.01	0.01	0.02	0.03
3.5-4.0	0.04	0.02	0.02	0.01	0.01
4.0-4.5	0.02	0.02	0.01	0.01	0.01
4.5-5.0	0.01	0.01	0.01	0.01	0.02
5.0-5.5	0.02	0.01	0.01	0.01	0.01
5.5-6.0	0.03	0.02	0.03	0.01	0.00
6.0-6.5	0.01	0.01	0.01	0.01	0.01
6.5-7.0	0.01	0.01	0.01	0.01	0.01
7.0-7.5	0.02	0.02	0.01	0.00	0.00
7.5-8.0	0.03	0.01	0.01	0.01	0.01
8.0-8.5	0.02	0.01	0.01	0.02	0.01
8.5-9.0	0.03	0.03	0.01	0.02	0.01
9.0-9.5	0.02	0.02	0.01	0.01	0.01
9.5-10.0	0.02	0.02	0.01	0.02	0.01

Concentrations of Fe in agarose gel after electrophoretic extraction in NaOH of porewater from selected depth of LT1

	Depth in sed				
distance	4 cm	8 cm	12 cm	17 cm	20 cm
0.0-0.5	0.015	0.008	0.004	0.005	0.008
0.5-1.0	0.075	0.101	0.056	0.057	0.084
1.0-1.5	0.028	0.034	0.014	0.021	0.014
1.5-2.0	0.032	0.034	0.026	0.032	0.033
2.0-2.5	0.008	0.022	0.014	0.025	0.043
2.5-3.0	0.001	0.002	0.002	0.006	0.006
3.0-3.5	0.001	N/A	N/A	0.000	0.002
3.5-4.0	N/A	N/A	N/A	N/A	N/A
4.0-4.5	N/A	N/A	N/A	N/A	N/A
4.5-5.0	N/A	N/A	N/A	N/A	N/A
5.0-5.5	N/A	N/A	N/A	N/A	N/A
5.5-6.0	N/A	N/A	N/A	N/A	N/A
6.0-6.5	N/A	N/A	N/A	N/A	N/A
6.5-7.0	N/A	N/A	N/A	N/A	N/A
7.0-7.5	N/A	N/A	N/A	N/A	N/A
7.5-8.0	0.001	N/A	N/A	N/A	N/A
8.0-8.5	0.002	0.001	N/A	0.001	0.001
8.5-9.0	0.002	0.001	0.001	0.001	N/A
9.0-9.5	0.002	0.001	0.001	0.001	0.001
9.5-10.0	0.002	0.002	0.001	0.001	0.002

Concentrations of Mn in agarose gel after electrophoretic extraction in NaOH of porewater from selected depth of LT1

Depth in sed					
distance	4 cm	8 cm	12 cm	17 cm	20 cm
0.0-0.5	0.042	0.070	0.063	0.082	0.058
0.5-1.0	0.069	0.077	0.068	0.101	0.107
1.0-1.5	0.046	0.059	0.059	0.106	0.028
1.5-2.0	0.063	0.056	0.032	0.069	0.072
2.0-2.5	0.032	0.062	0.053	0.053	0.055
2.5-3.0	0.055	0.056	0.054	0.066	0.052
3.0-3.5	0.071	0.070	0.032	0.050	0.040
3.5-4.0	0.047	0.051	0.070	0.067	0.060
4.0-4.5	0.039	0.070	0.042	0.060	0.051
4.5-5.0	0.046	0.046	0.059	0.056	0.046
5.0-5.5	0.049	0.062	0.041	0.043	0.066
5.5-6.0	0.058	0.068	0.063	0.055	0.028
6.0-6.5	0.049	0.031	0.046	0.051	0.051
6.5-7.0	0.056	0.030	0.060	0.046	0.023
7.0-7.5	0.053	0.048	0.046	0.037	0.019
7.5-8.0	0.048	0.053	0.061	0.037	0.059
8.0-8.5	0.047	0.050	0.029	0.064	0.066
8.5-9.0	0.075	0.033	0.072	0.055	0.048
9.0-9.5	0.046	0.057	0.041	0.074	0.044
9.5-10.0	0.056	0.044	0.047	0.060	0.051

Concentrations of P in agarose gel after electrophoretic extraction in NaOH of porewater from selected depth of LT1

Depth in sed					
distance	4 cm	8 cm	12 cm	17 cm	20 cm
0.0-0.5	N/A	0.007	0.047	0.043	0.061
0.5-1.0	N/A	0.049	N/A	0.059	0.085
1.0-1.5	N/A	0.088	N/A	N/A	0.100
1.5-2.0	0.018	0.038	N/A	0.041	0.029
2.0-2.5	N/A	N/A	N/A	0.013	0.040
2.5-3.0	0.033	N/A	N/A	0.040	0.061
3.0-3.5	N/A	0.071	0.004	0.084	0.067
3.5-4.0	0.001	0.004	0.018	0.027	0.018
4.0-4.5	N/A	N/A	0.042	N/A	0.037
4.5-5.0	0.027	0.077	N/A	0.068	0.031
5.0-5.5	N/A	0.009	0.059	N/A	0.070
5.5-6.0	0.008	0.041	0.002	N/A	N/A
6.0-6.5	N/A	0.014	0.007	0.006	0.029
6.5-7.0	0.014	0.016	N/A	0.057	0.035
7.0-7.5	0.031	0.022	N/A	0.050	N/A
7.5-8.0	N/A	0.005	N/A	N/A	N/A
8.0-8.5	N/A	0.037	N/A	0.013	0.034
8.5-9.0	N/A	0.024	0.011	0.034	0.056
9.0-9.5	N/A	0.010	0.045	0.065	0.020
9.5-10.0	N/A	N/A	N/A	0.050	0.019

Concentrations of Pb in agarose gel after electrophoretic extraction in NaOH of porewater from selected depth of LT1

Depth in sed					
distance	4 cm	8 cm	12 cm	17 cm	20 cm
0.0-0.5	0.53	0.11	0.09	0.30	0.37
0.5-1.0	0.88	0.15	0.13	0.52	1.04
1.0-1.5	0.42	0.05	0.03	0.33	0.11
1.5-2.0	0.24	0.08	0.02	0.22	0.27
2.0-2.5	0.30	0.06	0.01	0.41	0.13
2.5-3.0	0.30	0.03	0.01	0.28	0.25
3.0-3.5	0.17	0.02	0.03	0.22	0.10
3.5-4.0	0.26	0.03	0.06	0.44	0.10
4.0-4.5	0.51	0.08	0.01	0.09	0.08
4.5-5.0	0.18	0.05	0.02	0.23	0.18
5.0-5.5	0.15	0.08	0.09	0.23	0.13
5.5-6.0	0.20	0.06	0.03	0.34	0.07
6.0-6.5	0.48	0.10	0.02	0.27	0.31
6.5-7.0	0.35	0.04	0.02	0.16	0.15
7.0-7.5	0.41	0.06	0.06	0.24	0.06
7.5-8.0	0.42	0.01	0.04	0.05	0.11
8.0-8.5	0.26	0.01	0.01	0.06	0.06
8.5-9.0	0.36	0.06	0.03	0.14	0.06
9.0-9.5	0.08	0.03	0.01	0.06	0.09
9.5-10.0	0.27	0.01	0.07	1.17	0.08

Concentrations of Si in agarose gel after electrophoretic extraction in NaOH of porewater from selected depth of LT1

Depth in sed					
distance across gel	4 cm	8 cm	12 cm	17 cm	20 cm
0.0-0.5	0.091	0.031	0.029	0.220	0.155
0.5-1.0	0.128	0.032	0.032	0.220	0.241
1.0-1.5	0.081	0.024	0.054	0.242	0.023
1.5-2.0	0.103	0.034	0.024	0.230	0.080
2.0-2.5	0.071	0.029	0.023	0.265	0.039
2.5-3.0	0.108	0.016	0.062	0.179	0.063
3.0-3.5	0.076	0.014	0.022	0.176	0.067
3.5-4.0	0.106	0.029	0.017	0.175	0.026
4.0-4.5	0.082	0.025	0.012	0.033	0.030
4.5-5.0	0.065	0.015	0.029	0.146	0.028
5.0-5.5	0.076	0.024	0.066	0.168	0.023
5.5-6.0	0.083	0.035	0.023	0.164	0.016
6.0-6.5	0.089	0.022	0.017	0.190	0.049
6.5-7.0	0.075	0.027	0.028	0.172	0.032
7.0-7.5	0.092	0.019	0.016	0.192	0.019
7.5-8.0	0.068	0.023	0.020	0.024	0.133
8.0-8.5	0.064	0.018	0.046	0.032	0.053
8.5-9.0	0.084	0.020	0.041	0.036	0.030
9.0-9.5	0.054	0.028	0.014	0.043	0.034
9.5-10.0	0.091	0.031	0.013	0.055	0.046

Concentrations of Zn in agarose gel after electrophoretic extraction in NaOH of porewater from selected depth of LT1

Depth in sed					
distance across gel	5 cm	9 cm	13 cm	17 cm	20 cm
0.0-0.5	0.084	0.173	0.068	0.094	0.081
0.5-1.0	0.142	0.374	0.637	0.383	0.027
1.0-1.5	0.002	0.050	0.046	0.046	0.047
1.5-2.0	0.006	0.071	0.067	0.084	0.018
2.0-2.5	0.009	0.041	0.082	0.075	0.008
2.5-3.0	0.014	0.036	0.055	0.073	0.011
3.0-3.5	0.016	0.008	0.030	0.046	0.051
3.5-4.0	0.017	0.010	0.047	0.056	0.057
4.0-4.5	0.005	N/A	0.090	0.035	0.041
4.5-5.0	N/A	0.003	0.012	0.028	N/A
5.0-5.5	N/A	0.005	0.093	0.049	0.013
5.5-6.0	0.017	0.024	0.047	N/A	0.016
6.0-6.5	0.002	0.023	0.113	0.015	0.025
6.5-7.0	0.001	0.005	0.087	0.133	0.000

Concentrations of Al in agarose gel after electrophoretic extraction in Tris-HCl of porewater from selected depth of LT1

Depth in sed					
distance across gel	4 cm	8 cm	12 cm	17 cm	20 cm
0.0-0.5	0.015	0.005	0.016	0.007	0.008
0.5-1.0	0.005	0.005	0.010	0.007	0.007
1.0-1.5	0.005	0.007	0.005	0.003	0.004
1.5-2.0	0.002	N/A	0.003	0.002	0.003
2.0-2.5	0.006	0.002	0.002	0.003	0.005
2.5-3.0	0.016	0.006	0.006	0.011	0.011
3.0-3.5	0.009	0.020	0.015	0.005	0.010
3.5-4.0	0.016	0.013	0.009	0.001	0.032
4.0-4.5	0.014	0.022	0.013	N/A	0.008
4.5-5.0	0.015	0.016	0.006	0.000	0.006
5.0-5.5	0.006	0.006	0.017	0.003	0.008
5.5-6.0	0.010	0.012	0.009	0.011	0.008
6.0-6.5	0.011	0.029	0.011	0.001	0.002
6.5-7.0	0.010	0.013	0.010	0.006	0.005

Concentrations of Cu in agarose gel after electrophoretic extraction in Tris-HCl of porewater from selected depth of LT1

Depth in sed					
distance across gel	4 cm	8 cm	12 cm	17 cm	20 cm
0.0-0.5	0.97	1.99	0.48	0.26	0.30
0.5-1.0	2.70	5.05	5.56	3.16	0.09
1.0-1.5	0.09	0.57	0.38	0.22	0.06
1.5-2.0	0.09	0.86	0.20	0.23	0.12
2.0-2.5	0.07	0.56	0.19	0.21	0.06
2.5-3.0	0.07	0.27	0.14	0.09	0.07
3.0-3.5	0.06	0.08	0.06	0.06	0.08
3.5-4.0	0.05	0.16	0.06	0.06	0.12
4.0-4.5	0.06	0.04	0.19	0.05	0.06
4.5-5.0	0.04	0.04	0.05	0.04	0.04
5.0-5.5	0.13	0.03	0.09	0.04	0.05
5.5-6.0	0.10	0.05	0.06	0.83	0.05
6.0-6.5	0.05	0.06	0.09	0.07	0.10
6.5-7.0	0.04	0.10	0.10	0.34	N/A

Concentrations of Fe in agarose gel after electrophoretic extraction in Tris-HCl of porewater from selected depth of LT1

Depth in sed					
distance across gel	4 cm	8 cm	12 cm	17 cm	20 cm
0.0-0.5	0.0248	0.0476	0.0123	0.0176	0.0137
0.5-1.0	0.0531	0.0953	0.0802	0.0999	0.0063
1.0-1.5	0.0010	0.0088	0.0055	0.0084	0.0037
1.5-2.0	0.0011	0.0098	0.0053	0.0052	0.0032
2.0-2.5	0.0010	0.0065	0.0019	0.0060	0.0010
2.5-3.0	0.0006	0.0030	0.0045	0.0047	0.0073
3.0-3.5	0.0008	0.0014	0.0012	0.0016	0.0022
3.5-4.0	0.0008	0.0014	0.0026	0.0027	0.0025
4.0-4.5	0.0001	0.0004	0.0103	0.0020	0.0028
4.5-5.0	N/A	0.0003	0.0033	0.0144	0.0031
5.0-5.5	N/A	N/A	0.0044	0.0031	0.0016
5.5-6.0	0.0007	0.0007	0.0051	0.0021	0.0019
6.0-6.5	0.0005	0.0011	0.0053	0.0019	0.0031
6.5-7.0	0.0005	0.0008	0.0057	0.0479	N/A

Concentrations of Mn in agarose gel after electrophoretic extraction in Tris-HCl of porewater from selected depth of LT1

Depth in sed					
distance across gel	4 cm	8 cm	12 cm	17 cm	20 cm
0.0-0.5	0.047	0.036	0.055	0.053	0.078
0.5-1.0	0.046	0.067	0.171	0.127	0.056
1.0-1.5	0.021	0.054	0.022	0.030	0.049
1.5-2.0	0.026	0.040	0.034	0.043	0.037
2.0-2.5	0.017	0.026	0.029	0.042	0.062
2.5-3.0	0.044	0.025	0.036	0.051	0.081
3.0-3.5	0.044	0.048	0.052	0.019	0.084
3.5-4.0	0.048	0.046	0.032	0.047	0.105
4.0-4.5	0.023	0.053	0.052	0.008	0.089
4.5-5.0	0.036	0.030	0.072	0.045	0.089
5.0-5.5	0.039	0.010	0.065	0.076	0.077
5.5-6.0	0.062	0.020	0.058	0.075	0.055
6.0-6.5	0.042	0.055	0.037	0.046	0.069
6.5-7.0	0.033	0.044	0.029	0.091	N/A

Concentrations of P in agarose gel after electrophoretic extraction in Tris-HCl of porewater from selected depth of LT1

Depth in sed					
distance across gel	4 cm	8 cm	12 cm	17 cm	20 cm
0.0-0.5	N/A	0.068	0.017	0.054	0.071
0.5-1.0	0.014	0.129	0.104	0.087	0.056
1.0-1.5	N/A	0.079	0.070	0.067	0.017
1.5-2.0	N/A	0.096	0.076	0.059	0.046
2.0-2.5	N/A	0.062	0.036	0.020	0.069
2.5-3.0	0.019	0.039	0.020	0.051	0.056
3.0-3.5	0.015	0.031	0.039	0.119	0.044
3.5-4.0	N/A	0.073	N/A	0.039	0.007
4.0-4.5	N/A	0.092	0.023	0.017	0.036
4.5-5.0	0.121	0.020	0.088	0.054	0.068
5.0-5.5	0.022	0.054	0.076	0.032	0.091
5.5-6.0	0.014	0.091	0.042	0.135	0.012
6.0-6.5	0.028	0.053	0.118	0.037	0.003
6.5-7.0	N/A	N/A	0.011	0.074	N/A

Concentrations of P in agarose gel after electrophoretic extraction in Tris-HCl of porewater from selected depth of LT1

Depth in sed					
distance across gel	4 cm	8 cm	12 cm	17 cm	20 cm
0.0-0.5	0.303	0.438	0.161	0.343	0.135
0.5-1.0	0.207	0.442	0.636	0.358	0.055
1.0-1.5	0.188	0.125	0.091	0.166	0.444
1.5-2.0	0.120	0.293	0.374	0.317	0.026
2.0-2.5	0.136	0.119	0.231	0.249	0.033
2.5-3.0	0.179	0.154	0.146	0.204	0.059
3.0-3.5	0.139	0.120	0.148	0.121	0.215
3.5-4.0	0.120	0.148	0.067	0.179	0.055
4.0-4.5	0.167	0.140	0.281	0.178	0.046
4.5-5.0	0.135	0.164	0.331	0.019	0.026
5.0-5.5	0.104	0.124	0.190	0.031	0.056
5.5-6.0	0.283	0.178	0.232	0.029	0.048
6.0-6.5	0.148	0.181	0.307	0.102	0.102
6.5-7.0	0.144	0.181	0.296	0.188	0.000

Concentrations of Si in agarose gel after electrophoretic extraction in Tris-HCl of porewater from selected depth of LT1

Depth in sed					
distance	4 cm	8 cm	12 cm	17 cm	20 cm
0.0-0.5	0.014	0.034	0.136	0.085	0.054
0.5-1.0	0.033	0.020	0.079	0.061	0.062
1.0-1.5	0.015	0.024	0.032	0.007	0.105
1.5-2.0	0.009	0.013	0.008	0.192	0.031
2.0-2.5	0.000	0.018	0.021	0.028	0.043
2.5-3.0	0.003	0.010	0.153	0.020	0.035
3.0-3.5	0.008	0.020	0.007	0.007	0.038
3.5-4.0	0.001	0.139	0.195	0.010	0.054
4.0-4.5	N/A	0.006	0.072	0.027	0.049
4.5-5.0	0.005	0.007	0.209	0.051	0.038
5.0-5.5	N/A	0.009	0.040	0.037	0.046
5.5-6.0	0.006	0.007	0.042	0.023	0.063
6.0-6.5	0.008	0.016	0.124	0.049	0.081
6.5-7.0	0.009	0.011	0.209	0.096	0.000

Concentrations of Zn in agarose gel after electrophoretic extraction in Tris-HCl of porewater from selected depth of LT1

Appendix 16: Results from LT1 electrophoresis of sediment

Depth in Sed core	1 cm	2 cm	3 cm	4 cm	5 cm
distance across gel					
0-0.5	0.156	0.112	0.225	0.428	0.312
0.5-1.0	0.342	0.307	0.653	0.787	0.486
1.0-1.5	0.111	0.126	0.304	0.203	0.247
1.5-2.0	0.185	0.082	0.254	0.223	0.175
2.0-2.5	0.135	0.103	0.207	0.167	0.188
2.5-3.0	0.096	0.063	0.118	0.168	0.197
3.0-3.5	0.065	0.065	0.127	0.123	0.125
3.5-4.0	0.032	0.049	0.109	0.140	0.092
4.0-4.5	0.026	0.035	0.053	0.094	0.042
4.5-5.0	0.025	0.019	0.067	0.073	0.058
5.0-5.5	0.057	0.001	0.069	0.284	0.069
5.5-6.0	0.042	0.003	0.052	0.059	0.084
6.0-6.5	0.048	0.017	0.029	0.110	0.075

Concentrations of Al in agarose gel after electrophoretic extraction of sediments LT1.1-5

Depth in Sed core	1 cm	2 cm	3 cm	4 cm	5 cm
distance across gel					
0-0.5	0.98	0.53	0.61	1.12	0.88
0.5-1.0	4.25	2.22	3.05	3.04	2.18
1.0-1.5	1.68	1.00	1.47	0.99	1.12
1.5-2.0	1.98	0.95	1.63	1.38	1.13
2.0-2.5	1.49	0.95	1.12	1.04	0.95
2.5-3.0	0.56	0.50	0.45	0.63	0.62
3.0-3.5	0.25	0.23	0.66	0.30	0.21
3.5-4.0	0.13	0.17	0.28	0.32	0.19
4.0-4.5	0.14	0.11	0.13	0.15	0.13
4.5-5.0	0.06	0.08	0.15	0.12	0.12
5.0-5.5	0.13	0.06	0.15	0.18	0.23
5.5-6.0	0.09	0.07	0.13	0.17	0.16
6.0-6.5	0.17	0.07	0.12	0.44	0.17

Concentrations of Fe in agarose gel after electrophoretic extraction of sediments LT1.1-

Depth in Sed core	1 cm	2 cm	3 cm	4 cm	5 cm
distance across gel					
0-0.5	0.0088	0.0064	0.0030	0.0025	0.0123
0.5-1.0	0.0162	0.0000	0.0083	0.0052	0.0063
1.0-1.5	0.0031	0.0000	0.0065	0.0045	0.0137
1.5-2.0	0.0051	0.0080	0.0053	0.0014	0.0105
2.0-2.5	0.0063	0.0058	0.0017	0.0048	0.0092
2.5-3.0	0.0017	0.0094	0.0051	0.0184	0.0048
3.0-3.5	0.0022	0.0110	0.0077	0.0042	0.0440
3.5-4.0	0.0007	0.0088	0.0000	0.0045	0.0087
4.0-4.5	0.0029	0.0178	0.0080	0.0021	0.0060
4.5-5.0	0.0136	0.0144	0.0060	0.0097	0.0066
5.0-5.5	0.0131	0.0014	0.0017	0.0073	0.0073
5.5-6.0	0.0092	0.0024	0.0065	0.0000	0.0106
6.0-6.5	0.0166	0.0016	0.0066	0.0081	0.0090

Concentrations of Cu in agarose gel after electrophoretic extraction of sediments LT1.1-

Depth in Sed core					
distance across gel	1 cm	2 cm	3 cm	4 cm	5 cm
0-0.5	0.266	0.221	0.030	0.097	0.122
0.5-1.0	0.522	0.226	0.116	0.133	0.070
1.0-1.5	0.111	0.155	0.043	0.027	0.034
1.5-2.0	0.101	0.024	0.024	0.040	0.037
2.0-2.5	0.097	0.021	0.091	0.018	0.016
2.5-3.0	0.032	0.017	0.008	0.014	0.011
3.0-3.5	0.030	0.012	0.060	0.012	0.008
3.5-4.0	0.026	0.005	0.021	0.024	0.011
4.0-4.5	0.014	0.011	0.006	0.009	0.004
4.5-5.0	0.007	0.013	0.007	0.005	0.006
5.0-5.5	0.010	0.004	0.007	0.011	0.007
5.5-6.0	0.012	0.005	0.006	0.006	0.006
6.0-6.5	0.095	0.004	0.040	0.033	0.008

Concentrations of Mn in agarose gel after electrophoretic extraction of sediments LT1.1-

Depth in Sed core	[Pb]				
distance across gel	1 cm	2 cm	3 cm	4 cm	5 cm
0-0.5	0.024	0.027	0.052	0.087	0.030
0.5-1.0	0.085	0.046	0.000	0.022	0.058
1.0-1.5	0.012	0.059	0.033	0.018	0.017
1.5-2.0	0.036	0.090	0.093	0.023	0.055
2.0-2.5	0.149	0.015	0.078	0.000	0.023
2.5-3.0	0.118	0.030	0.017	0.067	0.008
3.0-3.5	0.051	0.046	0.002	0.042	0.005
3.5-4.0	0.063	0.086	0.032	0.003	0.073
4.0-4.5	0.046	0.058	0.012	0.005	0.000
4.5-5.0	0.049	0.068	0.000	0.000	0.002
5.0-5.5	0.000	0.059	0.032	0.000	0.007
5.5-6.0	0.034	0.007	0.012	0.065	0.028
6.0-6.5	0.058	0.025	0.000	0.003	0.062

Concentrations of Pb in agarose gel after electrophoretic extraction of sediments LT1.1-

Depth in Sed core	[P]				
distance across gel	1 cm	2 cm	3 cm	4 cm	5 cm
0-0.5	0.089	0.065	0.028	0.070	0.062
0.5-1.0	0.126	0.075	0.119	0.102	0.102
1.0-1.5	0.069	0.065	0.047	0.046	0.070
1.5-2.0	0.051	0.075	0.251	0.078	0.061
2.0-2.5	0.087	0.094	0.051	0.077	0.077
2.5-3.0	0.040	0.079	0.073	0.073	0.076
3.0-3.5	0.068	0.081	0.035	0.062	0.057
3.5-4.0	0.069	0.051	0.053	0.060	0.049
4.0-4.5	0.070	0.082	0.048	0.046	0.042
4.5-5.0	0.087	0.071	0.041	0.061	0.065
5.0-5.5	0.081	0.022	0.040	0.055	0.057
5.5-6.0	0.085	0.055	0.038	0.049	0.047
6.0-6.5	0.086	0.074	0.023	0.062	0.077

Concentrations of P in agarose gel after electrophoretic extraction of sediments LT1.1-5

Depth in Sed core	[Si]				
distance across gel	1 cm	2 cm	3 cm	4 cm	5 cm
0-0.5	0.28	0.16	0.23	0.51	0.31
0.5-1.0	0.28	0.20	0.81	0.68	0.36
1.0-1.5	0.09	0.07	0.32	0.21	0.15
1.5-2.0	0.14	0.04	0.25	0.39	0.06
2.0-2.5	0.11	0.05	0.25	0.15	0.10
2.5-3.0	0.12	0.05	0.15	0.21	0.09
3.0-3.5	0.06	0.05	0.22	0.22	0.06
3.5-4.0	0.04	0.04	0.18	0.17	0.09
4.0-4.5	0.04	0.14	0.16	0.14	0.07
4.5-5.0	0.03	0.03	0.18	0.19	0.05
5.0-5.5	0.08	0.02	0.09	0.10	0.04
5.5-6.0	0.21	0.02	0.13	0.06	0.15
6.0-6.5	0.16	0.02	0.08	0.07	0.06

Concentrations of Si in agarose gel after electrophoretic extraction of sediments LT1.1-5

Depth in Sed core	[Zn]				
distance across gel	1 cm	2 cm	3 cm	4 cm	5 cm
0-0.5	0.052	0.070	0.022	0.091	0.019
0.5-1.0	0.078	0.044	0.026	0.030	0.029
1.0-1.5	0.045	0.070	0.025	0.011	0.094
1.5-2.0	0.063	0.116	0.081	0.023	0.037
2.0-2.5	0.049	0.152	0.021	0.014	0.030
2.5-3.0	0.054	0.183	0.043	0.044	0.074
3.0-3.5	0.074	0.152	0.035	0.045	0.062
3.5-4.0	0.122	0.065	0.044	0.060	0.016
4.0-4.5	0.177	0.118	0.025	0.015	0.020
4.5-5.0	0.164	0.223	0.024	0.018	0.034
5.0-5.5	0.201	0.021	0.017	0.024	0.052
5.5-6.0	0.134	0.098	0.011	0.016	0.013
6.0-6.5	0.197	0.028	0.026	0.077	0.045

Concentrations of Zn in agarose gel after electrophoretic extraction of sediments LT1.1-

Depth in Sed core	4 cm	8 cm	12 cm	17 cm	20 cm
distance across gel					
0-0.5	0.035	0.066	0.084	0.190	0.201
0.5-1.0	0.149	0.181	0.080	0.065	0.065
1.0-1.5	0.035	0.072	0.044	0.011	0.053
1.5-2.0	0.061	N/A	0.021	N/A	0.035
2.0-2.5	0.019	N/A	N/A	0.029	0.029
2.5-3.0	0.018	0.006	N/A	0.010	0.007
3.0-3.5	0.016	N/A	N/A	N/A	N/A
3.5-4.0	N/A	N/A	0.002	N/A	N/A
4.0-4.5	N/A	N/A	N/A	N/A	N/A
4.5-5.0	N/A	N/A	N/A	N/A	N/A
5.0-5.5	N/A	N/A	N/A	N/A	N/A
5.5-6.0	N/A	N/A	N/A	N/A	N/A
6.0-6.5	N/A	0.204	0.185	0.095	N/A

Concentrations of Al in agarose gel after electrophoretic extraction of selected depths of sediments LT1

Depth in Sed core	4 cm	8 cm	12 cm	17 cm	20 cm
distance across gel					
0-0.5	0.18	0.25	0.51	0.76	0.80
0.5-1.0	0.94	0.81	0.51	0.40	0.41
1.0-1.5	0.63	0.59	0.34	0.25	0.28
1.5-2.0	0.59	0.32	0.14	0.14	0.16
2.0-2.5	0.32	0.18	0.06	0.08	0.09
2.5-3.0	0.15	0.15	1.00	0.06	0.08
3.0-3.5	0.08	0.34	0.35	0.04	0.05
3.5-4.0	0.05	0.07	0.33	0.03	0.06
4.0-4.5	0.04	0.04	0.04	0.03	0.03
4.5-5.0	0.07	0.03	0.08	0.05	0.05
5.0-5.5	0.03	0.35	0.03	0.04	0.03
5.5-6.0	0.05	0.03	0.02	0.05	N/A
6.0-6.5	0.07	0.43	0.43	0.55	N/A

Concentrations of Fe in agarose gel after electrophoretic extraction of selected depths of sediments LT1

Depth in Sed core	4 cm	8 cm	12 cm	17 cm	20 cm
distance across gel					
0-0.5	0.008	0.006	0.003	0.009	0.011
0.5-1.0	0.005	0.009	0.076	0.010	0.012
1.0-1.5	0.003	0.001	0.012	0.003	0.006
1.5-2.0	0.005	0.021	0.023	N/A	0.008
2.0-2.5	N/A	0.013	0.020	0.005	0.094
2.5-3.0	0.011	0.048	0.071	N/A	0.014
3.0-3.5	0.003	0.052	0.023	N/A	0.008
3.5-4.0	0.006	0.022	0.037	N/A	0.042
4.0-4.5	0.005	0.101	0.006	N/A	0.007
4.5-5.0	0.004	0.009	0.032	0.006	0.219
5.0-5.5	0.007	0.041	0.085	0.034	0.033
5.5-6.0	0.008	0.009	0.040	0.004	N/A
6.0-6.5	0.004	0.032	0.005	0.014	N/A

Concentrations of Cu in agarose gel after electrophoretic extraction of selected depths of sediments LT1

Depth in Sed core					
distance across gel	4 cm	8 cm	12 cm	17 cm	20 cm
0-0.5	0.026	0.012	0.015	0.020	0.022
0.5-1.0	0.026	0.020	0.012	0.006	0.006
1.0-1.5	0.014	0.008	0.007	0.002	0.005
1.5-2.0	0.015	0.003	0.004	0.001	0.002
2.0-2.5	0.009	0.002	0.003	0.001	0.002
2.5-3.0	0.008	0.007	0.007	0.001	0.001
3.0-3.5	0.007	0.004	0.004	0.000	0.001
3.5-4.0	0.003	0.001	0.005	0.001	0.012
4.0-4.5	0.002	0.000	0.000	0.000	0.002
4.5-5.0	0.001	0.000	0.001	0.000	0.002
5.0-5.5	0.001	0.002	N/A	0.002	0.000
5.5-6.0	0.001	0.001	N/A	0.001	N/A
6.0-6.5	0.000	0.021	0.018	0.012	N/A

Concentrations of Mn in agarose gel after electrophoretic extraction of selected depths of sediments LT1

Depth in Sed core	[P]				
distance across gel	4 cm	8 cm	12 cm	17 cm	20 cm
0-0.5	0.040	0.068	0.053	0.078	0.098
0.5-1.0	0.081	0.081	0.096	0.077	0.098
1.0-1.5	0.056	0.072	0.042	0.061	0.070
1.5-2.0	0.073	0.075	0.080	0.059	0.074
2.0-2.5	0.084	0.034	0.072	0.062	0.101
2.5-3.0	0.066	0.071	0.098	0.060	0.050
3.0-3.5	0.089	0.105	0.048	0.063	0.091
3.5-4.0	0.067	0.070	0.096	0.070	0.105
4.0-4.5	0.072	0.098	0.057	0.064	0.043
4.5-5.0	0.087	0.028	0.066	0.053	0.173
5.0-5.5	0.082	0.087	0.078	0.096	0.102
5.5-6.0	0.072	0.037	0.039	0.045	N/A
6.0-6.5	0.059	0.124	0.098	0.093	N/A

Concentrations of P in agarose gel after electrophoretic extraction of selected depths of sediments LT1

Depth in Sed core	[Pb]				
distance across gel	4 cm	8 cm	12 cm	17 cm	20 cm
0-0.5	0.056	N/A	N/A	0.092	0.011
0.5-1.0	0.023	0.019	0.036	N/A	0.095
1.0-1.5	0.054	N/A	0.024	N/A	0.066
1.5-2.0	0.065	0.008	0.082	0.059	0.018
2.0-2.5	0.005	0.046	0.044	N/A	0.084
2.5-3.0	N/A	0.079	N/A	0.010	N/A
3.0-3.5	0.054	0.062	0.010	0.018	0.005
3.5-4.0	0.016	0.052	0.006	0.069	0.046
4.0-4.5	0.084	0.039	N/A	0.039	0.067
4.5-5.0	0.051	0.005	0.056	0.019	0.060
5.0-5.5	0.056	0.031	0.069	0.018	0.008
5.5-6.0	0.080	N/A	0.047	0.008	N/A
6.0-6.5	N/A	0.064	0.034	N/A	N/A

Concentrations of Pb in agarose gel after electrophoretic extraction of selected depths of sediments LT1

Depth in Sed core	[Si]				
distance across gel	4 cm	8 cm	12 cm	17 cm	20 cm
0-0.5	0.088	0.122	0.084	0.172	0.228
0.5-1.0	0.304	0.428	0.059	0.304	0.079
1.0-1.5	0.110	0.314	0.035	0.072	0.056
1.5-2.0	0.056	0.036	0.031	0.038	0.054
2.0-2.5	0.045	0.091	0.054	0.331	0.191
2.5-3.0	0.043	0.093	0.049	0.110	0.198
3.0-3.5	0.046	0.039	0.041	0.121	0.087
3.5-4.0	0.051	0.022	0.045	0.164	0.102
4.0-4.5	0.066	0.043	0.057	0.142	0.066
4.5-5.0	0.106	0.117	0.049	0.087	0.074
5.0-5.5	0.053	0.025	0.047	0.042	0.052
5.5-6.0	0.213	0.170	0.151	0.158	N/A
6.0-6.5	0.146	0.356	0.445	0.175	N/A

Concentrations of Si in agarose gel after electrophoretic extraction of selected depths of sediments LT1

Depth in Sed core	[Zn]				
distance across gel	4 cm	8 cm	12 cm	17 cm	20 cm
0-0.5	0.04	0.04	0.06	0.07	0.07
0.5-1.0	0.04	0.07	0.12	0.04	0.05
1.0-1.5	0.03	0.05	0.04	0.03	0.07
1.5-2.0	0.06	0.07	0.41	0.03	0.10
2.0-2.5	0.19	0.12	0.11	0.03	0.11
2.5-3.0	0.06	0.38	0.17	0.16	0.05
3.0-3.5	0.06	0.12	0.26	0.03	0.08
3.5-4.0	0.17	0.09	0.22	0.17	0.09
4.0-4.5	0.09	0.10	0.06	0.08	0.05
4.5-5.0	0.84	0.05	0.10	0.06	0.19
5.0-5.5	0.63	0.11	0.34	0.11	0.06
5.5-6.0	0.61	0.27	0.16	0.06	N/A
6.0-6.5	0.39	0.30	0.04	0.09	N/A

Concentrations of Zn in agarose gel after electrophoretic extraction of selected depths of sediments LT1